



University of  
**Strathclyde**  
Science

The University of Strathclyde  
Strathclyde Institute of Pharmacy and Biomedical  
Sciences

**DEVELOPMENT OF NOVEL COMBINATION  
THERAPIES FOR THE TREATMENT OF  
PANCREATIC CANCER**

Calum Mullen

A thesis presented in fulfilment of the requirements  
for the degree of Doctor of Philosophy

March 2024

“Improvise, Adapt, Overcome!” – Bear Grylls

## **DECLARATION**

This thesis is the result of the author's original research. It has been composed by the author and has not been previously submitted for examination which has led to the award of a degree.

The copyright of this thesis belongs to the author under the terms of the United Kingdom Copyright Acts as qualified by University of Strathclyde Regulation 3.50. Due acknowledgement must always be made of the use of any material contained in, or derived from, this thesis.

**Signed:**

A handwritten signature in black ink, appearing to read 'Gullu', written in a cursive style.

**Date:** 27<sup>th</sup> March 2024

## **COVID IMPACT STATEMENT**

The laboratory work carried out as part of this thesis began in October 2019 and was completed in August 2023, thus the project was severely impacted due to lockdown limitations put in place during the COVID-19 pandemic.

From March 2020 to August 2020 there was no access to the laboratory due to the national lockdown in Scotland. From August 2020 to March 2021 there was reduced and restricted laboratory access due to institute social distancing measures, which limited the number of persons that could access the lab at a given time. As a result of this, I only had access to the lab approximately 3 days a week, which restricted my ability to do experiments.

In addition to restricting access, the COVID-19 pandemic also delayed my ability to be trained in the operation of the X-Rad225 irradiator, which was an essential part of my project as radiotherapy was required for experiments. I was finally able to be trained in the operation of the machine in October 2020, one full year after starting my PhD.

Additionally, the supply and delivery of essential plastics was severely impacted by COVID, which limited my ability to carry out experiments. In particular, the supply of the 96-well plates that were integral to my spheroid experiments was delayed by 6 months.

As a result of the pandemic the original scope and plan of my project was altered to allow for the completion of lab work within the allotted timeframe.

## **ACKNOWLEDGEMENTS**

It's strange sitting here at the end of this journey reflecting on the last 4 years, I can honestly say that I never expected to be in the position that I am now, and I wouldn't change a thing. Now I will attempt the hardest part – write something personal.

I would like to say thank you to my supervisor Dr Marie Boyd for guiding me through this process over the years. I would like to thank everyone in the Boyd lab, Yasir; Hannah; Rosh; Samantha; Reem; Olena; Sara; and Manal for your friendship over the years and making the tissue culture room a fun place to be during all the countless hours I spent in it. I would also like to thank all the honours and Master's students I have had the pleasure of working with over the years, you helped make this experience great.

I would like to say a big thank you to my family for supporting me throughout all the highs and lows that this process brings and keeping me level-headed. Without your support I wouldn't have made it.

Finally, I would like to say thank you to my girlfriend Emma, words can't express how grateful I am for you. You have encouraged me both in and out the lab, and your unwavering support is irreplaceable.

## **ABSTRACT**

### **Introduction**

In the UK, pancreatic cancer is the 5<sup>th</sup> most common cause of cancer related deaths, with an average 5-year survival rate of 7.3% and a 10-year survival rate of only 1%, which has remained unchanged since the 1970s. Currently the only curative treatment for pancreatic cancer is surgical resection, however 80% of patients are ineligible for resection as the majority of cases are diagnosed in the later stages of the disease and are inoperable, leaving chemotherapy as the only treatment option. Gemcitabine was first introduced in 1997 and remains a main staple of therapy for pancreatic cancer patients, whether as a monotherapy or in combination. However, despite its widespread use, gemcitabine resistance remains a widespread problem clinically, owing to both intrinsic and acquired resistance mechanisms present in over 80% of pancreatic cancers. There is, therefore, a significant clinical need for alternative treatment options in pancreatic cancer, and to this end we propose the use of the repurposed fumarate drugs dimethyl fumarate (DMF) and monomethyl fumarate (MMF). Both DMF and MMF were previously used for the treatment of multiple sclerosis but have since shown promise as anticancer agents, as DMF and MMF downregulate NRF2 activity, the major transcription factor responsible for the antioxidant response, which we hypothesise enhances the effect of other chemotherapies and radiotherapy in combination. The aims of this project were therefore to develop novel combination therapies utilising DMF and MMF in combination with chemotherapy and external beam radiotherapy (EXBR), which we hypothesise would show promise in inducing reduction in clonogenicity in pancreatic cancer cell lines.

## **Materials and methods**

Pancreatic cancer cell lines, Panc-1 and Mia PaCa-2 were cultured in both 2D and 3D cell models via the clonogenic and spheroid growth assays respectively to investigate the efficacy of both DMF and MMF in combination with gemcitabine or radiotherapy. Additionally, to determine the effects of scheduling the developed combinations, three schedules were tested: simultaneous administration (schedule 1); drug administered 24 hours before EXBR (schedule 2); and fumaric drug administered 24 hours before gemcitabine (schedule 3). To assess the effectiveness of the developed combinations *in vitro*, two-dimensional (2D) clonogenic and three-dimensional (3D) spheroid studies were carried out, followed by mechanistic studies investigating DNA damage and repair; distribution of cells throughout the cell cycle following treatment; cell death via apoptosis; and finally, glutathione levels within the cell following treatment to investigate the mechanisms underpinning the effects observed by the combinations.

## **Results**

From all of the developed combinations, five combinations were selected to go forward for further analysis based on the results obtained from the clonogenic assay. These combinations were: MMF + EXBR (schedule 1 & 2), MMF + gemcitabine (schedule 1 & 3) and DMF + EXBR (schedule 2). Of these five combinations, we believe MMF + EXBR (schedule 1 & 2), and MMF + gemcitabine (schedule 1) to be the most promising combinations based on the results experimentally obtained.

In Panc-1, the combination of 0.6  $\mu\text{M}$  MMF + 0.5 Gy EXBR (schedule 1) induced an average reduction in clonogenicity of  $49.08 \pm 3.18\%$ , whereas 0.6  $\mu\text{M}$  MMF induced a reduction in clonogenicity of  $26.48 \pm 6.34\%$  and 0.5 Gy EXBR  $30.56 \pm 4.27\%$ . When looking at the cell cycle, the combination caused S phase arrest (57.53% of cells in

the population), which corresponded with an increase in DNA damage (12.8%) and apoptosis (8.9%). However, this did not correspond with a decrease in glutathione as hypothesised as the glutathione levels remained the same as that of the untreated control. When testing this combination in spheroids, it resulted in a  $45.08 \pm 15.96\%$  reduction in spheroid growth when compared with the untreated control, whereas MMF monotherapy resulted in a  $31.88 \pm 13.11\%$  and EXBR  $35.77 \pm 14.30\%$  reduction. In Mia PaCa-2, the combination of  $0.6 \mu\text{M}$  MMF +  $0.5 \text{ Gy}$  EXBR (schedule 1) induced an average reduction in clonogenicity of  $32.47 \pm 11.05\%$ , whereas  $0.6 \mu\text{M}$  MMF induced a reduction in clonogenicity of  $27.33 \pm 5.91\%$  and  $0.5 \text{ Gy}$  EXBR  $20.82 \pm 6.94\%$ . When looking at the cell cycle, the combination caused G2/M phase arrest (43.22% of cells in the population), which corresponded with an increase in DNA damage (11.29%) and apoptosis (30.5%). However, this did not correspond with a decrease in glutathione as hypothesised as the glutathione levels remained the same as that of the untreated control. When testing this combination in spheroids, it resulted in a  $62.66 \pm 9.23\%$  reduction in spheroid growth when compared with the untreated control, whereas MMF monotherapy resulted in a  $62.21 \pm 5.53\%$  and EXBR  $23.5 \pm 6.37\%$  reduction.

In Panc-1, the combination of  $0.6 \mu\text{M}$  MMF +  $0.16 \mu\text{M}$  gemcitabine (schedule 1) induced an average reduction in clonogenicity of  $55.19 \pm 3\%$ , whereas  $0.6 \mu\text{M}$  MMF induced a reduction in clonogenicity of  $22.97 \pm 4.7\%$  and  $0.16 \mu\text{M}$  gemcitabine  $2.22 \pm 2.18\%$ . When looking at the cell cycle, the combination caused G2/M phase arrest (61.21% of cells in the population), which corresponded with an increase in DNA damage (2.77%) and apoptosis (8.17%). However, this did not correspond with a decrease in glutathione as hypothesised as the glutathione levels remained the same as that of the untreated control. When testing this combination in spheroids, it resulted in a  $96.50 \pm 5.15\%$  reduction in spheroid growth when compared with the untreated

control, whereas MMF monotherapy resulted in a  $31.11 \pm 10.24\%$  and gemcitabine  $94.88 \pm 3.36\%$  reduction. In Mia PaCa-2, the combination of  $0.6 \mu\text{M}$  MMF +  $0.16 \mu\text{M}$  gemcitabine (schedule 1) induced an average reduction in clonogenicity of  $14.97 \pm 7.17\%$ , whereas  $0.6 \mu\text{M}$  MMF induced a reduction in clonogenicity of  $30.33 \pm 2.15\%$  and  $0.16 \mu\text{M}$  gemcitabine  $15.52 \pm 6.13\%$ . When looking at the cell cycle, the combination caused G2/M phase arrest (61.21% of cells in the population), which corresponded with an increase in DNA damage (2.06%) and apoptosis (30.31%). However, this did not correspond with a decrease in glutathione as hypothesised as the glutathione levels remained the same as that of the untreated control. When testing this combination in spheroids, it resulted in a  $92.56 \pm 4.73\%$  reduction in spheroid growth when compared with the untreated control, whereas MMF monotherapy resulted in a  $60.21 \pm 8.51\%$  and gemcitabine  $90.13 \pm 6.36\%$  reduction.

In Panc-1, the combination of  $0.6 \mu\text{M}$  MMF + 0.5 Gy EXBR (schedule 2) induced an average reduction in clonogenicity of  $48.74 \pm 9.35\%$ , whereas  $0.6 \mu\text{M}$  MMF induced a reduction in clonogenicity of  $27 \pm 3.27\%$  and 0.5 Gy EXBR  $32.08 \pm 5.41\%$ . When looking at the cell cycle, the combination had no effect on the cell cycle or induced lasting DNA damage and glutathione levels remained the same as the untreated control, however there was an increase in apoptosis (12.9%). When testing this combination in spheroids, it resulted in a  $41.76 \pm 10.85\%$  reduction in spheroid growth when compared with the untreated control, whereas MMF monotherapy resulted in a  $46.40 \pm 17.28\%$  and EXBR  $46.71 \pm 11.72\%$  reduction.

In Mia PaCa-2, the combination of  $0.6 \mu\text{M}$  MMF + 0.5 Gy EXBR (schedule 2) induced an average reduction in clonogenicity of  $36.54 \pm 14.9\%$ , whereas  $0.6 \mu\text{M}$  MMF induced a reduction in clonogenicity of  $29.09 \pm 6.74\%$  and 0.5 Gy EXBR  $18.02 \pm 3.52\%$ . When looking at the cell cycle, the combination had no effect on the cell cycle, however there was an increase in DNA damage (2.19%) and apoptosis (25.05%). However, this did not

correspond with a decrease in glutathione as hypothesised as the glutathione levels remained the same as that of the untreated control. When testing this combination in spheroids, it resulted in a  $44.03 \pm 15.40\%$  reduction in spheroid growth when compared with the untreated control, whereas MMF monotherapy resulted in a  $29.73 \pm 11.90\%$  and EXBR  $4.11 \pm 2.72\%$  reduction

In Panc-1, the combination of  $20 \mu\text{M}$  DMF +  $0.5 \text{ Gy}$  EXBR (schedule 2) induced an average reduction in clonogenicity of  $36.13 \pm 4.17\%$ , whereas  $0.5 \text{ Gy}$  EXBR induced a reduction in clonogenicity of  $28.06 \pm 2.57\%$  and  $20 \mu\text{M}$  DMF had no effect on clonogenicity. The combination had no effect on glutathione levels, the distribution of cells throughout the cell cycle or induced any lasting DNA damage, however there was an increase in apoptosis ( $9.74\%$ ). When testing this combination in spheroids, it resulted in a  $63.80 \pm 6.65\%$  reduction in spheroid growth when compared with the untreated control, whereas DMF monotherapy resulted in a  $28.33 \pm 12.24\%$  and EXBR  $40.20 \pm 13.84\%$  reduction. In Mia PaCa-2, the combination of  $20 \mu\text{M}$  DMF +  $0.5 \text{ Gy}$  EXBR (schedule 2) induced an average reduction in clonogenicity of  $48.67 \pm 6.10\%$ , whereas  $20 \mu\text{M}$  DMF induced a reduction in clonogenicity of  $11.13 \pm 3.83\%$  and  $0.5 \text{ Gy}$  EXBR  $19.94 \pm 4.04\%$ . When looking at the cell cycle, the combination had no effect on the cell cycle, however there was an increase in DNA damage ( $3.49\%$ ) and apoptosis ( $22\%$ ). However, this did not correspond with a decrease in glutathione as hypothesised as the glutathione levels remained the same as that of the untreated control. When testing this combination in spheroids, it resulted in a  $55.24 \pm 12.67\%$  reduction in spheroid growth when compared with the untreated control, whereas DMF monotherapy resulted in a  $10.26 \pm 12.58\%$  and EXBR  $6.87 \pm 4.86\%$  reduction.

In Panc-1, the combination of  $0.6 \mu\text{M}$  MMF +  $0.16 \mu\text{M}$  gemcitabine (schedule 3) induced an average reduction in clonogenicity of  $13.28 \pm 6.37\%$ , whereas  $0.6 \mu\text{M}$  MMF induced a reduction in clonogenicity of  $25.71 \pm 4.79\%$  and  $0.16 \mu\text{M}$  gemcitabine

3.2 ± 1.52%. The combination had no effect on glutathione levels, the distribution of cells throughout the cell cycle or induced any lasting DNA damage, however there was an increase in apoptosis (9.53%). When testing this combination in spheroids, it resulted in a 96.65 ± 3.86% reduction in spheroid growth when compared with the untreated control, whereas MMF monotherapy resulted in a 16.97 ± 12.49% and gemcitabine a 97.04 ± 2.19% reduction. In Mia PaCa-2, the combination of 0.6 µM MMF + 0.16 µM gemcitabine (schedule 3) induced an average reduction in clonogenicity of 25.15 ± 2.96%, whereas 0.6 µM MMF induced a reduction in clonogenicity of 24.94 ± 5.47% and 0.5 Gy EXBR 21.42 ± 5.04%. When looking at the cell cycle, the combination caused G2/M phase arrest (38.31% of cells in the population), which corresponded with an increase in DNA damage (6.63%) and apoptosis (27.27%). However, this did not correspond with a decrease in glutathione as hypothesised as the glutathione levels remained the same as that of the untreated control. When testing this combination in spheroids, it resulted in a 93.13 ± 2.93% reduction in spheroid growth when compared with the untreated control, whereas MMF monotherapy resulted in a 42.14 ± 4.46% and gemcitabine a 90.91 ± 5.83% reduction.

### **Conclusion**

The combinations of MMF + EXBR and MMF + gemcitabine show promise as a potential candidate for the treatment of pancreatic cancers, however further studies investigating the effects of the combination *in vivo* would be required prior to potential clinical studies.

From the obtained results we were unable to confirm the mechanism of action of DMF/MMF, therefore further studies would be required to elucidate the mechanism of cell death and confirm if glutathione levels are being reduced as hypothesised.

## **ABBREVIATIONS**

2D = two-dimensional

3D = three-dimensional

ACS = American Cancer Society

ATP = adenosine triphosphate

AUC = area under the curve

Bcl-2 = B-cell lymphoma 2

*CDKN2A* = cyclin-dependent kinase 2A

CES1 = carboxylesterase 1

CT = computed tomography

D<sub>50</sub> = irradiation dose to reduce the survival rate to 50%

dCK = deoxycytidine kinase

dCTP = deoxycytidine triphosphate

dFdCMP = gemcitabine monophosphate

dFdCTP = gemcitabine triphosphate

DJ-1 = protein deglycase

DMEM = Dulbecco's modified Eagle medium

DMF = dimethyl fumarate

DDR = DNA damage response

DSBs = double-strand breaks

EMA = European Medicines Agency

EXBR = external beam radiotherapy

FBS = Fetal Bovine Serum

FDA = Food and Drug Administration

FITC = fluorescein isothiocyanate

FOLFIRINOX = folinic acid, fluorouracil, irinotecan, and oxaliplatin

G1 phase = gap one phase

G2 phase = gap two phase

GI = gastrointestinal

GSH = glutathione

GSSG = glutathione disulphide

IAP = inhibitors of apoptosis  
IARC = International Agency for Research on Cancer  
IC<sub>50</sub> = half-maximal inhibitory concentration  
KEAP1 = Kelch-like ECH-associated protein 1  
KRAS = Kirsten rat sarcoma viral oncogene homolog  
LINAC = medical linear accelerator  
M = metastasis  
M phase = mitotic phase  
MDR = multidrug resistance  
MMF = monomethyl fumarate  
MRI = magnetic resonance imaging  
MRP1 = multidrug resistance protein 1  
N = lymph nodes  
NCI = National Cancer Institute  
NDPK = nucleoside diphosphate kinase  
NF-κB = nuclear factor-κB  
NICE = National Institute for Health and Care Excellence  
NMPK = monophosphate kinase  
NRF2 = nuclear factor erythroid 2-related factor 2  
NTPs = nucleoside triphosphates  
p53 = tumour protein 53  
PanCAN = Pancreatic Cancer Action Network  
PARP = Poly (ADP-ribose) polymerase  
PBS = phosphate-buffered saline  
PDAC = pancreatic ductal adenocarcinoma  
P-gp = P-glycoprotein  
PI = propidium iodide  
Poly-HEMA = poly (2-hydroxyethyl methacrylate)  
PS = phosphatidylserine  
RNase A = Ribonuclease A  
ROS = reactive oxygen species

RRMS = relapsing-remitting multiple sclerosis

S phase = DNA synthesis phase

SABR = stereotactic ablative radiotherapy

SBRT = stereotactic body radiation therapy

sG1 = sub G1

SSBs = single-strand breaks

T = tumour grade

TBE = Tris Borate EDTA

TMZ = temozolomide

TNM = tumour, node, metastasis

*TP53* = tumour protein 53

U.K. = United Kingdom

U.S. = United States

WCRF = World Cancer Research Fund

WHO = World Health Organisation

## Table of Contents

<b>DECLARATION</b> .....	3
<b>COVID IMPACT STATEMENT</b> .....	4
<b>ACKNOWLEDGEMENTS</b> .....	5
<b>ABSTRACT</b> .....	6
<b>ABBREVIATIONS</b> .....	12
<b>CHAPTER 1: Introduction</b> .....	26
<b>1.1: Cancer Incidence &amp; Mortality</b> .....	27
<b>1.2: Biology and Hallmarks of Cancer</b> .....	27
<b>1.3: DNA damage response</b> .....	29
<b>1.4: The Cell Cycle</b> .....	30
<b>1.5: Modes of Cell Death</b> .....	31
<b>1.3: Pancreatic Cancer</b> .....	34
<b>1.4: Pancreatic Cancer Incidence</b> .....	37
<b>1.5: Diagnosis and Staging of Pancreatic Cancer</b> .....	37
<b>1.6: Pancreatic Cancer Mortality</b> .....	39
<b>1.7: Pancreatic Cancer Survival Rates</b> .....	39
<b>1.8: Molecular Characteristics of Pancreatic Cancer</b> .....	41
<b>1.9: Pancreatic Cancer Treatment</b> .....	42
<b>1.10: Radiobiology</b> .....	45
<b>1.11: Gemcitabine</b> .....	46
<b>1.12: Chemoresistance in Pancreatic Cancer</b> .....	49
<b>1.13: Drug Repurposing</b> .....	50
<b>1.14: Fumaric acid &amp; Glutathione Metabolism</b> .....	50
<b>1.14: Dimethyl Fumarate</b> .....	51
<b>1.15: Dimethyl Fumarate and Cancer</b> .....	54
<b>1.16: Monomethyl Fumarate</b> .....	58
<b>1.17: Glutathione and Pancreatic Cancer</b> .....	58
<b>1.18: Aims</b> .....	59
<b>CHAPTER 2: Evaluation of the cytotoxic effect of single therapeutic agents and EXBR on pancreatic cancer cell survival in 2D &amp; 3D cell models</b> .....	60
<b>2.1: INTRODUCTION</b> .....	61
<b>2.2: AIMS</b> .....	63
<b>2.3: MATERIALS AND METHODS</b> .....	63

2.3.1: Cell Lines and Culture Conditions .....	63
2.3.2: Treatments.....	64
2.3.3: Cell Doubling Time Assay .....	65
2.3.4: Clonogenic Assay.....	66
2.3.5: Preparation of Low Attachment 96-well Plates for Spheroid Growth Delay Assay .....	67
2.3.6: Spheroid Growth Delay Assay .....	68
2.3.7: Spheroid Growth Analysis .....	68
2.3.8: Statistical Analysis.....	69
<b>2.4: RESULTS.....</b>	<b>69</b>
2.4.1: Growth characteristics of pancreatic cells <i>in vitro</i> .....	69
2.4.2: Cytotoxic effect of gemcitabine on pancreatic cell clonogenicity <i>in vitro</i> .....	72
2.4.3: Cytotoxic effect of DMF on pancreatic cell clonogenicity <i>in vitro</i> ....	76
2.4.4: Cytotoxic effect of MMF on pancreatic cell clonogenicity <i>in vitro</i> ...	80
2.4.5: EXBR induced cytotoxicity on pancreatic cell clonogenicity <i>in vitro</i> .....	83
2.4.6: Interrogation of the effect of gemcitabine on pancreatic cancer spheroid growth <i>in vitro</i> .....	87
2.4.7: Interrogation of the effect of DMF on pancreatic cancer spheroid growth <i>in vitro</i> .....	95
2.4.8: Interrogation of the effect of MMF on pancreatic cancer spheroid growth <i>in vitro</i> .....	101
2.4.9: Interrogation of the effect of EXBR on pancreatic cancer spheroid growth <i>in vitro</i> .....	108
<b>2.5: DISCUSSION.....</b>	<b>114</b>
2.5.1: Cell growth characteristics .....	114
2.5.2: Cytotoxicity of gemcitabine <i>in vitro</i> .....	116
2.5.3: Cytotoxicity of DMF <i>in vitro</i> .....	118
2.5.4: Cytotoxicity of MMF <i>in vitro</i> .....	119
2.5.5: EXBR induced cytotoxicity <i>in vitro</i> .....	120
2.5.6: Conclusions .....	121
<b>CHAPTER 3: Development and evaluation of combination therapies in pancreatic cancer cell line 2D &amp; 3D cell models.....</b>	<b>122</b>
3.1: INTRODUCTION.....	123
3.2: AIMS .....	124
3.3: MATERIALS AND METHODS .....	125

3.3.1: Cell Lines and Culture Conditions .....	125
3.3.2: Treatments.....	125
3.3.3: Clonogenic Assay.....	127
3.3.4: Preparation of Low Attachment 96-well Plates for Spheroid Growth Assay.....	127
3.3.5: Spheroid Growth Assay .....	127
3.3.6: Spheroid Growth Analysis .....	127
3.3.7: Statistical Analysis.....	127
3.4: RESULTS.....	128
3.4.1: Development of schedule 1 combinations.....	128
3.4.2: Analysis of schedule 1 combinations .....	132
3.4.3: Development of schedule 2 combinations.....	157
3.4.4: Analysis of schedule 2 combinations .....	162
3.4.4: Development of schedule 3 combinations.....	180
3.4.5: Analysis for schedule 3 combinations.....	183
3.5: DISCUSSION.....	195
3.5.1: Gemcitabine + EXBR.....	195
3.5.2: DMF + EXBR .....	199
3.5.3: MMF + EXBR .....	201
3.5.4: DMF + gemcitabine.....	202
3.5.5: MMF + gemcitabine .....	204
3.5.6: Summary of combination therapies .....	206
CHAPTER 4: Mechanistic studies of developed combinations .....	208
4.1: INTRODUCTION.....	209
4.1.1: Cell Cycle.....	209
4.1.2: Apoptosis.....	210
4.1.3: DNA damage .....	211
4.1.4: Glutathione .....	212
4.2: AIMS .....	212
4.3: MATERIALS AND METHODS .....	212
4.3.1: Cell Lines and Culture Conditions .....	212
4.3.2: Treatments.....	213
4.3.3: Cell Cycle Analysis.....	213
4.3.4: Apoptosis Assay .....	214
4.3.5: Comet Assay (single cell gel electrophoresis) .....	215

4.3.6: Glutathione Assay .....	217
4.3.7: Statistical Analysis .....	218
4.4: RESULTS .....	219
4.4.1: Cell cycle studies on developed combinations .....	219
4.4.2: Apoptosis studies on developed combinations .....	255
4.4.3: DNA damage studies on developed combinations .....	287
4.4.4: Glutathione studies on developed combinations .....	299
4.5: DISCUSSION .....	312
4.5.1: Monotherapies .....	312
4.5.2: MMF + EXBR .....	314
4.5.3: MMF + gemcitabine .....	316
4.5.4: DMF + EXBR .....	319
4.5.5: Summary .....	321
CHAPTER 5: Discussion, conclusions, & future work .....	323
5.2: Discussion & Future work .....	324
5.2: Limitations .....	329
5.3: Final Conclusions .....	330
APPENDIX .....	332
REFERENCES .....	344

## **Table of Figures:**

Figure 1.1: Anatomy of the Pancreas.....	36
Figure 1.2: Pancreatic Cancer Incidence & Survival Rates .....	40
Figure 1.3: Gemcitabine Mechanism of Action.....	48
Figure 1.4: DMF Metabolism .....	53
Figure 1.5: DMF Mechanism of Action .....	57
Figure 2.1: Panc-1 and Mia PaCa-2 growth characteristics .....	70
Figure 2.2: Cytotoxic effect of gemcitabine on Panc-1 and Mia PaCa-2.....	73
Figure 2.3: Cytotoxic effect of DMF on Panc-1 and Mia PaCa-2.....	77
Figure 2.4: Cytotoxic effect of MMF on Panc-1 and Mia PaCa-2.....	81
Figure 2.5: Effect of EXBR on Panc-1 and Mia PaCa-2 .....	85
Figure 2.6: Effect of gemcitabine on Panc-1 spheroid growth .....	88
Figure 2.7: Effect of gemcitabine on Mia PaCa-2 spheroid growth.....	92
Figure 2.8: Effect of DMF on Panc-1 spheroid growth.....	96
Figure 2.9: Effect of DMF on Mia PaCa-2 spheroid growth .....	99
Figure 2.10: Effect of MMF on Panc-1 spheroid growth.....	102
Figure 2.11: Effect of MMF on Mia PaCa-2 spheroid growth .....	105
Figure 2.12: Effect of EXBR on Panc-1 spheroid growth.....	109
Figure 2.13: Effect of EXBR on Mia PaCa-2 spheroid growth .....	112
Figure 3.1: Scheduling of combination therapies .....	126
Figure 3.2 .....	129
Figure 3.3: Schedule 1 spheroid growth pilot study in Panc-1 .....	131
Figure 3.4: Schedule 1 – MMF + EXBR analysis.....	133
Figure 3.5: Schedule 1 – MMF + EXBR spheroid growth assay in Panc-1 and MiaPaCa-2...	135
Figure 3.6: Schedule 1 – MMF + gemcitabine analysis .....	139
Figure 3.7: Schedule 1 – MMF + gemcitabine spheroid growth assay in Panc-1 and MiaPaCa-2 .....	141
Figure 3.8: Schedule 1 – DMF + gemcitabine analysis .....	145
Figure 3.9: Schedule 1 – DMF + gemcitabine spheroid growth assay in Panc-1 and Mia PaCa-2 .....	147
Figure 3.10: Schedule 1 – gemcitabine + EXBR spheroid growth assay in Panc-1 and Mia PaCa-2 .....	151
Figure 3.11: Schedule 1 – DMF + EXBR spheroid growth assay in Panc-1 and MiaPaCa-2..	154
Figure 3.12: Schedule 2 combinations in pancreatic cancer cell lines.....	158
Figure 3.13: Schedule 2 spheroid growth pilot study in Panc-1 .....	161
Figure 3.14: Schedule 2 – gemcitabine + EXBR analysis .....	163
Figure 3.15: Schedule 1 – gemcitabine + EXBR spheroid growth assay in Panc-1 and MiaPaCa-2 .....	165
Figure 3.16: Schedule 2 – DMF + EXBR analysis.....	169
Figure 3.17: Schedule 2 – DMF + EXBR spheroid growth assay in Panc-1 and MiaPaCa-2..	171
Figure 3.18: Schedule 2 – MMF + EXBR combination analysis .....	175
Figure 3.19: Schedule 2 – MMF + EXBR spheroid growth assay in Panc-1 and MiaPaCa-2.	177
Figure 3.20: Schedule 3 combinations in pancreatic cancer cell lines.....	181
Figure 3.21: Schedule 3 – DMF + gemcitabine analysis.....	184

Figure 3.22: Schedule 3 – DMF + gemcitabine spheroid growth assay in Panc-1 and Mia PaCa-2 .....	186
Figure 3.23: Schedule 3 – MMF + gemcitabine analysis .....	190
Figure 3.24: Schedule 3 – MMF + gemcitabine spheroid growth assay in Panc-1 and Mia PaCa-2 .....	192
Figure 4.1: Cell cycle analysis of combination therapies in Panc-1 .....	220
Figure 4.2: Cell cycle analysis of combination therapies in Mia PaCa-2 .....	238
Figure 4.3: Apoptosis analysis of combination therapies in Panc-1 .....	256
Figure 4.4: Apoptosis analysis of combination therapies in Mia PaCa-2 .....	272
Figure 4.5: DNA damage analysis of combination therapies in Panc-1 .....	288
Figure 4.6: DNA damage analysis of combination therapies in Mia PaCa-2 .....	293
Figure 4.7: Glutathione analysis of combination therapies in Panc-1 .....	300
Figure 4.8: Glutathione analysis of combination therapies in Mia PaCa-2 .....	305

## **Table of Tables:**

Table 1.1: Pancreatic cancer tumour grades .....	38
Table 1.2: Pancreatic cancer tumour staging .....	38
Table 1.3: Mutation Frequency in Pancreatic Cancer .....	42
Table 2.1: Preparation of Drug Stocks .....	65
Table 2.2: Treatment Concentrations .....	65
Table 2.4: Summary table of one-way ANOVA analysis of gemcitabine concentrations vs control for pancreatic cell lines.....	75
Table 2.6: Summary table of one-way ANOVA analysis of DMF concentrations vs control for pancreatic cell lines.....	79
Table 2.8: Summary table of one-way ANOVA analysis of MMF concentrations vs control for pancreatic cell lines.....	83
Table 2.10: Summary table of one-way ANOVA analysis of radiation doses vs control for pancreatic cell lines.....	86
Table 2.11: Summary table of Kruskal-Wallis test of V/V0 for gemcitabine treated Panc-1 spheroids.....	90
Table 2.12: Summary table of Kruskal-Wallis test of AUC for gemcitabine treated Panc-1 spheroids.....	91
Table 2.13: Summary table of Kruskal-Wallis test of V/V0 for gemcitabine treated Mia PaCa-2 spheroids.....	93
Table 2.14: Summary table of Kruskal-Wallis test of AUC for gemcitabine treated Mia PaCa-2 spheroids.....	94
Table 2.15: Summary table of Kruskal-Wallis test of V/V0 for DMF treated Panc-1 spheroids .....	97
Table 2.16: Summary table of Kruskal-Wallis test of AUC for DMF in Panc-1 spheroids .....	98
Table 2.17: Summary table of Kruskal-Wallis test of DMF treated Mia PaCa-2 spheroids .	100
Table 2.18: Summary table of Kruskal-Wallis test of AUC for DMF treated Mia PaCa-2 spheroids.....	101
Table 2.19: Summary table of Kruskal-Wallis test of V/V0 for MMF treated Panc-1 spheroids .....	103
Table 2.20: Summary table of Kruskal-Wallis test of AUC for MMF treated Panc-1 spheroids .....	104
Table 2.21: Summary table of Kruskal-Wallis test of V/V0 for MMF treated Mia PaCa-2 spheroids.....	106
Table 2.22: Summary table of Kruskal-Wallis test of AUC for MMF treated Mia PaCa-2 spheroids.....	107
Table 2.23: Summary table of Kruskal-Wallis test of V/V0 for EXBR treated Panc-1 spheroids .....	110
Table 2.24: Summary table of Kruskal-Wallis test of AUC for EXBR treated Panc-1 spheroids .....	111
Table 2.25: Summary table of Kruskal-Wallis test of V/V0 for EXBR treated Mia PaCa-2 spheroids.....	113
Table 2.26: Summary table of Kruskal-Wallis test of AUC for EXBR treated Mia PaCa-2 spheroids.....	114

Table 3.1: Statistical comparisons for schedule 1 MMF + EXBR spheroid growth and AUC assay in Panc-1 and Mia PaCa-2.....	137
Table 3.2: Statistical comparisons for schedule 1 MMF + gemcitabine spheroid growth and AUC assay in Panc-1 and Mia PaCa-2.....	143
Table 3.3: Statistical comparisons for schedule 1 MMF + gemcitabine spheroid growth and AUC assay in Panc-1 and Mia PaCa-2.....	149
Table 3.4: Statistical comparisons for schedule 1 gemcitabine + EXBR spheroid growth and AUC assay in Panc-1 and Mia PaCa-2.....	153
Table 3.5: Statistical comparisons for schedule 1 DMF + EXBR spheroid growth and AUC assay in Panc-1 and Mia PaCa-2.....	156
Table 3.6: Summary of the Schedule 1 combinations .....	157
Table 3.7: Statistical comparisons for schedule 2 gemcitabine + EXBR spheroid growth and AUC assay in Panc-1 and Mia PaCa-2.....	167
Table 3.8: Statistical comparisons for schedule 2 DMF + EXBR spheroid growth and AUC assay in Panc-1 and Mia PaCa-2.....	173
Table 3.9: Statistical comparisons for schedule 2 MMF + EXBR spheroid growth and AUC assay in Panc-1 and Mia PaCa-2.....	179
Table 3.10: Summary of the Schedule 2 combinations .....	180
Table 3.11: Statistical comparisons for schedule 3 DMF + gemcitabine spheroid growth and AUC assay in Panc-1 and Mia PaCa-2.....	188
Table 3.12: Statistical comparisons for schedule 3 MMF + gemcitabine spheroid growth and AUC assay in Panc-1 and Mia PaCa-2.....	194
Table 3.14: Summary of the Schedule 3 combinations .....	194
Table 4.1: Statistical comparisons of the distribution of treated Panc-1 cells throughout the cell cycle versus the untreated control zero hours post treatment. Sch = schedule, M = MMF, D = MMF, G = gemcitabine, R = EXBR, ns = not significant. ....	225
Table 4.2: Statistical comparisons of the distribution of treated Panc-1 cells throughout the cell cycle versus monotherapies zero hours post treatment. Sch = schedule, M = MMF, D = MMF, G = gemcitabine, R = EXBR, ns = not significant. ....	226
Table 4.3: Statistical comparisons of the distribution of treated Panc-1 cells throughout the cell cycle versus the untreated control one hour post treatment. Sch = schedule, M = MMF, D = MMF, G = gemcitabine, R = EXBR, ns = not significant. ....	227
Table 4.4: Statistical comparisons of the distribution of treated Panc-1 cells throughout the cell cycle versus monotherapies one hour post treatment. Sch = schedule, M = MMF, D = MMF, G = gemcitabine, R = EXBR, ns = not significant. ....	228
Table 4.5: Statistical comparisons of the distribution of treated Panc-1 cells throughout the cell cycle versus the untreated control four hours post treatment. Sch = schedule, M = MMF, D = MMF, G = gemcitabine, R = EXBR, ns = not significant. ....	229
Table 4.6: Statistical comparisons of the distribution of treated Panc-1 cells throughout the cell cycle versus monotherapies four hours post treatment. Sch = schedule, M = MMF, D = MMF, G = gemcitabine, R = EXBR, ns = not significant. ....	230
Table 4.7: Statistical comparisons of the distribution of treated Panc-1 cells throughout the cell cycle versus the untreated control 24 hours post treatment. Sch = schedule, M = MMF, D = MMF, G = gemcitabine, R = EXBR, ns = not significant. ....	231

Table 4.8: Statistical comparisons of the distribution of treated Panc-1 cells throughout the cell cycle versus monotherapies 24 hours post treatment. Sch = schedule, M = MMF, D = MMF, G = gemcitabine, R = EXBR, ns = not significant. ....	232
Table 4.9: Statistical comparisons of the distribution of treated Panc-1 cells throughout the cell cycle versus the untreated control 36 hours post treatment. Sch = schedule, M = MMF, D = MMF, G = gemcitabine, R = EXBR, ns = not significant. ....	233
Table 4.10: Statistical comparisons of the distribution of treated Panc-1 cells throughout the cell cycle versus monotherapies 36 hours post treatment. Sch = schedule, M = MMF, D = MMF, G = gemcitabine, R = EXBR, ns = not significant. ....	234
Table 4.11: Statistical comparisons of the distribution of treated Mia PaCa-2 cells throughout the cell cycle versus the untreated control zero hours post treatment. Sch = schedule, M = MMF, D = MMF, G = gemcitabine, R = EXBR, ns = not significant. ....	243
Table 4.12: Statistical comparisons of the distribution of treated Mia PaCa-2 cells throughout the cell cycle versus monotherapies zero hours post treatment. Sch = schedule, M = MMF, D = MMF, G = gemcitabine, R = EXBR, ns = not significant. ....	244
Table 4.13: Statistical comparisons of the distribution of treated Mia PaCa-2 cells throughout the cell cycle versus the untreated control one hour post treatment. Sch = schedule, M = MMF, D = MMF, G = gemcitabine, R = EXBR, ns = not significant. ....	245
Table 4.14: Statistical comparisons of the distribution of treated Mia PaCa-2 cells throughout the cell cycle versus monotherapies one hour post treatment. Sch = schedule, M = MMF, D = MMF, G = gemcitabine, R = EXBR, ns = not significant. ....	246
Table 4.15: Statistical comparisons of the distribution of treated Mia PaCa-2 cells throughout the cell cycle versus the untreated control four hours post treatment. Sch = schedule, M = MMF, D = MMF, G = gemcitabine, R = EXBR, ns = not significant. ....	247
Table 4.16: Statistical comparisons of the distribution of treated Mia PaCa-2 cells throughout the cell cycle versus monotherapies four hours post treatment. Sch = schedule, M = MMF, D = MMF, G = gemcitabine, R = EXBR, ns = not significant. ....	248
Table 4.17: Statistical comparisons of the distribution of treated Mia PaCa-2 cells throughout the cell cycle versus the untreated control 24 hours post treatment. Sch = schedule, M = MMF, D = MMF, G = gemcitabine, R = EXBR, ns = not significant. ....	249
Table 4.18: Statistical comparisons of the distribution of treated Mia PaCa-2 cells throughout the cell cycle versus monotherapies 24 hours post treatment. Sch = schedule, M = MMF, D = MMF, G = gemcitabine, R = EXBR, ns = not significant. ....	250
Table 4.19: Statistical comparisons of the distribution of treated Mia PaCa-2 cells throughout the cell cycle versus the untreated control 36 hours post treatment. Sch = schedule, M = MMF, D = MMF, G = gemcitabine, R = EXBR, ns = not significant. ....	251
Table 4.20: Statistical comparisons of the distribution of treated Mia PaCa-2 cells throughout the cell cycle versus monotherapies 36 hours post treatment. Sch = schedule, M = MMF, D = MMF, G = gemcitabine, R = EXBR, ns = not significant. ....	252
Table 4.21: Statistical comparisons of the distribution of apoptotic Panc-1 cells versus the untreated control zero hours post treatment. Sch = schedule, M = MMF, D = MMF, G = gemcitabine, R = EXBR, ns = not significant. ....	260
Table 4.22: Statistical comparisons of the distribution of apoptotic Panc-1 cells versus monotherapies zero hours post treatment. Sch = schedule, M = MMF, D = MMF, G = gemcitabine, R = EXBR, ns = not significant. ....	261

Table 4.23: Statistical comparisons of the distribution of apoptotic Panc-1 cells versus the untreated control one hour post treatment. Sch = schedule, M = MMF, D = MMF, G = gemcitabine, R = EXBR, ns = not significant. ....	262
Table 4.24: Statistical comparisons of the distribution of apoptotic Panc-1 cells versus monotherapies one hour post treatment. Sch = schedule, M = MMF, D = MMF, G = gemcitabine, R = EXBR, ns = not significant. ....	263
Table 4.25: Statistical comparisons of the distribution of apoptotic Panc-1 cells versus the untreated control four hours post treatment. Sch = schedule, M = MMF, D = MMF, G = gemcitabine, R = EXBR, ns = not significant. ....	264
Table 4.26: Statistical comparisons of the distribution of apoptotic Panc-1 cells versus monotherapies four hours post treatment. Sch = schedule, M = MMF, D = MMF, G = gemcitabine, R = EXBR, ns = not significant. ....	265
Table 4.27: Statistical comparisons of the distribution of apoptotic Panc-1 cells versus the untreated control 24 hours post treatment. Sch = schedule, M = MMF, D = MMF, G = gemcitabine, R = EXBR, ns = not significant. ....	266
Table 4.28: Statistical comparisons of the distribution of apoptotic Panc-1 cells versus monotherapies 24 hours post treatment. Sch = schedule, M = MMF, D = MMF, G = gemcitabine, R = EXBR, ns = not significant. ....	267
Table 4.29: Statistical comparisons of the distribution of apoptotic Panc-1 cells versus the untreated control 36 hours post treatment. Sch = schedule, M = MMF, D = MMF, G = gemcitabine, R = EXBR, ns = not significant. ....	268
Table 4.30: Statistical comparisons of the distribution of apoptotic Panc-1 cells versus monotherapies 36 hours post treatment. Sch = schedule, M = MMF, D = MMF, G = gemcitabine, R = EXBR, ns = not significant. ....	269
Table 4.31: Statistical comparisons of the distribution of apoptotic Mia PaCa-2 cells versus the untreated control zero hours post treatment. Sch = schedule, M = MMF, D = MMF, G = gemcitabine, R = EXBR, ns = not significant. ....	276
Table 4.32: Statistical comparisons of the distribution of apoptotic Mia PaCa-2 cells versus monotherapies zero hours post treatment. Sch = schedule, M = MMF, D = MMF, G = gemcitabine, R = EXBR, ns = not significant. ....	277
Table 4.33: Statistical comparisons of the distribution of apoptotic Mia PaCa-2 cells versus the untreated control one hour post treatment. Sch = schedule, M = MMF, D = MMF, G = gemcitabine, R = EXBR, ns = not significant. ....	278
Table 4.34: Statistical comparisons of the distribution of apoptotic Mia PaCa-2 cells versus monotherapies one hour post treatment. Sch = schedule, M = MMF, D = MMF, G = gemcitabine, R = EXBR, ns = not significant. ....	279
Table 4.35: Statistical comparisons of the distribution of apoptotic Mia PaCa-2 cells versus the untreated control four hours post treatment. Sch = schedule, M = MMF, D = MMF, G = gemcitabine, R = EXBR, ns = not significant. ....	280
Table 4.36: Statistical comparisons of the distribution of apoptotic Mia PaCa-2 cells versus monotherapies four hours post treatment. Sch = schedule, M = MMF, D = MMF, G = gemcitabine, R = EXBR, ns = not significant. ....	281
Table 4.37: Statistical comparisons of the distribution of apoptotic Mia PaCa-2 cells versus the untreated control 24 hours post treatment. Sch = schedule, M = MMF, D = MMF, G = gemcitabine, R = EXBR, ns = not significant. ....	282

Table 4.38: Statistical comparisons of the distribution of apoptotic Mia PaCa-2 cells versus monotherapies 24 hours post treatment. Sch = schedule, M = MMF, D = MMF, G = gemcitabine, R = EXBR, ns = not significant. ....	283
Table 4.39: Statistical comparisons of the distribution of apoptotic Mia PaCa-2 cells versus the untreated control 36 hours post treatment. Sch = schedule, M = MMF, D = MMF, G = gemcitabine, R = EXBR, ns = not significant. ....	284
Table 4.40: Statistical comparisons of the distribution of apoptotic Mia PaCa-2 cells versus monotherapies 36 hours post treatment. Sch = schedule, M = MMF, D = MMF, G = gemcitabine, R = EXBR, ns = not significant. ....	285
Table 4.41: Statistical comparisons of DNA damage of treated Panc-1 cells throughout the time course versus the untreated control. Sch = schedule, M = MMF, D = MMF, G = gemcitabine, R = EXBR, ns = not significant. ....	290
Table 4.42: Statistical comparisons of DNA damage of treated Panc-1 cells throughout the time course versus the untreated control. Sch = schedule, M = MMF, D = MMF, G = gemcitabine, R = EXBR, ns = not significant. ....	291
Table 4.43: Statistical comparisons of DNA damage of treated Mia PaCa-2 cells throughout the time course versus the untreated control. Sch = schedule, M = MMF, D = MMF, G = gemcitabine, R = EXBR, ns = not significant. ....	296
Table 4.44: Statistical comparisons of DNA damage of treated Mia PaCa-2 cells throughout the time course versus the untreated control. Sch = schedule, M = MMF, D = MMF, G = gemcitabine, R = EXBR, ns = not significant. ....	297
Table 4.45: Statistical comparisons of glutathione levels in treated Panc-1 cells throughout the time course versus the untreated control. Sch = schedule, M = MMF, D = MMF, G = gemcitabine, R = EXBR, ns = not significant. ....	302
Table 4.46: Statistical comparisons of glutathione levels in treated Panc-1 cells throughout the time course versus the untreated control. Sch = schedule, M = MMF, D = MMF, G = gemcitabine, R = EXBR, ns = not significant. ....	303
Table 4.47: Statistical comparisons of glutathione levels in treated Mia PaCa-2 cells throughout the time course versus the untreated control. Sch = schedule, M = MMF, D = MMF, G = gemcitabine, R = EXBR, ns = not significant. ....	307
Table 4.48: Statistical comparisons of glutathione levels in treated Mia PaCa-2 cells throughout the time course versus the untreated control. Sch = schedule, M = MMF, D = MMF, G = gemcitabine, R = EXBR, ns = not significant. ....	308
Table 4.49: Summary of mechanistic results for combination therapies in Panc-1 cells vs the untreated control.....	310
Table 4.50: Summary of mechanistic results for combination therapies in Mia PaCa-2 cells vs the untreated control .....	311

## CHAPTER 1: Introduction

### **1.1: Cancer Incidence & Mortality**

In humans, cancer is the second highest cause of mortality (1 in 6 deaths), second only to heart disease [1]. In 2020 alone, over 18 million individuals were diagnosed with cancer, with 9.8 million cancer related deaths reported [2, 3]. Incident rates of cancer in the United Kingdom (U.K.) exceeds those in other areas of the world by 90%, with around 375,000 annual cancer diagnoses. Cancer incidence rates are higher in males (51%) compared with females (49%) in the U.K. (and globally), resulting from differences in lifestyle, genetic and hormonal profiles [4, 5]. However, despite the mortality rate of all cancers in the U.K. falling by 10% in the last decade, the global cancer burden is predicted to increase by 47% by the year 2040 [6].

### **1.2: Biology and Hallmarks of Cancer**

Cancer is an invasive disease caused by the accumulation of genetic abnormalities within a cell, leading to abnormal gene expression and uncontrolled proliferation, otherwise known as oncogenesis. Most cancers arise due to mutations in somatic cells, with a minority of rare hereditary cancers being caused by germline mutation [7, 8]. Cancer development is driven by two main types of genes: oncogenes and tumour suppressor genes. Oncogenes are mutated variants of normal cellular genes known as proto-oncogenes, which are responsible for controlling cellular processes such as proliferation, invasion, and survival. In a healthy cell, proto-oncogenes are highly regulated to prevent uncontrolled cell growth, however they are phenotypically dominant, meaning that a single mutated copy is sufficient for oncogenesis to occur. Tumour suppressor genes are normal cellular genes involved with processes such as cell cycle and apoptosis, which inhibit cell proliferation and survival. Tumour suppressor genes are phenotypically recessive, meaning that both copies of the gene must be mutated for oncogenesis to occur [7]. There are thought to be ten distinct hallmarks of cancer that explain the changes that occur in cancer: resisting cell death;

evasion of growth suppressors; sustainment of proliferative signalling; angiogenesis; replicative immortality; genome instability/mutation; tumour promoting inflammation; deregulating cellular metabolism; avoiding immune destruction and activation of invasion and metastasis [9]. As it stands, this work sits within the “resisting cell death” and “deregulating cellular metabolism” hallmarks of cancer, as we aim to develop novel combinations to overcome treatment resistance and the novel drugs we are assessing alter cellular metabolism through modulation of glutathione synthesis.

Cancer is a complex and dynamic disease. Even after the occurrence of the initial malignant transformation within the cell, cancer cells continue to evolve as genomic instability occurs, driving further mutation and destabilisation of cellular processes. As a result, cancers tend to become more heterogeneous over the course of the disease as tumours are composed of molecularly distinct masses of tumour which display differential molecular pathology and therapeutic sensitivity. Tumour heterogeneity can be divided into two categories: intertumoural and intratumoural heterogeneity [10].

Intratumoural heterogeneity is more diverse than intertumoural heterogeneity and can be subdivided into spatial and temporal. Spatial heterogeneity refers to the irregular distribution of genetically distinct tumour subpopulations across a primary tumour and/or multiple metastatic sites of an individual. Spatial heterogeneity is thought to occur due to differences in tumour microenvironments and site-specific stressors that pressure the cells into adapting. Temporal heterogeneity refers to dynamic variations that occur in a single tumour over time as the disease progresses or in response to pressure from therapies [10]. Furthermore, tumour heterogeneity has been implicated in treatment resistance in cancers as different subpopulations of cells have varying degrees of sensitivity to chemo/radiotherapy, enabling a degree of cancer clonogenicity and therefore, continued progression of disease [10].

### **1.3: DNA damage response**

The DNA damage response (DDR) is a critical cellular mechanism that ensures genomic stability by detecting and repairing DNA lesions. This complex network involves multiple signalling pathways and repair mechanisms that address various types of DNA damage, including double-strand breaks, base mismatches, and cross-linking. Key components of the DDR include damage sensors, transducer kinases, and effectors that work together to maintain genome integrity and prevent mutations that can lead to cancer [11, 12].

Cancer development is often linked to defects in the DDR, as these defects can lead to genomic instability and an accumulation of mutations that drive tumorigenesis. When DDR pathways fail or are overwhelmed, cells can undergo uncontrolled proliferation, leading to cancer. Notably, certain cancers exploit DDR deficiencies to their advantage, downregulating specific DNA repair proteins to enhance mutational adaptability and survival [11, 12].

Understanding DDR mechanisms has opened new avenues for cancer therapy. Targeting DDR pathways can make cancer cells more susceptible to treatments that induce DNA damage, such as radiation and chemotherapy. A prime example of this therapeutic strategy is the use of PARP inhibitors in cancers with BRCA1/2 mutations. These inhibitors exploit the concept of synthetic lethality, where cancer cells reliant on compensatory DNA repair pathways are selectively targeted, leading to cell death while sparing normal cells [11, 12].

Moreover, research continues to uncover new components and interactions within the DDR network, which could lead to the development of novel therapeutic agents. For instance, recent advances in structural biology and genomic analysis are enhancing our understanding of DDR mechanisms and identifying potential new targets for drug

development. This ongoing research is crucial for developing more effective cancer therapies and improving patient outcomes [11, 12].

#### **1.4: The Cell Cycle**

The cell cycle is a fundamental process through which cells grow, replicate their DNA, and divide. It consists of several phases: gap one (G1); gap two (G2); DNA synthesis (S) and mitosis (M). Regulation of the cell cycle is tightly controlled by various checkpoints and molecular signals to ensure that cells divide correctly and maintain genetic integrity. As previously mentioned, one of the key driving factors contributing to the development of cancer arises from uncontrolled cell proliferation due to mutations in genes that regulate the cell cycle [13-15].

In G1 phase the cell grows in size and synthesises mRNA and proteins (such as enzymes) that are necessary for DNA synthesis. This phase ensures that the cell is ready to replicate its DNA. In S phase the cell synthesises a complete copy of the DNA in its nucleus [13, 16, 17]. Each chromosome is replicated to form two sister chromatids, which are connected by a centromere. In G2 phase the cell continues to grow and produces proteins necessary for mitosis (cell division). This phase includes additional cell growth and organelle duplication. M phase consists of two processes: mitosis and cytokinesis. Mitosis is the process in which the cell's nucleus and contents divide to create two daughter nuclei, which can be divided into five stages; prophase; prometaphase; metaphase; anaphase; and telophase. In prophase the chromosomes condense and become visible, and the mitotic spindle begins to form. In prometaphase the nuclear envelope breaks down and spindle fibres attach to kinetochores. In metaphase chromosomes line up along the metaphase plate. In anaphase sister chromatids separate and are pulled to opposite poles of the cell. Finally, in telophase the nuclear membranes reform around each set of

chromosomes, which begin to decondense. Cytokinesis is the process in which the cytoplasm of the cell divides, resulting in two separate daughter cells [13, 16, 17].

Cell cycle checkpoints are surveillance mechanisms that monitor and regulate the progression of cells through the cell cycle, ensuring that each phase is properly completed before the next one begins [13, 16, 17]. There are four major cell cycle checkpoints that are crucial for maintaining genomic integrity and preventing uncontrolled cell division. The G1/S checkpoint functions to ensure that the cell is ready for DNA synthesis. The intra-S checkpoint functions to ensure the integrity of DNA is maintained during DNA replication and is activated in response to DNA damage. The G2/M checkpoint ensures that DNA replication is complete and checks for DNA damage before mitosis. Lastly, the spindle assembly checkpoint ensures that all chromosomes are properly attached to the mitotic spindle before anaphase. [13, 16, 17].

The key regulators involved throughout the cell cycle are cyclins and cyclin-dependent kinases (CDKs). Cyclins are proteins whose levels fluctuate depending on the stage of the cell cycle and activate CDKs to exhibit their regulatory effect. CDKs are enzymes that once activated, phosphorylate target proteins to drive the cell cycle forward, with different cyclin-CDK complexes active at each stage of the cell cycle. In G1 phase cyclin D and CDK4/6 level are increased. Whereas in S phase cyclin E/CDK2 and cyclin A/CDK2 are involved in the transition from G1 to S phase. In G2 phase cyclin A/CDK1 levels are increased. In M phase, cyclin B/CDK1 control the transition from G2 to M phase [18-21].

### **1.5: Modes of Cell Death**

There are several mechanisms in which damaged cells can die, including but not limited to: apoptosis, necrosis, autophagy, and ferroptosis. Apoptosis, or programmed cell death, is a tightly regulated and energy-dependent process that

allows cells to die in a controlled manner, which is essential for maintaining the health and stability of multicellular organisms. There are two apoptotic pathways in which cells can undergo programmed cell death: intrinsic and extrinsic [22-25].

The intrinsic, or mitochondrial pathway, is activated by internal signals such as the release of cytochrome c from the mitochondria. The key proteins involved in the intrinsic pathway are Apaf-1 and caspases, with caspase-9 and caspase-3 being the most prevalent. When cytochrome c is released from the mitochondria, Apaf-1 binds to cytochrome c to form the apoptosome. Once formed, the apoptosome activates caspase-9, leading to the activation of additional caspases, including caspase-3, which ultimately leads to cell death [24, 25]. The extrinsic, or death receptor pathway, is activated by external signals binding to death receptors present on the cell surface, such as Fas ligand binding to the Fas receptor. The key proteins involved with the extrinsic pathway are death receptors, adaptor proteins, and caspases, particularly caspase-8 and caspase-3. The binding of ligands to death receptors recruits adaptor proteins to form the death-inducing signalling complex. This complex then activates caspase-8, which in turn activates caspase-3, leading to cell death [22, 23].

Apoptosis is a tightly controlled process, with a balance of pro-apoptotic and anti-apoptotic proteins present to ensure correct activation of apoptosis. Pro-apoptotic proteins, such as Bax, function to promote apoptosis by enabling cytochrome c release from the mitochondria, which enables subsequent caspase activation. Anti-apoptotic proteins, such as Bcl-2, inhibit apoptosis by preventing cytochrome c release and subsequent caspase activation [22, 23]. Another major protein involved in apoptosis is p53, which induces apoptosis in response to DNA damage and other stress signals [22-25].

Unlike apoptosis, necrosis is an uncontrolled form of cell death, that results in the premature death of cells, typically caused by factors external to the cell, such as toxins or trauma. The activation of necrosis leads to the uncontrolled destruction of cell components and the release of harmful substances into the surrounding tissue, which often results in inflammation and scarring. There are several mechanisms in which necrosis can be activated, including mitochondrial dysfunction and rupturing of the plasma membrane [26-28]. Necrosis is associated with the development of cancers and can promote invasion and migration [29].

Autophagy is a cellular degradation and recycling process involving lysosomal degradation that is essential for maintaining cellular homeostasis and regulating cellular metabolism [26, 30, 31]. Key regulators of autophagy include the mechanistic target of rapamycin (mTOR) and AMP-activated protein kinase (AMPK). Under nutrient rich conditions mTOR inhibits autophagy, whereas AMPK activates autophagy under nutrient deprived conditions [26, 30, 31]. Autophagy is initiated in response to various stress signals such as nutrient deprivation; hypoxia; or damaged organelles. Once initiated, a double membrane structure known as the phagophore is formed, which expands and engulfs cytoplasmic material, including damaged organelles; protein aggregates; and pathogens, to form the autophagosome. The mature autophagosome fuses with a lysosome to form the autolysosome, which triggers the degradation of the autolysosome components by lysosomal enzymes. The resulting amino acids, nucleotides, and fatty acids are recycled back into the cytoplasm for reuse in cellular processes [26, 30, 31]. In some cancers, such as pancreatic cancer, autophagy can play a tumour promoting role as cancers can use autophagy as a means of survival when under stress to promote cell growth by recycling damaged cells [26, 30, 31].

Ferroptosis is a distinct form of regulated cell death, characterised by the iron-dependent accumulation of lipid peroxides to lethal levels. Ferroptosis is driven by iron, which catalyses the formation of reactive oxygen species (ROS). Excessive free iron contributes to lipid peroxidation, a process where ROS oxidise polyunsaturated fatty acids (PUFAs) in cellular membranes, resulting in lipid hydroperoxides. Glutathione peroxidase 4 (GPX4) is a critical enzyme that reduces lipid hydroperoxides to non-toxic lipid alcohols using glutathione (GSH) as a substrate. Depletion of GSH or direct inhibition of GPX4 leads to the accumulation of lipid peroxides and the induction of cell death [32-35].

### **1.3: Pancreatic Cancer**

The pancreas is a glandular organ located in the posterior of the abdomen, which is divided into three main sections: head, body, and tail as seen in **figure 1.1**. The pancreas has both exocrine and endocrine functions, with approximately 80% of the pancreas being composed of exocrine tissue [36-38]. Pancreatic acini are responsible for the exocrine function of the pancreas which have the highest protein synthesis rate of any mammalian organ, and are involved in the secretion of digestive enzymes, such as amylase and lipase, which aid in the digestion of foods [37, 38]. The endocrine function of the pancreas is carried out by cells within the islets of Langerhans, which secrete the hormones pro-insulin and glucagon, that are involved in carbohydrate metabolism [36, 37]. Originating from pancreatic duct epithelia, pancreatic ductal adenocarcinoma (PDAC) is a highly aggressive exocrine malignancy accounting for over 90% of pancreatic cancer cases, with 70% of cases arising in the head of the pancreas [39]. Tumours within the head of the pancreas are associated with a better prognosis than tumours originating in the body or tail. Although rare, malignancy of the endocrine portion of the pancreas, known as pancreatic neuroendocrine tumours, can also occur but are associated with a better

prognosis than exocrine tumours [39, 40]. As PDAC is the most prevalent subtype of pancreatic tumour, PDAC will be referred to as pancreatic cancer going forward. The symptoms of pancreatic cancer are often non-specific, including abdominal pain; jaundice; back pain; and weight loss, which are often wrongly attributed to alternative benign causes. The symptoms experienced by patients can depend on the origin of the tumour within the pancreas, with jaundice resulting from biliary obstruction being more prevalent in tumours of the head of the pancreas. However, tumours of the pancreas body tend to invade surrounding tissues and structures, which manifests as back pain, while tumours of the tail tend to be asymptomatic until the disease has metastasised [41, 42].

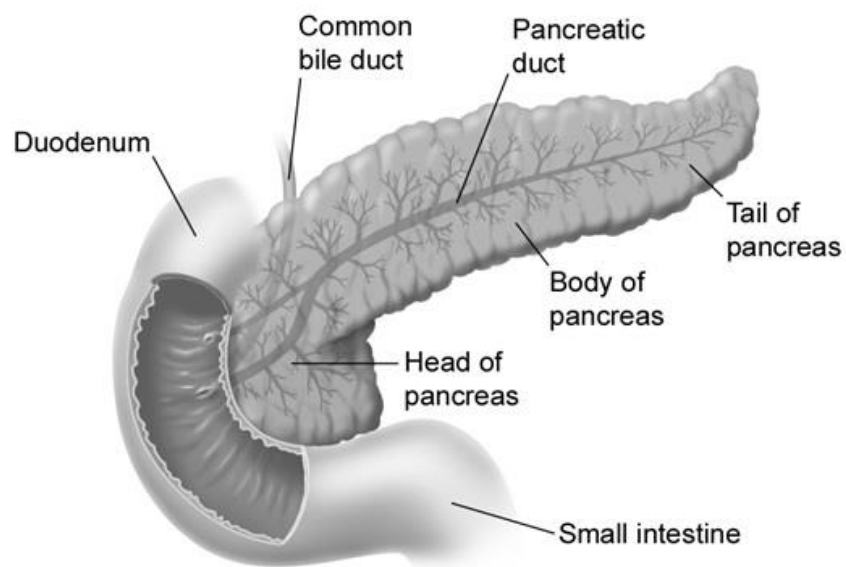


**Figure 1.1: Anatomy of the Pancreas.** Illustration of the pancreas and some of the surrounding organs and tissues. The pancreas is divided into three main areas: the head, body, and tail. The most common form of pancreatic cancer originates in the epithelium of the pancreatic duct. Adapted from: Bliss, 2001 [43].

#### **1.4: Pancreatic Cancer Incidence**

Pancreatic cancer is the 12<sup>th</sup> most common cancer globally, with over 495,000 new cases diagnosed in 2022, with a higher documented incidence in males compared with females [2, 44]. In the U.K., pancreatic cancer is the 10<sup>th</sup> most common cancer, accounting for approximately 3% of annual cancer diagnoses, with people over the age of 75 accounting for 47% of all pancreatic cancer cases diagnosed [41]. The incidence rate of pancreatic cancer has risen by 9% in the U.K. within the last decade and is predicted to increase by a further 6% by the year 2035. The main risk factor for pancreatic cancer is age, however, obesity, smoking, chronic pancreatitis, and diabetes (more prevalent in type 2) have also been linked to disease occurrence [41, 45, 46].

#### **1.5: Diagnosis and Staging of Pancreatic Cancer**

Pancreatic tumours can be divided into five grades: Tis; T1; T2; T3; and T4, and a summary of tumour grades can be found in **table 1.1**. The initial diagnosis of pancreatic cancers is typically performed through a computed tomography (CT) scan, with endoscopic ultrasound and magnetic resonance imaging (MRI) being performed for further investigation [41, 42, 47-49]. As the most common symptoms of pancreatic cancer, including but not limited to abdominal pain and jaundice, are often unspecific, the disease is often diagnosed in its advanced stages. Such symptoms have led to over 80% of all cases being diagnosed in the advanced stages, highlighting the difficulty in achieving early diagnosis for better patient outcomes [45]. Pancreatic tumours are defined in accordance with the tumour, node, metastasis (TNM) staging system, which is based on tumour grade (T), if the tumour has spread to the lymph nodes (N) and if the tumour has metastasised (M). There are seven TNM stages of pancreatic cancer: 0; IA; IB; IIA; IIB; III; and IV [48, 49]. A summary of the stages can be found in **table 1.2**. Stages 0 and IA pancreatic cancer are considered early stage

and are localised to the pancreas. Whereas stages IIB and III pancreatic cancer are considered locally advanced, with the tumour spreading to nearby tissues and possibly into the lymph nodes. Stage IV pancreatic cancer is considered advanced stage tumours with distant metastases and invasion into the lymph nodes. Pancreatic cancer can also be classified as localised; regional; or distant. Localised tumours are those that have not spread outside the pancreas, regional are those that have spread from the pancreas to nearby tissues or lymph nodes and distant are tumours that have metastasised [50].

**Table 1.1: Pancreatic cancer tumour grades.**

<u>Tumour Grade</u>	<u>Description</u>
Tis	Early-stage tumour
T1	≤ 2 cm in length, localised to pancreas
T2	> 2 cm in length, localised to pancreas
T3	> 4 cm in length, extended beyond the pancreas
T4	Metastasised

**Table 1.2: Pancreatic cancer tumour staging.**

<u>Stage</u>	<u>Tumour Grade</u>	<u>Lymph Node Invasion (+/-)</u>	<u>Distant Metastases (+/-)</u>
0	Tis	-	-
IA	T1	-	-
IB	T2	-	-
IIA	T3	-	-
IIB	T1/T2/T3	+	-
III	T4	+/-	-
IV	T1/T2/T3/T4	+/-	+

### **1.6: Pancreatic Cancer Mortality**

Pancreatic cancer is one of the most lethal cancers and is the 7<sup>th</sup> leading cause of cancer related deaths globally [51]. The mortality rate of pancreatic cancer increases with age, with the majority of deaths occurring in individuals over 80 years old. In the U.K. the mortality rate has risen by approximately 5.5% between 1990 and 2019, showing that the disease burden continues to steadily grow [51].

### **1.7: Pancreatic Cancer Survival Rates**

The net survival rates for pancreatic cancer in England between the years 2013 - 2017 are: 25.4% one-year post diagnosis; 7.3% five years post diagnosis; and 5% ten years post diagnosis [52]. A graph depicting these statistics is displayed in **figure 1.2A**. The survival rate for pancreatic cancer is largely dependent on the stage in which the cancer is diagnosed, with earlier diagnosis having a more favourable outcome. In America the five-year survival rates for pancreatic cancer stage are as follows: localised 43.9%; regional 14.7%; and distant 3.1% [53]. However, most cases globally are diagnosed in the distant stage of the disease. Between 2013 to 2017 in the U.K. 67.6% of cases were diagnosed in the distant stage. As shown in **figure 1.2B**, between the years 2012 – 2014, New Zealand had the highest rate (67.4%) of distant stage pancreatic cancer; however, the overall global average for distant stage pancreatic cancer diagnosis was 65.5%, highlighting the global issue of late-stage diagnosis of pancreatic cancer and emphasising the need for improved early detection methods and awareness [54].

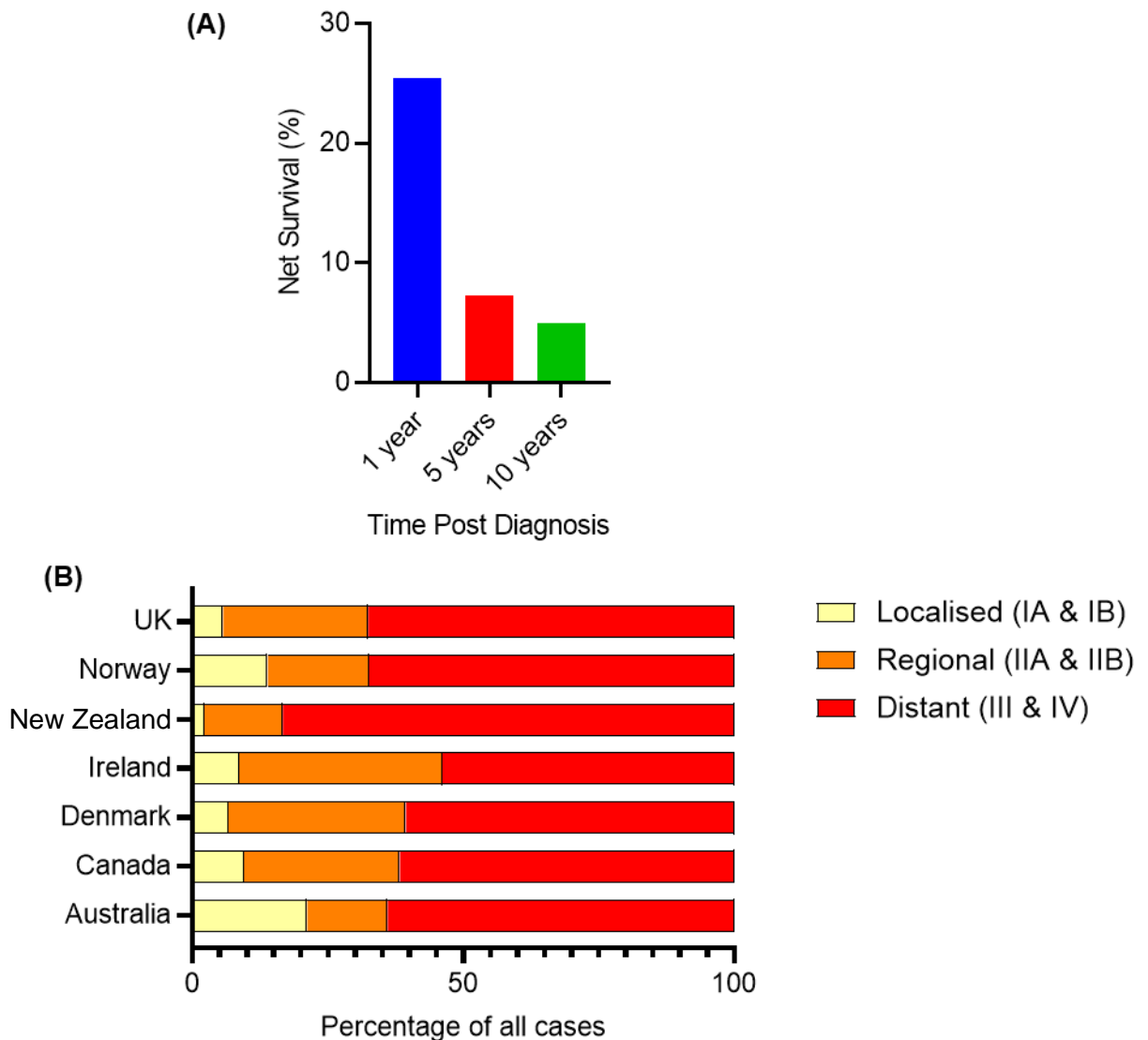


**Figure 1.2: Pancreatic Cancer Incidence & Survival Rates.** The survival rates and diagnosis rates are displayed (A) The net survival rates for patients in England between 2013 - 2017 are displayed. Data adapted from Cancer Research UK – data accessed 8<sup>th</sup> January 2024. (B) The percentage of cases diagnosed in each stage of the disease in various countries around the world between 2012 - 2014 is displayed. Data adapted from International Agency for Research on Cancer [54] – data accessed 8<sup>th</sup> January 2024.

### **1.8: Molecular Characteristics of Pancreatic Cancer**

The tumour mutation profile in pancreatic cancer is highly diverse, however a well-defined set of prevalent driver mutations has been established, including, but not limited to mutations in the following genes: cyclin-dependent kinase 2A (*CDKN2A*); Kirsten rat sarcoma viral oncogene homolog (*KRAS*); and tumour protein 53 (*TP53*). The most commonly occurring mutation in pancreatic cancer is inactivation of *CDKN2A*, which occurs in 95% of cases, resulting in the loss of the cell cycle regulatory protein p16, and increased cell proliferation. The next most prevalent mutation is the activation of *KRAS*, which occurs in 90% of pancreatic cancers, which is responsible for the production of the protein K-Ras, causing activation of downstream signalling pathways, leading to cell cycle progression and increased cell survival/invasion. Inactivation of *TP53* occurs in 70% of pancreatic cancers, resulting in evasion of apoptotic signals and DNA repair checkpoints [41, 42, 48, 49, 55, 56]. A summary of the frequency of gene mutations in pancreatic cancer can be found in **table 1.3**.

**Table 1.3: Mutation Frequency in Pancreatic Cancer.**

<u>Gene</u>	<u>Type</u>	<u>Main signalling/system</u>	<u>Mutation frequency (approximate %)</u>
<i>CDKN2A</i>	Tumour Suppressor	Cell cycle	95%
<i>KRAS</i>	Proto-oncogene	Ras/Raf/MAPK	90%
<i>TP53</i>	Tumour Suppressor	Apoptosis/DNA repair/Cell cycle	70%
<i>HER2</i>	Proto-oncogene	Cell cycle	70%
<i>FHIT</i>	Tumour Suppressor	Apoptosis/DNA repair	70%
<i>SMAD4</i>	Tumour Suppressor	TGF $\beta$	50%
<i>CDKN2B</i>	Tumour Suppressor	Cell cycle	48%
<i>AKT2</i>	Proto-oncogene	Cell cycle/glucose metabolism	20%
<i>APC</i>	Tumour Suppressor	Wnt	16%
<i>MYB</i>	Proto-oncogene	Haematopoiesis	10%
<i>RB1</i>	Tumour Suppressor	Cell cycle	10%
<i>PIK3CA</i>	Proto-oncogene	PTEN/PI3K/AKT	5%
<i>STK11</i>	Tumour Suppressor	AMPK	5%
<i>CTNNB1</i>	Proto-oncogene	Wnt	4%
<i>MAP2K4</i>	Tumour Suppressor	MAPK	4%
<i>MLH1</i>	Tumour Suppressor	DNA repair	3%
<i>BRCA2</i>	Tumour Suppressor	DNA repair	2%
<i>ALK5</i>	Tumour Suppressor	TGF $\beta$	1%

### **1.9: Pancreatic Cancer Treatment**

Pancreatic cancers in the earlier stages of the disease - stages IA, IB, and IIA - are typically considered resectable, although resection may be attempted in later stages where the tumour is deemed borderline resectable, depending on the surgeon/patient [50, 57]. Surgical resection is considered the only curative treatment for pancreatic cancer, however due to late diagnosis and tumour location, only 15 – 20% of patients are eligible for resection [58]. Furthermore, despite surgery being the only curative treatment, the patient prognosis following surgical resection is poor, with frequent complications, high morbidity rate, recurrence (~90%), and a median survival rate

between 12 to 19 months [58-62]. Even with a successful curative resection, 71% of patients have disease recurrence [58]. In addition to surgical intervention patients with resectable tumours may undergo adjuvant or neoadjuvant chemotherapy [63-65]. Adjuvant chemotherapy has been shown to increase the five-year survival rate of patients from 10% with surgery alone to 20 – 25% [66], whilst the benefit of neoadjuvant chemotherapy remains under investigation in clinical trials [62, 64, 65].

In the case of patients with unresectable tumours in advanced disease stages (IIB, III, and IV), chemotherapy is the main treatment strategy. The role and schedule of the chemotherapy is dependent on whether the disease is locally advanced (stages IIB & III) or metastatic (stage IV) [41, 42, 57].

In locally advanced pancreatic cancer, the disease may be borderline resectable, but the majority of patients do not have the opportunity to undergo surgery. Surgical limitations owe to the aggressive nature of the disease progression, or invasion of the disease into the major vasculature in close proximity to the pancreas [67, 68]. For patients with unresectable tumours chemotherapy and chemoradiation are the two most commonly administered treatment modalities [67]. Chemotherapy for locally advanced pancreatic cancer consists of several treatment options: including gemcitabine plus oxaliplatin; gemcitabine plus nab-paclitaxel; folinic acid, fluorouracil, irinotecan, and oxaliplatin (FOLFIRINOX); or gemcitabine monotherapy, depending on disease progression and patient fitness [67, 69].

Radiotherapy may also be administered simultaneously with chemotherapy (chemoradiotherapy) to patients with locally advanced pancreatic cancer. However, the role of radiotherapy in the treatment of pancreatic cancer remains debated due to the limitations represented by the poor radiotolerance of the organs surrounding the pancreas - mainly the stomach; duodenum; and bowel - and the minimal patient benefit which is often observed clinically [70-72]. Standard fractionated radiotherapy

may be given along with chemotherapy in a dose ranging from 40 – 60 Gy in 1.8 – 2 Gy fractions, however limited benefit to median patient survival of approximately two months, has been observed clinically [71]. An emerging radiotherapeutic technique for locally advanced pancreatic cancer is stereotactic body radiation therapy (SBRT), otherwise known as stereotactic ablative radiotherapy (SABR), which delivers fewer yet higher doses of radiation to the target area when compared with conventional fractionated radiotherapy [73]. The efficacy of SBRT in the treatment of pancreatic cancer is still under assessment, as there are contrasting reports of SBRT efficacy in the literature which may be due to differences in delivery and dosimetry methodologies. However, the majority of studies reported increased quality of patient life, with lower toxicity, pain relief and improved overall survival when compared with conventional fractionated radiotherapy [70, 71, 74-76].

For patients with metastatic pancreatic cancer, treatment options are limited and are solely based on patient performance status, which is defined as the ability to carry out daily living activities unassisted. In patients with a poor performance status, treatment is typically palliative to help reduce the symptoms, but in some cases gemcitabine monotherapy may be administered. In contrast, patients with a good performance status may also receive gemcitabine monotherapy or combination therapies such as the FOLFIRINOX regimen or gemcitabine plus nab-paclitaxel. The average median overall survival is approximately 6.2 months for patients with metastatic disease who undergo gemcitabine monotherapy; 11.1 months for FOLFIRINOX; and 8.5 months for gemcitabine plus nab-paclitaxel [77]. However, these combination therapies are associated with higher rates of adverse side effects when compared with gemcitabine monotherapy [77].

### **1.10: Radiobiology**

Radiotherapy uses ionising radiation, such as X-rays, which are absorbed by water within tissues to induce cell damage. The majority of damage induced by ionising radiation is indirect, resulting from the interaction between tissue absorbed radiation and water molecules, known as the Compton effect (or Compton scatter). The Compton effect refers to the process in which rapidly moving photons interact with slow moving free electrons, causing photons to lose energy and electrons to gain energy [78]. The accelerated movement of electrons can cause direct damage to cells by cleaving DNA bonds and indirect damage through the subsequent generation of free radicals. Free radicals are highly reactive unstable atoms which are produced by ionisation of other molecules which can inflict further damage on the cell. In this case the resulting free radicals are caused by the ionisation (or radiolysis) of water, resulting in hydroxyl ( $\text{OH}^\cdot$ ) and hydrogen ( $\text{H}^\cdot$ ) radicals. The hydroxyl radical is the most reactive and toxic radical produced, as it causes oxidative damage to DNA, resulting in both single- and double-strand breaks (SSBs, DSBs) [78-80].

The most common type of radiotherapy is external beam radiotherapy (EXBR), which delivers a targeted beam of radiation to a specific area of the body to minimise damage to the surrounding tissues. EXBR is typically administered to patients by a medical linear accelerator (LINAC), which delivers high energy X-rays to the target area [81]. The full dose of radiation required for treatment is not delivered at once but is preferentially divided into several smaller doses known as fractions which are delivered daily over numerous weeks. Fractionated radiotherapy is used to allow the healthy cells in the body to recover between doses of radiation, to minimise side effects [81]. Standard fractionated radiotherapy doses are in the range of 1.8 – 2 Gy up to a total dose of 40 – 60 Gy. The typical side effects of radiotherapy include tiredness, weakness, sore skin, and loss of hair in the treatment area [81].

### **1.11: Gemcitabine**

Since its introduction in 1997, gemcitabine, also known as 2',2'-difluoro-2'-deoxycytidine (dFdC), has been a first line therapeutic drug for the treatment of pancreatic cancer and is still commonly used as a monotherapy or in combination with other chemotherapeutic drugs [82, 83]. Gemcitabine is a deoxycytidine nucleoside analogue, which ultimately integrates into DNA in place of cytosine and blocks DNA synthesis, leading to DNA breaks and inhibition of repair. Additionally, gemcitabine activates tumour protein 53 (p53), leading to gap one phase (G1) and DNA synthesis (S) phase cell cycle arrest and apoptosis [84]. Uptake of gemcitabine into the cell is dependent on a variety of human nucleoside transporters, which are a group of membrane transport proteins that are responsible for the transport of nucleoside substrates across the cell membrane [83]. Once in the cell, gemcitabine is phosphorylated into gemcitabine monophosphate (dFdCMP) by deoxycytidine kinase (dCK) and subsequent phosphorylation by monophosphate kinase (NMPK) and nucleoside diphosphate kinase (NDPK) results in the formation of the active metabolite gemcitabine triphosphate (dFdCTP) [83]. Gemcitabine triphosphate actively competes with the NTP deoxycytidine triphosphate (dCTP) for incorporation into DNA. Once incorporated into the DNA gemcitabine triphosphate causes premature termination of the growing DNA chain during DNA synthesis, inducing replication stress and the formation of stalled replication forks, signalling DNA damage to the cell [83]. The formation of stalled replication forks leads to the formation of DSBs, which the cell is ultimately unable to repair. A second mechanism in which DNA damage is induced by gemcitabine is caused by the second metabolite, gemcitabine diphosphate, which inhibits the enzyme ribonucleoside reductase, which is responsible for the formation of nucleoside triphosphates (NTPs), which are the molecular precursors of DNA [83]. Ribonucleoside reductase inhibition results in a depletion of dCTP and allows gemcitabine triphosphate to be more readily

incorporated into the DNA in place of dCTP, causing the inhibition of DNA synthesis as previously mentioned [83]. An overview of this mechanism of action can be found in **figure 1.3**. The DNA damage and replication stress caused by gemcitabine activate the DNA damage response pathways. Key proteins in these pathways, such as ATR (ataxia telangiectasia and Rad3-related protein) and Chk1 (checkpoint kinase 1), detect the stalled replication forks and initiate signalling cascades to halt the cell cycle (G1/S phase arrest) and attempt DNA repair [83, 85, 86]. However, in the presence of extensive DNA damage induced by gemcitabine, these repair mechanisms are often overwhelmed, leading to the activation of apoptosis pathways to eliminate the damaged cells [85, 86]. Key regulators like p53, a tumour suppressor protein, are upregulated in response to DNA damage. p53 activation promotes the transcription of pro-apoptotic genes, leading to programmed cell death [85-87]. This is a critical mechanism by which gemcitabine exerts its cytotoxic effects on cancer cells.

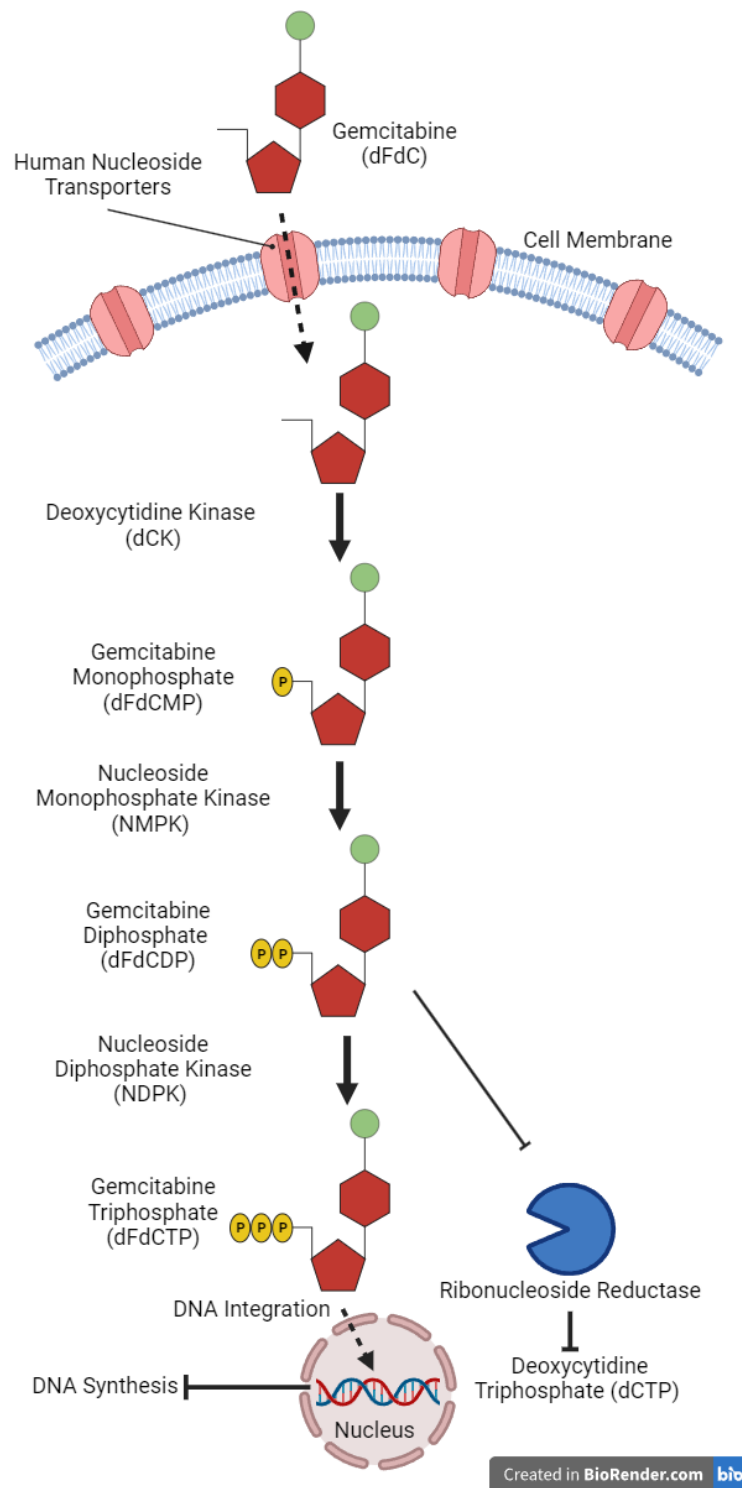


**Figure 1.3: Gemcitabine Mechanism of Action.** An overview of the mechanism of action for gemcitabine is displayed. Briefly, gemcitabine is transported into the cell via nucleoside transporters and undergoes phosphorylation to become the active metabolite gemcitabine triphosphate, which inhibits the production of nucleosides and allows its incorporation into the DNA of the cell, ultimately leading to the inhibition of DNA synthesis and induction of apoptosis.

### **1.12: Chemoresistance in Pancreatic Cancer**

Despite being the first line therapy for advanced and metastatic pancreatic cancers, resistance to gemcitabine occurs frequently in patients, with less than 20% of patients showing a response to gemcitabine [88]. The therapeutic efficacy of gemcitabine is severely limited by both intrinsic and acquired resistance, leading to treatment failure and the recurrence of disease in patients [89].

Intrinsic resistance refers to naturally occurring resistance within the patient that renders the chemotherapy ineffective from the start of treatment, which can be attributed to patient genetic factors and the tumour microenvironment [89]. One intrinsic resistance factor and hallmark of pancreatic cancer is the development of a dense fibrous scar tissue, known as desmoplasia, that surrounds the malignant epithelial cells. Desmoplasia can account for up to 90% of the total tumour volume and forms a physical barrier which prevents drug delivery, resulting in treatment failure [89, 90].

In addition to physical barriers hindering drug delivery, there are several molecular resistance mechanisms which present therapeutic limitations. The main molecular intrinsic resistance mechanism identified in pancreatic cancer is the upregulation of the transcription factor nuclear factor- $\kappa$ B (NF- $\kappa$ B). NF- $\kappa$ B regulates multiple aspects of the innate and adaptive immune response, as well as the inflammatory response [91]. Activation of NF- $\kappa$ B in pancreatic cancer suppresses apoptosis, allowing the cancer cells to evade programmed cell death [90]. In contrast to innate chemoresistance, acquired resistance typically occurs after repeated exposure to chemotherapy, resulting in the upregulation of anti-apoptotic genes such as B-cell lymphoma 2 (Bcl-2) and inhibitors of apoptosis (IAP) proteins [92].

### **1.13: Drug Repurposing**

Drug development is a highly time and money intensive process, with an average development process taking 17 years and \$2.6 billion to develop from molecule to market. Of all drug development initiatives, a mere 2.01% of drug compounds successfully make it to market [93]. Therefore, with these high cost and time investments, it makes drug repurposing, the name given to the process of using an already developed drug to treat diseases alternative to its initial purpose, a very lucrative option [93]. Repurposing drugs is hugely beneficial as the safety assessment and formulation of the drug is previously known due to the clinical trial process, allowing for an accelerated development time and reduced costs by approximately \$300 million [93].

Examples of previously repurposed drugs include duloxetine, which was originally developed for the treatment of depression and in treating urinary incontinence. A prime example of drug repurposing is the use of thalidomide, originally developed with the intention of treating nausea in pregnant women, which is now used for the treatment of cancers such as multiple myeloma [93, 94].

### **1.14: Fumaric acid & Glutathione Metabolism**

Fumaric acid is a critical intermediate involved in the tricarboxylic acid (TCA) cycle, which is a central metabolic pathway that generates energy, adenosine triphosphate (ATP), through the oxidation of acetyl-CoA. Fumaric acid is hydrated by the enzyme fumarase to form malate, which is subsequently oxidised into oxaloacetate, allowing the TCA cycle to renew. Additionally, the conversion of fumaric acid to malate is involved in the production of NADH and FADH<sub>2</sub>, which are essential electron carriers used in the production of ATP [95, 96].

The TCA cycle is also linked to glutathione (GSH) metabolism, as the TCA cycle aids in the production of NADPH. GSH is a ubiquitous tripeptide consisting of cysteine,

glycine, and glutamic acid, which plays a critical role in the antioxidant response. During the antioxidant response, GSH forms adducts with, and neutralises oxidants by acting as a reducing agent and following this, GSH is then oxidised to glutathione disulphide (GSSG) [97]. The ratio of GSH to GSSG is dependent on the exposure of cells to oxidative stress, with cells under normal conditions having a GSH:GSSG ratio of 100:1, yet comparatively, cells exposed to oxidative stress have a 10:1 ratio of GSH:GSSG [97]. NADPH is required by the enzyme glutathione reductase to convert GSSG to GSH, thus preserving the cellular redox state and protecting the cell against oxidative damage.

#### **1.14: Dimethyl Fumarate**

As previously mentioned, fumaric acid is an important intermediate involved in the TCA cycle, which is responsible for the production of energy in the formation of ATP within the mitochondria of the cell [98]. Fumarates, esters of fumaric acid, have shown to have immunomodulating, antioxidative and anti-inflammatory properties [98]. One such fumarate, dimethyl fumarate (DMF), is an oral disease modifying treatment used in the treatment of relapsing-remitting multiple sclerosis (RRMS) and psoriasis [99]. DMF was approved in 2013 for use in the United States (U.S.) by the U.S. Food and Drug Administration (FDA) for the treatment of RRMS in adults, and subsequently approved for use in the U.K. in 2014 by the National Institute for Health and Care Excellence (NICE) under the trade name Tecfidera®, which in the U.S. it is the most prescribed drug for RRMS [99-101]. In 2017 DMF was approved in the European Union and U.K. by the European Medicines Agency (EMA) and NICE respectively, for the treatment of moderate to severe plaque psoriasis in adults under the trade name Skilarence® but has yet to be approved in the U.S. [101-103].

As DMF is an approved drug used in various medical applications, the pharmacokinetics and safety profile of DMF have previously been thoroughly

characterised following oral administration. Once in the gastrointestinal (GI) tract, DMF is hydrolysed by esterases into monomethyl fumarate (MMF) and methanol in a 1:1 ratio [104]. An overview of this process is shown in **figure 1.4**. MMF is the active metabolite of the prodrug DMF, which exerts the desired therapeutic effect it exhibits, and methanol is converted into formic acid by alcohol dehydrogenases [104, 105]. The most commonly reported side effects of DMF are flushing (redness of skin), abdominal pain, nausea, and diarrhoea [100, 101, 103]. The production of methanol and subsequent formic acid is thought to be the main driving factor of the GI symptoms experienced by some patients following DMF administration [104]. Less commonly, some patients will develop mild lymphopenia (reduced white blood cell levels) after starting DMF treatment, and it has been observed clinically that this risk increases with the age of the patient [100, 101, 103, 105-107]. According to the literature, DMF can reportedly exhibit a degree of cytotoxicity to specific types of immune cells, particularly helper T and natural killer cells, which is thought to contribute to the lymphopenia observed in some cases [107, 108].

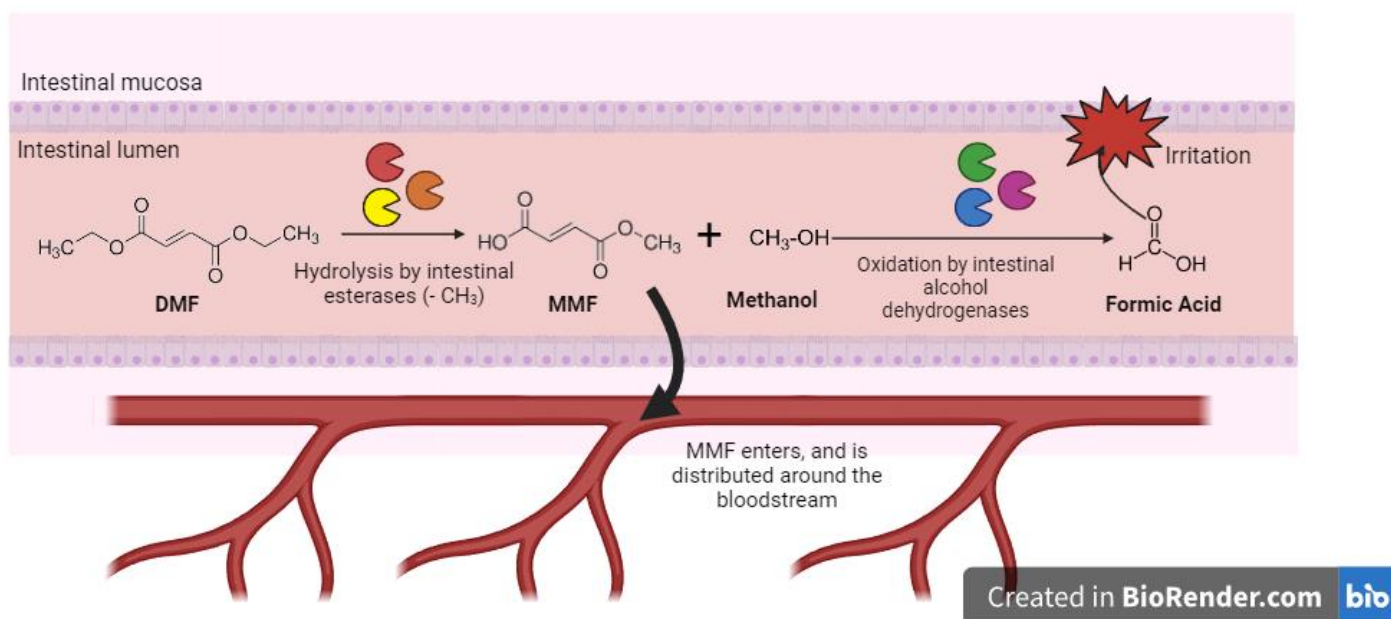


**Figure 1.4: DMF Metabolism.** An overview of the metabolism of DMF into MMF is displayed in the figure. Once in the small intestine DMF is hydrolysed by intestinal esterases to become MMF (the active metabolite) and methanol. MMF is absorbed into the bloodstream and distributed around the body. Methanol is metabolised into formic acid, which is thought to be responsible for the adverse gastrointestinal symptoms experienced by patients.

### **1.15: Dimethyl Fumarate and Cancer**

Recent studies have shown that DMF has anti-cancer properties, in cancers such as melanoma [109, 110], ovarian [111, 112], lung [113], colon [114] and breast [115], making it a promising candidate for the development of new combination therapies to treat cancer. Further highlighting this, in 2015 DMF in combination with temozolomide (TMZ) and standard radiotherapy was tested in a phase 1 clinical trial (NCT02337426) for the treatment of glioblastoma. The results published from this clinical trial indicate that no unexpected toxicities were observed and that DMF may be safely combined with the current therapies, but that a further phase 2 study would be necessary to determine if the effect on patient survival is meaningful [116]. Additionally, it has been reported in the literature that DMF has no significant cytotoxic effect on non-cancerous cells [112], again highlighting its potential as an anti-cancer drug.

The specific mechanism of action in which DMF elicits its anti-cancer activity is currently poorly understood, however several cellular targets of DMF have been identified [117]. The modulation of nuclear factor erythroid 2-related factor 2 (NRF2) activity is thought to be a key factor in the anti-cancer properties of DMF, and interestingly, NRF2 activity has been implemented in driving pancreatic cancer progression [118].

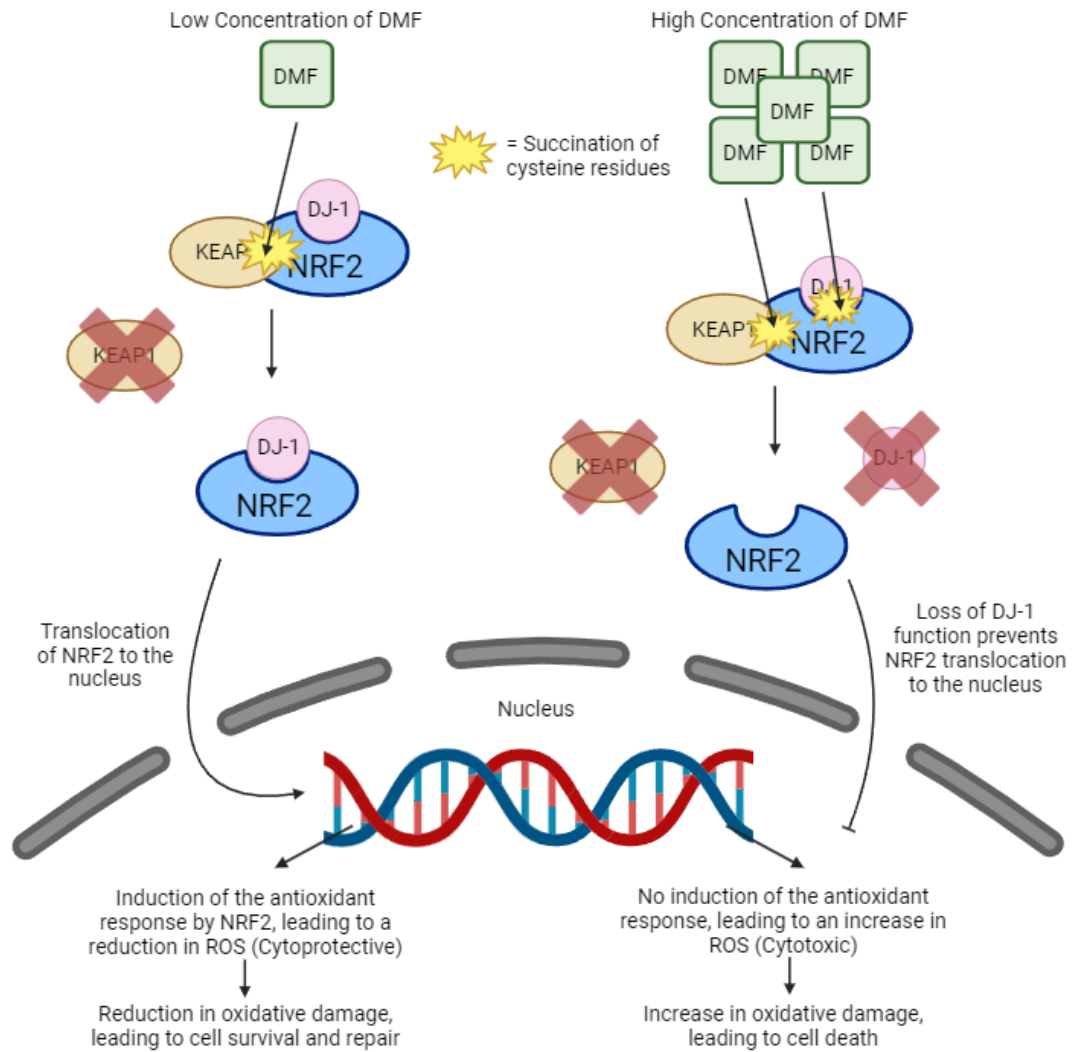
NRF2 is a ubiquitously expressed transcription factor and considered a “master redox switch” due to its control of the expression of numerous (> 200) cytoprotective genes involved in the antioxidant response [117]. One key pathway activated by NRF2 is the glutathione pathway, which is known to play a major role in tumorigenesis [119]. Under the control of NRF2 is glutamate-cysteine ligase and glutathione synthetase, both of which are key enzymes involved in glutathione regulation. Glutamate-cysteine ligase is responsible for the first step in glutathione synthesis, where it ligates cysteine and glutamic acid to form the intermediate molecule  $\gamma$ -glutamylcysteine [120].

Glutathione synthetase is the enzyme responsible for catalysing the condensation of  $\gamma$ -glutamylcysteine and glycine to form glutathione [121]. NRF2 is therefore deeply involved in glutathione metabolism by promoting the synthesis of glutathione in response to ROS [120, 121].

Under basal conditions NRF2 is held within the cytoplasm in an inactive complex with the repressor protein Kelch-like ECH-associated protein 1 (KEAP1), which is also responsible for NRF2 ubiquitination [111]. When the cell is under stress due to reactive oxygen species (ROS) or electrophiles, such as hydrogen radicals resulting from radiolysis of water following radiotherapy, the NRF2-KEAP1 complex is disrupted, allowing NRF2 to translocate to the nucleus, where it can upregulate the expression of genes involved in the antioxidant response [111, 117].

DMF modulates NRF2 activity in a concentration dependent manner, with lower doses of  $<10 \mu\text{M}$  activating NRF2, and higher doses of  $>25 \mu\text{M}$  having a cytotoxic effect via inhibition of NRF2 [111]. An overview of this mechanism is displayed in **figure 1.5**. At low concentrations DMF activates NRF2 by targeting cysteine residues of KEAP1 which causes conformational changes in the protein, resulting in the disruption of the NRF2-KEAP1 complex. Such disruption allows for the translocation of NRF2 to the nucleus, and subsequent activation of genes involved in the antioxidant response, protecting the cell from ROS induced damage [111]. However, at higher concentrations, DMF has an additional target called protein deglycase (DJ-1). DJ-1 is a regulator of NRF2 activity as it promotes the dissociation of the NRF2-KEAP1 complex, thus enabling NRF2 activity [111]. At high concentrations, DMF targets the cysteine 106 residue of NRF2, which binds DJ-1, resulting in the dissociation and loss of DJ-1 activity. Translocation of NRF2 to the nucleus is therefore prevented, with a subsequent upregulation of the antioxidant response, which leaves the cell vulnerable to ROS [111, 117]. The concentration dependant manner in which DMF works in

cancers highlights the need to evaluate the drug at varying concentrations, which could lead to issues in translating the drug clinically as a standard fixed dose may be unachievable. Therefore, through its modulation of NRF2, DMF has a direct impact on glutathione synthesis as it inhibits NRF2 translocation, preventing transcription of the key enzymes involved in glutathione synthesis.



Created in [BioRender.com](https://BioRender.com)

**Figure 1.5: DMF Mechanism of Action.** An overview of the proposed anti-cancer mechanism of action for DMF is displayed. At low concentrations (<math><10\ \mu\text{M}</math>) DMF activates NRF2 activity, leading to the upregulation of antioxidant genes, ultimately leading to cell survival. At high concentrations (>math>>25\ \mu\text{M}</math>) DMF inhibits NRF2 activity, leading to an increase in ROS, and ultimately cell death.

### **1.16: Monomethyl Fumarate**

As previously stated, MMF is the highly bioavailable active metabolite of DMF and is currently only FDA approved (in 2020) for use in the treatment of RRMS in adults in the U.S., under the trade name Bafiertam® [101, 122]. Until recently it was debated in literature whether or not MMF was responsible for the therapeutic action displayed after administration of the prodrug DMF, however it is now widely accepted that MMF is the active metabolite and functions mechanistically like DMF [122, 123]. The main differences between DMF and MMF are in its solubility and half-life, with DMF being reported as ten times more soluble in biological fluids than MMF [104]. DMF has a half-life of approximately 12 minutes inside the body, whereas MMF is 30 minutes, as MMF is less susceptible to hydrolysis by esterases in the small intestine [122-125]. In clinic, MMF has been observed causing fewer GI side effects compared with DMF [126].

### **1.17: Glutathione and Pancreatic Cancer**

Glutathione (GSH) plays a critical role in the antioxidant response, in which it neutralises oxidants to protect the cell from oxidative damage. Recent studies have reported that the downregulation/inhibition of glutathione synthesis enhances chemotherapeutic efficacy in pancreatic cancer [127, 128]. Further highlighting the importance of GSH and pancreatic cancer progression is that GSH is essential for the functionality and maintenance of pancreatic cancer stem cells [129].

Therefore, due to the promotion of GSH production by NRF2 activity, DMF/MMF has been deemed a promising candidate for the treatment of pancreatic cancer due to NRF2 inhibition by DMF/MMF activity, thus resulting in a decrease in GSH, in conjunction with chemo- and radiosensitisation of pancreatic cancer cells.

### **1.18: Aims**

The aims of this research were to investigate the efficacy of the repurposed drugs DMF and MMF as chemotherapeutic agents against pancreatic cancer cells, and to develop novel combination therapies involving these drugs.

Given that the only currently viable treatment option for the majority of pancreatic cancer patients is chemotherapy due to late diagnosis, the limited range and poor performance of current chemotherapies highlights pancreatic cancer as a cancer of unmet clinical need, emphasising the need for new and alternative therapies.

Although not fully elucidated at present, the known mechanism of action of DMF/MMF with regards to NRF2, is a promising target for pancreatic cancer as this pathway is essential to all cells, including cancerous ones, meaning the chances of resistance developing are low. The efficacy of NRF2 inhibitors DMF and MMF will be investigated in both 2D and 3D cell models, and novel combination therapies involving administration of DMF/MMF in conjunction with the current gold standard chemotherapeutic agent gemcitabine, as well as with radiotherapy.

It is hypothesised that DMF/MMF will sensitise the pancreatic cancer cells to both gemcitabine and radiotherapy through modulation of NRF2 activity, resulting in a reduced antioxidant response, such as lowered production of glutathione, allowing ROS generated by both gemcitabine and radiotherapy to induce DNA damage, and ultimately cancer cell death.

**CHAPTER 2: Evaluation of the cytotoxic effect of single  
therapeutic agents and EXBR on pancreatic cancer cell  
survival in 2D & 3D cell models**

## **2.1: INTRODUCTION**

Gemcitabine is a standard treatment for pancreatic cancer, particularly in the advanced stages of the disease, however despite its widespread use the efficacy of gemcitabine is limited. As a monotherapy, gemcitabine only provides limited improvement to overall survival rates (approximately 6 – 7 months) when compared with supportive care [86, 130-136]. The main obstacles to gemcitabine therapy are resistance (intrinsic and acquired), toxicity, and challenges in drug delivery. Over 80% of patients with pancreatic cancer have intrinsic resistance and are unresponsive to gemcitabine therapy [88]. Other patients will develop resistance over time with repeated exposure to gemcitabine through the upregulation of multiple mechanisms, such as the upregulation of cytidine deaminase, the enzyme responsible for inactivating gemcitabine. Gemcitabine is a highly cytotoxic drug, with severe hematologic toxicity which can lead to side effects such as neutropenia and thrombocytopenia, which can limit the dose and usage. Delivering gemcitabine to the tumour site remains a challenge as the dense desmoplasia surrounding the tumour prevents drug penetration, which leads to suboptimal concentrations of gemcitabine at the tumour site, decreasing the therapeutic efficacy [86, 130-136]. Therefore, as gemcitabine therapy faces several significant challenges, we aimed to evaluate the efficacy of DMF and MMF as novel therapeutic agents for the treatment for pancreatic cancer in the hopes of finding a treatment that may overcome some of the limitations faced by gemcitabine monotherapy by combining DMF/MMF with other agents in combination.

Before combining DMF/MMF in combination, the single agent activity first had to be established. To evaluate the efficacy of the fumarates (DMF and MMF) as novel therapeutic agents for the treatment of pancreatic cancer, the cytotoxic effects were examined in both 2D and 3D cell models in Panc-1 and Mia PaCa-2 cell lines, along

with the current therapies for pancreatic cancer, gemcitabine, and external beam radiotherapy (EXBR). The drugs were assessed in a 2D cell model via the clonogenic assay (**section 2.3.4**), and the results used to develop novel combinations for evaluation in further studies (**Chapter 3**). To assess DMF and MMF in a 3D cell model, a spheroid growth delay assay was used (**section 2.3.6**).

Panc-1 and Mia PaCa-2 cell lines were chosen as these cell lines are two of the most extensively used PDAC cell lines in literature, which would allow our work to build upon that which is already published [39]. Panc-1 originated from a pancreatic head tumour from a 56-year-old male, where duodenal wall invasion was observed. Mia PaCa-2 originated from a pancreatic body and tail tumour from a 65-year-old male with periaortic infiltration [137]. In comparison with Mia PaCa-2, Panc-1 has a higher affinity for adhesion to extracellular proteins, such as, type I collagen, fibronectin and collagen type IV [137]. Additionally, the two cell lines have alternate KRAS and TP53 mutation [137].

The clonogenic assay is a useful means of determining the cytotoxicity of an agent *in vitro*, as it tests the clonogenicity (ability of a single cell to undergo 'infinite' cell division and form a colony) of each cell within a given population, which in turn can determine the cytotoxic effect of a treatment when compared with an untreated control [138]. However, the clonogenic assay involves the culture of cells in a 2D monolayer, which inadequately emulates the conditions of a 3D tumour microenvironment *in vivo* as cell monolayers lack the heterogeneity and hypoxic regions found within real tumours [139]. Therefore, DMF and MMF were also tested in a 3D spheroid cell model which more accurately reflects the 3D tumour microenvironment, as spheroids consist of an outer layer of actively proliferating cells, an internal quiescent (dormant) zone caused by the limited distribution of nutrients and oxygen, and finally a necrotic core comprising of hypoxic, apoptotic, and necrotic cells [139, 140]. To assess the cytotoxic

effect of the drugs on the spheroids, the growth of the spheroids was monitored for 2 – 3 weeks to allow for the change in volume to be calculated.

This is the first stage in our assay cascade that allows us to establish the cytotoxicity of the single agents to allow us to better design combination therapies using these agents. Additionally, the agents were tested in both 2D and 3D models as a means of further validating the efficacy of these agents, as spheroids more accurately represent the conditions of a tumour *in vivo* when compared with a 2D monolayer. We use the clonogenic assay first to establish a dose range for future experiments.

## **2.2: AIMS**

The aims of this chapter were therefore to establish the growth characteristics of both Mia PaCa-2 and Panc-1 and determine the cytotoxicity of DMF, MMF, gemcitabine and external beam radiation *in vitro* using both 2D and 3D models. Additionally, the effect of exposure time on drug cytotoxicity was investigated in 2D culture.

## **2.3: MATERIALS AND METHODS**

### **2.3.1: Cell Lines and Culture Conditions**

The cell lines Panc-1 (ATCC CRL-1469) and Mia PaCa-2 (ATCC CRL-1420) were utilised for these studies. Both cell lines originate from epithelial cells of pancreatic ductal adenocarcinoma (PDAC). Cells were cultured with Dulbecco's modified Eagle medium (DMEM) (Thermo Fisher Scientific, Perth, UK) supplemented with 584 mg/L L-Glutamine (Thermo Fisher Scientific, Perth, UK), 10% Fetal Bovine Serum (FBS) (Thermo Fisher Scientific, Perth, UK), 50 U/mL Penicillin, 50 mg/mL Streptomycin (Thermo Fisher Scientific, Perth, UK), 250 µg/mL Amphotericin B (Sigma Aldrich, Irvine, UK), 110 mg/L Sodium pyruvate (Thermo Fisher Scientific, Perth, UK) and 4.5 g/L D-Glucose (Thermo Fisher Scientific, Perth, UK).

Cells were cultured in a 5% CO<sub>2</sub> humidified 37°C incubator to approximately 70% confluency before use or passage. To passage, cells were washed with 5 mL of 1X phosphate-buffered saline (PBS) (Thermo Fisher Scientific, Perth, UK) and incubated with 3 mL of 1X 0.05% trypsin-EDTA solution (Thermo Fisher Scientific, Perth, UK) for cell detachment before subculturing in vented T-75 flasks (Fisher Scientific, Renfrew, UK) containing 15 mL of complete DMEM media.

Cell stocks were prepared by suspending approximately 1×10<sup>6</sup> cells in 1 mL of complete media containing 10% DMSO (Sigma Aldrich, Irvine, UK) and 10% FBS within a cryovial (Starlab, Milton Keynes, UK) before freezing at -80°C. If a fresh batch of cells was required, a frozen vial was thawed at 37°C and added to a T-25 flask (Helena Biosciences, Sunderland, UK) containing 5 mL of complete DMEM media, then incubated at 37°C with 5% CO<sub>2</sub>. Following incubation, cells were detached from the flask surface using 1X 0.05% trypsin-EDTA solution once cells were approximately 70% confluent and added to a T-75 flask containing 15 mL of complete DMEM media to allow further growth.

### **2.3.2: Treatments**

The following drugs were purchased from Sigma Aldrich (Irvine, UK) and used to treat cells: gemcitabine, DMF, and MMF. From the powdered drugs, 100 mM stock solutions were prepared using the appropriate solvent and sterilised using a 0.2 µm filter (Sigma Aldrich, Irvine, UK) to a final volume of 10 mL, as shown in **table 2.1**. Working dilutions were prepared using the stock solutions by diluting with 1X PBS to a final concentration of 500 µM (50 µL of 100 mM drug diluted in 9.95 mL 1X PBS).

**Table 2.1: Preparation of Drug Stocks.**

Drug	Molecular Weight (g/mol)	Mass (mg)	Solvent Volume (mL)	Solvent	Concentration (mM)
Gemcitabine	299.66	299.66	10	PBS	100
DMF	144.127	144.127	10	DMSO	100
MMF	130.1	130.1	10	DMSO	100

From the 500  $\mu\text{M}$  working dilutions, the desired concentrations of each drug for cell treatment were prepared using complete DMEM media for dilution in the concentration ranges displayed in **table 2.2**.

**Table 2.2: Treatment Concentrations.**

Assay Type	DMF Concentrations ( $\mu\text{M}$ )	MMF Concentrations ( $\mu\text{M}$ )	Gemcitabine Concentrations ( $\mu\text{M}$ )
Clonogenic	0 - 100	0 - 10	0 - 10
Spheroid	0 - 100	0 - 10	0 - 10

Table displays the concentrations of drugs used in clonogenic and spheroid growth delay assays

### **2.3.3: Cell Doubling Time Assay**

To calculate the doubling time of Panc-1 and Mia PaCa-2 during the exponential growth phase,  $1 \times 10^5$  cells were seeded in T-25 flasks. Following 24 hours of growth cells were washed with 5 mL of 1X PBS and then detached by the addition of 2mL of 1X 0.05% trypsin-EDTA solution, then neutralised with 5 mL of complete DMEM media to create a cell suspension with a final volume of 7 mL. The resulting cell suspension was passed through a 23-gauge needle (Becton, Dickinson and Company, Plymouth, UK) to create a single cell suspension that could be counted on a haemocytometer (Scientific Laboratory Supplies, Nottingham, UK) to determine the total number of cells present. This process was repeated every subsequent 24 hours for a total of 5 days. The doubling time of Panc-1 and Mia PaCa-2 cell lines were mathematically determined via a modified (Y0 constraint set to 100,000) exponential

growth equation using GraphPad Prism version 10.1.2. Each doubling time assay was carried out in three biological repeats, with three technical repeats per biological repeat.

#### **2.3.4: Clonogenic Assay**

Prior to carrying out the clonogenic assay, the plating efficiency had to be established for both Panc-1 and Mia PaCa-2 to determine the optimal number of cells to seed for the clonogenic assay. To achieve this, cells were plated in 5 mL of complete media in 60 mm petri dishes (with three technical repeats per biological repeat in triplicate) at various densities from 500 – 2000 cells. Following 14 days of incubation to allow the development of visible colonies (> 50 cells in size), media was removed, and dishes washed with PBS. To fix cell colonies, the dishes were incubated with 100% methanol at room temperature for 10 minutes. To stain the colonies, dishes were incubated with 5% (v/v) Giemsa's solution (VWR, Leicestershire, UK) for 30 minutes. Colonies were counted by eye to determine the plating efficiency using the following equation:

$$\text{Plating efficiency: } \frac{\text{Number of colonies}}{\text{Number of cells seeded}}$$

To carry out the clonogenic assay, cells were seeded in T-25 flasks at a density of  $2 \times 10^5$  cells per flask and incubated until 70% confluent. Following incubation, media was removed and replaced with 1.5 mL of complete media containing the desired concentration of drug (**section 2.3.2**) or irradiated with 2 – 10 Gy EXBR using the X-Rad225 irradiator (Precision X-Ray, Connecticut, USA) at a dose rate of 2.3 Gy/min. Cells were incubated for a further 24 or 48 hours, depending on the experimental requirement, before removing the treatment and washing the cells with 5 mL of 1X PBS to remove any residual drug. Cells were then detached with 2mL of 1X 0.05% trypsin-EDTA solution which was neutralised by the addition of 5 mL of complete DMEM media to create a cell suspension. The resulting suspension was then passed

through a 23-gauge needle to create a single cell suspension which could be counted using a haemocytometer. The volume of cell suspension required to collect 500 cells was then determined and added to individual 60 mm petri dishes (Thermo Fisher Scientific, Perth, UK) in triplicate. The 60 mm petri dishes were then incubated for approximately 14 days to allow for the visible development of colonies over 50 cells in size. Following incubation, media was removed, and dishes washed with PBS. To fix cell colonies, the dishes were incubated with 100% methanol at room temperature for 10 minutes. To stain the colonies, dishes were incubated with 5% (v/v) Giemsa's solution (VWR, Leicestershire, UK) for 30 minutes. Colonies were counted by eye to determine the survival fraction using the following equation:

$$\text{Survival Fraction: } \frac{\text{Number of colonies in treated sample/number of cells seeded}}{\text{Number of control colonies/number of cells seeded}}$$

Each treatment was therefore compared to the plating efficiency of the untreated control. Each clonogenic assay was carried out in three biological repeats, with three technical repeats per biological repeat.

IC<sub>50</sub> values were determined using Hill-slope equation on GraphPad Prism version 10.1.2. For irradiated cells, D<sub>50</sub> values were determined using linear quadratic model on GraphPad Prism version 10.1.2

### **2.3.5: Preparation of Low Attachment 96-well Plates for Spheroid Growth Delay Assay**

Non-tissue culture treated round bottom 96-well plates were purchased from Fisher Scientific (Leicestershire, UK) and a poly (2-hydroxyethyl methacrylate) (poly-HEMA) coating solution was prepared as follows: 1.2 g of poly-HEMA (Sigma Aldrich, Irvine, UK) was dissolved in 40 mL of 95% ethanol (Fisher Scientific, Leicestershire, UK) and the resulting solution was incubated on a tube roller (Starlab, Milton Keynes, UK) at 37°C until the poly-HEMA was fully dissolved. To coat the round bottom 96-well

plates, 50  $\mu\text{L}$  of poly-HEMA coating solution was added to each individual well of the plate(s) and incubated in a biological safety cabinet with the plate lid removed until the solution had fully evaporated, leaving behind the coating to prevent cell attachment.

### **2.3.6: Spheroid Growth Delay Assay**

Cells were plated in low attachment round bottom 96-well plates (**section 2.3.5**) at a density of 700 cells per well. Each well was made up to a final volume of 200  $\mu\text{L}$  using complete DMEM media. The surrounding wells of the plate were filled with 200  $\mu\text{L}$  of 1X PBS to help hydrate the wells containing cells and to minimise the edge effect. Following 48 hours of growth, media was removed and replaced with 200  $\mu\text{L}$  of complete DMEM media containing drug (**section 2.3.2**) at the desired concentration or plates were irradiated with 0.5 – 6 Gy at a dose rate of 2.3 Gy/min, using the X-Rad225 irradiator, then incubated for 48 hours. Following incubation, the media containing the treatment was removed and the spheroids washed with 200  $\mu\text{L}$  of 1X PBS before the addition of 200  $\mu\text{L}$  of complete DMEM media. The media was then subsequently refreshed every 2 – 3 days with 50  $\mu\text{L}$  of fresh media for a total of 14 - 21 days. Spheroids were imaged every 2 – 3 days to monitor growth using the EVOS FL auto system (Life Technologies, Paisley, UK), with images being captured using the brightfield 4X objective. Each spheroid growth delay assay was carried out in three biological repeats, with sixteen technical repeats per biological repeat.

### **2.3.7: Spheroid Growth Analysis**

Spheroid images captured using the EVOS FL auto system were analysed using SpheroidSizer software [141] for MATLAB (version R2013a). Spheroid volumes were determined by the software using the following equation, with  $D_{\text{max}}$  representing the maximum diameter and  $D_{\text{min}}$  representing the minimum diameter of the spheroid:

$$\text{Spheroid Volume: } 0.5 (D_{\text{max}} \times (D_{\text{min}}^2))$$

The change in spheroid volume ( $V/V_0$ ) was then calculated for each time point by dividing the volume ( $V$ ) of each individual spheroid at the desired timepoint by its initial volume ( $V_0$ ). The area under the curve (AUC) for each treatment was then calculated using GraphPad Prism version 10.1.2.

### **2.3.8: Statistical Analysis**

All statistical analysis was carried out using GraphPad Prism version 10.1.2. Significance was assigned at an alpha ( $\alpha$ ) value  $\leq 0.05$ . Prior to carrying out any analysis on data, a Shapiro-Wilk normality test was used to determine if the data conformed to normal distribution (parametric or nonparametric), to allow for the selection of an appropriate statistical test. If the data was parametric, a one-way ANOVA with Bonferroni post hoc test was used. If the data was nonparametric, a Kruskal-Wallis with Dunn's post hoc test was used. The following labelling was used to convey significance: ns = not significant; \* =  $P \leq 0.05$ ; \*\* =  $P \leq 0.01$ , \*\*\* =  $P \leq 0.001$ ; and \*\*\*\* =  $P \leq 0.0001$ .

## **2.4: RESULTS**

### **2.4.1: Growth characteristics of pancreatic cells *in vitro***

To establish the doubling time of both Panc-1 and Mia PaCa-2, a doubling time assay was carried out as described in **section 2.3.3**. The doubling time is the time taken for a complete cell cycle, and subsequently the population of cells to double in number and the results shown in **figure 2.1**.

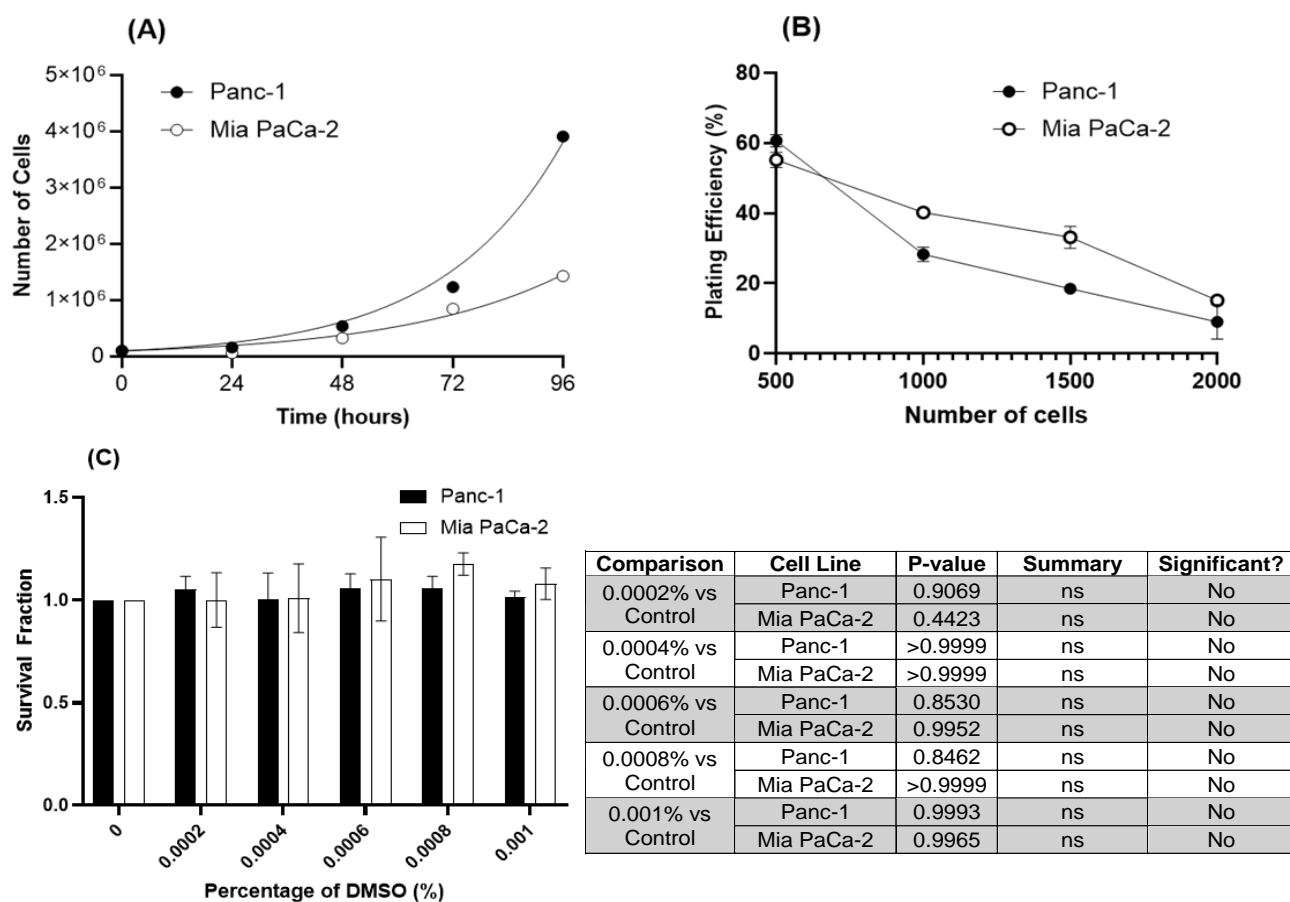


**Figure 2.1: Panc-1 and Mia PaCa-2 growth characteristics.** (A) Cell doubling time assay, the data represented as the average of three independent experiments carried out in triplicate  $\pm$  standard deviation (the error bars are too small to be shown). (B) Plating efficiency was calculated for varying numbers of cells. The data represented as the average of three independent experiments carried out in triplicate  $\pm$  standard deviation (some error bars are too small to be shown). (C) Clonogenic assay to determine pancreatic cancer cell response to DMSO concentrations equivalent to percentages present in treatments with DMF/MMF as these drugs are initially solubilised in DMSO prior to subsequent dilution in PBS and finally media (some error bars are too small to be shown). Table shows statistical comparisons using one-way ANOVA with Bonferroni post hoc test of DMSO treated cells with the untreated controls (0% DMSO) for both Panc-1 and Mia PaCa-2.

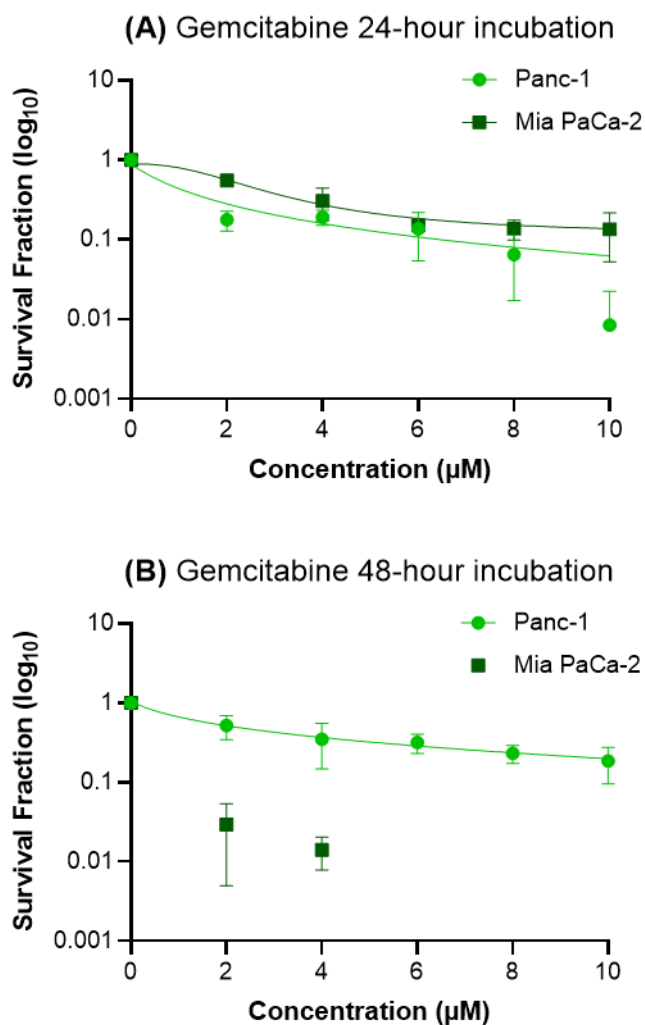
The doubling time of Panc-1 and Mia PaCa-2 cell lines were mathematically determined via a modified (Y0 constraint set to 100,000) exponential growth equation using GraphPad Prism version 10.1.2. Panc-1 was calculated to have a doubling time of  $18.27 \pm 0.02$  hours (**figure 2.1A**). Mia PaCa-2 was calculated to have a doubling time of  $24.82 \pm 0.5$  hours (**figure 2.1A**). Based on these results, a 24-hour incubation period would be sufficient to allow for one cell cycle, and 48 hours for two cell cycles in both Panc-1 and Mia PaCa-2, when exposing cells to drugs.

The optimal seeding density for Panc-1 and Mia PaCa-2 was determined to be 500 cells following the plating efficiency as this number of cells gave a plating efficiency value of >50% (**figure 2.1B**). Going forward 500 cells would be plated for the clonogenic assay.

To determine if the small percentage of DMSO present in DMF/MMF treatments would have a statistically significant effect on cell clonogenicity, cells were exposed to a range of DMSO concentrations equivalent to that present in treatments utilised (**figure 2.1C**). As can be seen in **figure 2.1C** all concentrations of DMSO tested did not statistically significantly vary from that of the untreated (0% DMSO) control, indicating that at the concentrations used the DMSO has no effect on cell clonogenicity in both cell lines ( $P > 0.442$ ). Therefore, a DMSO control was not included going forward and instead an untreated control used.

#### **2.4.2: Cytotoxic effect of gemcitabine on pancreatic cell clonogenicity *in vitro***

The clonogenic assay was carried out as described in **section 2.3.4** to assess the cytotoxicity of gemcitabine on pancreatic cells *in vitro*. Cells were incubated with gemcitabine for both 24- and 48-hours to determine if increasing the exposure time of the drug to the cells had any effect on cytotoxicity. The half-maximal inhibitory concentration (IC<sub>50</sub>) was then determined using GraphPad Prism version 10.1.2 and the results shown in **figure 2.2**.



Cell Line	Gemcitabine IC <sub>50</sub> with 24-hour incubation	Gemcitabine IC <sub>50</sub> with 48-hour incubation
Panc-1	1.021 ± 0.12 µM	2.002 ± 1.63 µM
Mia PaCa-2	2.271 ± 1.4 µM	N/A

**Figure 2.2: Cytotoxic effect of gemcitabine on Panc-1 and Mia PaCa-2.** Cells were exposed to varying concentrations (2 µM – 10 µM) of gemcitabine and the survival fraction determined. (A) Cytotoxic effect of gemcitabine following 24-hour incubation. (B) Cytotoxic effect of gemcitabine following 48-hour incubation. All data is represented as the average of three independent experiments carried out in triplicate ± standard deviation. No curve could be fit for Mia PaCa-2 at this time point.

In both cell lines and incubation periods, gemcitabine induced a dose dependent reduction in clonogenic survival. In Panc-1, after exposure of cells to gemcitabine for 24-hours (**figure 2.2A**), the highest concentration (10  $\mu$ M) of gemcitabine induced an average reduction in clonogenicity of  $99.16 \pm 1.38\%$  and, only  $81.48 \pm 8.9\%$  reduction in clonogenicity was induced with a 48-hour incubation (**figure 2.2B**). In Mia PaCa-2, the highest concentration of gemcitabine (10  $\mu$ M) induced an average reduction in clonogenicity of  $86.54 \pm 8.18\%$  following a 24-hour incubation (**figure 2.2A**), and 100% reduction in clonogenicity following a 48-hour incubation with gemcitabine (**figure 2.2B**). There was no statistically significant difference in clonogenicity ( $P = 0.0684$ ) between 24- and 48-hour incubations with gemcitabine for Panc-1, whereas there was a statistically significant decrease in clonogenicity between 24- and 48-hour incubations with gemcitabine in the Mia PaCa-2 cell line ( $P = 0.011$ ). There was no statistically significant difference in clonogenicity between Panc-1 and Mia PaCa-2 following a 24-hour incubation with gemcitabine ( $P = 0.6281$ ). However, there was a statistically significant difference in clonogenicity between Panc-1 and Mia PaCa-2 following a 48-hour incubation with gemcitabine, with more reduction in clonogenicity being induced in Mia PaCa-2 ( $P = 0.0004$ ).

The  $IC_{50}$  value for gemcitabine in Panc-1 following 24-hour incubation was calculated to be  $1.021 \pm 1.4 \mu$ M and  $2.022 \pm 1.63 \mu$ M for 48-hour incubation. The  $IC_{50}$  value for gemcitabine in Mia PaCa-2 following 24-hour incubation was calculated to be  $2.271 \pm 0.12 \mu$ M. As three of the concentrations tested (6 – 8  $\mu$ M) resulted in no surviving cells, an  $IC_{50}$  value could not be calculated for gemcitabine following a 48-hour incubation in Mia PaCa-2, nor could a curve be fit (**figure 2.2B**).

As the data conformed to normal distribution, according to the Shapiro-Wilk normality test, one-way ANOVA with Bonferroni post hoc test was used to assess the cytotoxic effect of the various concentrations of gemcitabine when compared with the untreated

control. A summary of this analysis can be found in **table 2.4**. In Panc-1 cells, all concentrations of gemcitabine tested (**figure 2.2**) induced significant reduction in clonogenicity when compared with the untreated control for both incubation periods ( $P < 0.0001$ ). In Mia PaCa-2, all concentrations of gemcitabine tested (**figure 2.2**) also induced significant reduction in clonogenicity when compared with the untreated control for both incubation periods ( $P < 0.0001$ ).

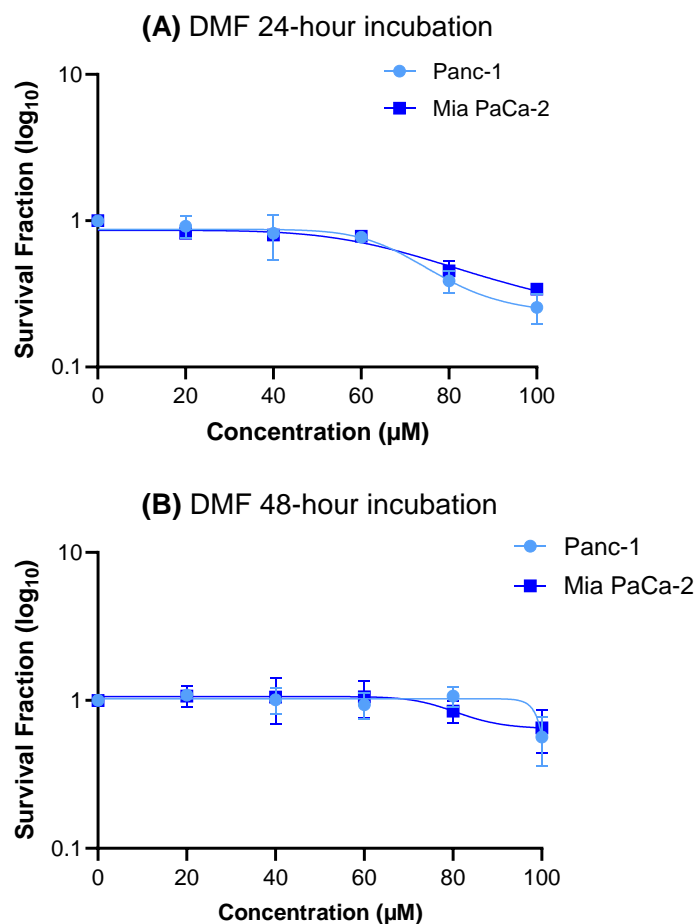
**Table 2.4: Summary table of one-way ANOVA analysis of gemcitabine concentrations vs control for pancreatic cell lines.**

Comparison	Cell Line	Incubation	P-value	Summary	Significant?
2 $\mu$ M vs Control	Panc-1	24 hrs	<0.0001	****	Yes
		48 hrs	<0.0001	****	Yes
4 $\mu$ M vs Control	Panc-1	24 hrs	<0.0001	****	Yes
		48 hrs	<0.0001	****	Yes
6 $\mu$ M vs Control	Panc-1	24 hrs	<0.0001	****	Yes
		48 hrs	<0.0001	****	Yes
8 $\mu$ M vs Control	Panc-1	24 hrs	<0.0001	****	Yes
		48 hrs	<0.0001	****	Yes
10 $\mu$ M vs Control	Panc-1	24 hrs	<0.0001	****	Yes
		48 hrs	<0.0001	****	Yes
2 $\mu$ M vs Control	Mia PaCa-2	24 hrs	<0.0001	****	Yes
		48 hrs	<0.0001	****	Yes
4 $\mu$ M vs Control	Mia PaCa-2	24 hrs	<0.0001	****	Yes
		48 hrs	<0.0001	****	Yes
6 $\mu$ M vs Control	Mia PaCa-2	24 hrs	<0.0001	****	Yes
		48 hrs	<0.0001	****	Yes
8 $\mu$ M vs Control	Mia PaCa-2	24 hrs	<0.0001	****	Yes
		48 hrs	<0.0001	****	Yes
10 $\mu$ M vs Control	Mia PaCa-2	24 hrs	<0.0001	****	Yes
		48 hrs	<0.0001	****	Yes

Overall, the results in **section 2.4.2** indicate that both cell lines are sensitive to gemcitabine as expected as this is the current gold standard chemotherapy for pancreatic cancer. Furthermore, the incubation period with gemcitabine significantly influences drug effectiveness in Mia PaCa-2 only, as can be seen by the  $IC_{50}$  values displayed in **table 2.3**.

#### **2.4.3: Cytotoxic effect of DMF on pancreatic cell clonogenicity *in vitro***

The clonogenic assay was carried out as described in **section 2.3.4** to assess the cytotoxicity of DMF on pancreatic cells *in vitro*. Cells were incubated with DMF (20 – 100  $\mu$ M) for both 24- and 48-hours to determine if increasing the exposure time had any effect on cytotoxicity. The results of this experiment are shown in **figure 2.3**.



Cell Line	DMF IC <sub>50</sub> with 24-hour incubation	DMF IC <sub>50</sub> with 48-hour incubation
Panc-1	71.22 ± 5.87 µM	104.5 ± 41.47 µM
Mia PaCa-2	76.73 ± 2.17 µM	79.79 ± 17.82 µM

**Figure 2.3: Cytotoxic effect of DMF on Panc-1 and Mia PaCa-2.** Cells were exposed to varying concentrations (20 µM – 100 µM) of DMF and the survival fraction determined. (A) Cytotoxic effect of DMF following 24-hour incubation. (B) Cytotoxic effect of DMF following 48-hour incubation. All data is represented as the average of three independent experiments carried out in triplicate ± standard deviation.

In both cell lines and incubation periods, DMF induced a dose dependent reduction in clonogenicity. In Panc-1, following a 24-hour incubation period with DMF (**figure 2.3A**), the highest concentration (100  $\mu$ M) of DMF induced an average reduction in clonogenicity of  $74.44 \pm 5.92\%$ , and only  $43.35 \pm 20.4\%$  reduction in clonogenicity was induced with a 48-hour incubation (**figure 2.3B**), with the 24-hour incubation period inducing significantly more reduction in clonogenicity when compared with the 48-hour incubation in Panc-1 cells ( $P = 0.0006$ ). In Mia PaCa-2, the highest concentration of DMF (100  $\mu$ M) induced an average reduction in clonogenicity of  $65.95 \pm 2.15\%$  with a 24-hour incubation (**figure 2.3A**), and only  $34.82\% \pm 20.92\%$  reduction in clonogenicity following a 48-hour incubation (**figure 2.3B**), with the 24-hour incubation period inducing significantly more reduction in clonogenicity when compared with the 48-hour incubation in Mia PaCa-2 cells ( $P = 0.0009$ ). There was no statistically significant difference in clonogenicity induced by DMF between Panc-1 and Mia PaCa-2 following both 24- and 48-hour incubations with DMF ( $P > 0.9999$ ).

The  $IC_{50}$  value for DMF in Panc-1 cells following 24-hour incubation was calculated to be  $71.22 \pm 5.87 \mu$ M, and  $104.5 \pm 41.47 \mu$ M following a 48-hour incubation with DMF. The  $IC_{50}$  value for DMF in Mia PaCa-2 cells following 24-hour incubation was calculated to be  $76.73 \pm 2.17 \mu$ M, and  $79.79 \pm 17.82 \mu$ M for 48-hour incubation.

As the data conformed to normal distribution, according to the Shapiro-Wilk normality test, one-way ANOVA with Bonferroni post hoc test was used to assess the cytotoxic effect of the various concentrations of DMF when compared with the untreated control. A summary of this analysis can be found in **table 2.6**. In Panc-1, incubation of the cells with only 20  $\mu$ M of DMF (**figure 2.3A**) did not induce statistically significant reduction in clonogenicity when compared with the untreated control for the 24-hour incubation period with DMF ( $P > 0.0009$ ). For the 48-hour incubation period in Panc-1, only 100  $\mu$ M DMF (**figure 2.3B**) induced significant reduction in clonogenicity when

compared with the untreated control ( $P < 0.0001$ ). In Mia PaCa-2, all concentrations of DMF tested following a 24-hour incubation with cells (**figure 2.3A**) induced significant reduction in clonogenicity when compared with the untreated control ( $P < 0.0001$ ). For the 48-hour incubation period with DMF in Mia PaCa-2 cells, only 100  $\mu\text{M}$  DMF (**figure 2.3B**) induced significant reduction in clonogenicity when compared with the untreated control ( $P = 0.0110$ ).

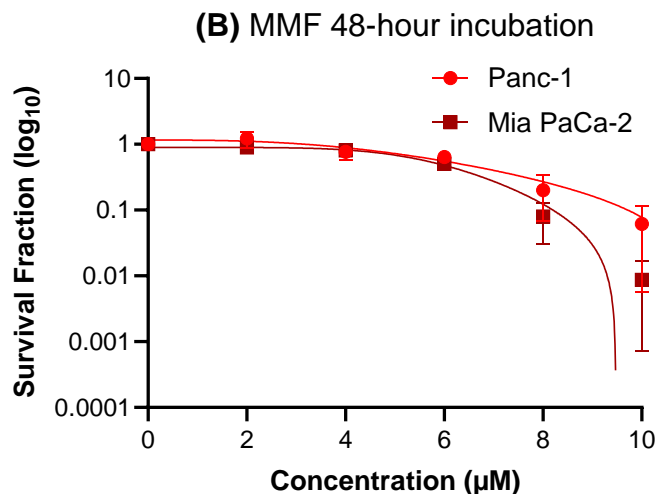
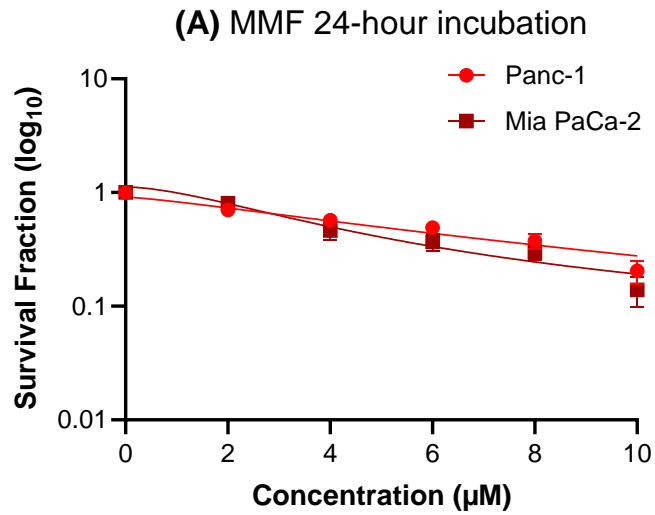
**Table 2.6: Summary table of one-way ANOVA analysis of DMF concentrations vs control for pancreatic cell lines.**

Comparison	Cell Line	Incubation	P-value	Summary	Significant?
20 $\mu\text{M}$ vs Control	Panc-1	24 hrs	>0.9999	ns	No
		48 hrs	>0.9999	ns	No
40 $\mu\text{M}$ vs Control	Panc-1	24 hrs	0.0457	*	Yes
		48 hrs	>0.9999	ns	No
60 $\mu\text{M}$ vs Control	Panc-1	24 hrs	0.0059	**	Yes
		48 hrs	>0.9999	ns	No
80 $\mu\text{M}$ vs Control	Panc-1	24 hrs	<0.0001	****	Yes
		48 hrs	>0.9999	ns	No
100 $\mu\text{M}$ vs Control	Panc-1	24 hrs	<0.0001	****	Yes
		48 hrs	<0.0001	****	Yes
20 $\mu\text{M}$ vs Control	Mia PaCa-2	24 hrs	<0.0001	****	Yes
		48 hrs	>0.9999	ns	No
40 $\mu\text{M}$ vs Control	Mia PaCa-2	24 hrs	<0.0001	****	Yes
		48 hrs	>0.9999	ns	No
60 $\mu\text{M}$ vs Control	Mia PaCa-2	24 hrs	<0.0001	****	Yes
		48 hrs	>0.99991	ns	No
80 $\mu\text{M}$ vs Control	Mia PaCa-2	24 hrs	<0.0001	****	Yes
		48 hrs	>0.9999	ns	No
100 $\mu\text{M}$ vs Control	Mia PaCa-2	24 hrs	<0.0001	****	Yes
		48 hrs	0.0110	*	Yes

Overall, the results in **section 2.4.3** indicate that both cell lines are sensitive to DMF, however much higher concentrations are required to reduce clonogenicity when compared with MMF and gemcitabine.

#### **2.4.4: Cytotoxic effect of MMF on pancreatic cell clonogenicity *in vitro***

The clonogenic assay was carried out as described in **section 2.3.4** to assess the cytotoxicity of MMF on pancreatic cells *in vitro*. Cells were incubated with MMF for both 24- and 48-hours to determine if increasing the exposure time had any effect on cytotoxicity. The results of this experiment are shown in **figure 2.4**.



Cell Line	MMF IC <sub>50</sub> with 24-hour incubation	MMF IC <sub>50</sub> with 48-hour incubation
Panc-1	6.512 ± 0.93 µM	6.752 ± 0.96 µM
Mia PaCa-2	3.312 ± 2.74 µM	6.388 ± 0.44 µM

**Figure 2.4: Cytotoxic effect of MMF on Panc-1 and Mia PaCa-2.** Cells were exposed to varying concentrations (2 µM – 10 µM) of MMF and the survival fraction determined. **(A)** Cytotoxic effect of MMF following 24-hour incubation. **(B)** Cytotoxic effect of MMF following 48-hour incubation. All data is represented as the average of three independent experiments carried out in triplicate ± standard deviation.

In both cell lines and incubation periods, MMF induced a dose dependent reduction in clonogenicity. In Panc-1, following a 24-hour incubation with MMF (**figure 2.4A**), the highest concentration (10  $\mu$ M) of MMF induced an average reduction in clonogenicity of  $79.5 \pm 4.73\%$  and  $93.85 \pm 5.6\%$  reduction in clonogenicity was induced with a 48-hour incubation (**figure 2.4B**). In Mia PaCa-2, the highest concentration of MMF (10  $\mu$ M) induced an average reduction in clonogenicity of  $86.1 \pm 4.1\%$  following a 24-hour incubation (**figure 2.4A**), and  $99.13 \pm 0.8\%$  reduction in clonogenicity following a 48-hour incubation with MMF (**figure 2.4B**). There was no statistically significant difference in clonogenicity between 24- and 48-hour incubations with MMF for both Panc-1 and Mia PaCa-2 cell lines ( $P > 0.9999$ ). There was also no statistically significant difference between Panc-1 and Mia PaCa-2 with both 24- and 48-hour incubations with MMF ( $P > 0.9999$ ).

The  $IC_{50}$  value for MMF following a 24-hour incubation in Panc-1 cells was calculated to be  $6.512 \pm 0.93 \mu$ M and  $6.752 \pm 0.96 \mu$ M for the 48-hour incubation. The  $IC_{50}$  value for MMF following 24-hour incubation in Mia PaCa-2 cells was calculated to be  $3.312 \pm 2.74 \mu$ M and  $6.388 \pm 0.44 \mu$ M for the 48-hour incubation. These  $IC_{50}$  values were lower than that of DMF, which will be addressed in the discussion of this chapter.

As the data conformed to normal distribution, according to the Shapiro-Wilk normality test, one-way ANOVA with Bonferroni post hoc test was used to assess the cytotoxic effect of the various concentrations of MMF when compared with the untreated control. A summary of this analysis can be found in **table 2.8**. In Panc-1, all concentrations of MMF tested following 24-hour incubation of the cells with MMF (**figure 2.4A**) induced a significant reduction in clonogenicity when compared with the untreated control ( $P < 0.0001$ ). For the 48-hour incubation with MMF in Panc-1 (**figure 2.4B**) all tested concentrations, with the exception of 2  $\mu$ M, induced a significant reduction in clonogenicity when compared with the untreated control ( $P < 0.05$ ). In

Mia PaCa-2, all concentrations of MMF tested (**figure 2.4**) induced a significant reduction in clonogenicity when compared with the untreated control for both incubation periods ( $P < 0.001$ ).

**Table 2.8: Summary table of one-way ANOVA analysis of MMF concentrations vs control for pancreatic cell lines.**

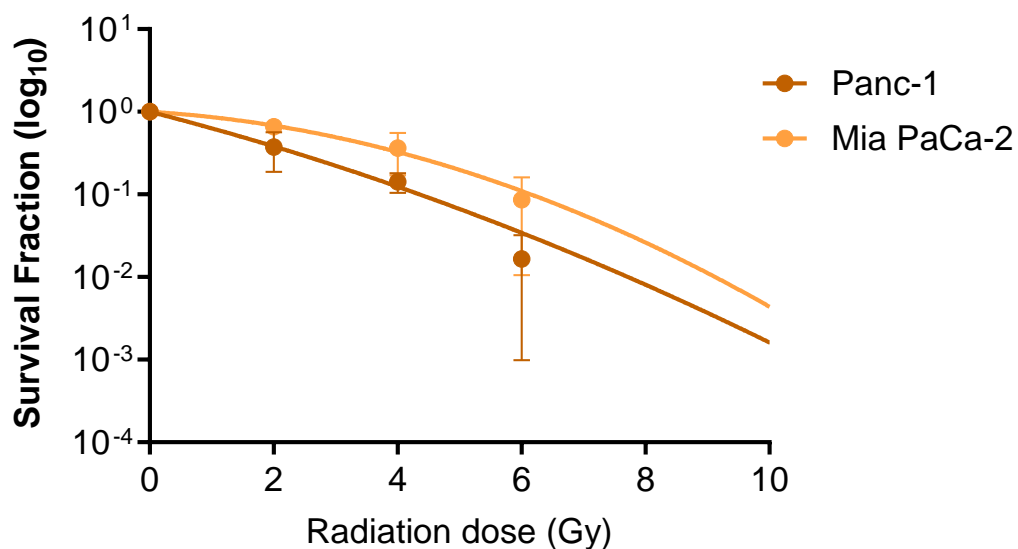
Comparison	Cell Line	Incubation	P-value	Summary	Significant?
2 $\mu$ M vs Control	Panc-1	24 hrs	<0.0001	****	Yes
		48 hrs	0.0517	ns	No
4 $\mu$ M vs Control	Panc-1	24 hrs	<0.0001	****	Yes
		48 hrs	0.0455	*	Yes
6 $\mu$ M vs Control	Panc-1	24 hrs	<0.0001	****	Yes
		48 hrs	0.0005	***	Yes
8 $\mu$ M vs Control	Panc-1	24 hrs	<0.0001	****	Yes
		48 hrs	<0.0001	****	Yes
10 $\mu$ M vs Control	Panc-1	24 hrs	<0.0001	****	Yes
		48 hrs	<0.0001	****	Yes
2 $\mu$ M vs Control	Mia PaCa-2	24 hrs	<0.0001	****	Yes
		48 hrs	0.0003	***	Yes
4 $\mu$ M vs Control	Mia PaCa-2	24 hrs	<0.0001	****	Yes
		48 hrs	<0.0001	****	Yes
6 $\mu$ M vs Control	Mia PaCa-2	24 hrs	<0.0001	****	Yes
		48 hrs	<0.0001	****	Yes
8 $\mu$ M vs Control	Mia PaCa-2	24 hrs	<0.0001	****	Yes
		48 hrs	<0.0001	****	Yes
10 $\mu$ M vs Control	Mia PaCa-2	24 hrs	<0.0001	****	Yes
		48 hrs	<0.0001	****	Yes

Overall, the results in **section 2.4.4** indicate that both cell lines are sensitive MMF, and that based upon the two incubation periods tested with MMF, the effectiveness of the drug is not influenced by treatment time.

#### **2.4.5: EXBR induced cytotoxicity on pancreatic cell clonogenicity *in vitro***

The clonogenic assay was carried out as described in **section 2.3.4**, to assess the effect of EXBR induced cytotoxicity on pancreatic cells *in vitro*. Cells were irradiated with a range of doses of EXBR (0 – 10 Gy) at a dose rate of 2.3 Gy/min. Data was analysed via a linear quadratic model using GraphPad Prism version 10.1.2 to

determine the  $D_{50}$  (irradiation dose to reduce the survival rate to 50%). The results of this experiment are shown in **figure 2.5**.



<u>Cell Line</u>	<u><math>\alpha</math> (Gy<sup>-1</sup>)</u>	<u><math>\beta</math> (Gy<sup>-1</sup>)</u>	<u><math>\alpha/\beta</math> ratio</u>	<u>D<sub>50</sub> (Gy)</u>
Panc-1	0.441	0.02	21.86	1.47 ± 0.71
Mia PaCa-2	0.104	0.04	2.39	2.95 ± 0.74

**Figure 2.5: Effect of EXBR on Panc-1 and Mia PaCa-2.** Cells were irradiated with varying doses (2 Gy – 10 Gy) of radiation and the survival fraction determined. Data is represented as the average of three independent experiments carried out in triplicate ± standard deviation.

The D<sub>50</sub> value for radiation in Panc-1 was calculated to be 1.47 ± 0.71 Gy and 2.95 ± 0.74 Gy for Mia PaCa-2.

As the data conformed to normal distribution, according to the Shapiro-Wilk normality test, one-way ANOVA with Bonferroni post hoc test was used to assess the toxicity of the various doses of EXBR in both Panc-1 and Mia PaCa-2 cells when compared with the unirradiated control. A summary of this analysis can be found in **table 2.10**. An unpaired t-test was used to compare EXBR induced cytotoxicity between Panc-1, and Mia PaCa-2 cell lines.

In both cell lines EXBR induced a dose dependent reduction in cell surviving fraction (**figure 2.5**). The highest dose of radiation tested (10 Gy) induced 100% reduction in clonogenicity in both cell lines (**figure 2.5**). All doses of EXBR induced a significant reduction in clonogenicity when compared with the untreated control (P < 0.0001). There was no statistically significant difference in clonogenicity induced by EXBR between Panc-1 and Mia PaCa-2 cell lines when exposed to any dose of EXBR (P = 0.1938).

**Table 2.10: Summary table of one-way ANOVA analysis of radiation doses vs control for pancreatic cell lines.**

Comparison	Cell Line	P-value	Summary	Significant?
2 Gy vs Control	Panc-1	<0.0001	****	Yes
4 Gy vs Control	Panc-1	<0.0001	****	Yes
6 Gy vs Control	Panc-1	<0.0001	****	Yes
8 Gy vs Control	Panc-1	<0.0001	****	Yes
10 Gy vs Control	Panc-1	<0.0001	****	Yes
2 Gy vs Control	Mia PaCa-2	<0.0001	****	Yes
4 Gy vs Control	Mia PaCa-2	<0.0001	****	Yes
6 Gy vs Control	Mia PaCa-2	<0.0001	****	Yes
8 Gy vs Control	Mia PaCa-2	<0.0001	****	Yes
10 Gy vs Control	Mia PaCa-2	<0.0001	****	Yes

Overall, the results from **section 2.4.5** indicate that both cell lines are sensitive to EXBR, with Panc-1 being more radiosensitive than Mia PaCa-2.

## **2.4.6: Interrogation of the effect of gemcitabine on pancreatic cancer spheroid growth *in vitro***

### **2.4.6-1: Interrogation of the effect of gemcitabine on Panc-1 spheroid growth**

The spheroid growth delay assay was carried out as described in **section 2.3.6** to assess the cytotoxicity of gemcitabine on spheroids grown from Panc-1 cells *in vitro*. Panc-1 spheroids were exposed to gemcitabine at a concentration range of 0 – 10  $\mu\text{M}$  for 48-hours to determine the effect on spheroid growth via change in volume ( $V/V_0$ ) and AUC analysis. The results are presented in **figure 2.6**.

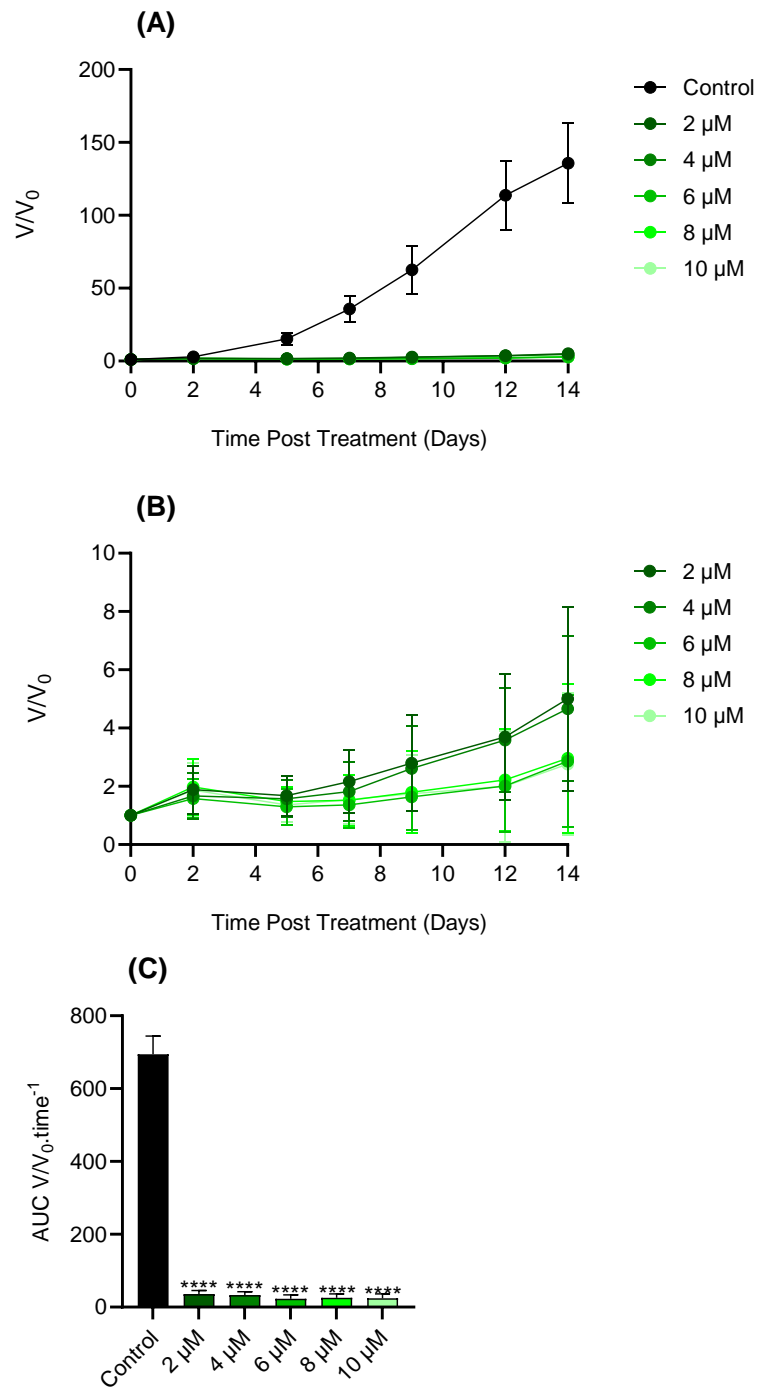


**Figure 2.6: Effect of gemcitabine on Panc-1 spheroid growth.** Panc-1 spheroids were exposed to varying concentrations (2  $\mu\text{M}$  – 10  $\mu\text{M}$ ) of gemcitabine and the change in volume ( $V/V_0$ ) and AUC calculated. (A)  $V/V_0$  for gemcitabine treated spheroids and untreated control. The data is represented as the average of three independent experiments carried out with 16 spheroids per treatment group (48 spheroids total)  $\pm$  standard deviation. (B)  $V/V_0$  for gemcitabine treated spheroids alone. (C) AUC for gemcitabine treated spheroids and untreated control, statistical significance shown in comparison with the untreated control. The data is represented as the average  $\pm$  standard deviation. \*\*\*\* =  $P \leq 0.0001$ .

As both  $V/V_0$  and AUC data obtained from Panc-1 spheroids incubated with gemcitabine did not conform to normal distribution following a Shapiro-Wilk normality test, a Kruskal-Wallis with Dunn's post hoc test was used to assess the effect of the gemcitabine on spheroid growth when compared with the untreated control. In Panc-1 spheroids (**figure 2.6A**), all concentrations of gemcitabine induced a statistically significant reduction in spheroid growth when compared with the untreated control spheroids ( $P < 0.0001$ ). The highest concentration of gemcitabine tested ( $10 \mu\text{M}$ ) resulted in a 50-fold reduction in spheroid volume when compared with the untreated control spheroids (**figure 2.6A**). As gemcitabine induced such a significant reduction in spheroid volume in Panc-1 spheroids when compared with the untreated control, an additional graph (**figure 2.6B**) showing only gemcitabine treated spheroids was generated to allow the differences between concentrations to be more clearly observed. When comparing the different concentrations of gemcitabine administered,  $6 \mu\text{M}$  induced a statistically greater reduction in spheroid volume when compared with the lower concentrations of  $2$  &  $4 \mu\text{M}$  gemcitabine ( $P < 0.0001$ ), however the higher concentrations ( $8$  &  $10 \mu\text{M}$ ) did not induce a statistically significantly greater reduction in spheroid volume when compared with  $6 \mu\text{M}$  of gemcitabine ( $P > 0.9999$ ), suggesting there was no additional benefit with respect to decreasing spheroid growth afforded by the administration of the higher concentrations of gemcitabine. A summary of these comparisons can be found in **table 2.11**.

**Table 2.11: Summary table of Kruskal-Wallis test of V/V0 for gemcitabine treated Panc-1 spheroids.**

Comparison	P-value	Summary	Significant?
2 $\mu$ M vs Control	<0.0001	****	Yes
4 $\mu$ M vs Control	<0.0001	****	Yes
6 $\mu$ M vs Control	<0.0001	****	Yes
8 $\mu$ M vs Control	<0.0001	****	Yes
10 $\mu$ M vs Control	<0.0001	****	Yes
2 $\mu$ M vs 4 $\mu$ M	>0.9999	ns	No
2 $\mu$ M vs 6 $\mu$ M	<0.0001	****	Yes
2 $\mu$ M vs 8 $\mu$ M	<0.0001	****	Yes
2 $\mu$ M vs 10 $\mu$ M	<0.0001	****	Yes
4 $\mu$ M vs 6 $\mu$ M	<0.0001	****	Yes
4 $\mu$ M vs 8 $\mu$ M	<0.0001	****	No
4 $\mu$ M vs 10 $\mu$ M	<0.0001	****	Yes
6 $\mu$ M vs 8 $\mu$ M	>0.9999	ns	No
6 $\mu$ M vs 10 $\mu$ M	>0.9999	ns	No
8 $\mu$ M vs 10 $\mu$ M	>0.9999	ns	No

When assessing the AUC for Panc-1 spheroids incubated with gemcitabine (**figure 2.6C**), all concentrations of gemcitabine induced a statistically significant reduction in AUC when compared with the untreated control ( $P < 0.0001$ ). When comparing the different concentrations of gemcitabine administered in Panc-1 spheroids, 10  $\mu$ M did not induce a statistically greater reduction in AUC compared with the lower concentrations of gemcitabine tested ( $P > 0.8567$ ), suggesting there was no additional benefit with respect to decreasing spheroid growth afforded by the administration of the higher concentrations of gemcitabine. A summary of these comparisons can be found in **table 2.12**.

**Table 2.12: Summary table of Kruskal-Wallis test of AUC for gemcitabine treated Panc-1 spheroids.**

Comparison	P-value	Summary	Significant?
2 $\mu$ M vs Control	<0.0001	****	Yes
4 $\mu$ M vs Control	<0.0001	****	Yes
6 $\mu$ M vs Control	<0.0001	****	Yes
8 $\mu$ M vs Control	<0.0001	****	Yes
10 $\mu$ M vs Control	<0.0001	****	Yes
2 $\mu$ M vs 4 $\mu$ M	0.9965	ns	No
2 $\mu$ M vs 6 $\mu$ M	0.8567	ns	No
2 $\mu$ M vs 8 $\mu$ M	0.9224	ns	No
2 $\mu$ M vs 10 $\mu$ M	0.8991	ns	No
4 $\mu$ M vs 6 $\mu$ M	0.9224	ns	No
4 $\mu$ M vs 8 $\mu$ M	0.9349	ns	No
4 $\mu$ M vs 10 $\mu$ M	0.9224	ns	No
6 $\mu$ M vs 8 $\mu$ M	0.9965	ns	No
6 $\mu$ M vs 10 $\mu$ M	0.9965	ns	No
8 $\mu$ M vs 10 $\mu$ M	0.9965	ns	No

The overall results of **section 2.4.6-1** suggest that Panc-1 spheroids are highly sensitive to gemcitabine monotherapy in the concentration range tested and that no additional reduction in spheroid growth was observed when increasing the concentration of gemcitabine above 2  $\mu$ M.

#### **2.4.6-2 Interrogation of the effect of gemcitabine on Mia PaCa-2 spheroid growth**

The spheroid growth delay assay was carried out as described in **section 2.3.6** to assess the cytotoxicity of gemcitabine on spheroids grown from Mia PaCa-2 cells *in vitro*. Mia PaCa-2 spheroids were exposed to gemcitabine at a concentration range of 0 – 10  $\mu$ M for 48-hours to determine the effect on spheroid growth via change in volume ( $V/V_0$ ) and AUC analysis. The results are presented in **figure 2.7**.

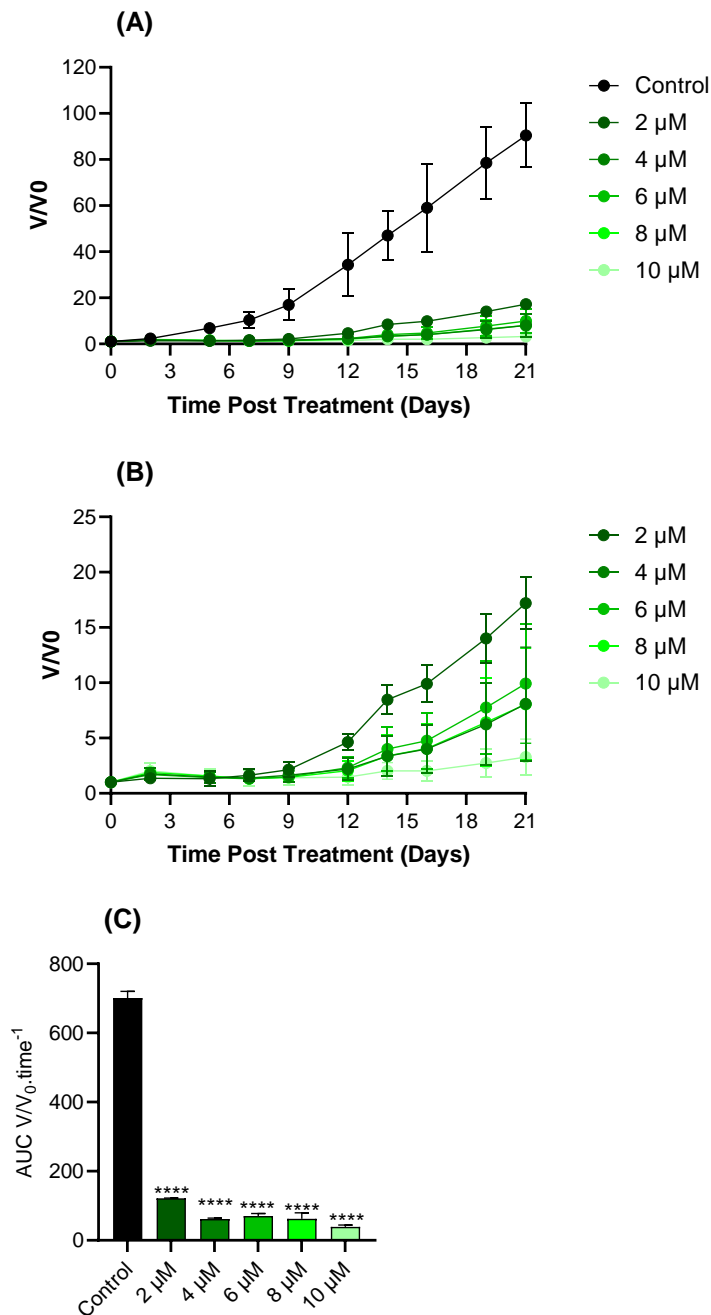


**Figure 2.7: Effect of gemcitabine on Mia PaCa-2 spheroid growth.** Mia PaCa-2 spheroids were exposed to varying concentrations (2  $\mu\text{M}$  – 10  $\mu\text{M}$ ) of gemcitabine and the change in volume ( $V/V_0$ ) and AUC calculated. (A)  $V/V_0$  for gemcitabine treated spheroids and untreated control. The data is represented as the average of three independent experiments carried out with 16 spheroids per treatment group (48 spheroids total)  $\pm$  standard deviation. (B)  $V/V_0$  for gemcitabine treated spheroids alone. (C) AUC for gemcitabine treated spheroids and untreated control, statistical significance shown in comparison with the untreated control. The data is represented as the average  $\pm$  standard deviation. \*\* =  $P \leq 0.01$ , \*\*\*\* =  $P \leq 0.0001$ .

As both  $V/V_0$  and AUC data obtained from Mia PaCa-2 spheroids incubated with gemcitabine did not conform to normal distribution following a Shapiro-Wilk normality test, a Kruskal-Wallis with Dunn's post hoc test was used to assess the effect of the gemcitabine on spheroid growth when compared with the untreated control. In Mia PaCa-2 spheroids (**figure 2.7A**), all concentrations of gemcitabine induced a statistically significant reduction in spheroid growth when compared with the untreated control spheroids ( $P < 0.0001$ ). The highest concentration of gemcitabine (10  $\mu\text{M}$ ) resulted in a 27-fold reduction in spheroid volume when compared with the untreated control spheroids (**figure 2.7A**). As gemcitabine induced such a significant reduction in Mia PaCa-2 spheroid volume when compared with the untreated control, an additional graph (**figure 2.7B**) showing only gemcitabine treated spheroids was generated to allow the differences between concentrations to be more clearly observed. When comparing the different administered concentrations, 4  $\mu\text{M}$  induced a statistically greater reduction in spheroid volume when compared with all lower concentrations ( $P < 0.0001$ ), with the exception of 10  $\mu\text{M}$  gemcitabine ( $P > 0.9999$ ). A summary of these comparisons can be found in **table 2.13**.

**Table 2.13: Summary table of Kruskal-Wallis test of  $V/V_0$  for gemcitabine treated Mia PaCa-2 spheroids.**

Comparison	P-value	Summary	Significant?
2 $\mu\text{M}$ vs Control	<0.0001	****	Yes
4 $\mu\text{M}$ vs Control	<0.0001	****	Yes
6 $\mu\text{M}$ vs Control	<0.0001	****	Yes
8 $\mu\text{M}$ vs Control	<0.0001	****	Yes
10 $\mu\text{M}$ vs Control	<0.0001	****	Yes
2 $\mu\text{M}$ vs 4 $\mu\text{M}$	<0.0001	****	Yes
2 $\mu\text{M}$ vs 6 $\mu\text{M}$	<0.0001	****	Yes
2 $\mu\text{M}$ vs 8 $\mu\text{M}$	<0.0001	****	Yes
2 $\mu\text{M}$ vs 10 $\mu\text{M}$	<0.0001	****	Yes
4 $\mu\text{M}$ vs 6 $\mu\text{M}$	>0.9999	ns	No
4 $\mu\text{M}$ vs 8 $\mu\text{M}$	>0.9999	ns	No
4 $\mu\text{M}$ vs 10 $\mu\text{M}$	<0.0001	****	Yes
6 $\mu\text{M}$ vs 8 $\mu\text{M}$	>0.9999	ns	No
6 $\mu\text{M}$ vs 10 $\mu\text{M}$	<0.0001	****	Yes
8 $\mu\text{M}$ vs 10 $\mu\text{M}$	<0.0001	****	Yes

When assessing the AUC for Mia PaCa-2 spheroids incubated with gemcitabine (**figure 2.7C**), all concentrations of gemcitabine induced a statistically significant reduction in AUC when compared with the untreated control ( $P < 0.0001$ ). When comparing the different concentrations of gemcitabine administered in Mia PaCa-2 spheroids, 10  $\mu\text{M}$  induced a statistically greater reduction in AUC when compared with 2  $\mu\text{M}$  gemcitabine ( $P < 0.0001$ ), however it was of no additional benefit when compared with all other concentrations tested ( $P > 0.2472$ ). A summary of these comparisons can be found in **table 2.14**.

**Table 2.14: Summary table of Kruskal-Wallis test of AUC for gemcitabine treated Mia PaCa-2 spheroids.**

Comparison	P-value	Summary	Significant?
2 $\mu\text{M}$ vs Control	<0.0001	****	Yes
4 $\mu\text{M}$ vs Control	<0.0001	****	Yes
6 $\mu\text{M}$ vs Control	<0.0001	****	Yes
8 $\mu\text{M}$ vs Control	<0.0001	****	Yes
10 $\mu\text{M}$ vs Control	<0.0001	****	Yes
2 $\mu\text{M}$ vs 4 $\mu\text{M}$	0.0002	***	No
2 $\mu\text{M}$ vs 6 $\mu\text{M}$	0.0010	***	Yes
2 $\mu\text{M}$ vs 8 $\mu\text{M}$	0.0003	***	Yes
2 $\mu\text{M}$ vs 10 $\mu\text{M}$	<0.0001	****	Yes
4 $\mu\text{M}$ vs 6 $\mu\text{M}$	0.9859	ns	No
4 $\mu\text{M}$ vs 8 $\mu\text{M}$	>0.9999	ns	No
4 $\mu\text{M}$ vs 10 $\mu\text{M}$	0.2554	ns	No
6 $\mu\text{M}$ vs 8 $\mu\text{M}$	0.9926	ns	No
6 $\mu\text{M}$ vs 10 $\mu\text{M}$	0.0519	ns	No
8 $\mu\text{M}$ vs 10 $\mu\text{M}$	0.2472	ns	No

The overall results of **section 2.4.6-2** suggest that Mia PaCa-2 spheroids were highly sensitive to gemcitabine monotherapy in the concentration range tested, with 10  $\mu\text{M}$  of gemcitabine inducing the greatest reduction in spheroid growth.

## **2.4.7: Interrogation of the effect of DMF on pancreatic cancer spheroid growth *in vitro***

### **2.4.7-1: Interrogation of the effect of DMF on Panc-1 spheroid growth**

The spheroid growth delay assay was carried out as described in **section 2.3.6** to assess the cytotoxicity of DMF on pancreatic spheroids *in vitro*. Panc-1 spheroids were incubated with DMF at a concentration range of 0 – 100  $\mu$ M for 48-hours to determine the effect on spheroid growth via change in volume ( $V/V_0$ ) and AUC analysis. The results are presented in **figure 2.8**.

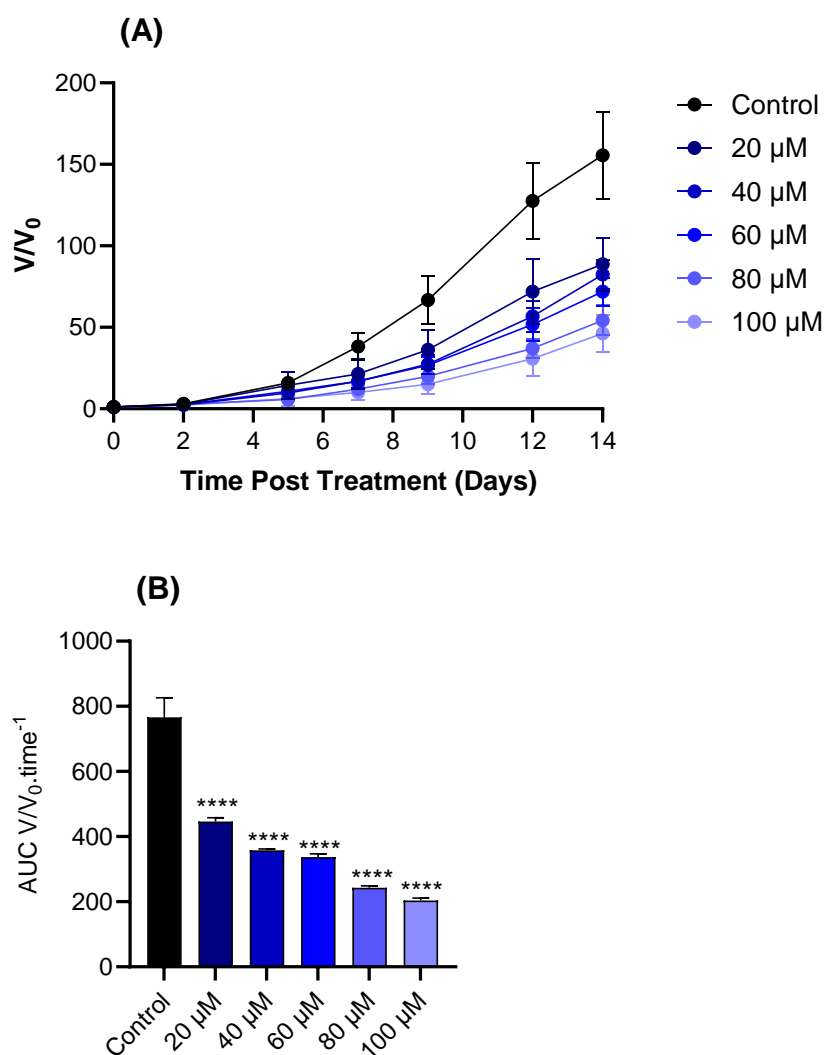


**Figure 2.8: Effect of DMF on Panc-1 spheroid growth.** Panc-1 spheroids were exposed to varying concentrations (20  $\mu\text{M}$  – 100  $\mu\text{M}$ ) of DMF and the change in volume ( $V/V_0$ ) and AUC calculated. (A)  $V/V_0$  for DMF treated spheroids and untreated control. The data is represented as the average of three independent experiments carried out with 16 spheroids per treatment group (48 spheroids total)  $\pm$  standard deviation. (B) AUC for DMF treated spheroids and untreated control, statistical significance shown in comparison with the untreated control. The data is represented as the average  $\pm$  standard deviation. \*\*\* =  $P \leq 0.001$  \*\*\*\* =  $P \leq 0.0001$ .

As both  $V/V_0$  and AUC data obtained from Panc-1 spheroids incubated with DMF did not conform to normal distribution following a Shapiro-Wilk normality test, a Kruskal-Wallis with Dunn's post hoc test was used to assess the effect of DMF on spheroid growth when compared with the untreated control. In Panc-1 spheroids (**figure 2.8A**), all concentrations of DMF tested induced a statistically significant reduction in spheroid growth when compared with the untreated control spheroids ( $P \leq 0.0026$ ). The highest concentration of DMF (100  $\mu\text{M}$ ) resulted in a 3-fold reduction in spheroid volume when compared with the untreated control spheroids (**figure 2.8A**). When comparing the different concentrations of DMF incubated with Panc-1 spheroids, 100  $\mu\text{M}$  of DMF induced a statistically greater reduction in spheroid volume when compared with the lower concentrations of 20; 40; & 60  $\mu\text{M}$  DMF administered ( $P \leq 0.0002$ ), however there was not a statistically significant greater reduction in spheroid volume when compared with 80  $\mu\text{M}$  of DMF ( $P = 0.9790$ ). A summary of these comparisons can be found in **table 2.15**.

**Table 2.15: Summary table of Kruskal-Wallis test of  $V/V_0$  for DMF treated Panc-1 spheroids.**

Comparison	P-value	Summary	Significant?
20 $\mu\text{M}$ vs Control	0.0026	**	Yes
40 $\mu\text{M}$ vs Control	<0.0001	****	Yes
60 $\mu\text{M}$ vs Control	<0.0001	****	Yes
80 $\mu\text{M}$ vs Control	<0.0001	****	Yes
100 $\mu\text{M}$ vs Control	<0.0001	****	Yes
20 $\mu\text{M}$ vs 40 $\mu\text{M}$	>0.9999	ns	No
20 $\mu\text{M}$ vs 60 $\mu\text{M}$	0.5388	ns	No
20 $\mu\text{M}$ vs 80 $\mu\text{M}$	<0.0001	****	Yes
20 $\mu\text{M}$ vs 100 $\mu\text{M}$	<0.0001	****	Yes
40 $\mu\text{M}$ vs 60 $\mu\text{M}$	>0.9999	ns	No
40 $\mu\text{M}$ vs 80 $\mu\text{M}$	<0.0001	*	No
40 $\mu\text{M}$ vs 100 $\mu\text{M}$	<0.0001	****	Yes
60 $\mu\text{M}$ vs 80 $\mu\text{M}$	0.0878	ns	No
60 $\mu\text{M}$ vs 100 $\mu\text{M}$	0.0002	***	No
80 $\mu\text{M}$ vs 100 $\mu\text{M}$	0.9790	ns	No

When assessing the AUC for Panc-1 spheroids treated with DMF (**figure 2.8B**), all concentrations of DMF tested induced a statistically significant reduction in AUC when compared with the untreated control ( $P < 0.0001$ ). When comparing the different concentrations of DMF in Panc-1 spheroids, 100  $\mu\text{M}$  of DMF induced a statistically greater reduction in AUC compared with all the lower concentrations of DMF tested ( $P < 0.0018$ ). A summary of these comparisons can be found in **table 2.16**.

**Table 2.16: Summary table of Kruskal-Wallis test of AUC for DMF in Panc-1 spheroids.**

Comparison	P-value	Summary	Significant?
20 $\mu\text{M}$ vs Control	<0.0001	****	Yes
40 $\mu\text{M}$ vs Control	<0.0001	****	Yes
60 $\mu\text{M}$ vs Control	<0.0001	****	Yes
80 $\mu\text{M}$ vs Control	<0.0001	****	Yes
100 $\mu\text{M}$ vs Control	0.0797	ns	No
20 $\mu\text{M}$ vs 40 $\mu\text{M}$	<0.0001	****	Yes
20 $\mu\text{M}$ vs 60 $\mu\text{M}$	<0.0001	****	Yes
20 $\mu\text{M}$ vs 80 $\mu\text{M}$	<0.0001	****	Yes
20 $\mu\text{M}$ vs 100 $\mu\text{M}$	<0.0001	****	Yes
40 $\mu\text{M}$ vs 60 $\mu\text{M}$	0.0018	**	Yes
40 $\mu\text{M}$ vs 80 $\mu\text{M}$	<0.0001	****	Yes
40 $\mu\text{M}$ vs 100 $\mu\text{M}$	<0.0001	****	Yes
60 $\mu\text{M}$ vs 80 $\mu\text{M}$	<0.0001	****	Yes
60 $\mu\text{M}$ vs 100 $\mu\text{M}$	<0.0001	****	Yes
80 $\mu\text{M}$ vs 100 $\mu\text{M}$	0.0797	ns	No

Overall, the results presented in **section 2.4.7-2** indicate that Panc-1 spheroid growth is inhibited by DMF in a dose dependent manner in Panc-1 spheroids.

#### **2.4.7-2: Interrogation of the effect of DMF on Mia PaCa-2 spheroid growth**

The spheroid growth delay assay was carried out as described in **section 2.3.6** to assess the cytotoxicity of DMF on pancreatic spheroids *in vitro*. Mia PaCa-2 spheroids were incubated with DMF at a concentration range of 0 – 100  $\mu\text{M}$  for 48-hours to determine the effect on spheroid growth via change in volume ( $V/V_0$ ) and AUC analysis. The results are presented in **figure 2.9**.

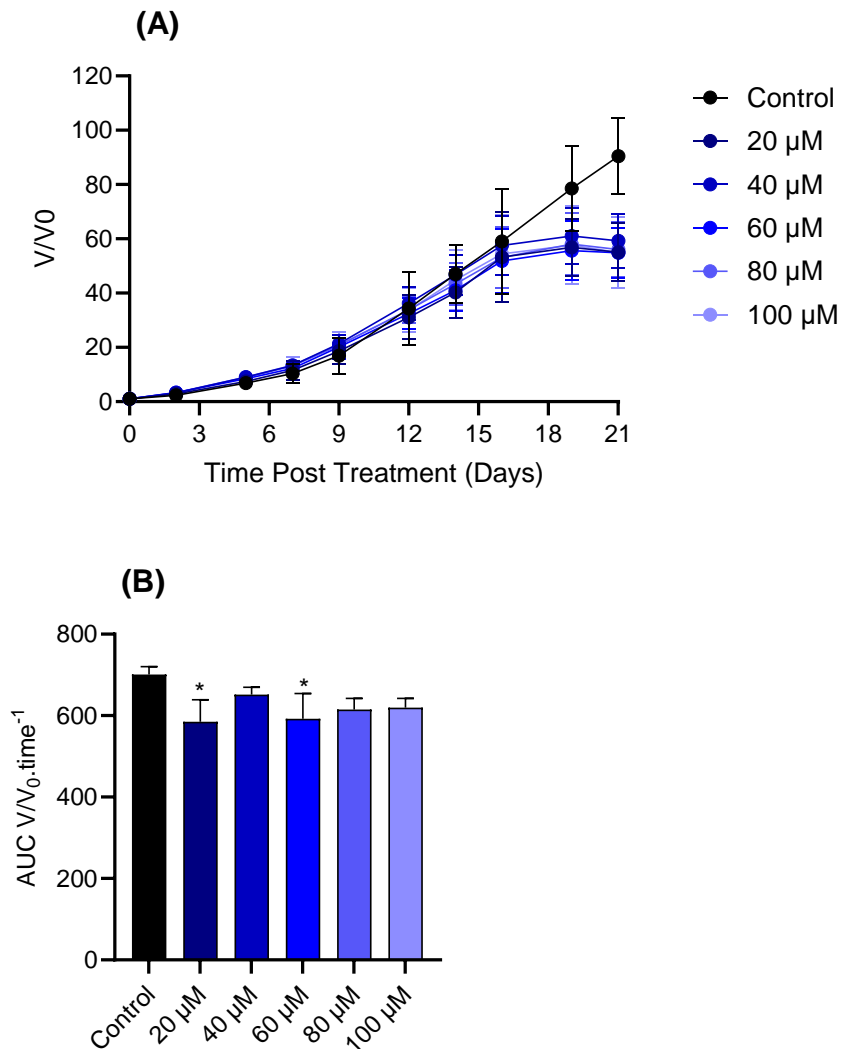


**Figure 2.9: Effect of DMF on Mia PaCa-2 spheroid growth.** Mia PaCa-2 spheroids were exposed to varying concentrations (20  $\mu\text{M}$  – 100  $\mu\text{M}$ ) of DMF and the change in volume ( $V/V_0$ ) and AUC calculated. (A)  $V/V_0$  for DMF treated spheroids and untreated control. The data is represented as the average of three independent experiments carried out with 16 spheroids per treatment group (48 spheroids total)  $\pm$  standard deviation. (B) AUC for DMF treated spheroids and untreated control, statistical significance shown in comparison with the untreated control. The data is represented as the average  $\pm$  standard deviation. \*\*\* =  $P \leq 0.001$  \*\*\*\* =  $P \leq 0.0001$ .

As both  $V/V_0$  and AUC data obtained from Mia PaCa-2 spheroids incubated with DMF did not conform to normal distribution following a Shapiro-Wilk normality test, a Kruskal-Wallis with Dunn's post hoc test was used to assess the effect of the DMF on spheroid growth when compared with the untreated control. In Mia PaCa-2 spheroids (**figure 2.9A**), no concentrations of DMF tested induced a statistically significant reduction in spheroid growth when compared with the untreated control spheroids ( $P \geq 0.2323$ ). A summary of these comparisons can be found in **table 2.17**. The highest concentration of DMF tested (100  $\mu\text{M}$ ) induced only a 1.6-fold reduction in spheroid volume when compared with the untreated control spheroids (**figure 2.9A**).

**Table 2.17: Summary table of Kruskal-Wallis test of DMF treated Mia PaCa-2 spheroids.**

Comparison	P-value	Summary	Significant?
20 $\mu\text{M}$ vs Control	0.2323	ns	No
40 $\mu\text{M}$ vs Control	>0.9999	ns	No
60 $\mu\text{M}$ vs Control	0.6620	ns	No
80 $\mu\text{M}$ vs Control	>0.9999	ns	No
100 $\mu\text{M}$ vs Control	>0.9999	ns	No

To further interrogate whether DMF induced any significant reduction in Mia PaCa-2 spheroid growth when compared with the untreated control, AUC was analysed. Out of all concentrations of DMF tested only the incubation of spheroids with 20  $\mu\text{M}$  ( $P = 0.0110$ ) and 60  $\mu\text{M}$  ( $P = 0.0168$ ) induced a statistically significant reduction in AUC when compared with the untreated control (**figure 2.9B**). However, there was no statistically significant difference in the growth of Mia PaCa-2 spheroids between incubation with 20 and 60  $\mu\text{M}$  of DMF ( $P > 0.9999$ ). A summary of these comparisons can be found in **table 2.18**.

**Table 2.18: Summary table of Kruskal-Wallis test of AUC for DMF treated Mia PaCa-2 spheroids.**

Comparison	P-value	Summary	Significant?
20 $\mu$ M vs Control	0.0110	*	Yes
40 $\mu$ M vs Control	0.4074	ns	No
60 $\mu$ M vs Control	0.0168	*	Yes
80 $\mu$ M vs Control	0.0616	ns	No
100 $\mu$ M vs Control	0.0804	ns	No

Overall, the results from **section 2.4.7-2** indicate that Mia PaCa-2 spheroids were not sensitive to DMF treatment, however when analysing AUC data, 20 & 60  $\mu$ M of DMF appear to have significantly reduced spheroid growth when compared with the untreated control.

#### **2.4.8: Interrogation of the effect of MMF on pancreatic cancer spheroid growth *in vitro***

##### **2.4.8-1: Interrogation of the effect of MMF on Panc-1 spheroid growth**

The spheroid growth delay assay was carried out as described in **section 2.3.6** to assess the cytotoxicity of MMF on pancreatic spheroids *in vitro*. Mia PaCa-2 spheroids were incubated with MMF at a concentration range of 0 – 10  $\mu$ M for 48-hours to determine the effect on spheroid growth via change in volume ( $V/V_0$ ) and AUC analysis. The results are presented in **figure 2.10**.

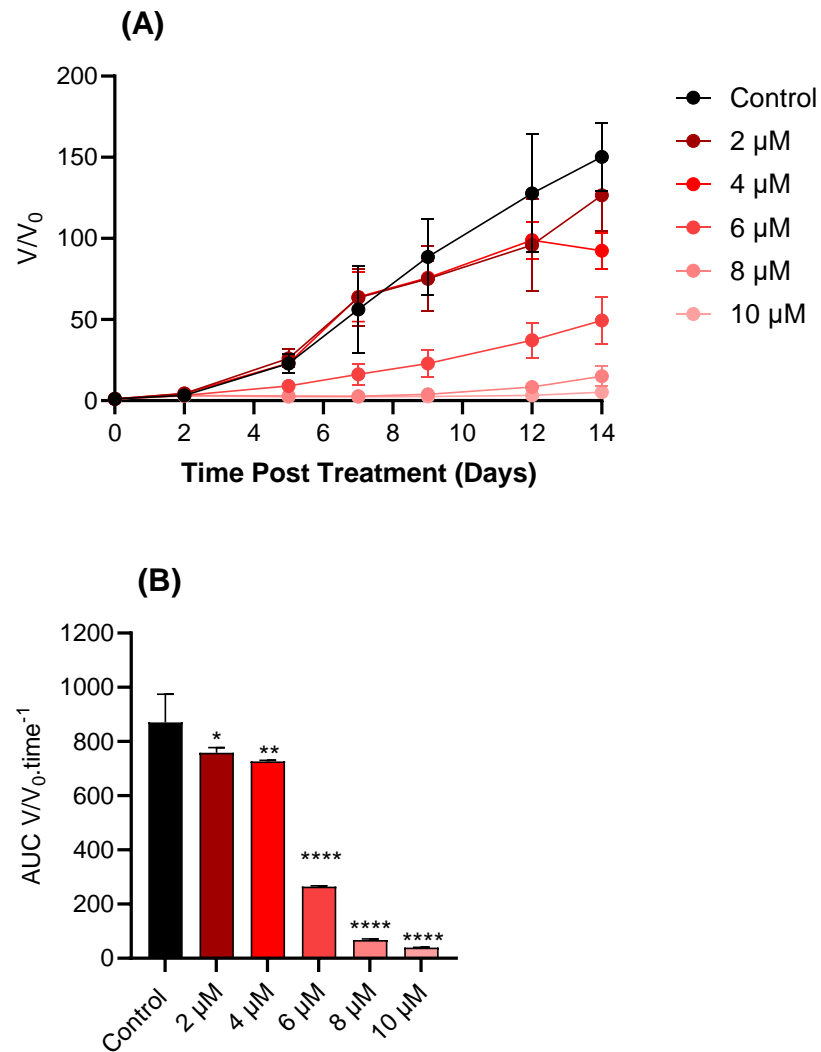


**Figure 2.10: Effect of MMF on Panc-1 spheroid growth.** Panc-1 spheroids were exposed to varying concentrations (2  $\mu\text{M}$  – 10  $\mu\text{M}$ ) of MMF and the change in volume ( $V/V_0$ ) and AUC calculated. (A)  $V/V_0$  for MMF treated spheroids and untreated control. The data is represented as the average of three independent experiments carried out with 16 spheroids per treatment group (48 spheroids total)  $\pm$  standard deviation. (B) AUC for MMF treated spheroids and untreated control, statistical significance shown in comparison with the untreated control. The data is represented as the average  $\pm$  standard deviation. \*\*\*\* =  $P \leq 0.0001$ .

As both  $V/V_0$  and AUC data obtained from Panc-1 spheroids incubated with MMF did not conform to normal distribution following a Shapiro-Wilk normality test, a Kruskal-Wallis with Dunn's post hoc test was used to assess the effect of the MMF on spheroid growth when compared with the untreated control. In Panc-1 spheroids (**figure 2.10A**), incubation with 6  $\mu\text{M}$ ; 8  $\mu\text{M}$ ; and 10  $\mu\text{M}$  of MMF induced a statistically significant reduction in spheroid growth when compared with the untreated control spheroids ( $P < 0.0001$ ). The highest concentration of MMF tested (10  $\mu\text{M}$ ) in Panc-1 spheroids induced a 28-fold reduction in spheroid volume when compared with the untreated control spheroids (**figure 2.10A**). When comparing the different concentrations of MMF incubated with Panc-1 spheroids, 10  $\mu\text{M}$  of MMF induced a statistically significantly greater reduction in Panc-1 spheroid growth when compared with all other concentrations ( $P \leq 0.0005$ ), a summary of these comparisons can be found in **table 2.19**.

**Table 2.19: Summary table of Kruskal-Wallis test of  $V/V_0$  for MMF treated Panc-1 spheroids.**

Comparison	P-value	Summary	Significant?
2 $\mu\text{M}$ vs Control	>0.9999	ns	No
4 $\mu\text{M}$ vs Control	>0.9999	ns	No
6 $\mu\text{M}$ vs Control	<0.0001	****	Yes
8 $\mu\text{M}$ vs Control	<0.0001	****	Yes
10 $\mu\text{M}$ vs Control	<0.0001	****	Yes
2 $\mu\text{M}$ vs 4 $\mu\text{M}$	>0.9999	ns	No
2 $\mu\text{M}$ vs 6 $\mu\text{M}$	<0.0001	****	Yes
2 $\mu\text{M}$ vs 8 $\mu\text{M}$	<0.0001	****	Yes
2 $\mu\text{M}$ vs 10 $\mu\text{M}$	<0.0001	****	Yes
4 $\mu\text{M}$ vs 6 $\mu\text{M}$	<0.0001	****	Yes
4 $\mu\text{M}$ vs 8 $\mu\text{M}$	<0.0001	****	Yes
4 $\mu\text{M}$ vs 10 $\mu\text{M}$	<0.0001	****	Yes
6 $\mu\text{M}$ vs 8 $\mu\text{M}$	<0.0001	***	Yes
6 $\mu\text{M}$ vs 10 $\mu\text{M}$	<0.0001	****	Yes
8 $\mu\text{M}$ vs 10 $\mu\text{M}$	0.0005	***	Yes

When assessing the AUC for Panc-1 spheroids incubated with MMF (**figure 2.10B**), all tested concentrations of MMF induced a statistically significant reduction in AUC when compared with the untreated control spheroids ( $P \leq 0.0310$ ). However, 10  $\mu\text{M}$  of MMF induced a statistically significant reduction in AUC when compared with all lower concentration of MMF tested ( $P \leq 0.0210$ ). A summary of comparisons can be found in **table 2.20**.

**Table 2.20: Summary table of Kruskal-Wallis test of AUC for MMF treated Panc-1 spheroids.**

Comparison	P-value	Summary	Significant?
2 $\mu\text{M}$ vs Control	0.0310	*	Yes
4 $\mu\text{M}$ vs Control	0.0065	**	Yes
6 $\mu\text{M}$ vs Control	<0.0001	****	Yes
8 $\mu\text{M}$ vs Control	<0.0001	****	Yes
10 $\mu\text{M}$ vs Control	<0.0001	****	Yes
2 $\mu\text{M}$ vs 4 $\mu\text{M}$	0.0118	*	Yes
2 $\mu\text{M}$ vs 6 $\mu\text{M}$	<0.0001	****	Yes
2 $\mu\text{M}$ vs 8 $\mu\text{M}$	<0.0001	****	Yes
2 $\mu\text{M}$ vs 10 $\mu\text{M}$	<0.0001	****	Yes
4 $\mu\text{M}$ vs 6 $\mu\text{M}$	<0.0001	****	Yes
4 $\mu\text{M}$ vs 8 $\mu\text{M}$	<0.0001	****	Yes
4 $\mu\text{M}$ vs 10 $\mu\text{M}$	<0.0001	****	Yes
6 $\mu\text{M}$ vs 8 $\mu\text{M}$	<0.0001	****	Yes
6 $\mu\text{M}$ vs 10 $\mu\text{M}$	<0.0001	****	Yes
8 $\mu\text{M}$ vs 10 $\mu\text{M}$	0.0210	*	Yes

Overall, the results in **section 2.4.8-1** indicate that Panc-1 spheroid growth was inhibited following incubation with MMF in the concentration range tested, with 10  $\mu\text{M}$  of MMF inducing the greatest reduction in spheroid volume.

#### **2.4.8-2: Interrogation of the effect of MMF on Mia PaCa spheroid growth**

The spheroid growth delay assay was carried out as described in **section 2.36** to assess the cytotoxicity of MMF on pancreatic spheroids *in vitro*. Mia PaCa-2 spheroids were incubated with MMF at a concentration range of 0 – 10  $\mu\text{M}$  for 48-hours to determine the effect on spheroid growth via change in volume ( $V/V_0$ ) and AUC analysis. The results are presented in **figure 2.11**.

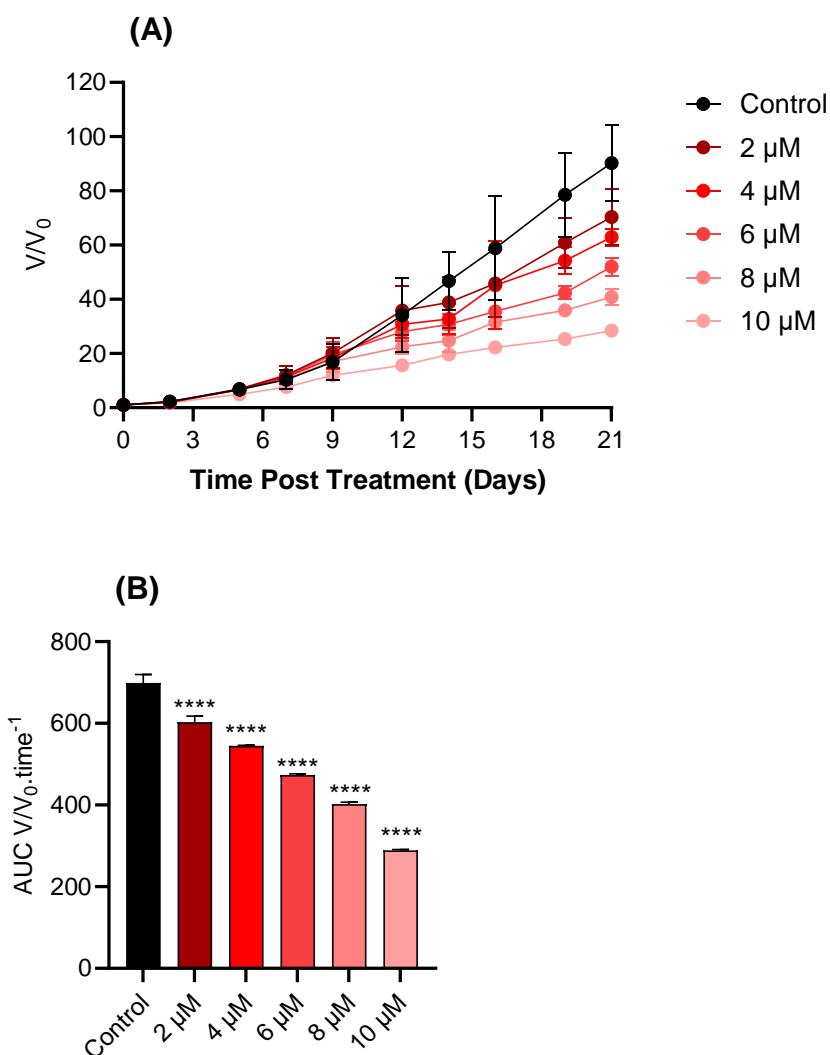


**Figure 2.11: Effect of MMF on Mia PaCa-2 spheroid growth.** Mia PaCa-2 spheroids were exposed to varying concentrations (2  $\mu\text{M}$  – 10  $\mu\text{M}$ ) of MMF and the change in volume ( $V/V_0$ ) and AUC calculated. (A)  $V/V_0$  for MMF treated spheroids and untreated control. The data is represented as the average of three independent experiments carried out with 16 spheroids per treatment group (48 spheroids total)  $\pm$  standard deviation. (B) AUC for MMF treated spheroids and untreated control, statistical significance shown in comparison with the untreated control. The data is represented as the average  $\pm$  standard deviation. \*\* =  $P \leq 0.01$  and \*\*\* =  $P \leq 0.0001$ .

As both  $V/V_0$  and AUC data obtained from Mia PaCa-2 spheroids incubated with MMF did not conform to normal distribution following a Shapiro-Wilk normality test, a Kruskal-Wallis with Dunn's post hoc test was used to assess the effect of the MMF on spheroid growth when compared with the untreated control. In Mia PaCa-2 spheroids, incubation with 6  $\mu\text{M}$  ( $P = 0.0118$ ); 8  $\mu\text{M}$  ( $P < 0.0001$ ); and 10  $\mu\text{M}$  ( $P < 0.0001$ ) of MMF induced a statistically significant reduction in spheroid growth when compared with the untreated control spheroids (**figure 2.11A**). Incubation with the highest concentration of MMF (10  $\mu\text{M}$ ) resulted in a 3.2-fold reduction in spheroid volume when compared with the untreated control spheroids (**figure 2.11A**). When comparing incubation with the different concentrations of MMF tested in Mia PaCa-2 spheroids, 10  $\mu\text{M}$  of MMF induced a statistically significantly greater reduction in Mia PaCa-2 spheroid growth when compared with all other concentrations ( $P < 0.0001$ ), a summary of these comparisons can be found in **table 2.21**.

**Table 2.21: Summary table of Kruskal-Wallis test of  $V/V_0$  for MMF treated Mia PaCa-2 spheroids.**

Comparison	P-value	Summary	Significant?
2 $\mu\text{M}$ vs Control	>0.9999	ns	No
4 $\mu\text{M}$ vs Control	0.3240	ns	No
6 $\mu\text{M}$ vs Control	0.0118	*	Yes
8 $\mu\text{M}$ vs Control	<0.0001	****	Yes
10 $\mu\text{M}$ vs Control	<0.0001	****	Yes
2 $\mu\text{M}$ vs 4 $\mu\text{M}$	>0.9999	ns	No
2 $\mu\text{M}$ vs 6 $\mu\text{M}$	0.1264	ns	No
2 $\mu\text{M}$ vs 8 $\mu\text{M}$	<0.0001	****	Yes
2 $\mu\text{M}$ vs 10 $\mu\text{M}$	<0.0001	****	Yes
4 $\mu\text{M}$ vs 6 $\mu\text{M}$	>0.9999	ns	No
4 $\mu\text{M}$ vs 8 $\mu\text{M}$	0.0039	**	Yes
4 $\mu\text{M}$ vs 10 $\mu\text{M}$	<0.0001	****	Yes
6 $\mu\text{M}$ vs 8 $\mu\text{M}$	0.1656	ns	No
6 $\mu\text{M}$ vs 10 $\mu\text{M}$	<0.0001	****	Yes
8 $\mu\text{M}$ vs 10 $\mu\text{M}$	<0.0001	****	Yes

When assessing the AUC for Mia PaCa-2 spheroids incubated with MMF (**figure 2.11B**), all concentrations tested induced a statistically significant reduction in AUC when compared with the untreated control spheroids ( $P < 0.0001$ ). However, 10  $\mu\text{M}$  of MMF induced a statistically significant reduction in AUC when compared with all lower concentrations of MMF tested ( $P < 0.0001$ ). A summary of comparisons can be found in **table 2.22**.

**Table 2.22: Summary table of Kruskal-Wallis test of AUC for MMF treated Mia PaCa-2 spheroids.**

Comparison	P-value	Summary	Significant?
2 $\mu\text{M}$ vs Control	<0.0001	****	Yes
4 $\mu\text{M}$ vs Control	<0.0001	****	Yes
6 $\mu\text{M}$ vs Control	<0.0001	****	Yes
8 $\mu\text{M}$ vs Control	<0.0001	****	Yes
10 $\mu\text{M}$ vs Control	<0.0001	****	Yes
2 $\mu\text{M}$ vs 4 $\mu\text{M}$	<0.0001	****	Yes
2 $\mu\text{M}$ vs 6 $\mu\text{M}$	<0.0001	****	Yes
2 $\mu\text{M}$ vs 8 $\mu\text{M}$	<0.0001	****	Yes
2 $\mu\text{M}$ vs 10 $\mu\text{M}$	<0.0001	****	Yes
4 $\mu\text{M}$ vs 6 $\mu\text{M}$	<0.0001	****	Yes
4 $\mu\text{M}$ vs 8 $\mu\text{M}$	<0.0001	****	Yes
4 $\mu\text{M}$ vs 10 $\mu\text{M}$	<0.0001	****	Yes
6 $\mu\text{M}$ vs 8 $\mu\text{M}$	<0.0001	****	Yes
6 $\mu\text{M}$ vs 10 $\mu\text{M}$	<0.0001	****	Yes
8 $\mu\text{M}$ vs 10 $\mu\text{M}$	<0.0001	****	Yes

Overall, the results in **section 2.4.8-2** indicate that Mia PaCa-2 spheroid growth was inhibited following incubation with MMF in the concentration range tested, with 10  $\mu\text{M}$  of MMF inducing the greatest reduction in spheroid volume.

## **2.4.9: Interrogation of the effect of EXBR on pancreatic cancer spheroid growth *in vitro***

### **2.4.9-1: Interrogation of the effect of EXBR on Panc-1 spheroid growth**

The spheroid growth delay assay was carried out as described in **section 2.3.6** to assess the effect of EXBR on pancreatic spheroid growth *in vitro*. Panc-1 spheroids were irradiated at a dose range of 0.5 – 6 Gy to determine the effect of EXBR on spheroid growth via change in volume ( $V/V_0$ ) and AUC analysis. The results are presented in **figure 2.12**.

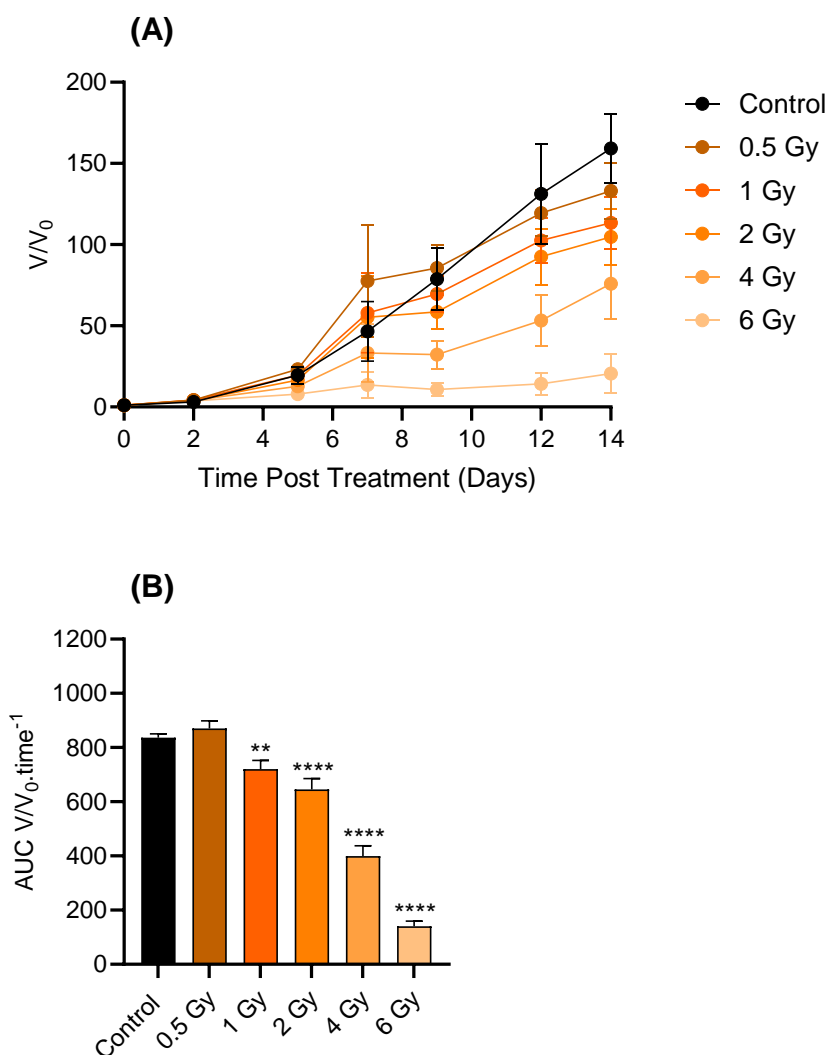


**Figure 2.12: Effect of EXBR on Panc-1 spheroid growth.** Panc-1 spheroids were exposed to varying doses (0.5 Gy – 6 Gy) EXBR and the change in volume ( $V/V_0$ ) and AUC calculated. (A)  $V/V_0$  for EXBR treated spheroids and untreated control. The data is represented as the average of three independent experiments carried out with 16 spheroids per treatment group (48 spheroids total)  $\pm$  standard deviation. (B) AUC for EXBR treated spheroids and untreated control, statistical significance shown in comparison with the untreated control. The data is represented as the average  $\pm$  standard deviation. \* =  $P \leq 0.05$ , \*\*\*\* =  $P \leq 0.0001$ .

As both  $V/V_0$  and AUC data obtained from Panc-1 spheroids treated with EXBR did not conform to normal distribution following a Shapiro-Wilk normality test, a Kruskal-Wallis with Dunn's post hoc test was used to assess the effect of the EXBR on spheroid growth when compared with the untreated control. In Panc-1 spheroids (**figure 2.12A**), only 4 Gy and 6 Gy of EXBR induced a statistically significant reduction in spheroid growth when compared with the untreated control spheroids ( $P < 0.0001$ ). Exposure to the highest dose of EXBR tested (6 Gy) induced in a 7.8-fold reduction in spheroid volume when compared with the untreated control spheroids (**figure 2.12A**). When comparing the different doses of EXBR tested in Panc-1 spheroids, 6 Gy of EXBR induced a statistically significantly greater reduction in Panc-1 spheroid growth when compared with all other doses tested ( $P < 0.0001$ ), a summary of these comparisons can be found in **table 2.23**.

**Table 2.23: Summary table of Kruskal-Wallis test of  $V/V_0$  for EXBR treated Panc-1 spheroids.**

Comparison	P-value	Summary	Significant?
0.5 Gy vs Control	0.8992	ns	No
1 Gy vs Control	>0.9999	ns	No
2 Gy vs Control	0.6031	ns	No
4 Gy vs Control	<0.0001	****	Yes
6 Gy vs Control	<0.0001	****	Yes
0.5 Gy vs 1 Gy	0.6135	ns	No
0.5 Gy vs 2 Gy	0.0240	*	Yes
0.5 Gy vs 4 Gy	<0.0001	****	Yes
0.5 Gy vs 6 Gy	<0.0001	****	Yes
1 Gy vs 2 Gy	>0.9999	ns	No
1 Gy vs 4 Gy	<0.0001	****	Yes
1 Gy vs 6 Gy	<0.0001	****	Yes
2 Gy vs 4 Gy	0.0043	**	Yes
2 Gy vs 6 Gy	<0.0001	****	Yes
4 Gy vs 6 Gy	<0.0001	****	Yes

When assessing the AUC for Panc-1 spheroids treated with EXBR (**figure 2.12B**), all doses induced a statistically significant reduction in AUC when compared with the untreated control spheroid ( $P \leq 0.020$ ), with the exception of spheroids treated with

0.5 Gy, whose growth did not statistically differ from the untreated control (P = 0.5229). However, 6 Gy induced a statistically significant reduction in AUC when compared with all lower concentration doses tested (P < 0.0001). A summary of comparisons can be found in **table 2.24**.

**Table 2.24: Summary table of Kruskal-Wallis test of AUC for EXBR treated Panc-1 spheroids.**

Comparison	P-value	Summary	Significant?
0.5 Gy vs Control	0.5229	ns	No
1 Gy vs Control	0.0020	**	Yes
2 Gy vs Control	<0.0001	****	Yes
4 Gy vs Control	<0.0001	****	Yes
6 Gy vs Control	<0.0001	****	Yes
0.5 Gy vs 1 Gy	0.0014	**	Yes
0.5 Gy vs 2 Gy	<0.0001	****	Yes
0.5 Gy vs 4 Gy	<0.0001	****	Yes
0.5 Gy vs 6 Gy	<0.0001	****	Yes
1 Gy vs 2 Gy	0.1003	ns	No
1 Gy vs 4 Gy	<0.0001	****	Yes
1 Gy vs 6 Gy	<0.0001	****	Yes
2 Gy vs 4 Gy	<0.0001	****	Yes
2 Gy vs 6 Gy	<0.0001	****	Yes
4 Gy vs 6 Gy	<0.0001	****	Yes

Overall, the results in **section 2.4.9-1** indicate that Panc-1 spheroid growth was inhibited following exposure to EXBR in the dose range tested, with 6 Gy inducing the greatest reduction in spheroid growth.

#### **2.4.9-2: Interrogation of the effect of EXBR on Mia PaCa-2 spheroid growth**

The spheroid growth delay assay was carried out as described in **section 2.3.6** to assess the effect of EXBR on pancreatic spheroid growth *in vitro*. Mia PaCa-2 spheroids were irradiated at a dose range of 0.5 – 6 Gy to determine the effect of EXBR on spheroid growth via change in volume ( $V/V_0$ ) and AUC analysis. The results are presented in **figure 2.13**.

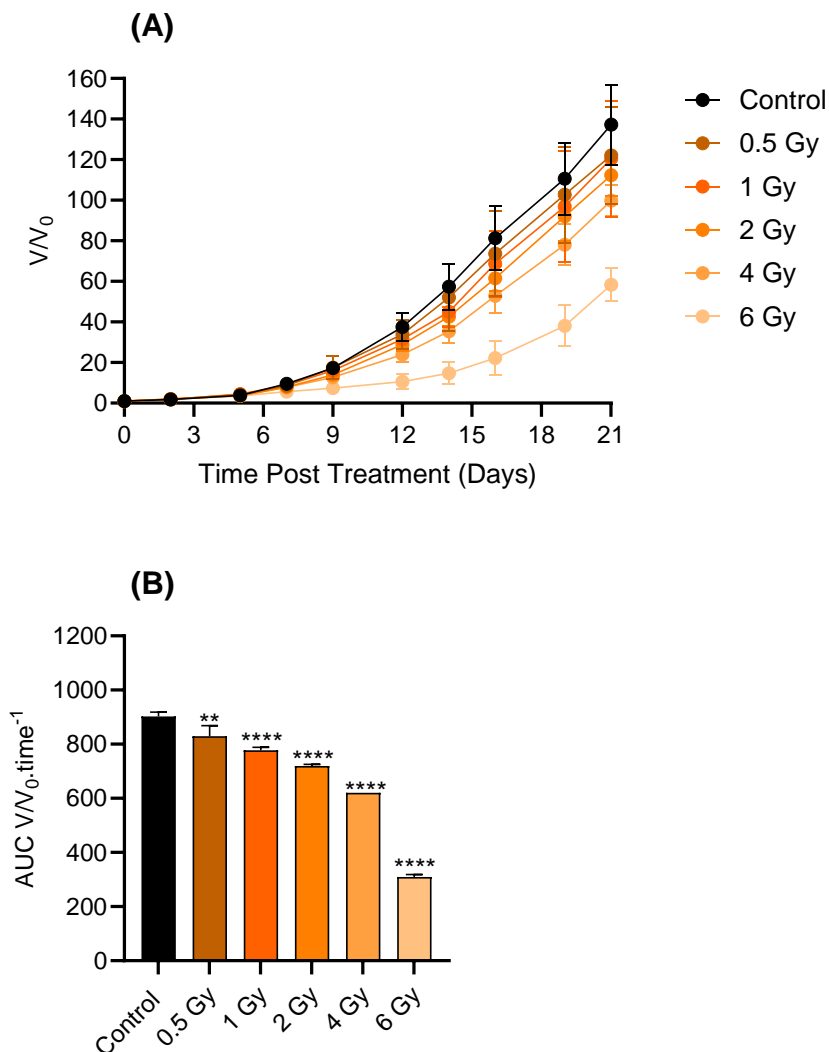


**Figure 2.13: Effect of EXBR on Mia PaCa-2 spheroid growth.** Mia PaCa-2 spheroids were exposed to varying doses (0.5 Gy – 6 Gy) EXBR and the change in volume ( $V/V_0$ ) and AUC calculated. (A)  $V/V_0$  for EXBR treated spheroids and untreated control. The data is represented as the average of three independent experiments carried out with 16 spheroids per treatment group (48 spheroids total)  $\pm$  standard deviation. (B) AUC for EXBR treated spheroids and untreated control, statistical significance shown in comparison with the untreated control. The data is represented as the average  $\pm$  standard deviation, some error bars too small to be shown on graph scale. \*\* =  $P \leq 0.01$ , \*\*\*\* =  $P \leq 0.0001$ .

As both  $V/V_0$  and AUC data obtained from Mia PaCa-2 spheroids treated with EXBR did not conform to normal distribution following a Shapiro-Wilk normality test, a Kruskal-Wallis with Dunn's post hoc test was used to assess the effect of the EXBR on spheroid growth when compared with the untreated control. In Mia PaCa-2 spheroids (**figure 2.13A**), only 4 Gy and 6 Gy of EXBR induced a statistically significant reduction in spheroid growth when compared with the untreated control spheroids ( $P \leq 0.0088$ ). Exposure to the highest dose of EXBR tested (6 Gy) induced a 2.35-fold reduction in spheroid growth when compared with the untreated control spheroids (**figure 2.13A**). When comparing the different doses of EXBR tested in Mia PaCa-2 spheroids, 6 Gy of EXBR induced a statistically significantly greater reduction in Mia PaCa-2 spheroid growth when compared with all other doses ( $P < 0.0001$ ), a summary of these comparisons can be found in **table 2.25**.

**Table 2.25: Summary table of Kruskal-Wallis test of  $V/V_0$  for EXBR treated Mia PaCa-2 spheroids.**

Comparison	P-value	Summary	Significant?
0.5 Gy vs Control	>0.9999	ns	No
1 Gy vs Control	0.9410	ns	No
2 Gy vs Control	0.2986	ns	No
4 Gy vs Control	0.0088	**	Yes
6 Gy vs Control	<0.0001	****	Yes
0.5 Gy vs 1 Gy	>0.9999	ns	No
0.5 Gy vs 2 Gy	>0.9999	ns	No
0.5 Gy vs 4 Gy	0.1746	ns	No
0.5 Gy vs 6 Gy	<0.0001	****	Yes
1 Gy vs 2 Gy	>0.9999	ns	No
1 Gy vs 4 Gy	0.7087	ns	No
1 Gy vs 6 Gy	<0.0001	****	Yes
2 Gy vs 4 Gy	>0.9999	ns	No
2 Gy vs 6 Gy	<0.0001	****	Yes
4 Gy vs 6 Gy	<0.0001	****	Yes

When assessing the AUC for Mia PaCa-2 spheroids treated with EXBR (**figure 2.13B**), all doses induced a statistically significant reduction in AUC when compared with the untreated control spheroids ( $P \leq 0.0014$ ). However, 6 Gy induced a

statistically significant reduction in AUC when compared with all lower concentration doses tested ( $P < 0.0001$ ). A summary of comparisons can be found in **table 2.26**.

**Table 2.26: Summary table of Kruskal-Wallis test of AUC for EXBR treated Mia PaCa-2 spheroids.**

Comparison	P-value	Summary	Significant?
0.5 Gy vs Control	0.0014	**	Yes
1 Gy vs Control	<0.0001	****	Yes
2 Gy vs Control	<0.0001	****	Yes
4 Gy vs Control	<0.0001	****	Yes
6 Gy vs Control	<0.0001	****	Yes
0.5 Gy vs 1 Gy	0.0420	*	Yes
0.5 Gy vs 2 Gy	0.0002	***	Yes
0.5 Gy vs 4 Gy	<0.0001	****	Yes
0.5 Gy vs 6 Gy	<0.0001	****	Yes
1 Gy vs 2 Gy	0.0214	*	Yes
1 Gy vs 4 Gy	<0.0001	****	Yes
1 Gy vs 6 Gy	<0.0001	****	Yes
2 Gy vs 4 Gy	0.0005	***	Yes
2 Gy vs 6 Gy	<0.0001	****	Yes
4 Gy vs 6 Gy	<0.0001	****	Yes

Overall, the results in **section 2.4.9-2** indicate that Mia PaCa-2 spheroid growth was inhibited following exposure to EXBR in the dose range tested, with 6 Gy inducing the greatest reduction in spheroid growth.

## 2.5: DISCUSSION

### 2.5.1: Cell growth characteristics

Before the cytotoxic effects of the selected agents could be assessed, the basic growth characteristics of each pancreatic cell line (Panc-1 and Mia PaCa-2) was established. We therefore investigated plating efficiency (colonies formed relative to the number of cells plated and cell doubling time (the time taken for one complete cell cycle) of Panc-1 and Mia PaCa-2. The results of these experiments were then used to establish the optimal protocol for the clonogenic assay (outlined in **section 2.3.4**), which would be used for assessing the cytotoxicity of the selected agents.

For the Panc-1 cell line the doubling time was experimentally determined to be  $18.27 \pm 0.02$  hours (**figure 2.1**). Based on literature research, the doubling time for Panc-1 cells appears highly variable and has been reported to range between 15.02 – 56 hours [142-144]. However, as methodology and conditions, as well as medium components vary considerably between laboratories and studies, this could explain the reported variability in doubling time.

For the Mia PaCa-2 cell line, the doubling time was experimentally determined to be  $24.82 \pm 0.5$  hours (**figure 2.1**). Based on literature research, the doubling time for Mia PaCa-2 cells appears highly variable and has been reported to range between 25.7 – 40 hours [137, 143].

Plating efficiency is a crucial metric in cell culture used for the assessment of consistency and reproducibility; the optimisation of culture conditions; and standardizing experimental procedures [145]. We therefore experimentally determined the optimal seeding density for Panc-1 and Mia PaCa-2. From the resulting data it was determined that 500 cells were the optimal seeding density as this number of cells gave a plating efficiency value of >50%, with Panc-1 at 60.6% and Mia PaCa-2 at 55.2% (**figure 2.1B**). Going forward 500 cells would be plated for the clonogenic assay.

DMF and MMF were solubilised in DMSO to create a drug solution. To determine if the DMSO present in the DMF/MMF treatments would have a statistically significant effect on cell clonogenicity, cells were exposed to a range of DMSO concentrations equivalent to that present in the treatments utilised in further experiments (**figure 2.1C**). None of the concentrations of DMSO tested statistically significantly varied from that of the untreated (0% DMSO) control, indicating that at the concentrations used, the DMSO has no effect on cell clonogenicity in both cell lines ( $P > 0.442$ ). Therefore, a DMSO control was not included going forward and instead an untreated

control used as DMSO had no effect and the use of an untreated control is one of the founding principles of the clonogenic assay [145, 146].

### **2.5.2: Cytotoxicity of gemcitabine *in vitro***

As previously mentioned, gemcitabine is the standard of care for the majority of patients with pancreatic cancer, whether in combination or as a monotherapy, therefore it was important to establish the sensitivity of the selected pancreatic cancer cell lines to this drug before testing any novel combination therapies. Gemcitabine cytotoxicity was tested via both the clonogenic (**section 2.4.2**) and spheroid growth delay assay (**section 2.4.6**), which as previously mentioned allow the effects of gemcitabine to be assessed in both 2D and 3D pancreatic cancer cell line models.

The results obtained from the clonogenic assay (**figure 2.2**) were as hypothesised, as gemcitabine effectively reduced pancreatic cancer clonogenicity in a dose dependent manner, as can be seen in the literature [147-149]. The IC<sub>50</sub> values obtained for both Panc-1 (1.021 µM following 24-hour incubation and 2.002 µM following 48-hour incubation) and Mia PaCa-2 (2.271 µM following 24-hour incubation and 0.7171 µM following 48-hour incubation) vary to that seen in the literature, however even within the literature itself, a wide variety of IC<sub>50</sub> values are reported. In Panc-1 IC<sub>50</sub> values have been reported ranging between 27 nM to 58 µM [148, 150] and 494 nM to 61 mM for Mia PaCa-2 [148, 151, 152], which implies that gemcitabine action is highly variable within these cell lines and dependant on exposure times & experimental parameters. In this particular instance the variability seen between incubation times could be due to intrinsic gemcitabine resistance within the cell lines caused by *TP53* mutation [137]. It has also been hypothesised in the literature that the treatment of pancreatic cells with a cytotoxic dose of gemcitabine elicits a rescue response in the surviving cells which allows them to better tolerate gemcitabine through modulation of transporter and exporter expression [153].

In the 3D pancreatic cancer cell line spheroid model, gemcitabine was highly effective at inhibiting spheroid growth (**section 2.4.2**) in both cell lines. This result was unexpected, as it was hypothesised that the spheroids would be more resistant to gemcitabine therapy as in the literature spheroids are reported to be more resistant to gemcitabine (and other chemotherapies) due to a multitude of factors including poor penetration of drug; the presence of quiescent and hypoxic cells; and increased multidrug resistance (MDR) gene expression [154-157]. Particularly multidrug resistance protein 1 (MRP1) and P-glycoprotein (P-gp) have been identified as key MDR proteins involved in resistance in spheroids, and are known to be overexpressed in pancreatic cancers, and further so in pancreatic spheroids [154, 155, 157]. The unexpected sensitivity to gemcitabine in spheroids of both cell lines could perhaps be explained by the overexpression of MRP1 and P-gp, as human cancer cell lines which over express these MDR proteins have been identified as more sensitive to gemcitabine due to an increase in deoxycytidine kinase (dCK) which coincides with increased MDR expression [158]. As previously mentioned dCK is the enzyme responsible for the phosphorylation of gemcitabine into gemcitabine monophosphate, which is the first key step in gemcitabine metabolism within the cell. Therefore, increased dCK expression in pancreatic spheroids could explain the increased sensitivity seen in **figures 2.6 & 2.7** as, gemcitabine would be more effectively converted into the active metabolite, gemcitabine triphosphate. To confirm this hypothesis further experimentation would be required, however in the literature studies carried out in 2D culture using both Panc-1 and Mia PaCa-2 cells indicated that dCK expression was greatly upregulated following the administration of gemcitabine [159].

### 2.5.3: Cytotoxicity of DMF *in vitro*

The effectiveness of DMF as a single treatment was investigated using both the clonogenic (**section 2.4.2**) and spheroid growth delay assay (**section 2.4.6**), which as previously mentioned allow the effects of DMF to be assessed in both 2D and 3D pancreatic cancer cell line models.

The rationale for selecting DMF as a candidate for pancreatic cancer therapy was due to its reported inhibitory effect on the transcription factor NRF2 [117], which could reduce the antioxidant response induced by conventional therapies and enhance therapeutic outcome in combination therapies. According to the literature, DMF was hypothesised to induce a cytotoxic effect at concentrations over 25  $\mu\text{M}$  [111], however these results were generated from a variety of types of cancer cell lines, not including pancreatic cancer cell lines. The results obtained in **figure 2.3** indicate that at 40  $\mu\text{M}$  and above DMF induced cytotoxicity in both cell lines.

In spheroids DMF proved to be more variable between the two pancreatic cell lines, with DMF having a lesser effect on reducing spheroid growth in Mia PaCa-2 (**figure 2.9**). Although there was no statistically significant reduction in spheroid growth in Mia PaCa-2 spheroids when treated with DMF, it can be observed that a reduction in spheroid growth began 16 days post treatment when compared with the untreated control. This result was unsurprising as spheroids are typically less sensitive to drugs when compared with 2D cell culture due to reduced drug penetration, pathophysiological differences due to hypoxia and alterations in the cell cycle [160]. However, in Panc-1 spheroids DMF induced a significant reduction in all concentration ranges tested (**figure 2.8**). This could be due to differences in spheroid composition, as studies in literature have identified that Panc-1 and Mia PaCa-2 spheroids differ in 3D structure, with Panc-1 forming a compact aggregate and Mia PaCa-2 forming a loose aggregate [161], based on this they determined that Panc-1

would be more suitable for 3D studies over Mia PaCa-2. Additionally, a studies identified that Panc-1 spheroids overexpress E-cadherin when compared with Mia PaCa-2 [162], again suggesting that the two cell lines fundamentally differ in 3D culture, as studies have shown that E-cadherin is essential to spheroid regulation and formation [163].

#### **2.5.4: Cytotoxicity of MMF *in vitro***

The efficacy of MMF as a single therapy was investigated using both the clonogenic (**section 2.4.2**) and spheroid growth delay assay (**section 2.4.6**), which as previously mentioned allow the effects of MMF to be assessed in both 2D and 3D pancreatic cancer cell models.

As previously mentioned, MMF is the active metabolite of DMF which results from the hydrolysis of DMF by digestive esterases in the small intestine of the body. In 2D studies utilising the clonogenic assay MMF was highly toxic in both cell lines (**figure 2.4**), with all concentrations tested inducing a significant reduction in clonogenicity when compared with the untreated control. Interestingly, MMF proved to be more cytotoxic than DMF, with much lower concentrations required to induce statistically significant reduction in clonogenicity (2  $\mu\text{M}$  MMF vs 40  $\mu\text{M}$  DMF) and lower  $\text{IC}_{50}$  values when using MMF vs DMF. This suggests that *in vitro* DMF is not converted into MMF at a high enough rate to induce the cytotoxicity seen when giving the drug directly as the active metabolite MMF. Therefore, it is hypothesised that the digestive esterases required for DMF metabolism are not highly expressed in *in vitro* studies. To confirm this hypothesis further studies would have to be undertaken as it is unclear from the literature whether digestive esterases are highly expressed by pancreatic cancer cell lines *in vitro*.

In spheroid studies (**figures 2.10 & 2.11**) MMF was highly effective in reducing spheroid growth in both cell lines, however a higher dose of 6  $\mu\text{M}$  MMF was required

to induce a significant reduction in spheroid growth when compared with the untreated control, which was three times higher than that of cells cultured in 2D. This result was expected, as previously mentioned spheroids tend to be more resistant to drug therapy when compared with 2D cell models.

### **2.5.5: EXBR induced cytotoxicity *in vitro***

The effectiveness of EXBR as a single therapy was investigated using both the clonogenic (**section 2.4.2**) and spheroid growth delay assay (**section 2.4.6**), which as previously mentioned allow the effects of EXBR to be assessed in both 2D and 3D pancreatic cancer cell models.

In 2D cell models, EXBR was highly effective at reducing clonogenicity in both cell lines (**figure 2.5**), with no statistical difference being observed between Panc-1 and Mia PaCa-2 when exposed to various doses of EXBR. The  $D_{50}$  value for Panc-1 has been reported in the literature to range between 2.19 – 3.31 Gy [164, 165], suggesting the obtained result of 1.47 Gy is slightly lower than would be anticipated, but the values reported in the literature again highlights the variability of the cell line. In Mia PaCa-2 the  $D_{50}$  determined to be 2.95 Gy, which is similar to values reported in literature of 2.47 Gy [166].

In the 3D spheroid model, both cell lines were less sensitive to EXBR than when exposed to EXBR in a 2D monolayer, with 4 Gy of radiation being required to induce significant reduction in spheroid volume when compared with the untreated control (**figures 2.12 & 2.13**). This result was expected, as previously mentioned spheroids tend to be more resistant to therapy, in particular radiotherapy, when compared with 2D cell models [167].

### 2.5.6: Conclusions

DMF exhibited limited cytotoxic effect as a single agent in both 2D and 3D studies, however as DMF is the prodrug, the result is not totally unexpected as DMF must undergo hydrolysis to become the active metabolite MMF to exhibit its cytotoxic effect. From this result we believe that DMF is not being effectively converted into MMF *in vitro*, however further studies would have to be carried out to validate or dispute this hypothesis.

Gemcitabine exhibited a cytotoxic effect in a dose dependent manner as we hypothesised and as seen in literature. Gemcitabine was highly effective at reducing pancreatic cancer spheroid growth, which was unexpected as spheroids are typically more resistant to therapy when compared with 2D cells. We believe this result was due to the increased expression of deoxycytidine kinase in the spheroids, which results in gemcitabine more readily metabolised into the active metabolite [158].

The results obtained from both 2D, and 3D cell studies show that MMF was highly cytotoxic to pancreatic cancer cells, unlike DMF. We believe these results suggest that MMF could have a potential role as a monotherapy for the treatment of pancreatic cancers, however given this would rely solely upon a single agent's cytotoxicity profile, it is likely that any potential treatments would be more efficacious in combination [168-170]. Therefore, the next steps in our investigation were to combine MMF with other agents in combination. DMF was still included going forward for comparisons sake.

**CHAPTER 3: Development and evaluation of combination  
therapies in pancreatic cancer cell line 2D & 3D cell models**

### **3.1: INTRODUCTION**

Now that the cytotoxic effects of the single therapies have been established in the previous chapter, the next phase of the project was to begin creating novel combination therapies utilising gemcitabine, DMF, MMF and EXBR.

Combination therapy refers to a treatment modality that combines two or more therapeutic agents together [168]. The development of new pharmaceutical anticancer agents is expensive and laborious, with an estimated 15 years required for the implementation of new agents into the pharmaceutical market following the developmental process [168]. Therefore, alternative approaches that combine existing anticancer agents together, and do not rely solely upon a single agent's originally developed cytotoxicity profile, to achieve a more efficient form of cancer therapy is an attractive option [168-170].

Conventional monotherapies often non-selectively target actively proliferating cells, which ultimately leads to the death of both cancerous and non-cancerous cells, meaning chemotherapy is typically toxic to the patient, leading to a multitude of side effects leaving the patient at risk of further complications/disease [168]. For example, gemcitabine is known to cause myelosuppression, leading to an increased chance of infection [171]. The use of combination therapy tends to decrease the toxicity of therapy as lower doses of the cytotoxic agents can be used [169, 170].

Another factor which can influence the potency of combination therapy is scheduling, where the sequence; duration; and dosing of agents can have a substantial effect on the efficacy of the combination [172] which has been demonstrated countless times in the literature [173-178]. For example, studies found that simultaneous administration of topotecan with Poly (ADP-ribose) polymerase (PARP) inhibitor PJ34 was more effective than administering topotecan 24 hours before or after PJ34 in the treatment of neuroblastoma [178].

For the purposes of this study, three different combination schedules were investigated: simultaneous administration of agents (schedule 1); drug administered 24 hours before EXBR (schedule 2); and fumarate administered 24 hours before gemcitabine (schedule 3).

The rationale for combining DMF/MMF with EXBR was as follows; 60% of the damage caused by radiation is due to the production of ROS as a result of the radiolysis of water molecules in cells [78]. In response to ROS, NRF2 is upregulated and initiates the antioxidant response, which includes the production of glutathione, to reduce ROS levels and protect the cell from oxidative stress [117]. As DMF/MMF is reported in the literature to be an inhibitor of NRF2 [117], and studies from our own lab have shown that DMF decreases the level of glutathione produced in the cell, we hypothesised that DMF/MMF would decrease the antioxidant response and allow the therapeutic effect of EXBR to be maximised.

The rationale for combining DMF/MMF with gemcitabine was as follows; gemcitabine is known to produce ROS through multiple mechanisms, for example gemcitabine can cause mitochondrial dysfunction, which leads to the leakage of electrons from the electron transport chain, resulting in the production of ROS and oxidative stress on the cell [179]. As the production of ROS elicits the antioxidant response through the upregulation of NRF2, we hypothesise that giving DMF/MMF in combination with gemcitabine would be beneficial as the antioxidant response would be diminished and allow the cytotoxic effect of gemcitabine to be maximised in the cell.

### **3.2: AIMS**

The aims of this chapter were therefore to develop novel combination therapies for the treatment of pancreatic cancer using *in vitro* 2D cell models. Following 2D cell

studies, the developed combinations were tested in 3D spheroid models. Additionally, the effect of different scheduling of components of the combinations was investigated.

### **3.3: MATERIALS AND METHODS**

#### **3.3.1: Cell Lines and Culture Conditions**

Cell lines were cultured as described previously in **section 2.3.1**.

#### **3.3.2: Treatments**

Drug solutions were prepared and diluted as previously described in **section 2.3.2**. For schedule 1 combinations both agents were administered simultaneously and incubated with the cells for a total of 48 hours. For schedule 2 combinations, the respective drug was added and incubated with the cells for 24 hours before irradiating the cells with 0.5 Gy of EXBR and incubating for a subsequent 24 hours (48-hour incubation total). For schedule 3 combinations the fumarate was added to the cells and incubated for 24 hours, before the addition of gemcitabine and incubated for a further 24 hours (48-hour incubation total). A diagrammatic representation of the schedules can be found in **figure 3.1**.

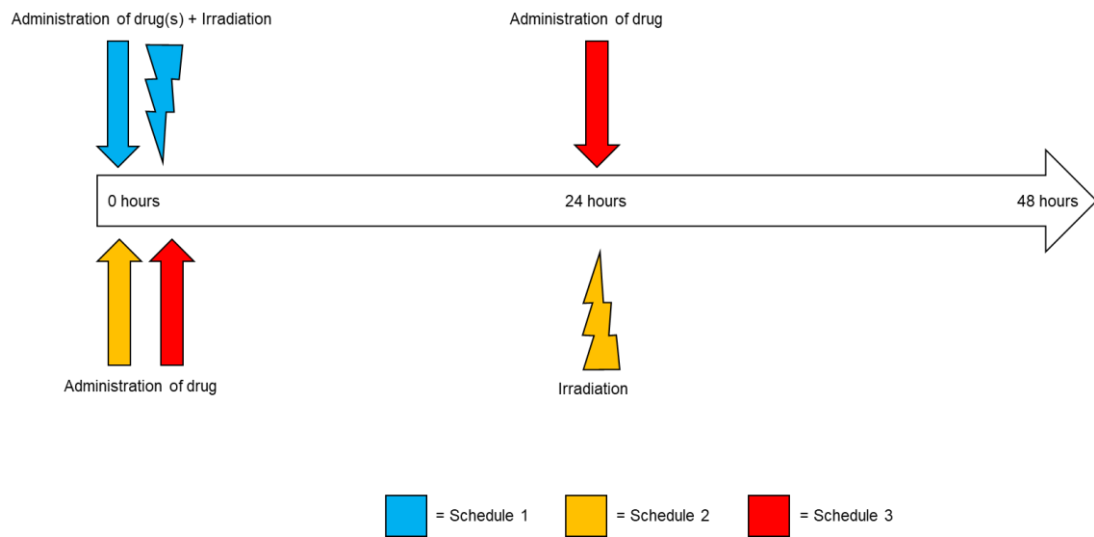


**Figure 3.1: Scheduling of combination therapies.** A diagrammatic representation of the three different schedules utilised are shown, with each treatment type lasting a total of 48 hours.

### **3.3.3: Clonogenic Assay**

The clonogenic assay was carried out as previously described in **section 2.3.4**, with the only modification being the treatment timings depending upon the combination schedule as described in **section 3.3.2**. Each clonogenic assay was carried out in triplicate, with three technical repeats per biological repeat.

### **3.3.4: Preparation of Low Attachment 96-well Plates for Spheroid Growth Assay**

Low attachment plates were prepared as previously described in **section 2.3.5**.

### **3.3.5: Spheroid Growth Assay**

The spheroid growth assay was carried out as previously described in **section 2.3.6**, with the only modification being the treatment timings depending upon the combination schedule as described in **section 3.3.2**. Each spheroid growth assay was carried out in triplicate, with sixteen technical repeats per biological repeat.

### **3.3.6: Spheroid Growth Analysis**

Spheroid growth analysis was carried out as previously described in **section 2.3.7**.

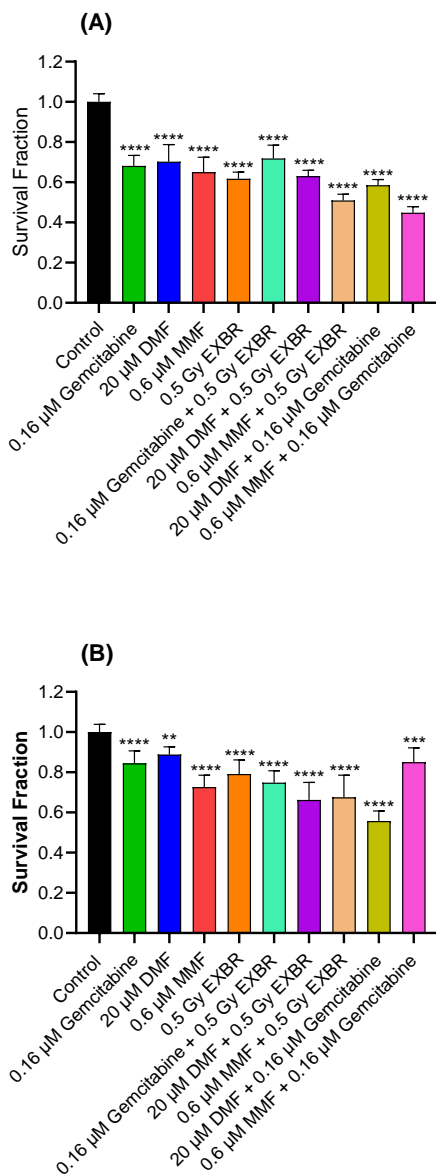
### **3.3.7: Statistical Analysis**

All statistical analysis was carried out using Graphpad Prism 10.1.2. Significance was assigned at an alpha ( $\alpha$ ) value  $\leq 0.05$ . Prior to carrying out any analysis on data, a Shapiro-Wilk normality test was used to determine if the data conformed to normal distribution (parametric or nonparametric), to allow for the selection of an appropriate statistical test. If the data was parametric a one-way ANOVA with Bonferroni post hoc test was used. If the data was nonparametric a Kruskal-Wallis with Dunn's post hoc test was used. For comparing between cell lines, a two-way ANOVA with Bonferroni post hoc test was used. The following labelling was used to convey significance: ns = not significant; \* =  $P \leq 0.05$ ; \*\* =  $P \leq 0.01$ ; \*\*\* =  $P \leq 0.001$ ; and \*\*\*\* =  $P \leq 0.0001$ .

## **3.4: RESULTS**

### **3.4.1: Development of schedule 1 combinations**

The clonogenic assay was carried out as described in **section 3.3.3** to assess the efficacy of schedule 1 combinations. In schedule 1 agents were administered simultaneously. This scheduling was tested as most conventional combination therapies are given simultaneously, e.g. FOLFIRINOX, as it improves patient compliance by simplifying the treatment regime and can lead to enhanced efficacy (Wei *et al.*, 2023). The dosing for drugs in the schedule 1 combinations are approximately  $IC_{10}$  values, based on the  $IC_{50}$  values obtained for both Panc-1 and Mia PaCa-2 presented in **chapter 2** to allow for the effect of the combination to be seen, as higher doses may have resulted in an inability to distinguish the effect of the combination from that of the single agent activity. The radiation dose was kept at 0.5 Gy as both cell lines were highly sensitive (**figure 2.5**) to EXBR and this was the lowest dose with the equipment available. The results are presented in **figure 3.2**.



(C)

Comparison	Cell Line	P-value	Summary	Significant?
0.16 $\mu$ M gemcitabine vs Control	Panc-1	<0.0001	****	Yes
	Mia PaCa-2	<0.0001	****	Yes
20 $\mu$ M DMF vs Control	Panc-1	<0.0001	****	Yes
	Mia PaCa-2	0.0030	**	Yes
0.6 $\mu$ M MMF vs Control	Panc-1	<0.0001	****	Yes
	Mia PaCa-2	<0.0001	****	Yes
0.5 Gy EXBR vs Control	Panc-1	<0.0001	****	Yes
	Mia PaCa-2	<0.0001	****	Yes
0.16 $\mu$ M gemcitabine + 0.5 Gy EXBR vs Control	Panc-1	<0.0001	****	Yes
	Mia PaCa-2	<0.0001	****	Yes
20 $\mu$ M DMF + 0.5 Gy EXBR vs Control	Panc-1	<0.0001	****	Yes
	Mia PaCa-2	<0.0001	****	Yes
0.6 $\mu$ M MMF + 0.5 Gy EXBR vs Control	Panc-1	<0.0001	****	Yes
	Mia PaCa-2	<0.0001	****	Yes
20 $\mu$ M DMF + 0.16 $\mu$ M gemcitabine vs Control	Panc-1	<0.0001	****	Yes
	Mia PaCa-2	<0.0001	****	Yes
0.6 $\mu$ M MMF + 0.16 $\mu$ M gemcitabine vs Control	Panc-1	<0.0001	****	Yes
	Mia PaCa-2	0.0001	***	Yes
0.16 $\mu$ M gemcitabine vs 0.6 $\mu$ M MMF + 0.16 $\mu$ M gemcitabine	Panc-1	0.6562	ns	No
	Mia PaCa-2	0.0066	**	Yes
0.16 $\mu$ M gemcitabine vs 20 $\mu$ M DMF + 0.16 $\mu$ M gemcitabine	Panc-1	0.0042	**	Yes
	Mia PaCa-2	<0.0001	****	Yes
0.16 $\mu$ M gemcitabine vs 0.6 $\mu$ M MMF + 0.16 $\mu$ M gemcitabine	Panc-1	<0.0001	****	Yes
	Mia PaCa-2	>0.9999	ns	No
20 $\mu$ M DMF vs 20 $\mu$ M DMF + 0.5 Gy EXBR	Panc-1	0.0320	*	Yes
	Mia PaCa-2	<0.0001	****	Yes
20 $\mu$ M DMF vs 20 $\mu$ M DMF + 0.16 $\mu$ M gemcitabine	Panc-1	0.0004	***	Yes
	Mia PaCa-2	<0.0001	****	Yes
0.6 $\mu$ M MMF vs 0.6 $\mu$ M MMF + 0.5 Gy EXBR	Panc-1	<0.0001	****	Yes
	Mia PaCa-2	0.7550	ns	No
0.6 $\mu$ M MMF vs 0.6 $\mu$ M MMF + 0.16 $\mu$ M gemcitabine	Panc-1	<0.0001	****	Yes
	Mia PaCa-2	0.0005	***	Yes
0.5 Gy EXBR vs 0.16 $\mu$ M gemcitabine + 0.5 Gy EXBR	Panc-1	0.0007	***	Yes
	Mia PaCa-2	0.6082	ns	No
0.5 Gy EXBR vs 20 $\mu$ M DMF + 0.5 Gy EXBR	Panc-1	>0.9999	ns	No
	Mia PaCa-2	0.0005	***	Yes
0.5 Gy EXBR vs 0.6 $\mu$ M MMF + 0.5 Gy EXBR	Panc-1	0.0002	***	Yes
	Mia PaCa-2	0.0109	*	Yes

**Figure 3.2: Schedule 1 combinations in pancreatic cancer cell lines.** (A) Survival fractions in Panc-1 cell line following treatment. (B) Survival fractions in Mia PaCa-2 cell line following treatment. Data is shown as the average of three independent experiments carried out in triplicate  $\pm$  standard deviation. Analysis was carried out via one-way ANOVA with Bonferroni post hoc test using GraphPad Prism 10.1.2. \*\* =  $P \leq 0.01$ ; \*\*\* =  $P \leq 0.001$ ; and \*\*\*\* =  $P \leq 0.0001$  in comparison with untreated control. (C) Statistical comparisons table.

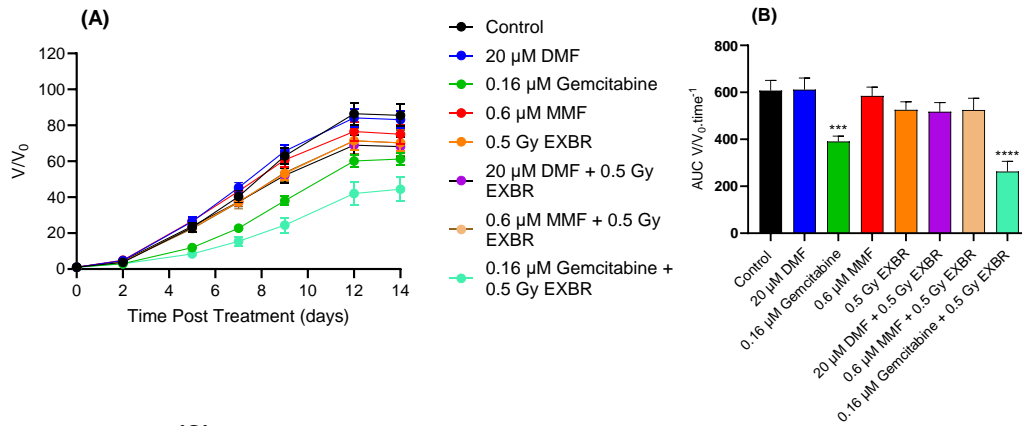
For a combination to be considered significant, it must have met the following criteria: induce significant reduction in clonogenicity when compared with the untreated control when compared with the individual components that make up the combination.

As can be seen in **figure 3.2** the schedule 1 combination of DMF + gemcitabine was the only combination to induce a statistically significant reduction in clonogenicity when compared with the untreated control ( $P < 0.0001$ ) in both Panc-1 and Mia PaCa-2. In Panc-1 the schedule 1 combinations of MMF + EXBR, and MMF + gemcitabine also induced a statistically significant reduction in clonogenicity when compared with the untreated control ( $P < 0.0001$ ). In Mia PaCa-2 the schedule 1 combination of DMF + EXBR also induced a statistically significant reduction in clonogenicity when compared with the untreated control ( $P < 0.0001$ ).

When comparing between the two cell lines using a two-way ANOVA with Bonferroni post hoc test, there was no statistically significant difference in clonogenicity between combinations in the cell lines ( $P > 0.9999$ ), with the exceptions of MMF + EXBR ( $P < 0.0001$ ) and MMF + gemcitabine ( $P < 0.0001$ ), which induced a statistically significantly greater reduction in clonogenicity in the Panc-1 cell line when compared with Mia PaCa-2.

Based on the results obtained in **figure 3.2** the schedule 1 combinations of MMF + EXBR; MMF + gemcitabine; and DMF + gemcitabine was selected to go forward for further analysis in **section 3.4.2**.

Prior to carrying out any spheroid experiments with the developed combinations, a small pilot study was carried out in Panc-1 spheroids using the schedule 1 combinations of DMF + EXBR, MMF + EXBR and gemcitabine + EXBR to aid in determining the appropriate dosing for future experiments. These results of this pilot study are presented in **figure 3.3**.



**(C)**

Comparison	Being Assessed	P-value	Summary	Significant?
Control vs 20 μM DMF	Spheroid growth	>0.9999	ns	No
	AUC	>0.9999	ns	No
Control vs 0.6 μM MMF	Spheroid growth	>0.9999	ns	No
	AUC	>0.9999	ns	No
Control vs 0.16 μM gemcitabine	Spheroid growth	0.0001	***	Yes
	AUC	<0.0001	****	Yes
Control vs 0.5 Gy EXBR	Spheroid growth	>0.9999	ns	No
	AUC	0.1479	ns	No
Control vs 20 μM DMF + 0.5 Gy EXBR	Spheroid growth	0.9168	ns	No
	AUC	0.1305	ns	No
Control vs 0.6 μM MMF + 0.5 Gy EXBR	Spheroid growth	>0.9999	ns	No
	AUC	0.3791	ns	No
Control vs 0.16 μM gemcitabine + 0.5 Gy EXBR	Spheroid growth	<0.0001	****	Yes
	AUC	<0.0001	****	Yes
20 μM DMF vs 20 μM DMF + 0.5 Gy EXBR	Spheroid growth	0.0439	*	Yes
	AUC	0.0014	**	Yes
0.5 Gy EXBR vs 20 μM DMF + 0.5 Gy EXBR	Spheroid growth	>0.9999	ns	No
	AUC	>0.9999	ns	No
0.6 μM MMF vs 0.6 μM MMF + 0.5 Gy EXBR	Spheroid growth	0.3718	ns	No
	AUC	0.4174	ns	No
0.5 Gy EXBR vs 0.6 μM MMF + 0.5 Gy EXBR	Spheroid growth	>0.9999	ns	No
	AUC	>0.9999	ns	No
0.16 μM gemcitabine vs 0.16 μM gemcitabine + 0.5 Gy EXBR	Spheroid growth	0.0025	**	Yes
	AUC	0.0020	**	Yes
0.5 Gy EXBR vs 0.16 μM gemcitabine + 0.5 Gy EXBR	Spheroid growth	<0.0001	****	Yes
	AUC	<0.0001	****	Yes

**Figure 3.3: Schedule 1 spheroid growth pilot study in Panc-1.** (A) Spheroid growth following treatment, data is represented as an average  $\pm$  standard deviation. Experiment was carried out in triplicate with 12 spheroids per treatment group per biological repeat (36 spheroids total). (B) AUC of spheroids following treatment, data is represented as an average  $\pm$  standard deviation (n = 3). Analysis was carried out via Kruskal-Wallis with Dunn's post hoc test using GraphPad Prism 10.1.2. \*\*\* = P  $\leq$  0.001 and \*\*\*\* = P  $\leq$  0.0001 in comparison with untreated control. (C) Statistical table of comparisons of combinations and monotherapies.

As can be seen in **figure 3.3**, 0.16  $\mu$ M + 0.5 Gy EXBR was the only combination to have induced a statistically significant effect on spheroid growth and AUC ( $P < 0.0001$ ). Based on this result it was decided that higher concentrations of combinations would likely need to be used going forward in spheroid experiments.

### **3.4.2: Analysis of schedule 1 combinations**

To assess the efficacy of the selected combinations from schedule 1, the clonogenic assay was repeated using alternative concentrations of the applicable drugs.

#### **3.4.2-1: Schedule 1 – MMF + EXBR**

Based on the results obtained in **figure 3.2** the schedule 1 combination of MMF + EXBR was selected for further analysis through the assay cascade as we believe MMF to overall be the most promising drug between DMF and MMF, as lower concentrations are required for a statistically significant effect when compared with DMF. The dosing for this combination was based on the monotherapy results obtained in **chapter 2**, and the dosing kept below the  $IC_{50}$  value to enable the effect of the combination to be seen. The dose of radiation was kept consistent at 0.5 Gy as both cell lines were highly sensitive to EXBR (**figure 2.5**) and this was the lowest dose with the equipment available. The incubation time of 48 hours was chosen to allow for comparison with the other schedules. The clonogenic assay was carried out as described in **section 3.3.3**, and the results presented in **figure 3.4**.

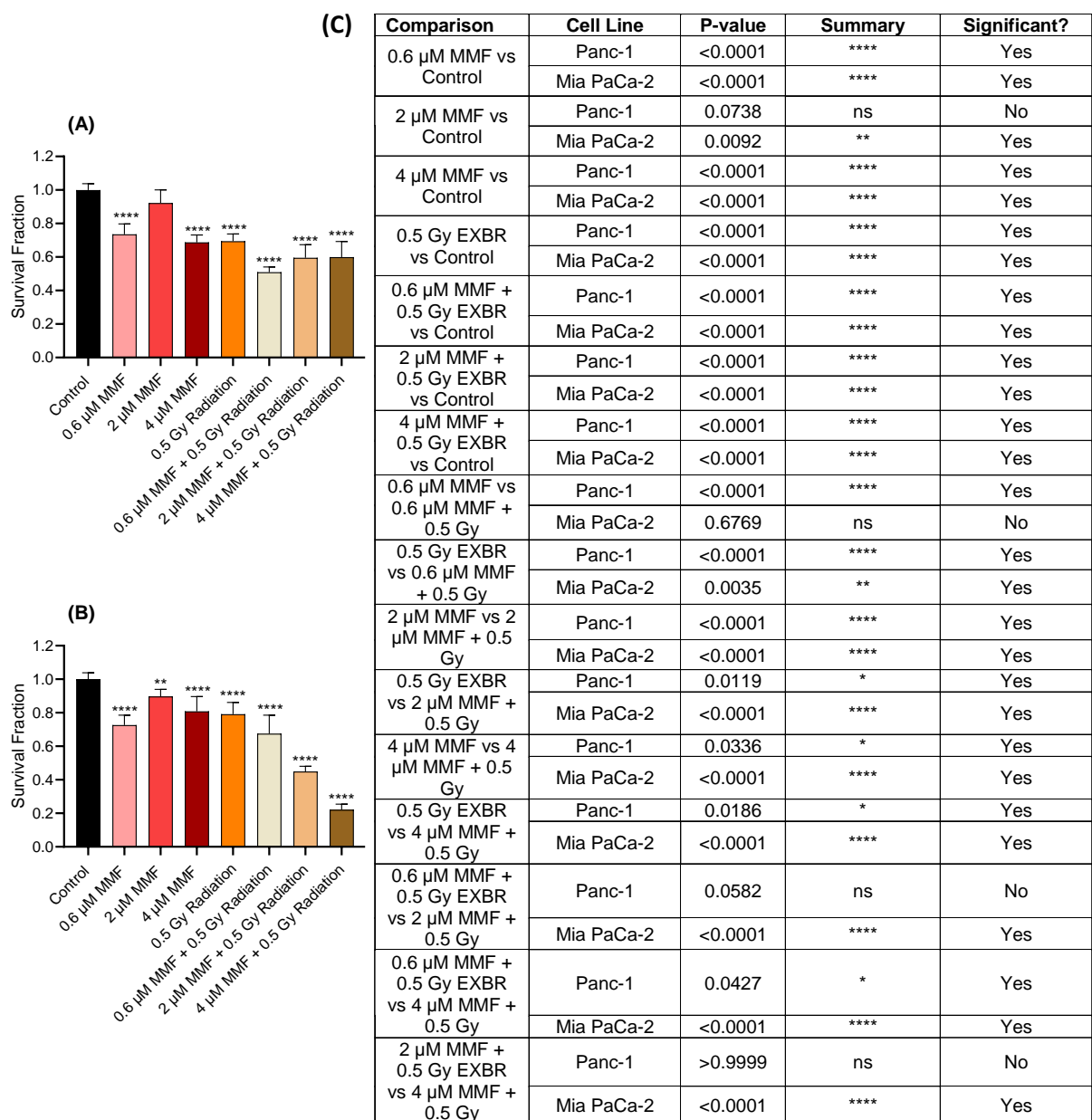


**Figure 3.4: Schedule 1 – MMF + EXBR analysis.** (A) Survival fractions in Panc-1 cell line following treatment. (B) Survival fractions in Mia PaCa-2 cell line following treatment. Analysis was carried out via one-way ANOVA with Bonferroni post hoc test using GraphPad Prism 10.1.2. \*\* =  $P \leq 0.01$  and \*\*\*\* =  $P \leq 0.0001$  in comparison with untreated control. (C) Statistical table of comparisons of combinations and monotherapies.

As can be seen in **figure 3.4** the schedule 1 combination of MMF + EXBR induced a significant reduction in clonogenicity when compared with the untreated control ( $P < 0.0001$ ) and monotherapies ( $P < 0.0186$ ) in both cell lines, with the exception of  $0.6 \mu\text{M}$  MMF +  $0.5 \text{ Gy}$  EXBR in Mia PaCa-2, as it did not induce a statistically significantly greater reduction in clonogenicity than  $0.6 \mu\text{M}$  MMF alone ( $P = 0.6769$ ).

In Panc-1 (**figure 3.4A**) the lowest concentration of the schedule 1 combination ( $0.6 \mu\text{M}$  MMF +  $0.5 \text{ Gy}$  EXBR) induced a significantly greater reduction in clonogenicity ( $P = 0.0427$ ) than the highest concentration ( $4 \mu\text{M}$  MMF +  $0.5 \text{ Gy}$  EXBR), however there was no statistical difference when compared with  $2 \mu\text{M}$  MMF +  $0.5 \text{ Gy}$  EXBR ( $P = 0.0582$ ). All concentrations of the combination induced a statistically significantly greater reduction in clonogenicity when compared with the monotherapies in Panc-1 cells ( $P \leq 0.0336$ ).

In Mia PaCa-2 (**figure 3.4B**)  $4 \mu\text{M}$  MMF +  $0.5 \text{ Gy}$  EXBR induced a significantly greater reduction in clonogenicity than both other concentrations tested ( $P < 0.0001$ ). All concentrations of the combination, except  $0.6 \mu\text{M}$  MMF +  $0.5 \text{ Gy}$  EXBR, induced a statistically significantly greater reduction in clonogenicity when compared with the monotherapies in Mia PaCa-2 cells ( $P < 0.0001$ ).

Following this test, the highest concentration of  $4 \mu\text{M}$  MMF +  $0.5 \text{ Gy}$  EXBR, was then tested in the 3D spheroid growth assay as described in **section 3.3.5**, and the results presented in **figure 3.5**. This dosing of the combination was selected as spheroids typically require higher dosing to elicit an effect when compared with 2D cell models, as indicated by the results in **figure 3.3**.

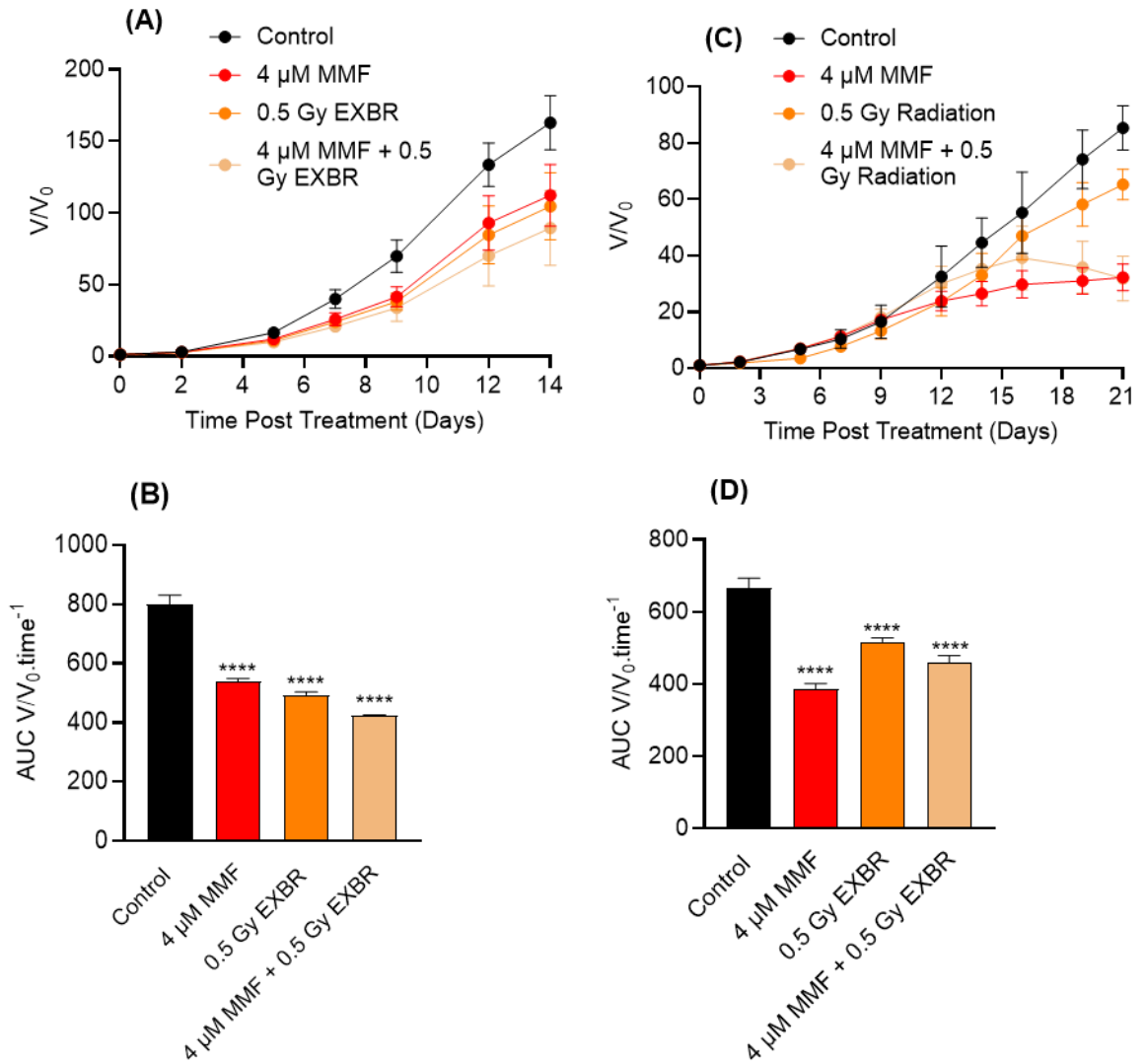


**Figure 3.5: Schedule 1 – MMF + EXBR spheroid growth assay in Panc-1 and MiaPaCa-2.** (A & C) Spheroid growth ( $V/V_0$ ) following treatment. The data is represented as the average of three independent experiments carried out with 16 spheroids per treatment group (48 spheroids total)  $\pm$  standard deviation. (B & D) AUC for treated spheroids and untreated control is shown. The data is represented as the average  $\pm$  standard deviation. Analysis was carried out via Kruskal-Wallis with Dunn's post hoc test using GraphPad Prism 10.1.2. \*\*\*\* =  $P \leq 0.0001$  in comparison with untreated control.

When interrogating change in volume ( $V/V_0$ ) in Panc-1 (**figure 3.5A**), the schedule 1 combination of 4  $\mu\text{M}$  MMF + 0.5 Gy EXBR induced a statistically significant reduction in spheroid growth when compared with the untreated control ( $P < 0.0001$ ). However, the combination did not induce a statistically significantly greater reduction in spheroid growth when compared with 4  $\mu\text{M}$  MMF ( $P = 0.1025$ ) and 0.5 Gy EXBR ( $P = 0.4663$ ) alone, suggesting there was no additional benefit to using the agents in combination in Panc-1 spheroids. To further investigate this observation the AUC was analysed (**figure 3.5B**) and the combination of 4  $\mu\text{M}$  MMF + 0.5 Gy EXBR induced a statistically significant reduction in the AUC when compared with the untreated control ( $P < 0.0001$ ). The combination induced a statistically significantly greater reduction in AUC when compared with 4  $\mu\text{M}$  MMF ( $P = < 0.0001$ ) and 0.5 Gy EXBR ( $P = 0.0016$ ), indicating the agents were of additional benefit in combination in Panc-1 spheroids.

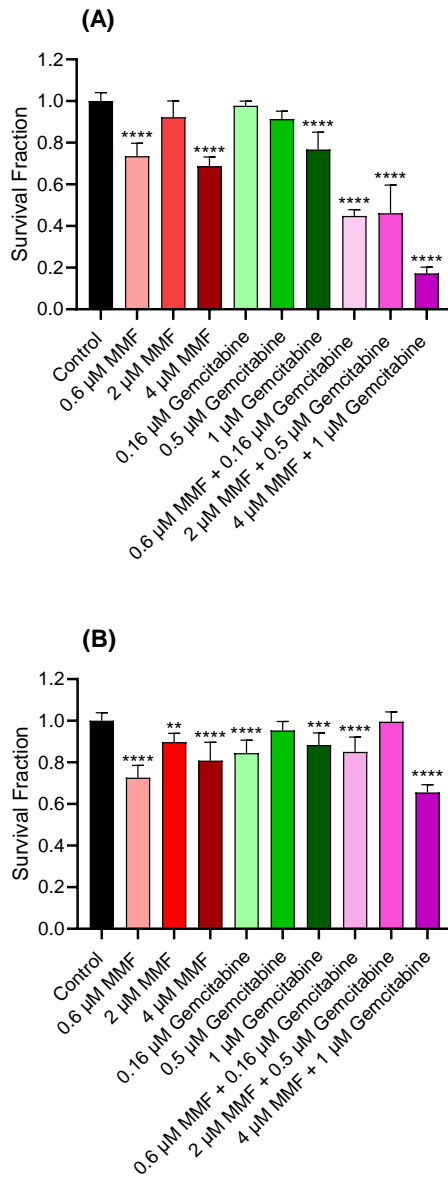
When interrogating the change in volume ( $V/V_0$ ) in Mia PaCa-2 spheroids (**figure 3.5C**), the schedule 1 combination of 4  $\mu\text{M}$  MMF + 0.5 Gy EXBR induced a statistically significant reduction in spheroid growth when compared with the untreated control ( $P = 0.0006$ ). However, the combination did not induce a statistically significantly greater reduction in spheroid growth when compared with 4  $\mu\text{M}$  MMF ( $P = 0.0543$ ) and 0.5 Gy EXBR ( $P > 0.9999$ ) alone, suggesting there was no additional benefit to using the agents in combination in Mia PaCa-2 spheroids. To further investigate this observation the AUC was analysed (**figure 3.5D**) and the combination of 4  $\mu\text{M}$  MMF + 0.5 Gy EXBR induced a statistically significant reduction in the AUC when compared with the untreated control ( $P = < 0.0001$ ). The combination induced a statistically significantly greater reduction in AUC when compared with 4  $\mu\text{M}$  MMF ( $P = 0.0045$ ) and 0.5 Gy EXBR ( $P = 0.0134$ ), indicating the agents were of additional benefit in combination in Mia PaCa-2 spheroids. A table depicting all statistical analysis carried out for **figure 3.5** can be found in **table 3.1**

**Table 3.1: Statistical comparisons for schedule 1 MMF + EXBR spheroid growth and AUC assay in Panc-1 and Mia PaCa-2.**

Comparison	Being Assessed	Cell Line	P-value	Summary	Significant?
4 $\mu$ M MMF vs Control	Spheroid growth	Panc-1	0.0029	**	Yes
		Mia PaCa-2	<0.0001	****	Yes
0.5 Gy EXBR vs Control	Spheroid growth	Panc-1	0.0002	***	Yes
		Mia PaCa-2	0.0060	**	Yes
4 $\mu$ M MMF + 0.5 Gy EXBR vs Control	Spheroid growth	Panc-1	<0.0001	****	Yes
		Mia PaCa-2	0.0006	****	Yes
4 $\mu$ M MMF vs 4 $\mu$ M MMF + 0.5 Gy	Spheroid growth	Panc-1	0.1025	ns	No
		Mia PaCa-2	0.0543	ns	No
0.5 Gy EXBR vs 4 $\mu$ M MMF + 0.5 Gy	Spheroid growth	Panc-1	0.4663	ns	No
		Mia PaCa-2	>0.9999	ns	No
4 $\mu$ M MMF vs Control	AUC	Panc-1	<0.0001	****	Yes
		Mia PaCa-2	<0.0001	****	Yes
0.5 Gy EXBR vs Control	AUC	Panc-1	<0.0001	****	Yes
		Mia PaCa-2	<0.0001	****	Yes
4 $\mu$ M MMF + 0.5 Gy EXBR vs Control	AUC	Panc-1	<0.0001	****	Yes
		Mia PaCa-2	<0.0001	****	Yes
4 $\mu$ M MMF vs 4 $\mu$ M MMF + 0.5 Gy	AUC	Panc-1	<0.0001	****	Yes
		Mia PaCa-2	0.0045	**	Yes
0.5 Gy EXBR vs 4 $\mu$ M MMF + 0.5 Gy	AUC	Panc-1	0.0016	**	Yes
		Mia PaCa-2	0.0134	*	Yes

### **3.4.2-2: Schedule 1 – MMF + gemcitabine**

Based on the results obtained in **figure 3.2** the schedule 1 combination of MMF + gemcitabine was selected for further analysis as we believe the combination showed promise, despite the result obtained for Mia PaCa-2 and hypothesised that altering the dosing may yield results in that cell line. The dosing for this combination was based on the monotherapy results obtained in **chapter 2**, and the dosing kept below the  $IC_{50}$  value to enable the effect of the combination to be seen. The incubation time of 48 hours was chosen to allow for comparison with the other schedules. The clonogenic assay was carried out as described in **section 3.3.3**, and the results presented in **figure 3.6**.



**(C)**

Comparison	Cell Line	P-value	Summary	Significant?
0.6 $\mu$ M MMF vs Control	Panc-1	<0.0001	****	Yes
	Mia PaCa-2	<0.0001	****	Yes
2 $\mu$ M MMF vs Control	Panc-1	0.1264	ns	No
	Mia PaCa-2	0.0022	**	Yes
4 $\mu$ M MMF vs Control	Panc-1	<0.0001	****	Yes
	Mia PaCa-2	<0.0001	****	Yes
0.16 $\mu$ M Gemcitabine vs Control	Panc-1	>0.9999	ns	No
	Mia PaCa-2	<0.0001	****	Yes
0.5 $\mu$ M Gemcitabine vs Control	Panc-1	0.0563	ns	No
	Mia PaCa-2	0.7925	ns	No
1 $\mu$ M Gemcitabine vs Control	Panc-1	<0.0001	****	Yes
	Mia PaCa-2	0.0004	***	Yes
0.6 $\mu$ M MMF + 0.16 $\mu$ M Gemcitabine vs Control	Panc-1	<0.0001	****	Yes
	Mia PaCa-2	<0.0001	****	Yes
2 $\mu$ M MMF + 0.5 $\mu$ M Gemcitabine vs Control	Panc-1	<0.0001	****	Yes
	Mia PaCa-2	>0.9999	ns	No
4 $\mu$ M MMF + 1 $\mu$ M Gemcitabine vs Control	Panc-1	<0.0001	****	Yes
	Mia PaCa-2	<0.0001	****	Yes
0.6 $\mu$ M MMF vs 0.6 $\mu$ M MMF + 0.16 $\mu$ M Gemcitabine	Panc-1	<0.0001	****	Yes
	Mia PaCa-2	0.0009	***	Yes
0.16 $\mu$ M Gemcitabine vs 0.6 $\mu$ M MMF + 0.16 $\mu$ M Gemcitabine	Panc-1	<0.0001	****	Yes
	Mia PaCa-2	>0.9999	ns	No
2 $\mu$ M MMF vs 2 $\mu$ M MMF + 0.5 $\mu$ M Gemcitabine	Panc-1	<0.0001	****	Yes
	Mia PaCa-2	0.0002	***	Yes
0.5 $\mu$ M Gemcitabine vs 2 $\mu$ M MMF + 0.5 $\mu$ M Gemcitabine	Panc-1	<0.0001	****	Yes
	Mia PaCa-2	0.1105	ns	No
4 $\mu$ M MMF vs 4 $\mu$ M MMF + 1 $\mu$ M Gemcitabine	Panc-1	<0.0001	****	Yes
	Mia PaCa-2	<0.0001	****	Yes
1 $\mu$ M Gemcitabine vs 4 $\mu$ M MMF + 1 $\mu$ M Gemcitabine	Panc-1	<0.0001	****	Yes
	Mia PaCa-2	<0.0001	****	Yes
0.6 $\mu$ M MMF + 0.16 $\mu$ M Gemcitabine vs 2 $\mu$ M MMF + 0.5 $\mu$ M Gemcitabine	Panc-1	>0.9999	ns	No
	Mia PaCa-2	<0.0001	****	Yes
0.6 $\mu$ M MMF + 0.16 $\mu$ M Gemcitabine vs 4 $\mu$ M MMF + 1 $\mu$ M Gemcitabine	Panc-1	<0.0001	****	Yes
	Mia PaCa-2	<0.0001	****	Yes
2 $\mu$ M MMF + 0.5 $\mu$ M Gemcitabine vs 4 $\mu$ M MMF + 1 $\mu$ M Gemcitabine	Panc-1	<0.0001	****	Yes
	Mia PaCa-2	<0.0001	****	Yes

**Figure 3.6: Schedule 1 – MMF + gemcitabine analysis.** (A) Survival fractions in Panc-1 cell line following treatment. (B) Survival fractions in Mia PaCa-2 cell line following treatment. (C) Statistical table of comparisons of combinations and monotherapies. Data is shown as the average of three independent experiments carried out in triplicate  $\pm$  standard deviation. Analysis was carried out via one-way ANOVA with Bonferroni post hoc test using GraphPad Prism 10.1.2. \*\* =  $P \leq 0.01$ , \*\*\* =  $P \leq 0.001$ ; and \*\*\*\* =  $P \leq 0.0001$  in comparison with untreated control.

As can be seen in **figure 3.6A** the schedule 1 combination of MMF + gemcitabine induced a significant reduction in clonogenicity when compared with the untreated control in Panc-1 cells at all concentrations tested ( $P < 0.0001$ ). However, in Mia PaCa-2 cells (**figure 3.6B**), only the highest concentration of the combination (4  $\mu$ M MMF + 1  $\mu$ M gemcitabine) induced a significant reduction in clonogenicity when compared with the untreated control ( $P < 0.0001$ ).

In Panc-1 cells (**figure 3.6A**) the highest concentration of the combination (4  $\mu$ M MMF + 1  $\mu$ M gemcitabine) a significant reduction in clonogenicity than the lower concentrations of the combination tested ( $P < 0.0001$ ). All concentrations of the combination induced a statistically significantly greater reduction in clonogenicity when compared with the monotherapies in Panc-1 cells ( $P < 0.0001$ ).

In Mia PaCa-2 (**figure 3.6B**) the highest concentration of the combination (4  $\mu$ M MMF + 1  $\mu$ M gemcitabine) induced a significant reduction in clonogenicity than the lower concentrations of the combination tested ( $P < 0.0001$ ). Only the highest concentration of the combination induced a statistically significantly greater reduction in clonogenicity when compared with the monotherapies in Mia PaCa-2 cells ( $P < 0.0001$ ).

Following this test, the highest concentration of 4  $\mu$ M MMF + 1  $\mu$ M gemcitabine, was then tested in the 3D spheroid growth assay as described in **section 3.3.5**, and the results presented in **figure 3.7**. This dosing of the combination was selected for spheroids as it was the only concentration to induce a statistically significantly greater reduction in clonogenicity when compared with the monotherapies in both cell lines ( $P < 0.0001$ ).

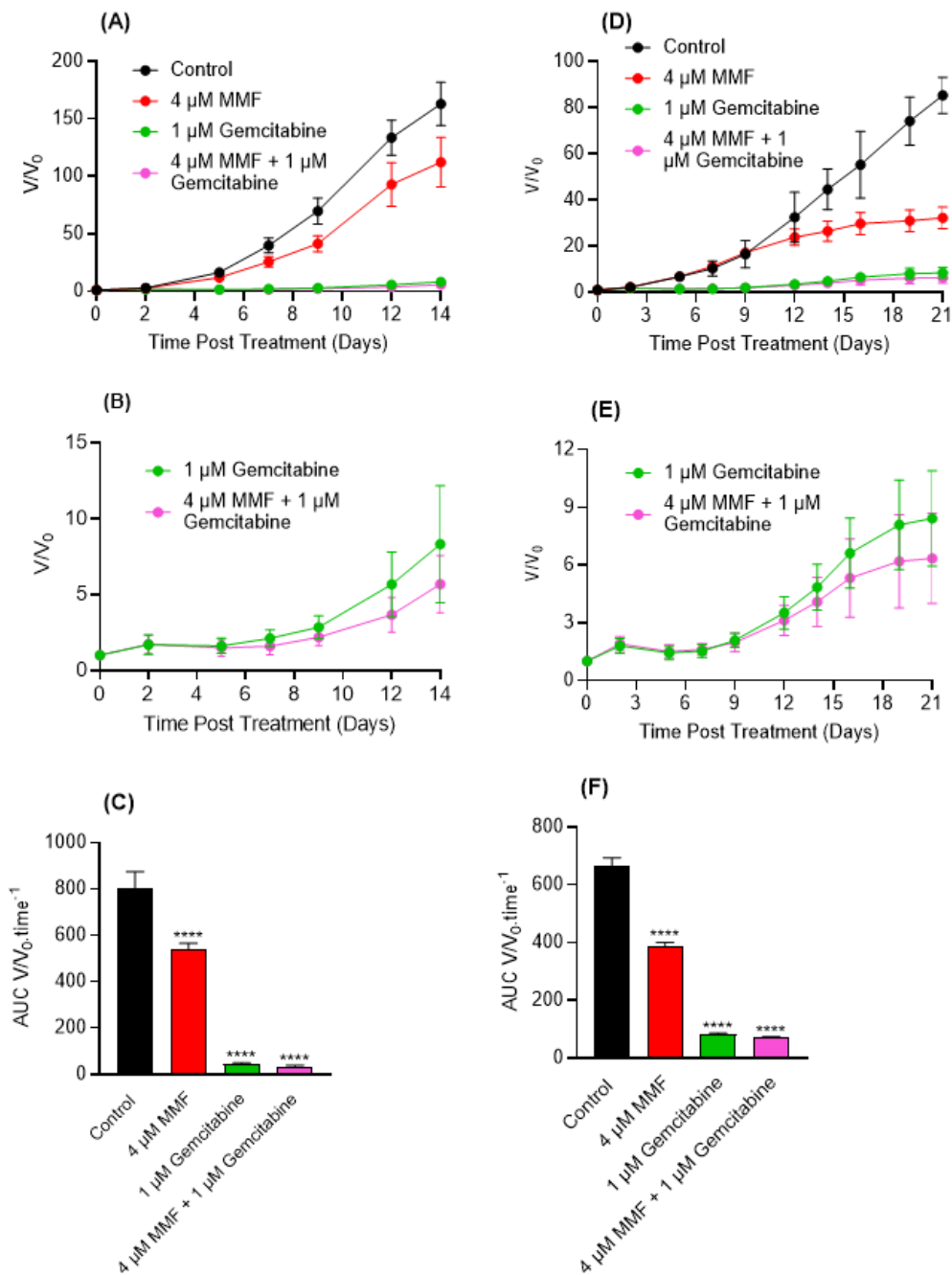


**Figure 3.7: Schedule 1 – MMF + gemcitabine spheroid growth assay in Panc-1 and MiaPaCa-2.** ((A&D) Spheroid growth (V/V<sub>0</sub>) following treatment. The data is represented as the average of three independent experiments carried out with 16 spheroids per treatment group (48 spheroids total) ± standard deviation. (B&E) V/V<sub>0</sub> for gemcitabine and MMF + gemcitabine treated spheroids alone is shown. (C&F) AUC for treated spheroids and untreated control is shown. The data is represented as the average ± standard deviation. Analysis was carried out via Kruskal-Wallis with Dunn's post hoc test using GraphPad Prism 10.1.2. \*\*\*\* = P ≤ 0.0001 in comparison with untreated control.

When interrogating the change in volume ( $V/V_0$ ) in Panc-1 (**figure 3.7A**), the schedule 1 combination of 4  $\mu\text{M}$  MMF + 1  $\mu\text{M}$  gemcitabine induced a statistically significant reduction in spheroid growth when compared with the untreated control ( $P < 0.0001$ ); 4  $\mu\text{M}$  MMF alone ( $P < 0.0001$ ); and 1  $\mu\text{M}$  gemcitabine (**figure 3.7B**) alone ( $P = 0.0408$ ), indicating the combination was of additional benefit in Panc-1 spheroids. To further investigate this observation, the AUC was analysed (**figure 3.7C**) and the combination of 4  $\mu\text{M}$  MMF + 1  $\mu\text{M}$  gemcitabine induced a statistically significant reduction in the AUC when compared with the untreated control and 4  $\mu\text{M}$  MMF alone ( $P < 0.0001$ ). However, the combination did not induce a statistically significantly greater reduction in AUC when compared with 1  $\mu\text{M}$  gemcitabine ( $P = 0.1968$ ), indicating the combination was of no additional benefit over gemcitabine monotherapy in Panc-1 spheroids.

In Mia PaCa-2 spheroids, the schedule 1 combination of 4  $\mu\text{M}$  MMF + 1  $\mu\text{M}$  gemcitabine (**figure 3.7D**) induced a statistically significant reduction in spheroid growth when compared with the untreated control ( $P < 0.0001$ ) and 4  $\mu\text{M}$  MMF alone ( $P < 0.0001$ ), however there was no statistically significant difference when compared with 1  $\mu\text{M}$  gemcitabine (**figure 3.7E**) alone ( $P = 0.2645$ ), suggesting there was no additional benefit to using the agents in combination in Mia PaCa-2 spheroids. To further investigate this observation, the AUC was analysed (**figure 3.7F**) and the combination of 4  $\mu\text{M}$  MMF + 1  $\mu\text{M}$  gemcitabine induced a statistically significant reduction in the AUC when compared with the untreated control ( $P < 0.0001$ ) and 4  $\mu\text{M}$  MMF ( $P < 0.0001$ ). However, when comparing the combination with 1  $\mu\text{M}$  gemcitabine alone, it did not induce a statistically significant reduction in AUC ( $P = 0.6811$ ), again indicating that there was no additional benefit to the drugs being administered in combination in Mia PaCa-2 spheroids when compared with the single

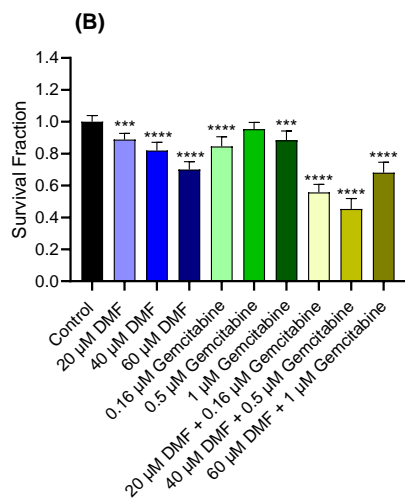
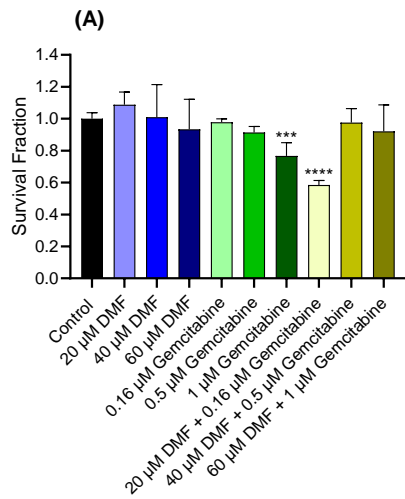
agents. A table depicting all statistical analysis carried out for **figure 3.7** can be found in **table 3.2**

**Table 3.2: Statistical comparisons for schedule 1 MMF + gemcitabine spheroid growth and AUC assay in Panc-1 and Mia PaCa-2.**

Comparison	Being Assessed	Cell Line	P-value	Summary	Significant?
4 $\mu$ M MMF vs Control	Spheroid growth	Panc-1	0.1339	ns	No
		Mia PaCa-2	0.0686	ns	No
1 $\mu$ M gemcitabine vs Control	Spheroid growth	Panc-1	<0.0001	****	Yes
		Mia PaCa-2	<0.0001	****	Yes
4 $\mu$ M MMF + 1 $\mu$ M gemcitabine vs Control	Spheroid growth	Panc-1	<0.0001	****	Yes
		Mia PaCa-2	<0.0001	****	Yes
4 $\mu$ M MMF vs 4 $\mu$ M MMF + 1 $\mu$ M gemcitabine	Spheroid growth	Panc-1	<0.0001	****	Yes
		Mia PaCa-2	<0.0001	****	Yes
1 $\mu$ M gemcitabine vs 4 $\mu$ M MMF + 1 $\mu$ M gemcitabine	Spheroid growth	Panc-1	0.0408	*	Yes
		Mia PaCa-2	0.2645	ns	No
4 $\mu$ M MMF vs Control	AUC	Panc-1	<0.0001	****	Yes
		Mia PaCa-2	<0.0001	****	Yes
1 $\mu$ M gemcitabine vs Control	AUC	Panc-1	<0.0001	****	Yes
		Mia PaCa-2	<0.0001	****	Yes
4 $\mu$ M MMF + 1 $\mu$ M gemcitabine vs Control	AUC	Panc-1	<0.0001	****	Yes
		Mia PaCa-2	<0.0001	****	Yes
4 $\mu$ M MMF vs 4 $\mu$ M MMF 1 $\mu$ M gemcitabine	AUC	Panc-1	<0.0001	****	Yes
		Mia PaCa-2	<0.0001	****	Yes
1 $\mu$ M gemcitabine vs 4 $\mu$ M MMF + 1 $\mu$ M gemcitabine	AUC	Panc-1	0.1968	ns	No
		Mia PaCa-2	0.6811	ns	No

### **3.4.2-3: Schedule 1 – DMF + gemcitabine**

Based on the results obtained in **figure 3.2** the schedule 1 combination of DMF + gemcitabine was selected for further analysis as we believe the combination showed promise, as the combination induced a statistically significantly greater effect than the individual monotherapies in both cell lines. The dosing for this combination was based on the monotherapy results obtained in **chapter 2**, and the dosing kept below the  $IC_{50}$  value to enable the effect of the combination to be seen. The incubation time of 48 hours was chosen to allow for comparison with the other schedules. The clonogenic assay was carried out as described in **section 3.3.3**, and the results presented in **figure 3.8**.



(C)

Comparison	Cell Line	P-value	Summary	Significant?
20 $\mu$ M DMF vs Control	Panc-1	0.9359	ns	No
	Mia PaCa-2	0.0002	***	Yes
40 $\mu$ M DMF vs Control	Panc-1	>0.9999	ns	No
	Mia PaCa-2	<0.0001	****	Yes
60 $\mu$ M DMF vs Control	Panc-1	>0.9999	ns	No
	Mia PaCa-2	<0.0001	****	Yes
0.16 $\mu$ M Gemcitabine vs Control	Panc-1	>0.9999	ns	No
	Mia PaCa-2	<0.0001	****	Yes
0.5 $\mu$ M Gemcitabine vs Control	Panc-1	>0.9999	ns	No
	Mia PaCa-2	0.6064	ns	No
1 $\mu$ M Gemcitabine vs Control	Panc-1	0.0004	***	Yes
	Mia PaCa-2	0.0001	***	Yes
20 $\mu$ M DMF + 0.16 $\mu$ M Gemcitabine vs Control	Panc-1	<0.0001	****	Yes
	Mia PaCa-2	<0.0001	****	Yes
40 $\mu$ M DMF + 0.5 $\mu$ M Gemcitabine vs Control	Panc-1	>0.9999	ns	No
	Mia PaCa-2	<0.0001	****	Yes
60 $\mu$ M DMF + 1 $\mu$ M Gemcitabine vs Control	Panc-1	>0.9999	ns	No
	Mia PaCa-2	<0.0001	****	Yes
20 $\mu$ M DMF vs 20 $\mu$ M DMF + 0.16 $\mu$ M Gemcitabine	Panc-1	<0.0001	****	Yes
	Mia PaCa-2	<0.0001	****	Yes
0.16 $\mu$ M Gemcitabine vs 20 $\mu$ M DMF + 0.16 $\mu$ M Gemcitabine	Panc-1	<0.0001	****	Yes
	Mia PaCa-2	<0.0001	****	Yes
40 $\mu$ M DMF vs 40 $\mu$ M DMF + 0.5 $\mu$ M Gemcitabine	Panc-1	0.9268	ns	No
	Mia PaCa-2	<0.0001	****	Yes
0.5 $\mu$ M Gemcitabine vs 40 $\mu$ M DMF + 0.5 $\mu$ M Gemcitabine	Panc-1	0.6846	ns	No
	Mia PaCa-2	<0.0001	****	Yes
60 $\mu$ M DMF vs 60 $\mu$ M DMF + 1 $\mu$ M Gemcitabine	Panc-1	0.9966	ns	No
	Mia PaCa-2	0.9273	ns	No
1 $\mu$ M Gemcitabine vs 60 $\mu$ M DMF + 1 $\mu$ M Gemcitabine	Panc-1	0.1255	ns	No
	Mia PaCa-2	<0.0001	****	Yes
20 $\mu$ M DMF + 0.16 $\mu$ M Gemcitabine vs 40 $\mu$ M DMF + 0.5 $\mu$ M Gemcitabine	Panc-1	<0.0001	****	Yes
	Mia PaCa-2	0.0038	**	Yes
20 $\mu$ M DMF + 0.16 $\mu$ M Gemcitabine vs 60 $\mu$ M DMF + 1 $\mu$ M Gemcitabine	Panc-1	<0.0001	****	Yes
	Mia PaCa-2	0.0007	***	Yes
40 $\mu$ M DMF + 0.5 $\mu$ M Gemcitabine vs 60 $\mu$ M DMF + 1 $\mu$ M Gemcitabine	Panc-1	0.6480	ns	No
	Mia PaCa-2	<0.0001	****	Yes

**Figure 3.8: Schedule 1 – DMF + gemcitabine analysis.** (A) Survival fractions in Panc-1 cell line following treatment. (B) Survival fractions in Mia PaCa-2 cell line following treatment. (C) Statistical table of comparisons of combinations and monotherapies. Data is shown as the average of three independent experiments carried out in triplicate  $\pm$  standard deviation. Analysis was carried out via one-way ANOVA with Bonferroni post hoc test using GraphPad Prism 10.1.2. \*\* =  $P \leq 0.01$ , \*\*\* =  $P \leq 0.001$ ; and \*\*\*\* =  $P \leq 0.0001$  in comparison with untreated control.

As can be seen in **figure 3.8A** only the lowest concentration of the schedule 1 DMF + gemcitabine (20  $\mu$ M DMF + 0.16  $\mu$ M gemcitabine) a significant reduction in clonogenicity when compared with the untreated control in Panc-1 cells ( $P < 0.0001$ ). However, in Mia PaCa-2 cells (**figure 3.8B**), the combination a significant reduction in clonogenicity at 40  $\mu$ M DMF + 0.5  $\mu$ M gemcitabine ( $P < 0.0001$ ) and 60  $\mu$ M DMF + 1  $\mu$ M gemcitabine ( $P < 0.0001$ ) when compared with the untreated control.

In Panc-1 cells (**figure 3.8A**) the lowest concentration of the schedule 1 combination (20  $\mu$ M DMF + 0.16  $\mu$ M gemcitabine) a significantly greater reduction in clonogenicity than the higher concentrations of the combination tested ( $P < 0.0001$ ). Only 20  $\mu$ M DMF + 0.16  $\mu$ M gemcitabine induced a statistically significantly greater reduction in clonogenicity than the individual monotherapies in Panc-1 cells ( $P < 0.0001$ ).

In Mia PaCa-2 cells (**figure 3.8B**) the lowest concentration of the combination (20  $\mu$ M DMF + 0.16  $\mu$ M gemcitabine) also induced a significant reduction in clonogenicity than the higher concentrations of the combination tested ( $P \leq 0.0038$ ). Both 20  $\mu$ M DMF + 0.16  $\mu$ M gemcitabine and 40  $\mu$ M DMF + 0.5  $\mu$ M gemcitabine induced a statistically significantly greater reduction in clonogenicity than the individual monotherapies in Mia PaCa-2 cells ( $P < 0.0001$ ).

Following this test, it was decided to assess a combination of 60  $\mu$ M DMF + 1  $\mu$ M gemcitabine, in the 3D spheroid growth assay as described in **section 3.3.5**, and the results presented in **figure 3.9**. These concentrations were selected as in previous experiments with alternative schedule 1 combinations, the lower concentrations in combination were ineffective at reducing spheroid growth when compared with the untreated control (**figure 3.3**), therefore it was decided to use the highest concentrations tested.

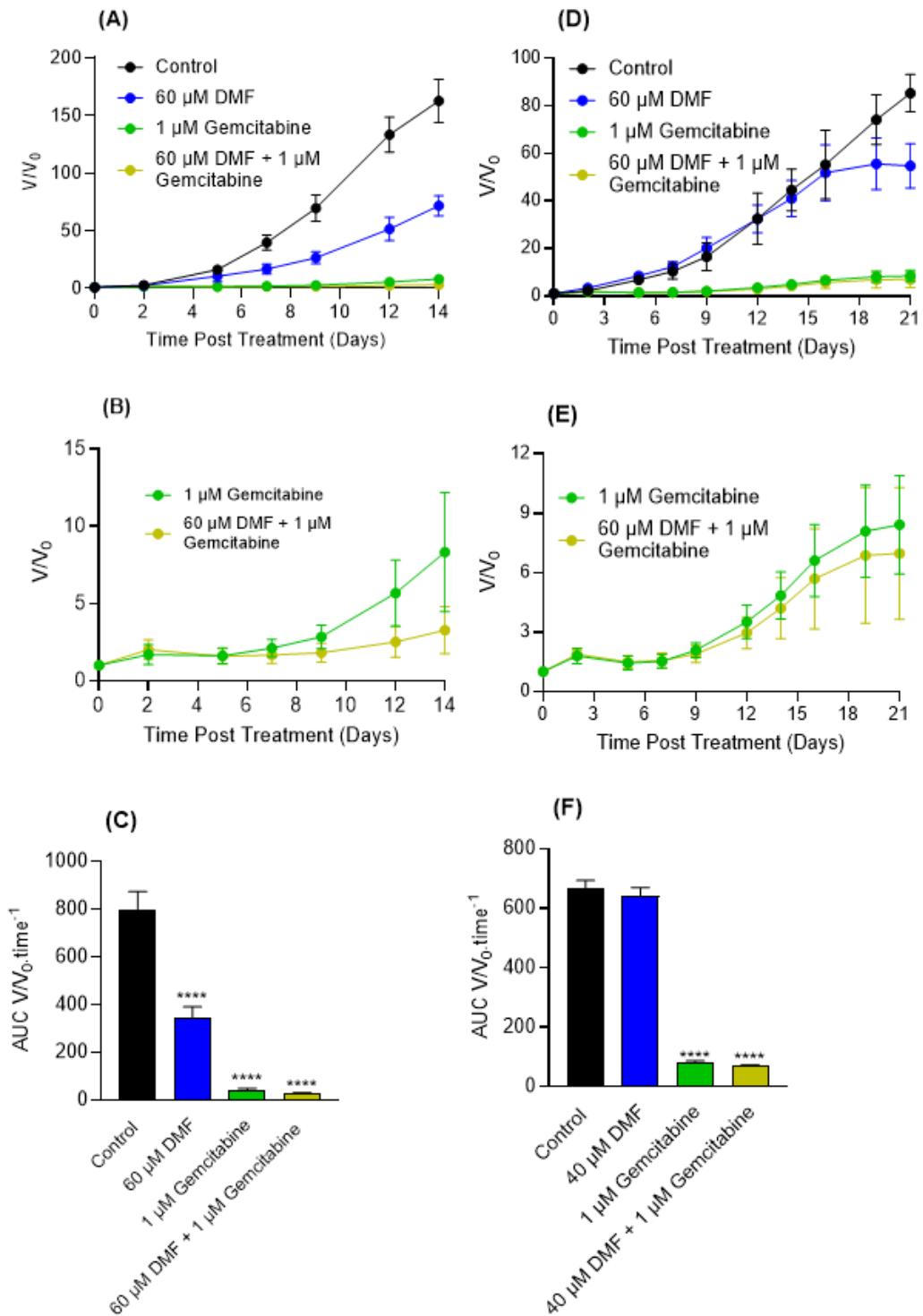


**Figure 3.9: Schedule 1 – DMF + gemcitabine spheroid growth assay in Panc-1 and Mia PaCa-2.** (A&D) Spheroid growth ( $V/V_0$ ) following treatment. The data is represented as the average of three independent experiments carried out with 16 spheroids per treatment group (48 spheroids total)  $\pm$  standard deviation. (B&E)  $V/V_0$  for gemcitabine and DMF + gemcitabine treated spheroids alone is shown. (C&F) AUC for treated spheroids and untreated control is shown. The data is represented as the average  $\pm$  standard deviation. Analysis was carried out via Kruskal-Wallis with Dunn's post hoc test using GraphPad Prism 10.1.2. \*\*\*\* =  $P \leq 0.0001$  in comparison with untreated control.

In Panc-1 spheroids (**figure 3.9A**), the schedule 1 combination of 60  $\mu\text{M}$  DMF + 1  $\mu\text{M}$  gemcitabine induced a statistically significant reduction in spheroid growth when compared with the untreated control ( $P < 0.0001$ ); 60  $\mu\text{M}$  DMF alone ( $P < 0.0001$ ); and 1  $\mu\text{M}$  gemcitabine (**figure 3.9B**) alone ( $P = 0.0001$ ), indicating that in contrast to the clonogenic assay, the agents in were of additional benefit in Panc-1 spheroids. To further investigate this observation, the AUC was analysed (**figure 3.9C**) and the combination of 60  $\mu\text{M}$  DMF + 1  $\mu\text{M}$  gemcitabine induced a statistically significant reduction in the AUC when compared with the untreated control ( $P < 0.0001$ ). When comparing the combination with its individual components, it induced a statistically significantly greater reduction in AUC when compared with 60  $\mu\text{M}$  DMF ( $P < 0.0001$ ) and 1  $\mu\text{M}$  gemcitabine ( $P = 0.0001$ ), again indicating the agents were of benefit in combination in Panc-1 spheroids.

In Mia PaCa-2 spheroids (**figure 3.9D**) the schedule 1 combination of 60  $\mu\text{M}$  DMF + 1  $\mu\text{M}$  gemcitabine induced a statistically significant reduction in spheroid growth when compared with the untreated control ( $P < 0.0001$ ) and 60  $\mu\text{M}$  DMF ( $P < 0.0001$ ), however there was no significant difference ( $P = 0.3501$ ) when compared with 1  $\mu\text{M}$  gemcitabine alone (**figure 3.9E**), indicating the agents were of no additional benefit in combination in Mia PaCa-2 spheroids. To further investigate this observation, the AUC (**figure 3.9F**) was analysed and the combination induced a significant reduction in AUC when compared with the untreated control ( $P < 0.0001$ ), as well as when compared with 60  $\mu\text{M}$  DMF alone ( $P < 0.0001$ ). However, there was no statistically significant difference between the combination of 60  $\mu\text{M}$  DMF + 1  $\mu\text{M}$  gemcitabine and 1  $\mu\text{M}$  gemcitabine alone ( $P = 0.8259$ ), again indicating the agents were of no additional benefit in combination in Mia PaCa-2 spheroids. A table depicting all statistical analysis carried out for **figure 3.9** can be found in **table 3.3**.

**Table 3.3: Statistical comparisons for schedule 1 MMF + gemcitabine spheroid growth and AUC assay in Panc-1 and Mia PaCa-2.**

Comparison	Being Assessed	Cell Line	P-value	Summary	Significant?
60 $\mu$ M DMF vs Control	Spheroid growth	Panc-1	0.4093	ns	No
		Mia PaCa-2	<0.9999	ns	No
1 $\mu$ M gemcitabine vs Control	Spheroid growth	Panc-1	<0.0001	****	Yes
		Mia PaCa-2	<0.0001	****	Yes
60 $\mu$ M DMF + 1 $\mu$ M gemcitabine vs Control	Spheroid growth	Panc-1	<0.0001	****	Yes
		Mia PaCa-2	<0.0001	****	Yes
60 $\mu$ M DMF vs 60 $\mu$ M DMF + 1 $\mu$ M gemcitabine	Spheroid growth	Panc-1	<0.0001	****	Yes
		Mia PaCa-2	<0.0001	****	Yes
1 $\mu$ M gemcitabine vs 60 $\mu$ M DMF + 1 $\mu$ M gemcitabine	Spheroid growth	Panc-1	0.0001	***	Yes
		Mia PaCa-2	0.3501	ns	No
60 $\mu$ M DMF vs Control	AUC	Panc-1	<0.0001	****	Yes
		Mia PaCa-2	0.3881	ns	No
1 $\mu$ M gemcitabine vs Control	AUC	Panc-1	<0.0001	****	Yes
		Mia PaCa-2	<0.0001	****	Yes
60 $\mu$ M DMF + 1 $\mu$ M gemcitabine vs Control	AUC	Panc-1	<0.0001	****	Yes
		Mia PaCa-2	<0.0001	****	Yes
60 $\mu$ M DMF vs 60 $\mu$ M DMF + 1 $\mu$ M gemcitabine	AUC	Panc-1	<0.0001	****	Yes
		Mia PaCa-2	<0.0001	****	Yes
1 $\mu$ M gemcitabine vs 60 $\mu$ M DMF + 1 $\mu$ M gemcitabine	AUC	Panc-1	0.2209	ns	No
		Mia PaCa-2	0.8259	ns	No

#### **3.4.2-4: Additional schedule 1 combination spheroid data**

In addition to the schedule 1 combinations presented previously, gemcitabine + EXBR and DMF + EXBR were also tested in Panc-1 and Mia PaCa-2 spheroids only, i.e. no additional clonogenic data was generated for these combinations in this schedule to allow for comparisons of the combination between schedules in spheroids.

The schedule 1 combination of 1  $\mu$ M gemcitabine + 0.5 Gy EXBR was tested in Panc-1 and Mia PaCa-2 spheroids, and the results presented in **figure 3.10**. This concentration was selected as it would allow comparison with the same combination in schedule 2.

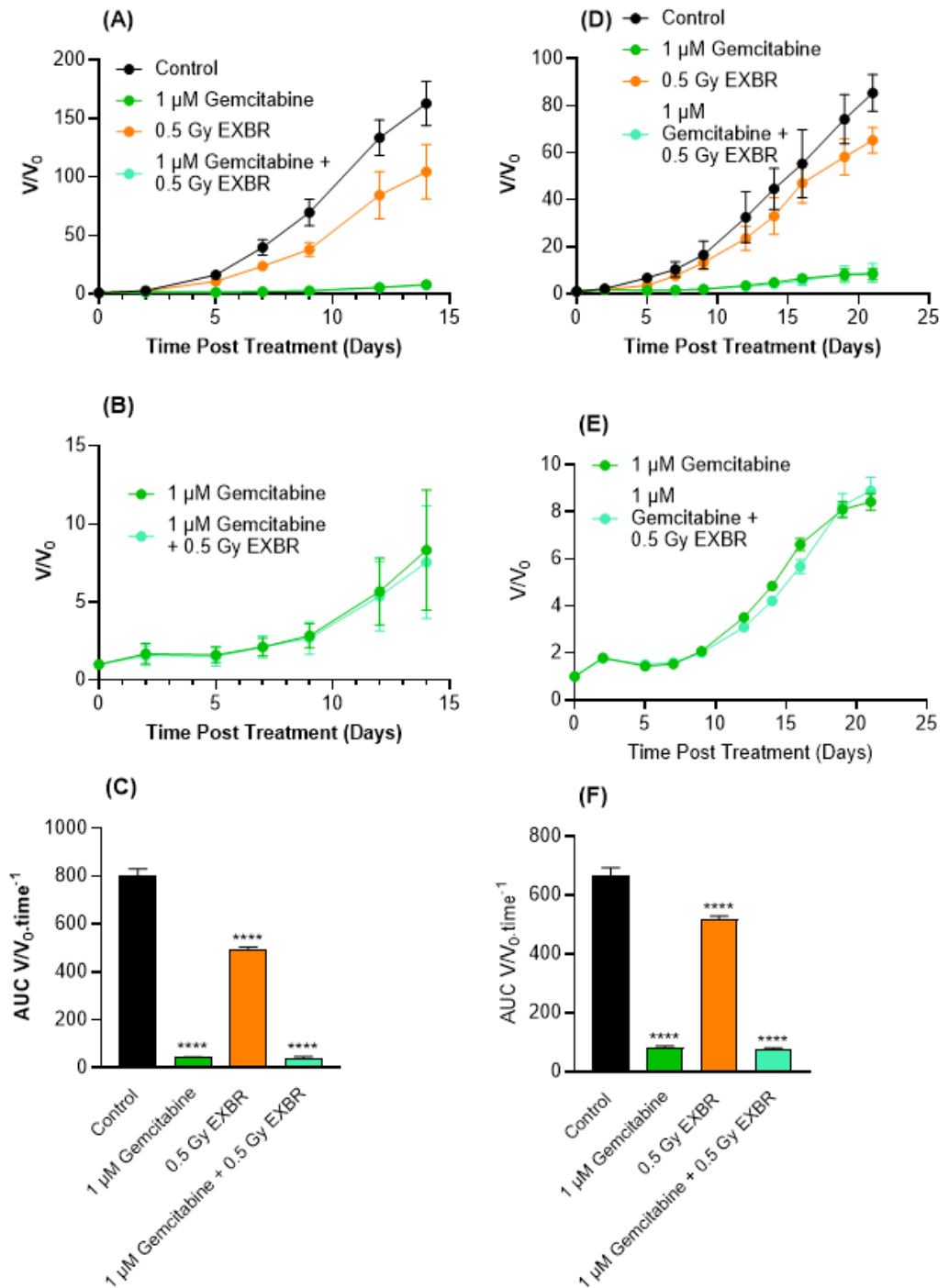


**Figure 3.10: Schedule 1 – gemcitabine + EXBR spheroid growth assay in Panc-1 and Mia PaCa-2.** ((A&D) Spheroid growth (V/V<sub>0</sub>) following treatment. The data is represented as the average of three independent experiments carried out with 16 spheroids per treatment group (48 spheroids total) ± standard deviation. (B&E) V/V<sub>0</sub> for gemcitabine and MMF + gemcitabine treated spheroids alone is shown. (C&F) AUC for treated spheroids and untreated control is shown. The data is represented as the average ± standard deviation. Analysis was carried out via Kruskal-Wallis with Dunn's post hoc test using GraphPad Prism 10.1.2. \*\*\*\* = P ≤ 0.0001 in comparison with untreated control.

When interrogating change in volume ( $V/V_0$ ) in Panc-1 (**figure 3.10A&B**), the schedule 1 combination of 1  $\mu\text{M}$  gemcitabine + 0.5 Gy EXBR induced a statistically significant reduction in spheroid growth when compared with the untreated control ( $P < 0.0001$ ). However, the combination did not induce a statistically significantly greater reduction in spheroid growth when compared with 1  $\mu\text{M}$  gemcitabine alone ( $P > 0.9999$ ), suggesting there was no additional benefit to using the agents in combination in Panc-1 spheroids. To further investigate this observation the AUC was analysed (**figure 3.10C**) and the combination of 1  $\mu\text{M}$  gemcitabine + 0.5 Gy EXBR induced a statistically significant reduction in the AUC when compared with the untreated control ( $P < 0.0001$ ), however there was no statistically significant difference when compared with 1  $\mu\text{M}$  gemcitabine alone ( $P = 0.9809$ ), again indicating the combination was of no additional benefit.

When interrogating the change in volume ( $V/V_0$ ) in Mia PaCa-2 spheroids (**figure 3.10D&E**), the schedule 1 combination of 1  $\mu\text{M}$  gemcitabine + 0.5 Gy EXBR induced a statistically significant reduction in spheroid growth when compared with the untreated control ( $P < 0.0001$ ). However, the combination did not induce a statistically significantly greater reduction in spheroid growth when compared with 1  $\mu\text{M}$  gemcitabine alone ( $P > 0.9999$ ), suggesting there was no additional benefit to using the agents in combination in Mia PaCa-2 spheroids. To further investigate this observation the AUC was analysed (**figure 3.10F**) and the combination of 1  $\mu\text{M}$  gemcitabine + 0.5 Gy EXBR induced a statistically significant reduction in the AUC when compared with the untreated control ( $P < 0.0001$ ), however there was no statistically significant difference when compared with 1  $\mu\text{M}$  gemcitabine alone ( $P > 0.9999$ ), again indicating the combination was of no additional benefit. A table depicting all statistical analysis carried out for **figure 3.10** can be found in **table 3.4**

**Table 3.4: Statistical comparisons for schedule 1 gemcitabine + EXBR spheroid growth and AUC assay in Panc-1 and Mia PaCa-2.**

Comparison	Being Assessed	Cell Line	P-value	Summary	Significant?
1 $\mu$ M gemcitabine vs Control	Spheroid growth	Panc-1	<0.0001	****	Yes
		Mia PaCa-2	<0.0001	****	Yes
0.5 Gy EXBR vs Control	Spheroid growth	Panc-1	0.0590	ns	No
		Mia PaCa-2	0.0300	*	Yes
1 $\mu$ M gemcitabine + 0.5 Gy EXBR vs Control	Spheroid growth	Panc-1	<0.0001	****	Yes
		Mia PaCa-2	<0.0001	****	Yes
1 $\mu$ M gemcitabine vs 1 $\mu$ M gemcitabine + 0.5 Gy	Spheroid growth	Panc-1	>0.9999	ns	No
		Mia PaCa-2	>0.9999	ns	No
0.5 Gy EXBR vs 1 $\mu$ M gemcitabine + 0.5 Gy	Spheroid growth	Panc-1	<0.0001	****	Yes
		Mia PaCa-2	<0.0001	****	Yes
1 $\mu$ M gemcitabine vs Control	AUC	Panc-1	<0.0001	****	Yes
		Mia PaCa-2	<0.0001	****	Yes
0.5 Gy EXBR vs Control	AUC	Panc-1	<0.0001	****	Yes
		Mia PaCa-2	<0.0001	****	Yes
1 $\mu$ M gemcitabine + 0.5 Gy EXBR vs Control	AUC	Panc-1	<0.0001	****	Yes
		Mia PaCa-2	<0.0001	****	Yes
1 $\mu$ M gemcitabine vs 1 $\mu$ M gemcitabine + 0.5 Gy	AUC	Panc-1	0.9809	ns	No
		Mia PaCa-2	0.9526	ns	No
0.5 Gy EXBR vs 1 $\mu$ M gemcitabine + 0.5 Gy	AUC	Panc-1	<0.0001	****	Yes
		Mia PaCa-2	<0.0001	****	Yes

The schedule 1 combination of 40  $\mu$ M DMF + 0.5 Gy EXBR was tested in Panc-1 and Mia PaCa-2 spheroids, and the results presented in **figure 3.11**. This concentration was selected as it would allow comparison with the same combination in schedule 2.

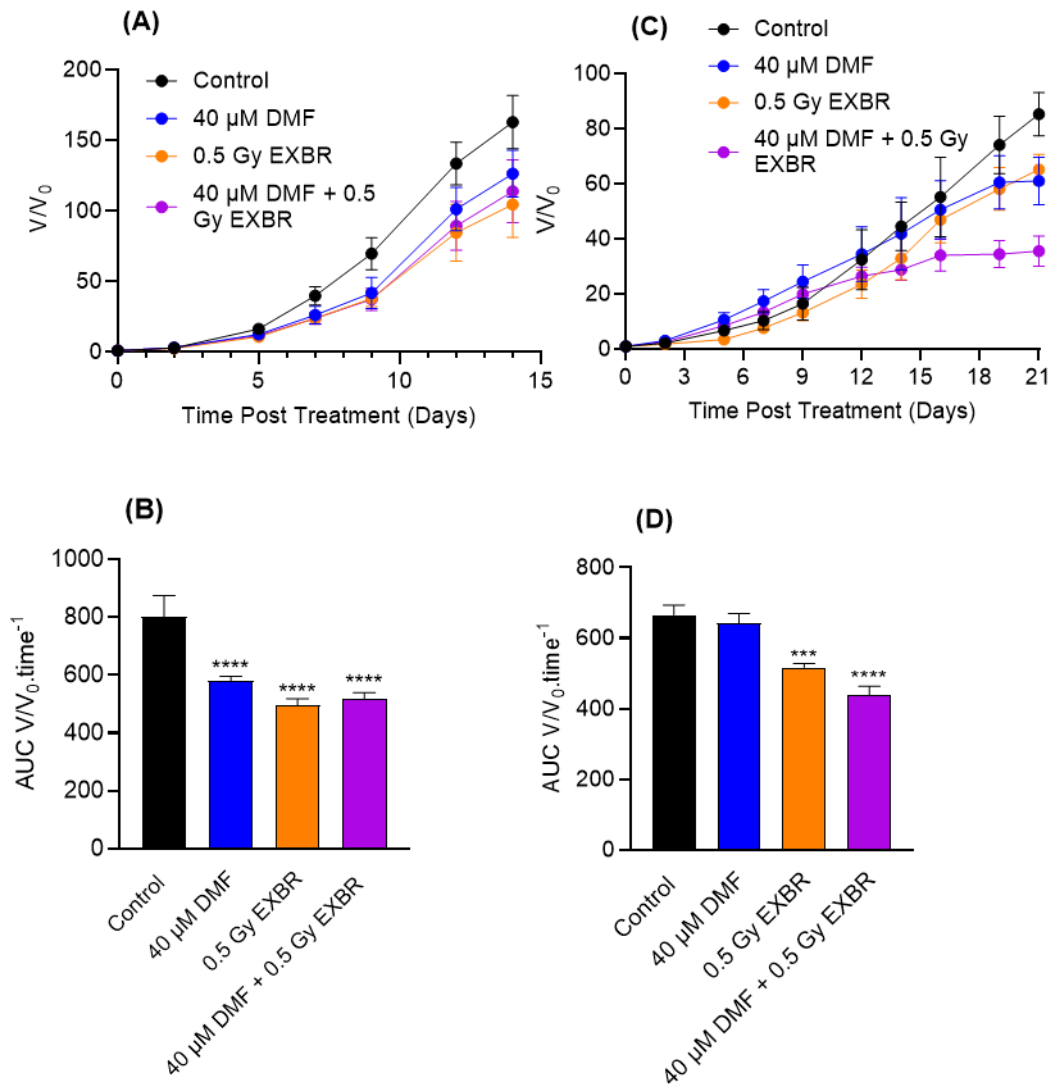


**Figure 3.11: Schedule 1 – DMF + EXBR spheroid growth assay in Panc-1 and MiaPaCa-2.** (A & C) Spheroid growth ( $V/V_0$ ) following treatment. The data is represented as the average of three independent experiments carried out with 16 spheroids per treatment group (48 spheroids total)  $\pm$  standard deviation. (B & D) AUC for treated spheroids and untreated control is shown. The data is represented as the average  $\pm$  standard deviation. Analysis was carried out via Kruskal-Wallis with Dunn's post hoc test using GraphPad Prism 10.1.2. \*\*\* =  $P \leq 0.001$ ; \*\*\*\* =  $P \leq 0.0001$  in comparison with untreated control.

When interrogating change in volume ( $V/V_0$ ) in Panc-1 (**figure 3.11A**), the schedule 1 combination of 40  $\mu$ M DMF + 0.5 Gy EXBR induced a statistically significant reduction in spheroid growth when compared with the untreated control ( $P = 0.0010$ ). However, the combination did not induce a statistically significantly greater reduction in spheroid growth when compared with 40  $\mu$ M DMF or 0.5 Gy EXBR alone ( $P > 0.9999$ ), suggesting there was no additional benefit to using the agents in combination in Panc-1 spheroids. To further investigate this observation the AUC was analysed (**figure 3.11B**) and the combination of 40  $\mu$ M DMF + 0.5 Gy EXBR induced a statistically significant reduction in the AUC when compared with the untreated control ( $P < 0.0001$ ). However, the combination did not induce a statistically significantly greater reduction in AUC when compared with 0.5 Gy EXBR alone ( $P = 0.2449$ ), again indicating the agents were not of additional benefit in combination in Panc-1 spheroids.

When interrogating change in volume ( $V/V_0$ ) in Mia PaCa-2 (**figure 3.11A**), the schedule 1 combination of 40  $\mu$ M DMF + 0.5 Gy EXBR induced a statistically significant reduction in spheroid growth when compared with the untreated control ( $P < 0.0001$ ). However, the combination did not induce a statistically significantly greater reduction in spheroid growth when compared with 0.5 Gy EXBR alone ( $P = 0.3798$ ), suggesting there was no additional benefit to using the agents in combination in Mia PaCa-2 spheroids. To further investigate this observation the AUC was analysed (**figure 3.11B**) and the combination of 40  $\mu$ M DMF + 0.5 Gy EXBR induced a statistically significant reduction in the AUC when compared with the untreated control ( $P < 0.0001$ ). The combination also induced a statistically significantly greater reduction in AUC when compared with 40  $\mu$ M DMF ( $P < 0.0001$ ) and 0.5 Gy EXBR ( $P = 0.0084$ ), indicating the agents were of additional benefit in combination in Mia PaCa-

2 spheroids. A table depicting all statistical analysis carried out for **figure 3.5** can be found in **table 3.5**.

**Table 3.5: Statistical comparisons for schedule 1 DMF + EXBR spheroid growth and AUC assay in Panc-1 and Mia PaCa-2.**

Comparison	Being Assessed	Cell Line	P-value	Summary	Significant?
40 $\mu$ M DMF vs Control	Spheroid growth	Panc-1	0.0203	*	Yes
		Mia PaCa-2	>0.9999	ns	No
0.5 Gy EXBR vs Control	Spheroid growth	Panc-1	<0.0001	****	Yes
		Mia PaCa-2	0.0031	**	Yes
40 $\mu$ M DMF + 0.5 Gy EXBR vs Control	Spheroid growth	Panc-1	0.0010	**	Yes
		Mia PaCa-2	<0.0001	****	Yes
40 $\mu$ M DMF vs 40 $\mu$ M DMF + 0.5 Gy	Spheroid growth	Panc-1	>0.9999	ns	No
		Mia PaCa-2	<0.0001	****	Yes
0.5 Gy EXBR vs 40 $\mu$ M DMF + 0.5 Gy	Spheroid growth	Panc-1	>0.9999	ns	No
		Mia PaCa-2	0.3798	ns	No
40 $\mu$ M DMF vs Control	AUC	Panc-1	<0.0001	****	Yes
		Mia PaCa-2	0.5267	ns	No
0.5 Gy EXBR vs Control	AUC	Panc-1	<0.0001	****	Yes
		Mia PaCa-2	0.0002	***	Yes
40 $\mu$ M DMF + 0.5 Gy EXBR vs Control	AUC	Panc-1	<0.0001	****	Yes
		Mia PaCa-2	<0.0001	****	Yes
40 $\mu$ M DMF vs 40 $\mu$ M DMF + 0.5 Gy	AUC	Panc-1	0.0033	**	Yes
		Mia PaCa-2	<0.0001	****	Yes
0.5 Gy EXBR vs 40 $\mu$ M DMF + 0.5 Gy	AUC	Panc-1	0.2449	ns	No
		Mia PaCa-2	0.0084	**	Yes

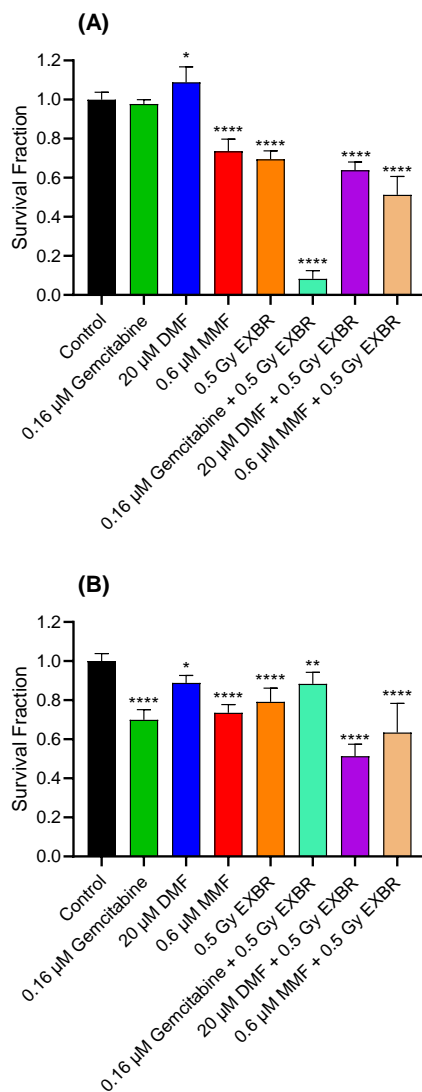
A summary of all tested schedule 1 combinations can be found in **table 3.6**.

**Table 3.6: Summary of the Schedule 1 combinations**

Schedule 1 combination	Greater effect than individual agents in Panc-1 cells?	Greater effect than individual agents in Panc-1 spheroids?	Greater effect than individual agents in Mia PaCa-2 cells?	Greater effect than individual agents in Mia PaCa-2 spheroids?
MMF + EXBR	Yes	Yes	Yes	No
MMF + Gemcitabine	Yes	Yes	Yes	No
DMF + Gemcitabine	No	Yes	Yes	No
Gemcitabine + EXBR	N/A	No	N/A	No
DMF + EXBR	N/A	No	N/A	Yes

**3.4.3: Development of schedule 2 combinations**

The clonogenic assay was carried out as described in **section 3.3.3** to assess the efficacy of schedule 2 combinations. For schedule 2 combinations, the respective drug was added and incubated with the cells for 24 hours before irradiating the cells with 0.5 Gy of EXBR and incubating for a subsequent 24 hours (48-hour incubation total). The dosing for drugs in the schedule 2 combinations are approximately IC<sub>10</sub> values, based on the IC<sub>50</sub> values obtained for both Panc-1 and Mia PaCa-2 presented in **chapter 2** to allow for the effect of the combination to be seen, as higher doses may have resulted in an inability to distinguish the effect of the combination from that of the single agent activity. The radiation dose was kept at 0.5 Gy as both cell lines were highly sensitive to EXBR (**figure 2.5**) and this was the lowest dose with the equipment available. The rationale for this scheduling was pre-treatment with DMF/MMF would decrease glutathione and allow EXBR to elicit a stronger cytotoxic effect. Gemcitabine + EXBR was included as a comparison to see how the novel combinations of DMF/MMF + EXBR performed, compared with the gold standard chemotherapy. The incubation time was 48 hours total to allow each component at least one full cell cycle following administration to illicit its effect. The results are presented in **figure 3.12**.



**(C)**

Comparison	Cell Line	P-value	Summary	Significant?
0.16 $\mu$ M Gemcitabine vs Control	Panc-1	<0.0001	****	Yes
	Mia PaCa-2	<0.0001	****	Yes
20 $\mu$ M DMF vs Control	Panc-1	0.1264	ns	No
	Mia PaCa-2	0.0022	**	Yes
0.6 $\mu$ M MMF vs Control	Panc-1	<0.0001	****	Yes
	Mia PaCa-2	<0.0001	****	Yes
0.5 Gy EXBR vs Control	Panc-1	>0.9999	ns	No
	Mia PaCa-2	<0.0001	****	Yes
0.16 $\mu$ M Gemcitabine + 0.5 Gy EXBR vs Control	Panc-1	0.0563	ns	No
	Mia PaCa-2	0.7925	ns	No
20 $\mu$ M DMF + 0.5 Gy EXBR vs Control	Panc-1	<0.0001	****	Yes
	Mia PaCa-2	0.0004	***	Yes
0.6 $\mu$ M MMF + 0.5 Gy EXBR vs Control	Panc-1	<0.0001	****	Yes
	Mia PaCa-2	<0.0001	****	Yes
0.16 $\mu$ M Gemcitabine vs Gemcitabine + 0.5 Gy EXBR	Panc-1	<0.0001	****	Yes
	Mia PaCa-2	<0.0001	****	Yes
0.5 Gy EXBR vs Gemcitabine + 0.5 Gy EXBR	Panc-1	<0.0001	****	Yes
	Mia PaCa-2	0.0076	**	Yes
20 $\mu$ M DMF vs 20 $\mu$ M DMF + 0.5 Gy EXBR	Panc-1	<0.0001	****	Yes
	Mia PaCa-2	<0.0001	****	Yes
0.5 Gy EXBR vs 20 $\mu$ M DMF + 0.5 Gy EXBR	Panc-1	0.0645	ns	No
	Mia PaCa-2	<0.0001	****	Yes
0.6 $\mu$ M MMF vs 0.6 $\mu$ M MMF + 0.5 Gy EXBR	Panc-1	<0.0001	****	Yes
	Mia PaCa-2	0.0770	ns	No
0.5 Gy EXBR vs 0.6 $\mu$ M MMF + 0.5 Gy EXBR	Panc-1	<0.0001	****	Yes
	Mia PaCa-2	0.0047	**	No

**Figure 3.12: Schedule 2 combinations in pancreatic cancer cell lines.** (A) Survival fractions in Panc-1 cell line following treatment. (B) Survival fractions in Mia PaCa-2 cell line following treatment. Data is shown as the average of three independent experiments carried out in triplicate  $\pm$  standard deviation. Analysis was carried out via one-way ANOVA with Bonferroni post hoc test using GraphPad Prism 10.1.2. \* =  $P \leq 0.05$ ; \*\* =  $P \leq 0.01$ ; and \*\*\*\* =  $P \leq 0.0001$  in comparison with untreated control.

For a combination to be considered significant, it must have met the following criteria: induce significant reduction in clonogenicity when compared with the untreated control when compared with the individual components that make up the combination.

As can be seen in **figure 3.12A** the schedule 2 combinations of gemcitabine + EXBR and MMF + EXBR were the only combinations tested to induce a statistically significant reduction in clonogenicity when compared with the untreated control and individual monotherapies in Panc-1 cells ( $P < 0.0001$ ). In Mia PaCa-2 cells (**figure 3.12B**) the schedule 2 combination of DMF + EXBR was the only combination tested to induce a statistically significant reduction in clonogenicity when compared with the untreated control and the individual monotherapies ( $P < 0.0001$ ).

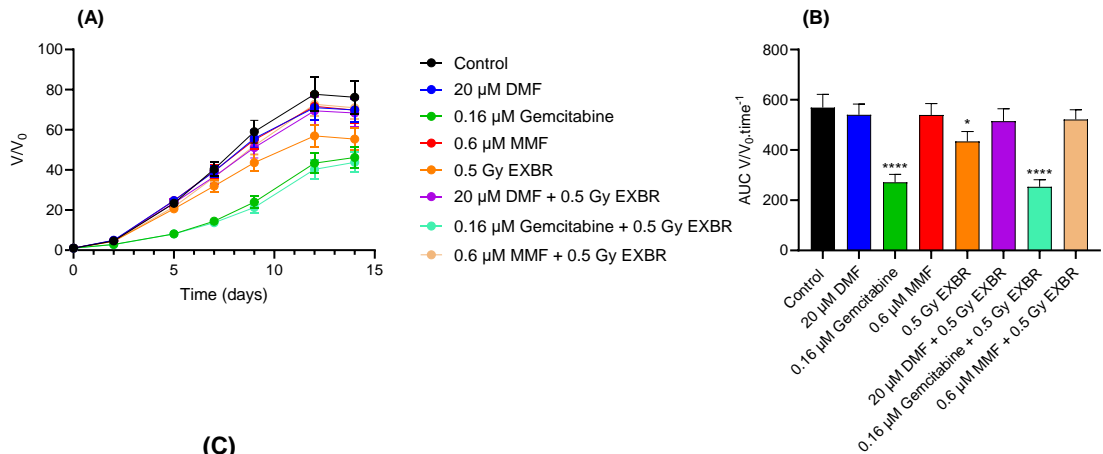
When comparing the reduction in clonogenicity induced by the combinations between the two cell lines using a two-way ANOVA with Bonferroni post hoc test, there was statistical difference in the reduction in clonogenicity between all three schedule 2 combinations in the cell lines. The combination of gemcitabine + EXBR induced a statistically significantly greater reduction in clonogenicity in Panc-1 cells when compared with Mia PaCa-2 cells ( $P < 0.0001$ ), as did the combination of MMF + radiation ( $P = 0.0011$ ). However, the combination of DMF + EXBR induced statistically significantly greater reduction in clonogenicity in Mia PaCa-2 cells than in Panc-1 cells ( $P = 0.0007$ ).

Based on the results obtained in **figure 3.12**, all three combinations assessed in schedule 2 were selected to go forward for further analysis in **section 3.4.4** as the combinations induced a greater reduction in clonogenicity than the respective single agents.

Prior to carrying out any spheroid experiments with the developed combinations, a small pilot study was carried out in Panc-1 spheroids using the schedule 2

combinations to aid in determining the appropriate dosing for future experiments.

These results of this pilot study are presented in **figure 3.13**.



**(C)**

Comparison	Being Assessed	P-value	Summary	Significant?
Control vs 20 μM DMF	Spheroid growth	>0.9999	ns	No
	AUC	>0.9999	ns	No
Control vs 0.6 μM MMF	Spheroid growth	>0.9999	ns	No
	AUC	>0.9999	ns	No
Control vs 0.16 μM gemcitabine	Spheroid growth	<0.0001	****	Yes
	AUC	<0.0001	****	Yes
Control vs 0.5 Gy EXBR	Spheroid growth	0.0700	ns	No
	AUC	0.0116	*	Yes
Control vs 20 μM DMF + 0.5 Gy EXBR	Spheroid growth	>0.9999	ns	No
	AUC	0.8221	ns	No
Control vs 0.6 μM MMF + 0.5 Gy EXBR	Spheroid growth	>0.9999	ns	No
	AUC	>0.9999	ns	No
Control vs 0.16 μM gemcitabine + 0.5 Gy EXBR	Spheroid growth	<0.0001	****	Yes
	AUC	<0.0001	****	Yes
20 μM DMF vs 20 μM DMF + 0.5 Gy EXBR	Spheroid growth	0.7818	ns	No
	AUC	0.4388	ns	No
0.5 Gy EXBR vs 20 μM DMF + 0.5 Gy EXBR	Spheroid growth	0.0477	*	Yes
	AUC	0.2394	ns	No
0.6 μM MMF vs 0.6 μM MMF + 0.5 Gy EXBR	Spheroid growth	0.8841	ns	No
	AUC	>0.9999	ns	No
0.5 Gy EXBR vs 0.6 μM MMF + 0.5 Gy EXBR	Spheroid growth	0.0340	*	Yes
	AUC	0.0248	*	Yes
0.16 μM gemcitabine vs 0.16 μM gemcitabine + 0.5 Gy EXBR	Spheroid growth	0.7642	ns	No
	AUC	>0.9999	ns	No
0.5 Gy EXBR vs 0.16 μM gemcitabine + 0.5 Gy EXBR	Spheroid growth	<0.0001	****	Yes
	AUC	<0.0001	****	Yes

**Figure 3.13: Schedule 2 spheroid growth pilot study in Panc-1.** (A) Spheroid growth following treatment, data is represented as an average  $\pm$  standard deviation. Experiment was carried out in triplicate with 12 spheroids per treatment group per biological repeat (36 spheroids total). (B) AUC of spheroids following treatment, data is represented as an average  $\pm$  standard deviation ( $n = 3$ ). Analysis was carried out via Kruskal-Wallis with Dunn's post hoc test using GraphPad Prism 10.1.2. \* =  $P \leq 0.05$ ; \*\* =  $P \leq 0.01$ ; and \*\*\*\* =  $P \leq 0.0001$  in comparison with untreated control. (C) Statistical table of comparisons of combinations and monotherapies.

As can be seen in **figure 3.13**, no combinations induced a statistically significantly greater reduction in spheroid growth when compared with the relevant monotherapies ( $P \geq 0.1455$ ), indicating that at the concentrations tested, the combinations were of no additional benefit in Panc-1 spheroids, and that going forward higher concentrations of DMF, MMF and gemcitabine should be tested in combination.

#### **3.4.4: Analysis of schedule 2 combinations**

To assess the efficacy of the selected combinations from schedule 2, the clonogenic assay was repeated using alternative concentrations of the applicable drugs. The dose of radiation was kept consistent at 0.5 Gy as both cell lines were highly sensitive (**figure 2.5**) to EXBR and this was the lowest dose with the equipment available.

##### **3.4.4-1: Schedule 2 – gemcitabine + EXBR**

Based on the results obtained in **figure 3.12** the schedule 2 combination of gemcitabine + EXBR was selected to undergo further analysis through the assay cascade as the combination showed particular promise in the Panc-1 cell line and would serve as a useful comparison for the other combinations in this schedule utilising DMF/MMF, as gemcitabine is the gold standard chemotherapy for pancreatic cancer. The dosing for this combination was based on the monotherapy results obtained in **chapter 2**, and the dosing kept below the  $IC_{50}$  value to enable the effect of the combination to be seen. The dose of radiation was kept consistent at 0.5 Gy as both cell lines were highly sensitive to EXBR (**figure 2.5**). Gemcitabine was incubated with the cell for 24 hours to allow at least one full cell cycle prior to irradiation, to allow DNA repair to be inhibited before irradiation, in the hopes of maximising the cytotoxic effect of EXBR. The clonogenic assay was carried out as described in **section 3.3.3**, and the presented in **figure 3.14**.

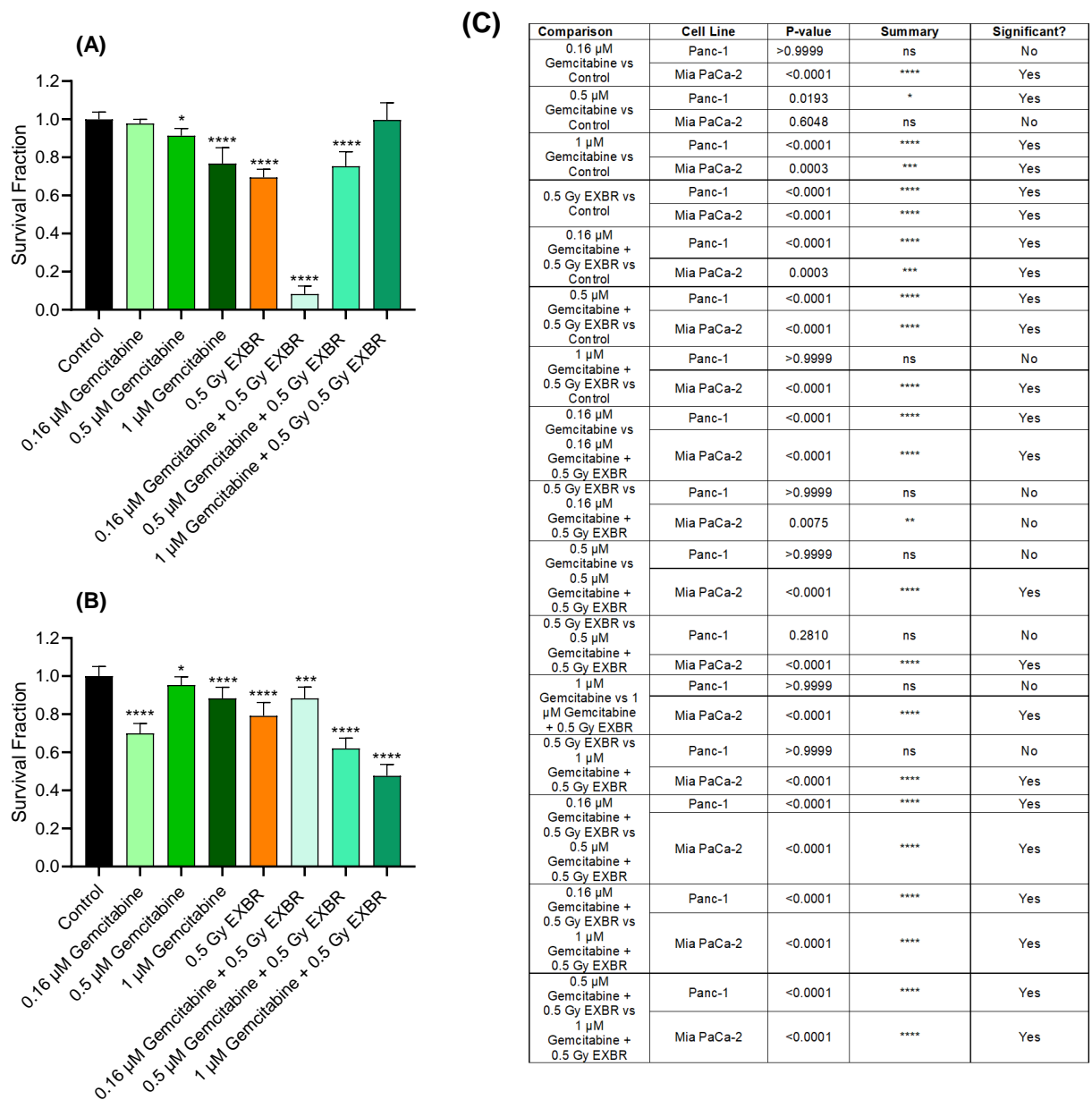


**Figure 3.14: Schedule 2 – gemcitabine + EXBR analysis.** (A) Survival fractions in Panc-1 cell line following treatment. (B) Survival fractions in Mia PaCa-2 cell line following treatment. Analysis was carried out via one-way ANOVA with Bonferroni post hoc test using GraphPad Prism 10.1.2. \* =  $P \leq 0.05$ ; \*\*\* =  $P \leq 0.001$ ; and \*\*\*\* =  $P \leq 0.0001$  in comparison with untreated control. (C) Statistical table of comparisons of combinations and monotherapies.

As can be seen in **figure 3.14A**, increasing the concentration of gemcitabine in the gemcitabine + EXBR schedule 2 combination did not lead to increased reduction in clonogenicity, with only the lowest concentration of gemcitabine (0.16  $\mu\text{M}$ ) in combination with 0.5 Gy EXBR inducing a statistically significant reduction in clonogenicity when compared with the untreated control in Panc-1 cells ( $P < 0.0001$ ). In Mia PaCa-2 cells (**figure 3.14B**), only 0.5  $\mu\text{M}$  and 1  $\mu\text{M}$  gemcitabine in combination with 0.5 Gy EXBR resulted in a statistically significant reduction in clonogenicity when compared with the untreated control ( $P < 0.0001$ ).

In Panc-1 cells (**figure 3.42A**) the lowest concentration of 0.16  $\mu\text{M}$  gemcitabine in combination with 0.5 Gy EXBR induced a significantly greater reduction in clonogenicity than both the higher concentrations of gemcitabine (0.5  $\mu\text{M}$  and 1  $\mu\text{M}$ ) in combination with 0.5 Gy EXBR ( $P < 0.0001$ ). Only 0.16  $\mu\text{M}$  gemcitabine + 0.5 Gy EXBR induced a statistically significantly greater reduction in clonogenicity when compared with both monotherapies in Panc-1 cells ( $P < 0.0001$ ).

In Mia PaCa-2 cells (**figure 3.14B**) the highest concentration of 0.16  $\mu\text{M}$  gemcitabine in combination with 0.5 Gy EXBR induced significantly more reduction in clonogenicity than both the higher concentrations of gemcitabine (0.5  $\mu\text{M}$  and 1  $\mu\text{M}$ ) in combination with 0.5 Gy EXBR ( $P < 0.0001$ ). Both 0.5  $\mu\text{M}$  gemcitabine + 0.5 Gy EXBR and 1  $\mu\text{M}$  gemcitabine + 0.5 Gy EXBR induced a statistically significantly greater reduction in clonogenicity when compared with both monotherapies in Mia PaCa-2 cells ( $P < 0.0001$ ).

Following this test, the highest concentration of 1  $\mu\text{M}$  gemcitabine + 0.5 Gy EXBR, was then tested in the 3D spheroid growth assay as described in **section 3.3.5**, and the results presented in **figure 3.15**. This concentration of the combination was selected as the preliminary study (**figure 3.11**) indicated that lower concentrations of combinations were ineffective in spheroids.

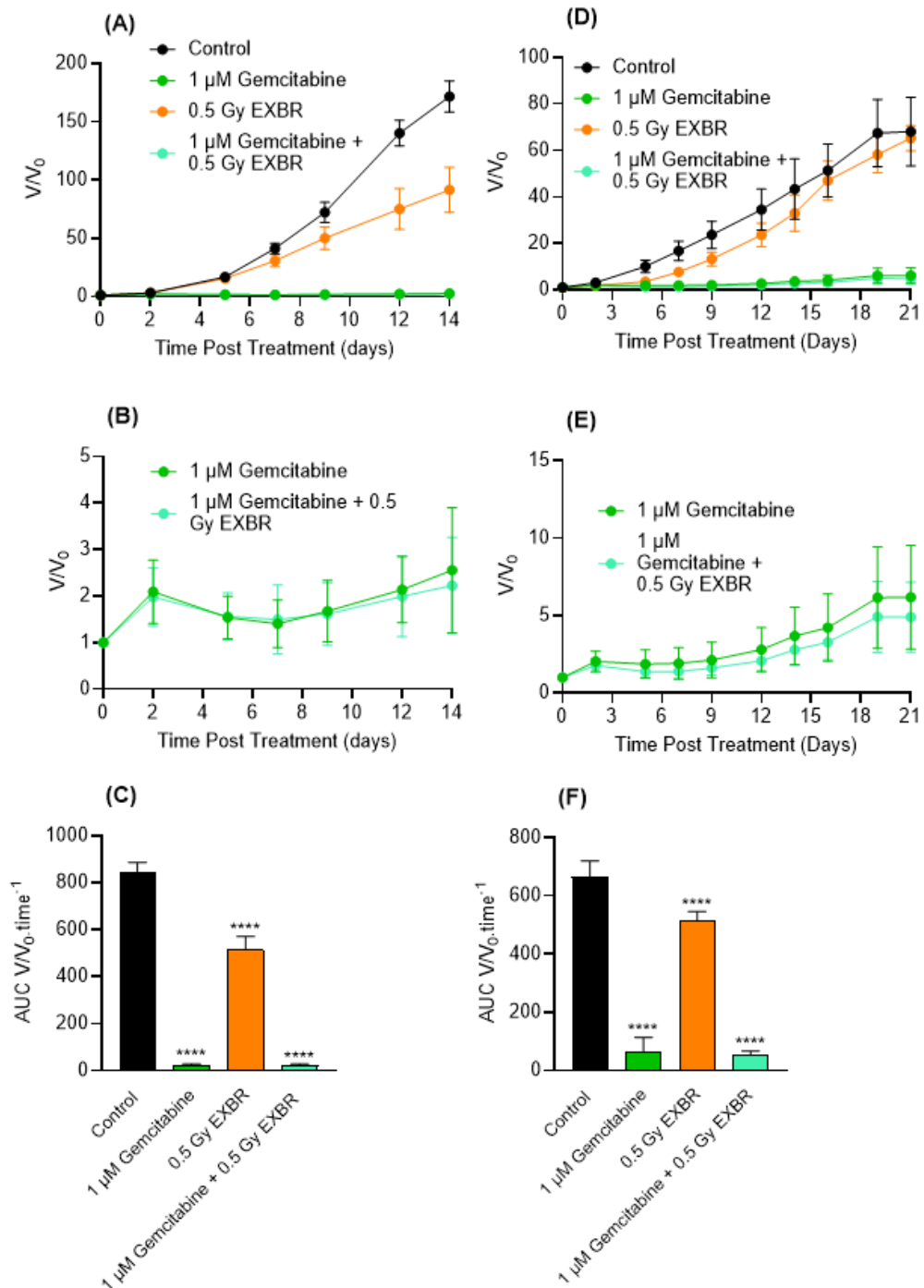


**Figure 3.15: Schedule 1 – gemcitabine + EXBR spheroid growth assay in Panc-1 and MiaPaCa-2.** ((A&D) Spheroid growth (V/V<sub>0</sub>) following treatment. The data is represented as the average of three independent experiments carried out with 16 spheroids per treatment group (48 spheroids total) ± standard deviation. (B&E) V/V<sub>0</sub> for gemcitabine and gemcitabine + EXBR treated spheroids alone is shown. (C&F) AUC for treated spheroids and untreated control is shown. The data is represented as the average ± standard deviation. Analysis was carried out via Kruskal-Wallis with Dunn's post hoc test using GraphPad Prism 10.1.2. \*\*\*\* = P ≤ 0.0001 in comparison with untreated control.

In Panc-1 spheroids (**figure 3.15A**), the schedule 2 combination of 1  $\mu\text{M}$  gemcitabine + 0.5 Gy EXBR statistically significantly reduced spheroid growth ( $V/V_0$ ) when compared with the untreated control and 0.5 Gy EXBR alone ( $P < 0.0001$ ). However, when compared with 1  $\mu\text{M}$  gemcitabine alone (**figure 3.15B**) there was no statistically significant difference ( $P = 0.8774$ ), indicating that the agents were of no additional benefit in in Panc-1 spheroids. To further investigate this observation, AUC was analysed. As can be seen in **figure 3.15C**, the combination of 1  $\mu\text{M}$  gemcitabine + 0.5 Gy EXBR induced a statistically significant reduction in AUC when compared with the untreated control ( $P < 0.0001$ ). The combination of 1  $\mu\text{M}$  gemcitabine + 0.5 Gy EXBR induced a statistically significantly greater reduction in AUC when compared with 0.5 Gy EXBR ( $P < 0.0001$ ), however when compared with 1  $\mu\text{M}$  gemcitabine alone there again was no statistical difference ( $P = 0.8774$ ), indicating the agents were of no additional benefit in combination in Panc-1 spheroids.

In Mia PaCa-2 spheroids (**figure 3.15D**), spheroid growth, as measured by the assessment of  $V/V_0$ , was statistically significantly reduced by the schedule 2 combination of 1  $\mu\text{M}$  gemcitabine + 0.5 Gy EXBR when compared with the untreated control; 1  $\mu\text{M}$  gemcitabine (**figure 3.15E**) alone; and 0.5 Gy EXBR alone ( $P \leq 0.0016$ ), implying that the agents were of additional benefit in Mia PaCa-2 spheroids. To further investigate this observation, the AUC was analysed (**figure 3.15F**) and the combination of 1  $\mu\text{M}$  gemcitabine + 0.5 Gy EXBR induced a statistically significant reduction in AUC when compared to the untreated control and 0.5 Gy EXBR alone ( $P < 0.0001$ ), however there was no statistically significant difference when compared to 1  $\mu\text{M}$  gemcitabine alone ( $P = 0.4102$ ), indicating the agents were not of additional benefit in combination in Mia PaCa-2 spheroids. A table depicting all statistical analysis carried out for **figure 3.15** can be found in **table 3.7**.

**Table 3.7: Statistical comparisons for schedule 2 gemcitabine + EXBR spheroid growth and AUC assay in Panc-1 and Mia PaCa-2.**

Comparison	Being Assessed	Cell Line	P-value	Summary	Significant?
1 $\mu$ M gemcitabine vs Control	Spheroid growth	Panc-1	<0.0001	****	Yes
		Mia PaCa-2	<0.0001	****	Yes
0.5 Gy EXBR vs Control	Spheroid growth	Panc-1	0.2334	ns	No
		Mia PaCa-2	0.0013	**	Yes
1 $\mu$ M gemcitabine + 0.5 Gy EXBR vs Control	Spheroid growth	Panc-1	<0.0001	****	Yes
		Mia PaCa-2	<0.0001	****	Yes
1 $\mu$ M gemcitabine vs 1 $\mu$ M gemcitabine + 0.5 Gy	Spheroid growth	Panc-1	0.8774	ns	No
		Mia PaCa-2	0.0016	**	Yes
0.5 Gy EXBR vs 1 $\mu$ M gemcitabine + 0.5 Gy	Spheroid growth	Panc-1	<0.0001	****	Yes
		Mia PaCa-2	<0.0001	****	Yes
1 $\mu$ M gemcitabine vs Control	AUC	Panc-1	<0.0001	****	Yes
		Mia PaCa-2	<0.0001	****	Yes
0.5 Gy EXBR vs Control	AUC	Panc-1	<0.0001	****	Yes
		Mia PaCa-2	<0.0001	****	Yes
1 $\mu$ M gemcitabine + 0.5 Gy EXBR vs Control	AUC	Panc-1	<0.0001	****	Yes
		Mia PaCa-2	<0.0001	****	Yes
1 $\mu$ M gemcitabine vs 1 $\mu$ M gemcitabine + 0.5 Gy	AUC	Panc-1	0.9962	ns	No
		Mia PaCa-2	0.4102	ns	No
0.5 Gy EXBR vs 1 $\mu$ M gemcitabine + 0.5 Gy	AUC	Panc-1	<0.0001	****	Yes
		Mia PaCa-2	<0.0001	****	Yes

#### **3.4.4-2: Schedule 2 – DMF + EXBR**

Based on the results obtained in **figure 3.12** the schedule 2 combination of DMF + EXBR was selected to undergo further analysis through the assay cascade as the combination showed particular promise in the Mia PaCa-2 cell line. The dosing for this combination was based on the monotherapy results obtained in **chapter 2**, and the dosing kept below the  $IC_{50}$  value to enable the effect of the combination to be seen. The dose of radiation was kept consistent at 0.5 Gy as both cell lines were highly sensitive to EXBR (**figure 2.5**). DMF was incubated with the cell for 24 hours to allow at least one full cell cycle prior to irradiation, to allow glutathione levels to be depleted by DMF in order to maximise the effect of radiation. The clonogenic assay was carried out as described in **section 3.3.3**, and the presented in **figure 3.16**.

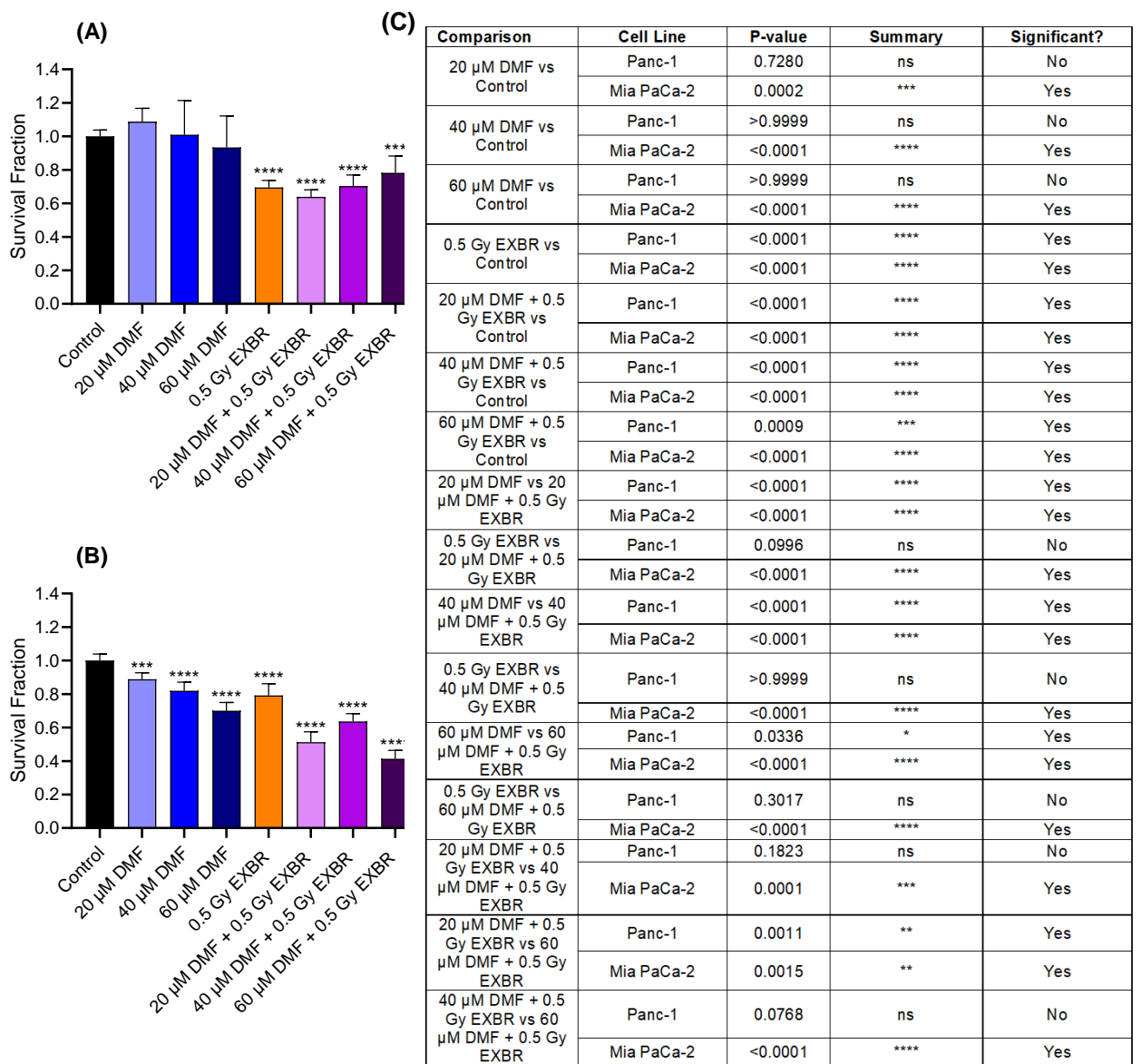


**Figure 3.16: Schedule 2 – DMF + EXBR analysis.** (A) Survival fractions in Panc-1 cell line following treatment. (B) Survival fractions in Mia PaCa-2 cell line following treatment. Analysis was carried out via one-way ANOVA with Bonferroni post hoc test using GraphPad Prism 10.1.2. \*\*\* =  $P \leq 0.001$  and \*\*\*\* =  $P \leq 0.0001$  in comparison with untreated control. (C) Statistical table of comparisons of combinations and monotherapies.

In Panc-1 cells, the schedule 2 combination of DMF + EXBR (**figure 3.16A**), induced a statistically significant increase in reduction in clonogenicity when compared with the untreated control at all concentrations tested ( $P \leq 0.0009$ ). However, all concentrations of the combination tested did not induce a statistically significantly greater reduction in clonogenicity when compared with 0.5 Gy EXBR alone ( $P \geq 0.3017$ ).

Conversely, in Mia PaCa-2 cells (**figure 3.16B**), the schedule 2 combination of DMF + EXBR induced statistically significantly greater reduction in clonogenicity when compared with the untreated control ( $P = < 0.0001$ ) and its individual components at all concentrations of DMF tested in combination ( $P < 0.0001$ ).

Following this test, the combination of 40  $\mu$ M DMF + 0.5 Gy EXBR, was then tested in the 3D spheroid growth assay as described in **section 3.3.5**, and the results presented in **figure 3.17**. These concentrations were selected as in the pilot experiment, the lower concentrations of combinations were ineffective at reducing spheroid growth (**figure 3.11**), therefore it was decided to use a higher concentration of DMF in combination. Moreover, 40  $\mu$ M DMF was selected as in Panc-1 cells, the combination of 60  $\mu$ M DMF + 0.5 Gy EXBR did not statistically significantly differ from 40  $\mu$ M DMF + 0.5 Gy EXBR ( $P = 0.0768$ ).

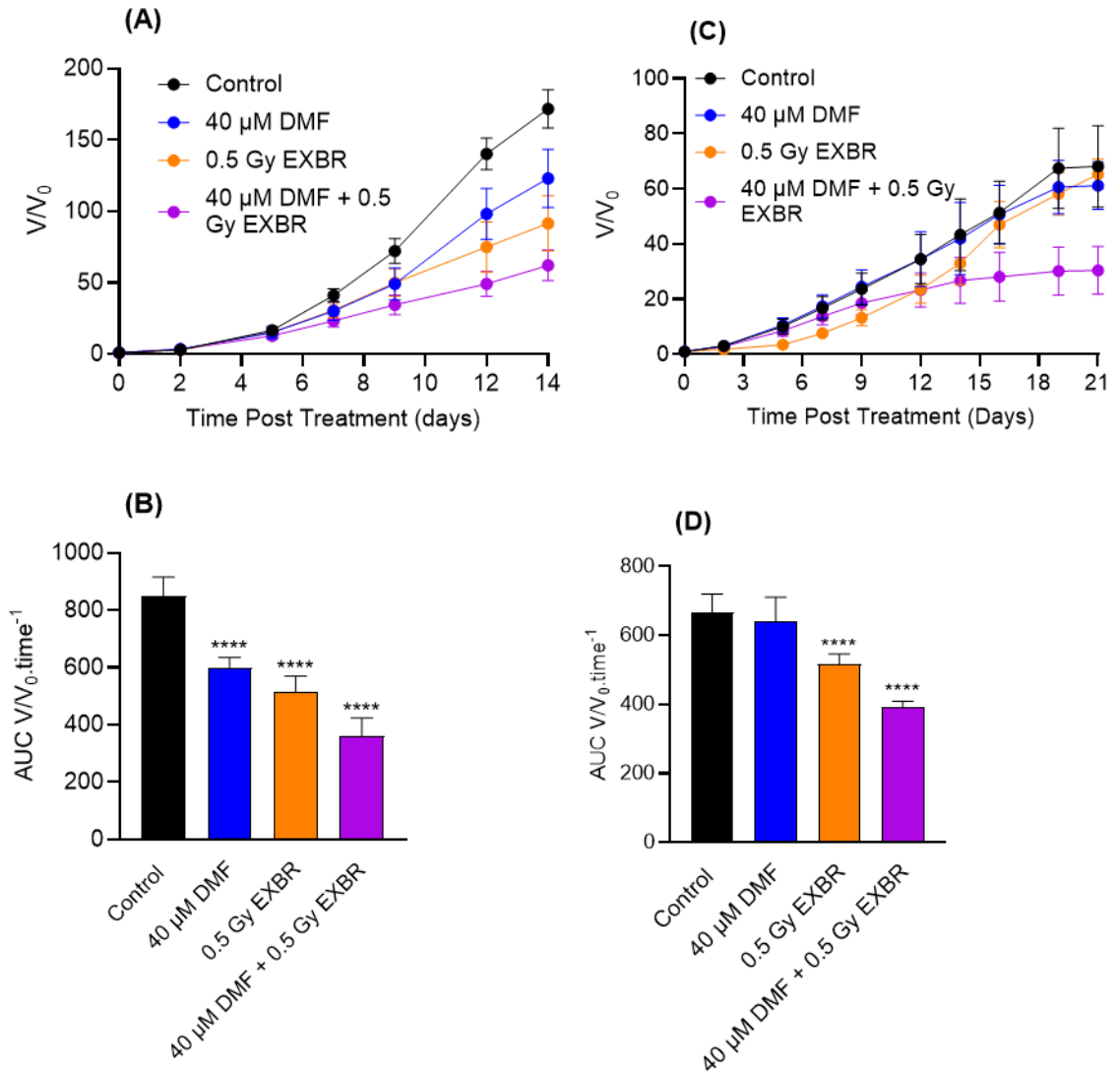


**Figure 3.17: Schedule 2 – DMF + EXBR spheroid growth assay in Panc-1 and MiaPaCa-2.** (A & C) Spheroid growth ( $V/V_0$ ) following treatment. The data is represented as the average of three independent experiments carried out with 16 spheroids per treatment group (48 spheroids total)  $\pm$  standard deviation. (B & D) AUC for treated spheroids and untreated control is shown. The data is represented as the average  $\pm$  standard deviation. Analysis was carried out via Kruskal-Wallis with Dunn's post hoc test using GraphPad Prism 10.1.2. \*\*\*\* =  $P \leq 0.0001$  in comparison with untreated control.

When interrogating the change in volume ( $V/V_0$ ) in Panc-1 spheroids (**figure 3.17A**), the schedule 2 combination of 40  $\mu\text{M}$  DMF + 0.5 Gy EXBR induced a statistically significant reduction in spheroid growth when compared with the untreated control and both individual agents ( $P \leq 0.0049$ ), indicating that agents were of additional benefit in combination in Panc-1 spheroids. To further investigate this observation, the AUC was analysed (**figure 3.17B**) and the combination of 40  $\mu\text{M}$  DMF + 0.5 Gy EXBR induced a statistically significant reduction in the AUC when compared with the untreated control and both individual agents ( $P \leq 0.0002$ ), again indicating that the agents were of additional benefit in combination in Panc-1 spheroids.

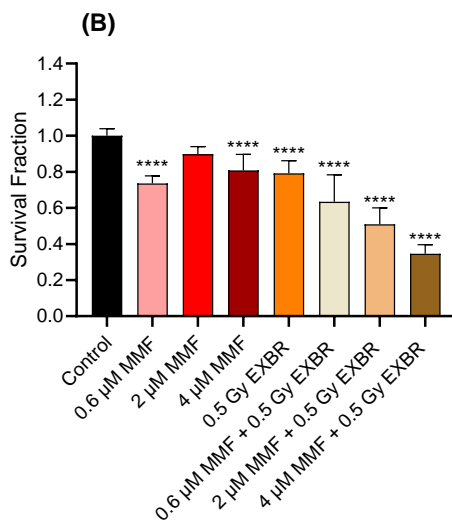
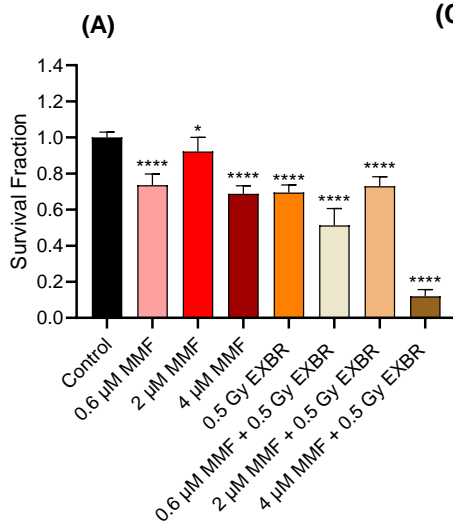
When interrogating the change in volume ( $V/V_0$ ) in Mia PaCa-2 spheroids (**figure 3.17C**), the schedule 2 combination of 40  $\mu\text{M}$  DMF + 0.5 Gy EXBR induced a statistically significant reduction in spheroid growth when compared with the untreated control and both individual agents ( $P \leq 0.0106$ ), indicating the agents were of additional benefit in Mia PaCa-2 spheroids. To further investigate this observation the AUC was analysed (**figure 3.17D**) and the combination of 40  $\mu\text{M}$  DMF + 0.5 Gy EXBR induced a statistically significant reduction in the AUC when compared with the untreated control and the individual components ( $P \leq 0.0003$ ), again indicating the agents were of additional benefit in Mia PaCa-2 spheroids. A table depicting all statistical analysis carried out for **figure 3.17** can be found in **table 3.8**.

**Table 3.8: Statistical comparisons for schedule 2 DMF + EXBR spheroid growth and AUC assay in Panc-1 and Mia PaCa-2.**

Comparison	Being Assessed	Cell Line	P-value	Summary	Significant?
40 $\mu$ M DMF vs Control	Spheroid growth	Panc-1	0.0379	*	Yes
		Mia PaCa-2	>0.9999	ns	No
0.5 Gy EXBR vs Control	Spheroid growth	Panc-1	0.0022	**	Yes
		Mia PaCa-2	<0.0001	****	Yes
40 $\mu$ M DMF + 0.5 Gy EXBR vs Control	Spheroid growth	Panc-1	<0.0001	****	Yes
		Mia PaCa-2	<0.0001	****	Yes
40 $\mu$ M DMF vs 40 $\mu$ M DMF + 0.5 Gy	Spheroid growth	Panc-1	0.0002	***	Yes
		Mia PaCa-2	<0.0001	****	Yes
0.5 Gy EXBR vs 40 $\mu$ M DMF + 0.5 Gy	Spheroid growth	Panc-1	0.0049	**	Yes
		Mia PaCa-2	0.0106	*	Yes
40 $\mu$ M DMF vs Control	AUC	Panc-1	<0.0001	****	Yes
		Mia PaCa-2	0.3565	ns	No
0.5 Gy EXBR vs Control	AUC	Panc-1	<0.0001	****	Yes
		Mia PaCa-2	<0.0001	****	Yes
40 $\mu$ M DMF + 0.5 Gy EXBR vs Control	AUC	Panc-1	<0.0001	****	Yes
		Mia PaCa-2	<0.0001	****	Yes
40 $\mu$ M DMF vs 40 $\mu$ M DMF + 0.5 Gy	AUC	Panc-1	<0.0001	****	Yes
		Mia PaCa-2	<0.0001	****	Yes
0.5 Gy EXBR vs 40 $\mu$ M DMF + 0.5 Gy	AUC	Panc-1	0.0002	***	Yes
		Mia PaCa-2	0.0003	***	Yes

#### **3.4.4-3: Schedule 2 – MMF + EXBR**

Based on the results obtained in **figure 3.12** the schedule 2 combination of MMF + EXBR was selected to undergo further analysis through the assay cascade as the combination showed particular promise in the Panc-1 cell line. The dosing for this combination was based on the monotherapy results obtained in **chapter 2**, and the dosing kept below the  $IC_{50}$  value to enable the effect of the combination to be seen. The dose of radiation was kept consistent at 0.5 Gy as both cell lines were highly sensitive to EXBR (**figure 2.5**). MMF was incubated with the cell for 24 hours to allow at least one full cell cycle prior to irradiation, to allow glutathione levels to be depleted by MMF in order to maximise the effect of radiation. The clonogenic assay was carried out as described in **section 3.3.3**, and the presented in **figure 3.18**.



**(C)**

Comparison	Cell Line	P-value	Summary	Significant?
0.6 μM MMF vs Control	Panc-1	<0.0001	****	Yes
	Mia PaCa-2	<0.0001	****	Yes
2 μM MMF vs Control	Panc-1	0.0476	*	Yes
	Mia PaCa-2	0.0560	ns	No
4 μM MMF vs Control	Panc-1	<0.0001	****	Yes
	Mia PaCa-2	<0.0001	****	Yes
0.5 Gy EXBR vs Control	Panc-1	<0.0001	****	Yes
	Mia PaCa-2	<0.0001	****	Yes
0.6 μM MMF + 0.5 Gy EXBR vs Control	Panc-1	<0.0001	****	Yes
	Mia PaCa-2	<0.0001	****	Yes
2 μM MMF + 0.5 Gy EXBR vs Control	Panc-1	<0.0001	****	Yes
	Mia PaCa-2	<0.0001	****	Yes
4 μM MMF + 0.5 Gy EXBR vs Control	Panc-1	<0.0001	****	Yes
	Mia PaCa-2	<0.0001	****	Yes
0.6 μM MMF vs 0.6 μM MMF + 0.5 Gy EXBR	Panc-1	<0.0001	****	Yes
	Mia PaCa-2	0.0786	ns	No
0.5 Gy EXBR vs 0.6 μM MMF + 0.5 Gy EXBR	Panc-1	<0.0001	****	Yes
	Mia PaCa-2	0.0047	**	Yes
2 μM MMF vs 2 μM MMF + 0.5 Gy EXBR	Panc-1	<0.0001	****	Yes
	Mia PaCa-2	<0.0001	****	Yes
0.5 Gy EXBR vs 2 μM MMF + 0.5 Gy EXBR	Panc-1	0.4364	ns	No
	Mia PaCa-2	<0.0001	****	Yes
4 μM MMF vs 4 μM MMF + 0.5 Gy EXBR	Panc-1	<0.0001	****	Yes
	Mia PaCa-2	<0.0001	****	Yes
	Mia PaCa-2	<0.0001	****	Yes
0.5 Gy EXBR vs 4 μM MMF + 0.5 Gy EXBR	Panc-1	<0.0001	****	Yes
	Mia PaCa-2	<0.0001	****	Yes
0.6 μM MMF + 0.5 Gy EXBR vs 2 μM MMF + 0.5 Gy EXBR	Panc-1	<0.0001	****	Yes
	Mia PaCa-2	0.0460	*	Yes
0.6 μM MMF + 0.5 Gy EXBR vs 4 μM MMF + 0.5 Gy EXBR	Panc-1	<0.0001	****	Yes
	Mia PaCa-2	<0.0001	****	Yes
2 μM MMF + 0.5 Gy EXBR vs 4 μM MMF + 0.5 Gy EXBR	Panc-1	<0.0001	****	Yes
	Mia PaCa-2	0.0084	**	Yes

**Figure 3.18: Schedule 2 – MMF + EXBR combination analysis.** (A) Survival fractions in Panc-1 cell line following treatment. (B) Survival fractions in Mia PaCa-2 cell line following treatment. Analysis was carried out via one-way ANOVA with Bonferroni post hoc test using GraphPad Prism 10.1.2. \* =  $P \leq 0.05$  and \*\*\*\* =  $P \leq 0.0001$  in comparison with untreated control. (C) Statistical table of comparisons of combinations and monotherapies.

In Panc-1 cells (**figure 3.18A**), all concentrations of the schedule 2 combination of MMF + EXBR induced significant reduction in clonogenicity when compared with the untreated control ( $P < 0.0001$ ). Both 0.6  $\mu\text{M}$  MMF + 0.5 Gy EXBR and 4  $\mu\text{M}$  MMF + 0.5 Gy EXBR induced a statistically significantly greater reduction in clonogenicity when compared with the individual monotherapies ( $P < 0.0001$ ). However, 2  $\mu\text{M}$  MMF + 0.5 Gy EXBR, did not induce a statistically significant decrease in clonogenicity when compared with 0.5 Gy EXBR alone ( $P = 0.4364$ ).

In Mia PaCa-2 cells (**figure 3.18B**), all concentrations of the schedule 2 combination of MMF + EXBR induced significant reduction in clonogenicity when compared with the untreated control ( $P < 0.0001$ ). Both 2  $\mu\text{M}$  MMF + 0.5 Gy EXBR and 4  $\mu\text{M}$  MMF + 0.5 Gy EXBR induced a statistically significantly greater reduction in clonogenicity when compared with the individual monotherapies ( $P < 0.0001$ ). However, 0.6  $\mu\text{M}$  MMF + 0.5 Gy EXBR, did not induce a statistically significant decrease in clonogenicity when compared with 0.6  $\mu\text{M}$  MMF alone ( $P = 0.0786$ ).

Following this test, the highest concentration of 4  $\mu\text{M}$  MMF + 0.5 Gy EXBR, was then tested in the 3D spheroid growth assay as described in **section 3.3.5**, and the results presented in **figure 3.19**. This dosing of the combination was selected as spheroids typically require higher dosing to elicit an effect when compared with 2D cell models, as indicated by the results in **figure 3.11**.

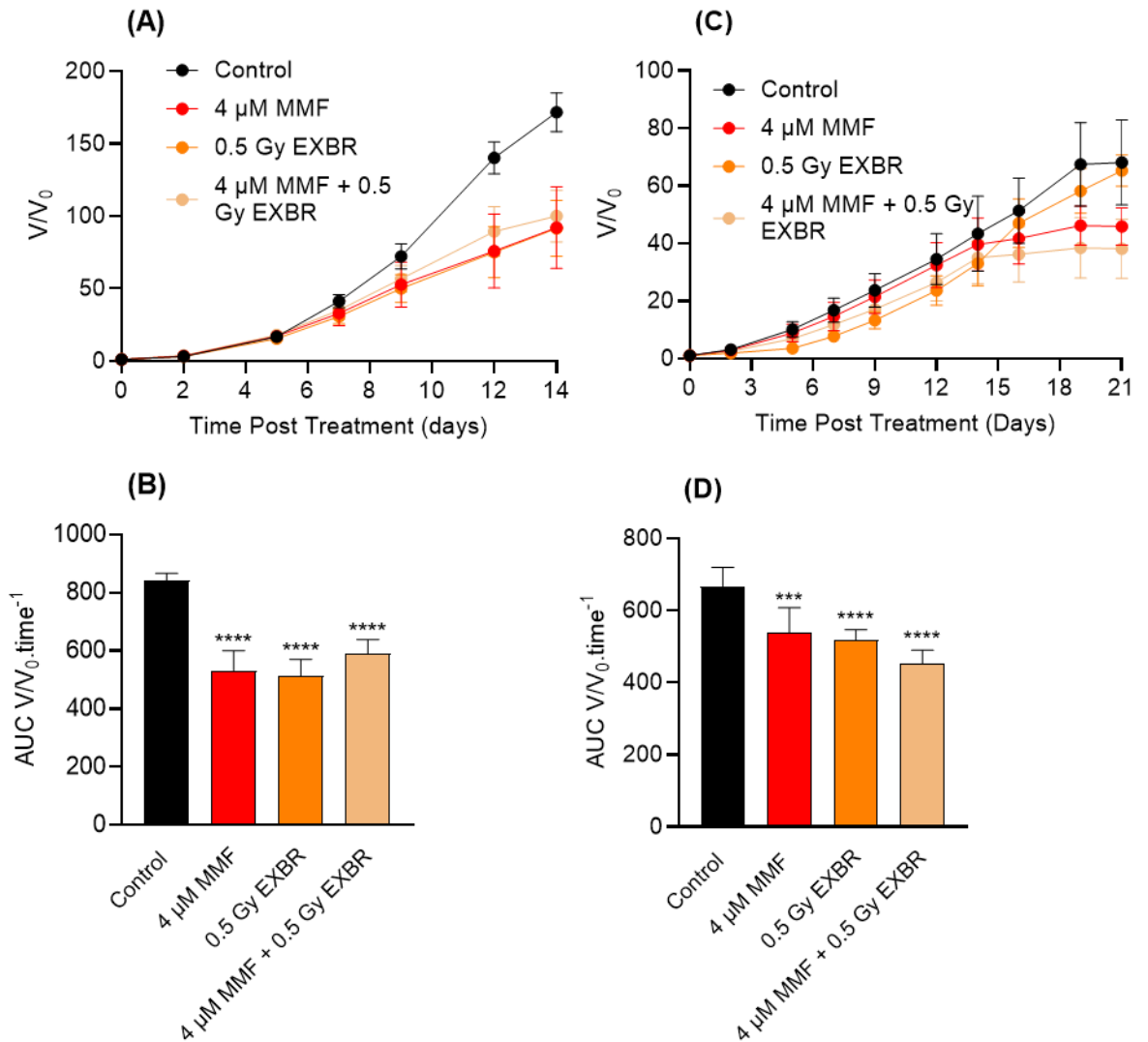


**Figure 3.19: Schedule 2 – MMF + EXBR spheroid growth assay in Panc-1 and MiaPaCa-2.** (A & C) Spheroid growth (V/V<sub>0</sub>) following treatment. The data is represented as the average of three independent experiments carried out with 16 spheroids per treatment group (48 spheroids total) ± standard deviation. (B & D) AUC for treated spheroids and untreated control is shown. The data is represented as the average ± standard deviation. Analysis was carried out via Kruskal-Wallis with Dunn's post hoc test using GraphPad Prism 10.1.2. \*\*\* = P ≤ 0.001 and \*\*\*\* = P ≤ 0.0001 in comparison with untreated control.

In Panc-1 spheroids (**figure 3.19A**), the schedule 2 combination of 4  $\mu\text{M}$  MMF + 0.5 Gy EXBR did not statistically significantly reduce the growth ( $V/V_0$ ) of Panc-1 spheroids when compared with the untreated control ( $P = 0.0946$ ). However, the individual components of 4  $\mu\text{M}$  MMF alone ( $P = 0.0024$ ) and 0.5 Gy EXBR alone ( $P = 0.0007$ ) statistically significantly reduced spheroid growth when compared with the untreated control in Panc-1 spheroids, suggesting the agents were not of additional benefit in Panc-1 spheroids. To further investigate whether the schedule 2 combination of 4  $\mu\text{M}$  MMF + 0.5 Gy EXBR induced a beneficial effect over the single agents, the AUC was analysed. As can be seen in **figure 3.19B**, the combination of 4  $\mu\text{M}$  MMF + 0.5 Gy EXBR induced a statistically significant reduction in AUC when compared with the untreated control, as did 4  $\mu\text{M}$  MMF and 0.5 Gy EXBR ( $P < 0.0001$ ) alone. However, both 4  $\mu\text{M}$  MMF and 0.5 Gy EXBR alone induced a statistically significantly greater reduction in AUC when compared with the combination ( $P \leq 0.0139$ ), again indicating the agents were not of additional benefit in Panc-1 spheroids.

In Mia PaCa-2 spheroids (**figure 3.19C**), the schedule 2 combination of 4  $\mu\text{M}$  MMF + 0.5 Gy EXBR statistically significantly reduced the growth ( $V/V_0$ ) of spheroids when compared with the untreated control, as did the individual components of the combination ( $P \leq 0.0946$ ). When comparing the combination with the individual components of 4  $\mu\text{M}$  MMF and 0.5 Gy EXBR alone, the schedule 2 combination of 4  $\mu\text{M}$  MMF + 0.5 Gy EXBR induced a statistically significantly greater reduction in spheroid growth when compared with 4  $\mu\text{M}$  MMF alone ( $P = 0.0048$ ), however there was no statistically significant difference when compared with 0.5 Gy EXBR alone ( $P = 0.2578$ ), indicating the agents were not of additional benefit in Mia PaCa-2 spheroids. To further investigate whether the schedule 2 combination of 4  $\mu\text{M}$  MMF + 0.5 Gy EXBR induced a beneficial effect over the individual agents, the AUC was analysed. As can be seen in **figure 3.19D**, the combination induced a statistically

significant reduction ( $P < 0.0001$ ) in AUC when compared with the untreated control, as did 4  $\mu\text{M}$  MMF and 0.5 Gy EXBR alone ( $P \leq 0.0002$ ). The schedule 2 combination of 4  $\mu\text{M}$  MMF + 0.5 Gy EXBR induced a statistically significant reduction in spheroid growth when compared with 4  $\mu\text{M}$  MMF and 0.5 Gy EXBR alone ( $P \leq 0.0139$ ), indicating that the combination was of additional benefit in Mia PaCa-2 spheroids. A table depicting all statistical analysis carried out for **figure 3.19** can be found in **table 3.9**.

**Table 3.9: Statistical comparisons for schedule 2 MMF + EXBR spheroid growth and AUC assay in Panc-1 and Mia PaCa-2.**

Comparison	Being Assessed	Cell Line	P-value	Summary	Significant?
4 $\mu\text{M}$ MMF vs Control	Spheroid growth	Panc-1	0.0024	**	Yes
		Mia PaCa-2	0.0096	**	Yes
0.5 Gy EXBR vs Control	Spheroid growth	Panc-1	0.0007	***	Yes
		Mia PaCa-2	<0.0001	****	Yes
4 $\mu\text{M}$ MMF + 0.5 Gy EXBR vs Control	Spheroid growth	Panc-1	0.0946	ns	No
		Mia PaCa-2	<0.0001	****	Yes
4 $\mu\text{M}$ MMF vs 4 $\mu\text{M}$ MMF + 0.5 Gy	Spheroid growth	Panc-1	0.3641	ns	No
		Mia PaCa-2	0.0048	**	Yes
0.5 Gy EXBR vs 4 $\mu\text{M}$ MMF + 0.5 Gy	Spheroid growth	Panc-1	0.1868	ns	No
		Mia PaCa-2	0.2578	ns	No
4 $\mu\text{M}$ MMF vs Control	AUC	Panc-1	<0.0001	****	Yes
		Mia PaCa-2	0.0002	***	Yes
0.5 Gy EXBR vs Control	AUC	Panc-1	<0.0001	****	Yes
		Mia PaCa-2	<0.0001	****	Yes
4 $\mu\text{M}$ MMF + 0.5 Gy EXBR vs Control	AUC	Panc-1	<0.0001	****	Yes
		Mia PaCa-2	<0.0001	****	Yes
4 $\mu\text{M}$ MMF vs 4 $\mu\text{M}$ MMF + 0.5 Gy	AUC	Panc-1	0.0439	*	Yes
		Mia PaCa-2	0.0029	**	Yes
0.5 Gy EXBR vs 4 $\mu\text{M}$ MMF + 0.5 Gy	AUC	Panc-1	0.0139	*	Yes
		Mia PaCa-2	0.0125	*	Yes

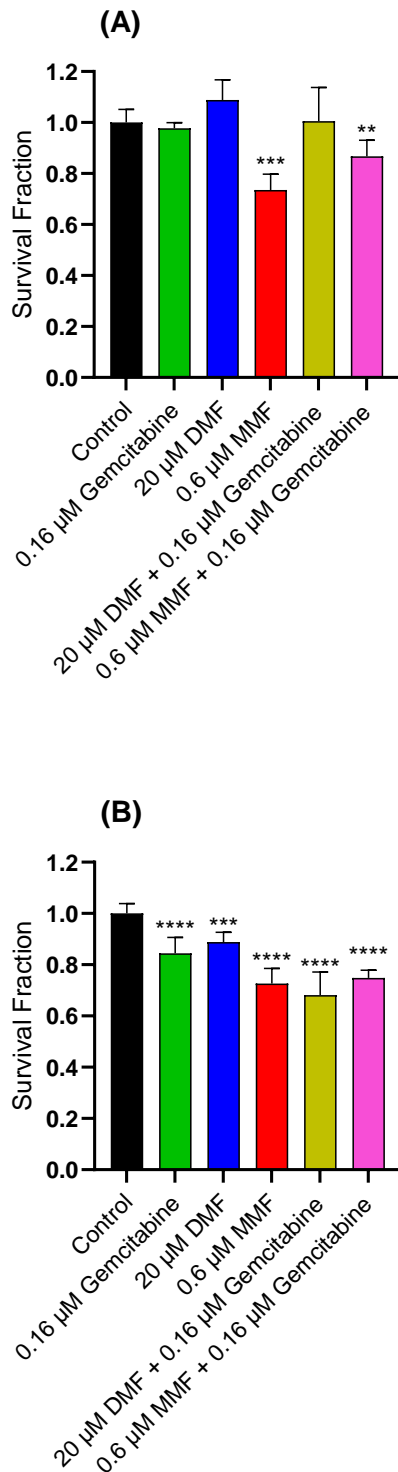
A summary of all tested schedule 2 combinations can be found in **table 3.10**.

**Table 3.10: Summary of the Schedule 2 combinations**

Schedule 2 combination	Greater effect than individual agents in Panc-1 cells?	Greater effect than individual agents in Panc-1 spheroids?	Greater effect than individual agents in Mia PaCa-2 cells?	Greater effect than individual agents in Mia PaCa-2 spheroids?
Gemcitabine + EXBR	No	No	Yes	No
DMF + EXBR	No	Yes	Yes	Yes
MMF + EXBR	Yes	No	Yes	Yes

#### 3.4.4: Development of schedule 3 combinations

The clonogenic assay was carried out as described in **section 3.3.3** to assess the efficacy of schedule 3 combinations. For schedule 3 combinations, the fumarate (DMF or MMF) was added to the cells and incubated for 24 hours, before the addition of gemcitabine and further incubation for 24 hours (48-hour incubation total). The dosing for drugs in the schedule 2 combinations are approximately IC<sub>10</sub> values, based on the IC<sub>50</sub> values obtained for both Panc-1 and Mia PaCa-2 presented in **chapter 2** to allow for the effect of the combination to be seen, as higher doses may have resulted in an inability to distinguish the effect of the combination from that of the single agent activity. The rationale for this scheduling was pre-treatment with DMF/MMF would decrease the antioxidant response and allow gemcitabine to elicit a greater cytotoxic effect. The incubation time was 48 hours total to allow each component at least one full cell cycle following administration to illicit its effect. The results are presented in **figure 3.20**.



**(C)**

Comparison	Cell Line	P-value	Summary	Significant?
0.16 $\mu$ M gemcitabine vs Control	Panc-1	0.9573	ns	No
	Mia PaCa-2	<0.0001	****	Yes
20 $\mu$ M DMF vs Control	Panc-1	0.0698	ns	No
	Mia PaCa-2	0.0006	***	Yes
0.6 $\mu$ M MMF vs Control	Panc-1	<0.0001	****	Yes
	Mia PaCa-2	<0.0001	****	Yes
20 $\mu$ M DMF + 0.16 $\mu$ M gemcitabine vs Control	Panc-1	>0.9999	ns	No
	Mia PaCa-2	<0.0001	****	Yes
0.6 $\mu$ M MMF + 0.16 $\mu$ M gemcitabine vs Control	Panc-1	0.0025	**	Yes
	Mia PaCa-2	<0.0001	****	Yes
20 $\mu$ M DMF vs 20 $\mu$ M DMF + 0.16 $\mu$ M gemcitabine	Panc-1	0.1455	ns	No
	Mia PaCa-2	<0.0001	****	Yes
0.16 $\mu$ M gemcitabine vs 20 $\mu$ M DMF + 0.16 $\mu$ M gemcitabine	Panc-1	0.7887	ns	No
	Mia PaCa-2	<0.0001	****	Yes
0.6 $\mu$ M MMF vs 0.6 $\mu$ M MMF + 0.16 $\mu$ M gemcitabine	Panc-1	<0.0001	****	Yes
	Mia PaCa-2	0.6542	ns	No
0.16 $\mu$ M gemcitabine vs 0.6 $\mu$ M MMF + 0.16 $\mu$ M gemcitabine	Panc-1	0.0005	***	Yes
	Mia PaCa-2	0.0018	**	Yes

**Figure 3.20: Schedule 3 combinations in pancreatic cancer cell lines.** (A) Survival fractions in Panc-1 cell line following treatment. (B) Survival fractions in Mia PaCa-2 cell line following treatment. Data is shown as the average of three independent experiments carried out in triplicate  $\pm$  standard deviation. Analysis was carried out via one-way ANOVA with Bonferroni post hoc test using GraphPad Prism 10.1.2. \*\* =  $P \leq 0.01$ ; \*\*\* =  $P \leq 0.001$ ; and \*\*\*\* =  $P \leq 0.0001$  in comparison with untreated control.

Prior to assigning any level of significant reduction in clonogenicity in the tested combinations, the combination must have met the following criteria: induce significant reduction in clonogenicity when compared with the untreated control and induce significantly more reduction in clonogenicity when compared with the individual components that make up the combination.

As can be seen in **figure 3.20B** the schedule 3 combination of 20  $\mu\text{M}$  DMF + 0.16  $\mu\text{M}$  gemcitabine induced a statistically significantly greater reduction in clonogenicity in Mia PaCa-2 cells when compared with the untreated control ( $P < 0.0001$ ). When compared with the individual components, 20  $\mu\text{M}$  DMF + 0.16  $\mu\text{M}$  gemcitabine induced statistically significantly greater reduction in clonogenicity than both DMF and gemcitabine monotherapies in Mia PaCa-2 cells ( $P < 0.0001$ ). In Panc-1, the schedule 3 combination of 20  $\mu\text{M}$  DMF + 0.16  $\mu\text{M}$  gemcitabine did not induce a statistically significant decrease in clonogenicity in comparison with the untreated control ( $P > 0.9999$ ) or the individual components ( $P \geq 0.1455$ ).

The schedule 3 combination of 0.6  $\mu\text{M}$  MMF + 0.16  $\mu\text{M}$  gemcitabine (**figure 3.20A&B**) induced statistically significantly greater kill in both cell lines when compared with the untreated control ( $P \leq 0.0025$ ), however in Mia PaCa-2 cells (**figure 3.20B**) the combination did not induce a statistically significantly greater reduction in clonogenicity when compared with 0.6  $\mu\text{M}$  MMF alone ( $P = 0.6542$ ), indicating the agents were not of additional benefit in combination in Mia PaCa-2 cells. In Panc-1 cells, the schedule 3 combination of 0.6  $\mu\text{M}$  MMF + 0.16  $\mu\text{M}$  gemcitabine induced a greater reduction in clonogenicity when compared with both monotherapies ( $P \leq 0.0005$ ).

In Panc-1 cells, the schedule 3 combination of 0.6  $\mu\text{M}$  MMF + 0.16  $\mu\text{M}$  gemcitabine induced a statistically significantly greater reduction in clonogenicity in Mia PaCa-2 cells when compared with Panc-1 cells ( $P = 0.0017$ ). The schedule 3 combination of

20  $\mu$ M DMF + 0.16  $\mu$ M gemcitabine induced a statistically significantly greater reduction in clonogenicity in Mia PaCa-2 cells, when compared Panc-1 cells ( $P < 0.0001$ ).

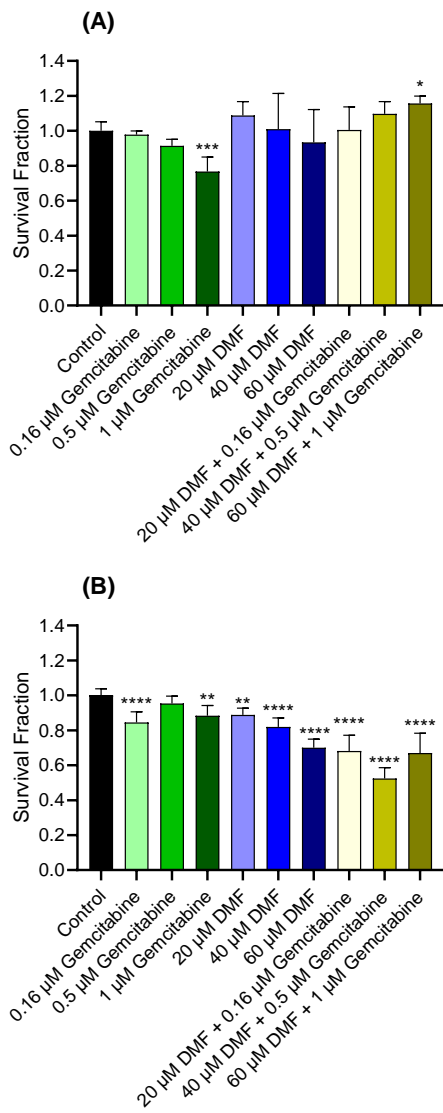
Based on the results obtained in **figure 3.20**, both combinations developed in schedule 3 were selected to go forward for further analysis in **section 3.4.5**.

### **3.4.5: Analysis for schedule 3 combinations**

To assess the efficacy of the selected combinations from schedule 3, the clonogenic assay was repeated using alternative concentrations of the applicable drugs.

#### **3.4.5-1: Schedule 3 – DMF + gemcitabine**

Based on the results obtained in **figure 3.20**, the schedule 3 combination of DMF + gemcitabine was selected for further analysis as we believe the combination showed promise, despite the result obtained for Panc-1, and hypothesised that altering the dosing may yield results in that cell line. The dosing for this combination was based on the monotherapy results obtained in **chapter 2**, and the dosing kept below the  $IC_{50}$  value to enable the effect of the combination to be seen. Additionally, this combination was kept at this stage for comparison with its schedule 3 MMF + gemcitabine counterpart. The incubation time was 48 hours total to allow each component at least one full cell cycle following administration to illicit its effect and we hypothesised that DMF would sensitise the cell through NRF2 inhibition, allowing gemcitabine to illicit a stronger cytotoxic effect. The clonogenic assay was carried out as described in **section 3.3.3**, and the results presented in **figure 3.21**.



Comparison	Cell Line	P-value	Summary	Significant?
20 μM DMF vs Control	Panc-1	0.4224	ns	No
	Mia PaCa-2	0.0035	**	Yes
40 μM DMF vs Control	Panc-1	>0.9999	ns	No
	Mia PaCa-2	<0.0001	****	Yes
60 μM DMF vs Control	Panc-1	0.7374	ns	No
	Mia PaCa-2	<0.0001	****	Yes
0.16 μM Gemcitabine vs Control	Panc-1	0.9996	ns	No
	Mia PaCa-2	<0.0001	****	Yes
0.5 μM Gemcitabine vs Control	Panc-1	0.4445	ns	No
	Mia PaCa-2	0.5587	ns	No
1 μM Gemcitabine vs Control	Panc-1	0.0002	***	Yes
	Mia PaCa-2	0.0020	**	No
20 μM DMF + 0.16 μM Gemcitabine vs Control	Panc-1	>0.9999	ns	No
	Mia PaCa-2	<0.0001	****	Yes
40 μM DMF + 0.5 μM Gemcitabine vs Control	Panc-1	0.3202	ns	No
	Mia PaCa-2	<0.0001	****	Yes
60 μM DMF + 1 μM Gemcitabine vs Control	Panc-1	0.0218	*	Yes
	Mia PaCa-2	<0.0001	****	Yes
20 μM DMF vs 20 μM DMF + 0.16 μM Gemcitabine	Panc-1	0.1455	ns	No
	Mia PaCa-2	<0.0001	****	Yes
0.16 μM Gemcitabine vs 20 μM DMF + 0.16 μM Gemcitabine	Panc-1	0.7887	ns	No
	Mia PaCa-2	<0.0001	****	Yes
40 μM DMF vs 40 μM DMF + 0.5 μM Gemcitabine	Panc-1	0.3291	ns	No
	Mia PaCa-2	<0.0001	****	Yes
0.5 μM Gemcitabine vs 40 μM DMF + 0.5 μM Gemcitabine	Panc-1	0.0138	*	Yes
	Mia PaCa-2	<0.0001	****	Yes
60 μM DMF vs 60 μM DMF + 1 μM Gemcitabine	Panc-1	0.0019	**	Yes
	Mia PaCa-2	0.8399	ns	No
1 μM Gemcitabine vs 60 μM DMF + 1 μM Gemcitabine	Panc-1	<0.0001	****	Yes
	Mia PaCa-2	<0.0001	****	Yes
20 μM DMF + 0.16 μM Gemcitabine vs 40 μM DMF + 0.5 μM Gemcitabine	Panc-1	0.0988	ns	No
	Mia PaCa-2	0.0031	**	Yes
20 μM DMF + 0.16 μM Gemcitabine vs 60 μM DMF + 1 μM Gemcitabine	Panc-1	0.0041	**	Yes
	Mia PaCa-2	0.9611	ns	No
40 μM DMF + 0.5 μM Gemcitabine vs 60 μM DMF + 1 μM Gemcitabine	Panc-1	0.3423	ns	No
	Mia PaCa-2	0.0060	**	Yes

**Figure 3.21: Schedule 3 – DMF + gemcitabine analysis.** (A) Survival fractions in Panc-1 cell line following treatment. (B) Survival fractions in Mia PaCa-2 cell line following treatment. Analysis was carried out via one-way ANOVA with Bonferroni post hoc test using GraphPad Prism 10.1.2. \* =  $P \leq 0.05$ ; \*\* =  $P \leq 0.01$ ; \*\*\* =  $P \leq 0.001$ ; and \*\*\*\* =  $P \leq 0.0001$  in comparison with untreated control. (C) Statistical table of comparisons of combinations and monotherapies.

In Panc-1 cells (**figure 3.21A**), the schedule 3 combination of DMF + gemcitabine did not induce a statistically significant reduction in clonogenicity when compared to the untreated control at any of the concentrations tested ( $P \geq 0.3202$ ), with the highest concentration combination (60  $\mu\text{M}$  DMF + 1  $\mu\text{M}$  gemcitabine) inducing a statistically significant increase in clonogenicity when compared with the untreated control ( $P = 0.0218$ ). This result indicates that the combination is of no additional benefit over the individual monotherapies in Panc-1 cells.

In Mia PaCa-2 cells (**figure 3.21B**), all concentrations of the schedule 3 combination of DMF + gemcitabine induced significant reduction in clonogenicity when compared with the untreated control ( $P < 0.0001$ ), however only the combinations of 20  $\mu\text{M}$  DMF + 0.16  $\mu\text{M}$  gemcitabine and 40  $\mu\text{M}$  DMF + 0.5  $\mu\text{M}$  gemcitabine induced statistically significantly more reduction in clonogenicity when compared with the individual drugs alone ( $P < 0.0001$ ). The highest concentration of the combination, 60  $\mu\text{M}$  DMF + 1  $\mu\text{M}$  gemcitabine, did not induce a statistically significantly greater level of reduction in clonogenicity when compared with 60  $\mu\text{M}$  DMF alone ( $P = 0.8399$ ).

Following this test, the highest concentration of 60  $\mu\text{M}$  DMF + 1  $\mu\text{M}$  gemcitabine, was then tested in the 3D spheroid growth assay as described in **section 3.3.5**, and the results presented in **figure 3.22**. This concentration was selected as pilot studies (**figure 3.3 & 3.11**) in Panc-1 spheroids using schedule 1 & 2 combinations indicated that lower concentrations of combinations were ineffective at reducing spheroid growth when compared with both the untreated control and monotherapies.

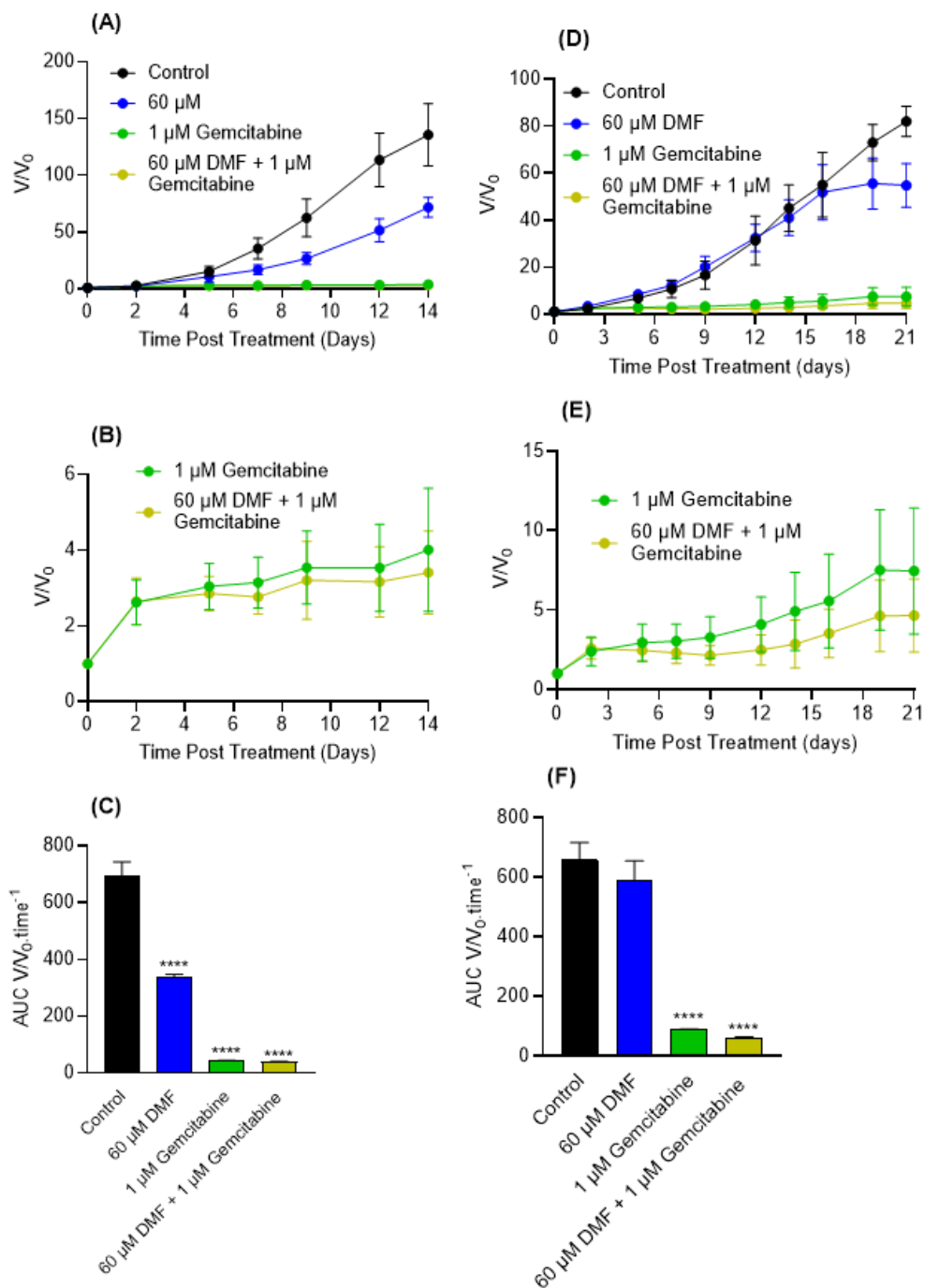


**Figure 3.22: Schedule 3 – DMF + gemcitabine spheroid growth assay in Panc-1 and Mia PaCa-2.** (A&D) Spheroid growth (V/V<sub>0</sub>) following treatment. The data is represented as the average of three independent experiments carried out with 16 spheroids per treatment group (48 spheroids total) ± standard deviation. (B&E) V/V<sub>0</sub> for gemcitabine and DMF + gemcitabine treated spheroids alone is shown. (C&F) AUC for treated spheroids and untreated control is shown. The data is represented as the average ± standard deviation. Analysis was carried out via Kruskal-Wallis with Dunn's post hoc test using GraphPad Prism 10.1.2. \*\*\*\* = P ≤ 0.0001 in comparison with untreated control.

In Panc-1 spheroids (**figure 3.22A**), the schedule 3 combination of 60  $\mu$ M DMF + 1  $\mu$ M gemcitabine induced a statistically significant reduction in spheroid growth when compared with the untreated control ( $P < 0.0001$ ). However, when compared with the individual components, the combination did not induce a statistically significantly greater reduction in spheroid growth when compared with 1  $\mu$ M gemcitabine (**figure 3.22B**) alone ( $P = 0.1001$ ), indicating that the agents were not of additional benefit in combination in Panc-1 spheroids. To further investigate this observation, the AUC was analysed. As can be seen in **figure 3.22C** the combination ( $P < 0.0001$ ) and both monotherapies statistically significantly reduced the AUC when compared with the untreated control ( $P < 0.0001$ ). However, the combination of 60  $\mu$ M DMF + 1  $\mu$ M did not statistically significantly reduce the AUC when compared with 1  $\mu$ M gemcitabine alone ( $P = 0.7777$ ), again indicating that the agents were not of additional benefit in combination in Panc-1 spheroids.

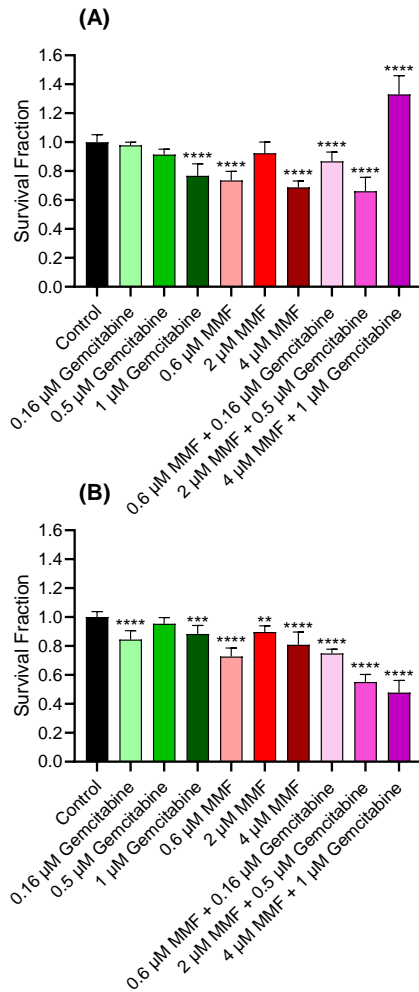
In Mia PaCa-2 spheroids (**figure 3.22D&E**), the schedule 3 combination of 60  $\mu$ M DMF + 1  $\mu$ M gemcitabine induced a statistically significant reduction in spheroid growth when compared with the untreated control and both monotherapies alone ( $P < 0.0001$ ), indicating that the agents were of additional benefit in combination in Mia PaCa-2 spheroids. To further investigate this observation, the AUC was analysed. As can be seen in **figure 3.22F** the combination and both monotherapies statistically significantly reduced the AUC when compared with the untreated control ( $P < 0.0001$ ). When comparing the combination of 60  $\mu$ M DMF + 1  $\mu$ M gemcitabine, it statistically significantly reduced the AUC when compared with 1  $\mu$ M gemcitabine and 60  $\mu$ M DMF ( $P \leq 0.0489$ ), again indicating that the agents were of additional benefit in combination in Mia PaCa-2 spheroids. A table depicting all statistical analysis carried out for **figure 3.22** can be found in **table 3.11**.

**Table 3.11: Statistical comparisons for schedule 3 DMF + gemcitabine spheroid growth and AUC assay in Panc-1 and Mia PaCa-2.**

Comparison	Being Assessed	Cell Line	P-value	Summary	Significant?
60 $\mu$ M DMF vs Control	Spheroid growth	Panc-1	0.0134	*	Yes
		Mia PaCa-2	>0.9999	ns	No
1 $\mu$ M gemcitabine vs Control	Spheroid growth	Panc-1	<0.0001	****	Yes
		Mia PaCa-2	<0.0001	****	Yes
60 $\mu$ M DMF + 1 $\mu$ M gemcitabine vs Control	Spheroid growth	Panc-1	<0.0001	****	Yes
		Mia PaCa-2	<0.0001	****	Yes
60 $\mu$ M DMF vs 60 $\mu$ M DMF + 1 $\mu$ M gemcitabine	Spheroid growth	Panc-1	<0.0001	****	Yes
		Mia PaCa-2	<0.0001	****	Yes
1 $\mu$ M gemcitabine vs 60 $\mu$ M DMF + 1 $\mu$ M gemcitabine	Spheroid growth	Panc-1	0.1001	ns	No
		Mia PaCa-2	<0.0001	****	Yes
60 $\mu$ M DMF vs Control	AUC	Panc-1	<0.0001	****	Yes
		Mia PaCa-2	0.2146	ns	No
1 $\mu$ M gemcitabine vs Control	AUC	Panc-1	<0.0001	****	Yes
		Mia PaCa-2	<0.0001	****	Yes
60 $\mu$ M DMF + 1 $\mu$ M gemcitabine vs Control	AUC	Panc-1	<0.0001	****	Yes
		Mia PaCa-2	<0.0001	****	Yes
60 $\mu$ M DMF vs 60 $\mu$ M DMF + 1 $\mu$ M gemcitabine	AUC	Panc-1	<0.0001	****	Yes
		Mia PaCa-2	<0.0001	****	Yes
1 $\mu$ M gemcitabine vs 60 $\mu$ M DMF + 1 $\mu$ M gemcitabine	AUC	Panc-1	0.7777	ns	No
		Mia PaCa-2	0.0489	*	No

#### **3.4.5-2: Schedule 3 – MMF + gemcitabine**

Based on the results obtained in **figure 3.20**, the schedule 3 combination of MMF + gemcitabine was selected for further analysis as we believe the combination showed promise and hypothesised that altering the dosing may yield more significant results. The dosing for this combination was based on the monotherapy results obtained in **chapter 2**, and the dosing kept below the IC<sub>50</sub> value to enable the effect of the combination to be seen. Additionally, this combination was kept at this stage for comparison with its schedule 3 MMF + gemcitabine counterpart. The incubation time was 48 hours total to allow each component at least one full cell cycle following administration to illicit its effect and we hypothesised that DMF would sensitise the cell through NRF2 inhibition, allowing gemcitabine to illicit a stronger cytotoxic effect. The clonogenic assay was carried out as described in **section 3.3.3**, and the results presented in **figure 3.23**.



**(C) Statistical Table of Comparisons**

Comparison	Cell Line	P-value	Summary	Significant?
0.6 $\mu$ M MMF vs Control	Panc-1	<0.0001	****	Yes
	Mia PaCa-2	<0.0001	****	Yes
2 $\mu$ M MMF vs Control	Panc-1	0.1608	ns	No
	Mia PaCa-2	0.0029	**	Yes
4 $\mu$ M MMF vs Control	Panc-1	<0.0001	****	Yes
	Mia PaCa-2	<0.0001	****	Yes
0.16 $\mu$ M Gemcitabine vs Control	Panc-1	0.9930	ns	No
	Mia PaCa-2	<0.0001	****	Yes
0.5 $\mu$ M Gemcitabine vs Control	Panc-1	0.0894	ns	No
	Mia PaCa-2	0.4486	ns	No
1 $\mu$ M Gemcitabine vs Control	Panc-1	<0.0001	****	Yes
	Mia PaCa-2	0.0005	***	Yes
0.6 $\mu$ M MMF + 0.16 $\mu$ M Gemcitabine vs Control	Panc-1	0.0019	**	Yes
	Mia PaCa-2	<0.0001	****	Yes
2 $\mu$ M MMF + 0.5 $\mu$ M Gemcitabine vs Control	Panc-1	<0.0001	****	Yes
	Mia PaCa-2	<0.0001	****	Yes
4 $\mu$ M MMF + 1 $\mu$ M Gemcitabine vs Control	Panc-1	<0.0001	****	Yes
	Mia PaCa-2	<0.0001	****	Yes
0.6 $\mu$ M MMF vs 0.6 $\mu$ M MMF + 0.16 $\mu$ M Gemcitabine	Panc-1	<0.0001	****	Yes
	Mia PaCa-2	>0.9999	ns	No
0.16 $\mu$ M Gemcitabine vs 0.6 $\mu$ M MMF + 0.16 $\mu$ M Gemcitabine	Panc-1	0.0005	***	Yes
	Mia PaCa-2	0.0019	**	Yes
2 $\mu$ M MMF vs 2 $\mu$ M MMF + 0.5 $\mu$ M Gemcitabine	Panc-1	<0.0001	****	Yes
	Mia PaCa-2	<0.0001	****	Yes
0.5 $\mu$ M Gemcitabine vs 2 $\mu$ M MMF + 0.5 $\mu$ M Gemcitabine	Panc-1	<0.0001	****	Yes
	Mia PaCa-2	<0.0001	****	Yes
4 $\mu$ M MMF vs 4 $\mu$ M MMF + 1 $\mu$ M Gemcitabine	Panc-1	<0.0001	****	Yes
	Mia PaCa-2	<0.0001	****	Yes
1 $\mu$ M Gemcitabine vs 4 $\mu$ M MMF + 1 $\mu$ M Gemcitabine	Panc-1	<0.0001	****	Yes
	Mia PaCa-2	<0.0001	****	Yes
0.6 $\mu$ M MMF + 0.16 $\mu$ M Gemcitabine vs 2 $\mu$ M MMF + 0.5 $\mu$ M Gemcitabine	Panc-1	0.0006	***	Yes
	Mia PaCa-2	<0.0001	****	Yes
0.6 $\mu$ M MMF + 0.16 $\mu$ M Gemcitabine vs 4 $\mu$ M MMF + 1 $\mu$ M Gemcitabine	Panc-1	<0.0001	****	Yes
	Mia PaCa-2	<0.0001	****	Yes
2 $\mu$ M MMF + 0.5 $\mu$ M Gemcitabine vs 4 $\mu$ M MMF + 1 $\mu$ M Gemcitabine	Panc-1	<0.0001	****	Yes
	Mia PaCa-2	0.0367	*	Yes

**Figure 3.23: Schedule 3 – MMF + gemcitabine analysis.** (A) Survival fractions in Panc-1 cell line following treatment. (B) Survival fractions in Mia PaCa-2 cell line following treatment. (C) Statistical table of comparisons of combinations and monotherapies. Data is shown as the average of three independent experiments carried out in triplicate  $\pm$  standard deviation. Analysis was carried out via one-way ANOVA with Bonferroni post hoc test using GraphPad Prism 10.1.2. \*\* =  $P \leq 0.01$  and \*\*\*\* =  $P \leq 0.0001$  in comparison with untreated control.

In Panc-1 cells (**figure 3. 23A**), the schedule 3 combination of MMF + gemcitabine induced a statistically significant reduction in clonogenicity when compared to the untreated control when given at 0.6  $\mu\text{M}$  MMF + 0.16  $\mu\text{M}$  gemcitabine ( $P < 0.0001$ ) and 2  $\mu\text{M}$  MMF + 0.5  $\mu\text{M}$  gemcitabine ( $P < 0.0001$ ). Unexpectedly the highest concentration of the combination (4  $\mu\text{M}$  MMF + 1  $\mu\text{M}$  gemcitabine) induced a statistically significant increase in clonogenicity when compared with the untreated control ( $P < 0.0001$ ). Both 0.6  $\mu\text{M}$  MMF + 0.16  $\mu\text{M}$  gemcitabine and 2  $\mu\text{M}$  MMF + 0.5  $\mu\text{M}$  gemcitabine induced a statistically significantly greater reduction in clonogenicity when compared with both monotherapies ( $P \leq 0.0019$ ). Conversely, 4  $\mu\text{M}$  MMF + 1  $\mu\text{M}$  gemcitabine induced a statistically significant increase in clonogenicity when compared with both monotherapies ( $P < 0.0001$ ).

In Mia PaCa-2 cells (**figure 3. 23B**), the schedule 3 combination of MMF + gemcitabine induced significant reduction in clonogenicity when compared with the untreated control ( $P < 0.0001$ ), however only the combinations of 2  $\mu\text{M}$  MMF + 0.5  $\mu\text{M}$  gemcitabine and 4  $\mu\text{M}$  MMF + 1  $\mu\text{M}$  gemcitabine were considered statistically significant as these combinations induced statistically significantly greater reduction in clonogenicity when compared with the individual drugs alone ( $P < 0.0001$ ). The lowest concentration of the combination, 0.6  $\mu\text{M}$  MMF + 0.16  $\mu\text{M}$  gemcitabine, did not induce a statistically significantly greater level of reduction in clonogenicity when compared with 0.6  $\mu\text{M}$  MMF alone ( $P > 0.9999$ ).

Following this test, the highest concentration of 4  $\mu\text{M}$  MMF + 1  $\mu\text{M}$  gemcitabine, was then tested in the 3D spheroid growth assay as described in **section 3.3.5**, and the results presented in **figure 3.24**. This concentration was selected as pilot studies (**figure 3.3 & 3.11**) in Panc-1 spheroids using schedule 1 & 2 combinations indicated that lower concentrations of combinations were ineffective at reducing spheroid growth when compared with both the untreated control and monotherapies.

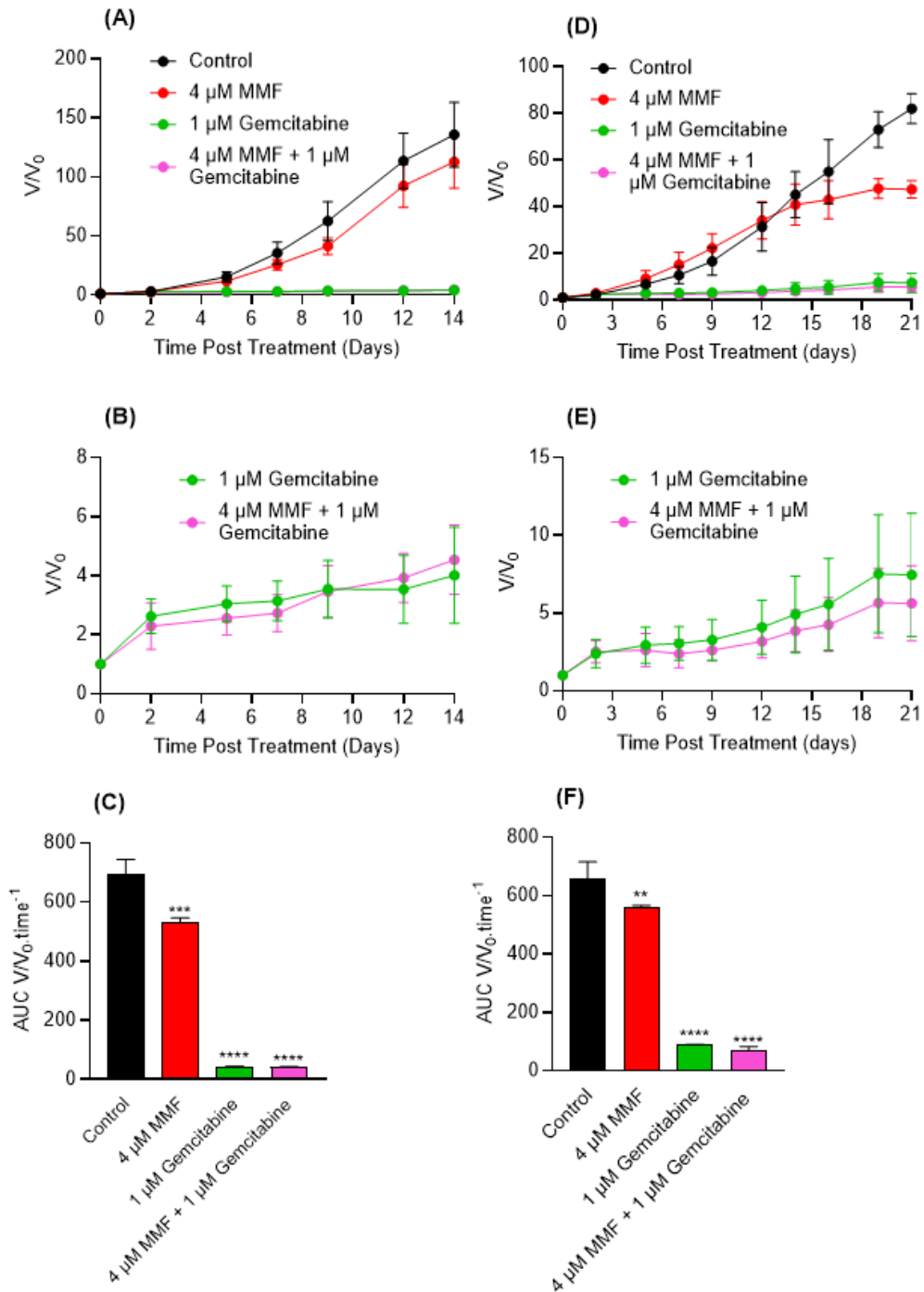


**Figure 3.24: Schedule 3 – MMF + gemcitabine spheroid growth assay in Panc-1 and Mia PaCa-2.** (A&D) Spheroid growth (V/V<sub>0</sub>) following treatment. The data is represented as the average of three independent experiments carried out with 16 spheroids per treatment group (48 spheroids total) ± standard deviation. (B&E) V/V<sub>0</sub> for gemcitabine and DMF + gemcitabine treated spheroids alone is shown. (C&F) AUC for treated spheroids and untreated control is shown. The data is represented as the average ± standard deviation. Analysis was carried out via Kruskal-Wallis with Dunn's post hoc test using GraphPad Prism 10.1.2. \*\*\* = P ≤ 0.001 and \*\*\*\* = P ≤ 0.0001 in comparison with untreated control.

In Panc-1 spheroids (**figure 3.24A**), the schedule 3 combination of 4  $\mu\text{M}$  MMF + 1  $\mu\text{M}$  gemcitabine induced a statistically significant reduction in spheroid growth when compared with the untreated control ( $P < 0.0001$ ), however when compared with 1  $\mu\text{M}$  gemcitabine alone (**figure 3.24B**) there was no statistically significant reduction ( $P > 0.9999$ ) in spheroid growth, indicating that the agents were not of additional benefit in combination in Panc-1 spheroids. To further investigate this observation, the AUC was analysed. As can be seen in **figure 3.24C**, the AUC was statistically significantly reduced by the combination and both monotherapies when compared with the untreated control ( $P \leq 0.0093$ ). However, when comparing the combination to the individual drugs, there was no statistically significant difference when comparing the combination to 1  $\mu\text{M}$  gemcitabine alone ( $P > 0.9631$ ), again indicating the agents were not of additional benefit in combination in Panc-1 spheroids.

In Mia PaCa-2 spheroids (**figure 3.24D&E**), the schedule 3 combination of 4  $\mu\text{M}$  MMF + 1  $\mu\text{M}$  gemcitabine induced a statistically significant reduction in spheroid growth when compared with the untreated control ( $P < 0.0001$ ); 4  $\mu\text{M}$  MMF ( $P < 0.0001$ ); and 1  $\mu\text{M}$  gemcitabine ( $P = 0.0074$ ), indicating that the agents were of additional benefit in combination in Mia PaCa-2 spheroids. To further investigate this observation, the AUC was analysed. As can be seen in **figure 3.24F**, the AUC was statistically significantly reduced by the combination and both monotherapies when compared with the untreated control ( $P \leq 0.0093$ ). When comparing the combination to the individual drugs, there was no statistically significant difference when comparing the combination to 1  $\mu\text{M}$  gemcitabine alone ( $P = 0.0710$ ), conversely indicating that the drugs were not of additional benefit in combination in Mia PaCa-2 spheroids. A table depicting all statistical analysis carried out for **figure 3.24** can be found in **table 3.12**.

**Table 3.12: Statistical comparisons for schedule 3 MMF + gemcitabine spheroid growth and AUC assay in Panc-1 and Mia PaCa-2.**

Comparison	Being Assessed	Cell Line	P-value	Summary	Significant?
4 $\mu$ M MMF vs Control	Spheroid growth	Panc-1	0.7611	ns	No
		Mia PaCa-2	>0.9999	ns	No
1 $\mu$ M gemcitabine vs Control	Spheroid growth	Panc-1	<0.0001	****	Yes
		Mia PaCa-2	<0.0001	****	Yes
4 $\mu$ M MMF + 1 $\mu$ M gemcitabine vs Control	Spheroid growth	Panc-1	<0.0001	****	Yes
		Mia PaCa-2	<0.0001	****	Yes
4 $\mu$ M MMF vs 4 $\mu$ M MMF + 1 $\mu$ M gemcitabine	Spheroid growth	Panc-1	<0.0001	****	Yes
		Mia PaCa-2	<0.0001	****	Yes
1 $\mu$ M gemcitabine vs 4 $\mu$ M MMF + 1 $\mu$ M gemcitabine	Spheroid growth	Panc-1	>0.9999	ns	No
		Mia PaCa-2	0.0074	**	Yes
4 $\mu$ M MMF vs Control	AUC	Panc-1	0.0002	***	Yes
		Mia PaCa-2	0.0093	**	Yes
1 $\mu$ M gemcitabine vs Control	AUC	Panc-1	<0.0001	****	Yes
		Mia PaCa-2	<0.0001	****	Yes
4 $\mu$ M MMF + 1 $\mu$ M gemcitabine vs Control	AUC	Panc-1	<0.0001	****	Yes
		Mia PaCa-2	<0.0001	****	Yes
4 $\mu$ M MMF vs 4 $\mu$ M MMF 1 $\mu$ M gemcitabine	AUC	Panc-1	<0.0001	****	Yes
		Mia PaCa-2	<0.0001	****	Yes
1 $\mu$ M gemcitabine vs 4 $\mu$ M MMF + 1 $\mu$ M gemcitabine	AUC	Panc-1	0.9631	ns	No
		Mia PaCa-2	0.0710	ns	No

A summary of all tested schedule 3 combinations can be found in **table 3.14** below.

**Table 3.14: Summary of the Schedule 3 combinations**

Schedule 3 combination	Greater effect than individual agents in Panc-1 cells?	Greater effect than individual agents in Panc-1 spheroids?	Greater effect than individual agents in Mia PaCa-2 cells?	Greater effect than individual agents in Mia PaCa-2 spheroids?
DMF + Gemcitabine	No	No	Yes	Yes
MMF + Gemcitabine	Yes	Yes	No	No

### **3.5: DISCUSSION**

As previously discussed, pancreatic cancer is most commonly diagnosed in the later stages of the disease, where therapeutic options are limited due to deteriorating patient health, therefore the therapeutic options are often limited in the clinic, with gemcitabine monotherapy being the most common treatment. However, gemcitabine resistance is prevalent clinically (Yin, *et al.*, 2016), therefore alternative treatments are greatly needed. In an attempt to combat this resistance, we developed various novel combination schedules incorporating DMF/MMF. Literature has shown that altering the schedule of combinations can greatly influence the therapeutic outcome (Modest *et al.*, 2019; McCluskey 2012), therefore we developed three different scheduling options.

We hypothesised that the addition of DMF/MMF with gemcitabine could enhance the therapeutic outcome, and that the utilising EXBR in combination with DMF/MMF could potentially remove the need for gemcitabine altogether, which could be more beneficial clinically due to the high levels of resistance seen.

#### **3.5.1: Gemcitabine + EXBR**

When treating cells and 3D spheroids with the gemcitabine + EXBR schedule 1 combination, gemcitabine and EXBR were administered simultaneously and incubated for 48 hours. It was hypothesised that this combination would be effective at killing both 2D cells and 3D spheroids, as in **chapter 2** it was shown that both Panc-1 and Mia PaCa-2 cells/spheroids were highly sensitive to both gemcitabine and EXBR monotherapy. It was also hypothesised that this scheduled combination would be effective as this combination has already been assessed clinically by phase II clinical trials in patients with locally advanced pancreatic cancer, in which gemcitabine was suggested to be a radiosensitiser, enhancing the effect of radiotherapy [180-183]. This combination was therefore included for comparison with novel combinations for

this schedule, as it has been shown promise in the literature. Using the clonogenic assay, it was determined that the schedule 1 combination of gemcitabine + EXBR administered simultaneously did not reduce clonogenicity in both Panc-1 and Mia PaCa-2 cells when compared with the single agents alone (**figure 3.2**), and based on this result, it was decided to not take this combination forward for further analysis. This result was unexpected, as based on previous results in **chapter 2** it was determined that Panc-1 and Mia PaCa-2 were highly sensitive to both gemcitabine and EXBR alone in both 2D cell monolayers and in the 3D spheroid model. To further evaluate this combination, it was tested in Panc-1 and Mia PaCa-2 spheroids (**figure 3.10**) and again, the combination did not induce any additional reduction in spheroid growth when compared with gemcitabine monotherapy. As previously stated, this combination and schedule of gemcitabine and EXBR has already been used clinically in patients with locally advanced pancreatic cancer. One phase two trial in 2011 reported that the combination can safely be administered to patients following activity and toxicology studies, but limited patient benefit was seen, with a median survival time of 10.3 months following treatment with the combination therapy [184], however this particular study did disclose the median survival time for untreated patients. In another study, the authors reported that the combination did not lead to any sustained disease-free survival in any of the patients in the study [183], again suggesting that the obtained results from the clonogenic assay are in fact to be expected and that the agents are of no additional benefit in combination, despite being effective as monotherapies.

For schedule 2, gemcitabine was given first and incubated with Panc-1 and Mia PaCa-2 cells/spheroids for 24 hours before being irradiated and incubated for a further 24 hours. For this schedule it was hypothesised that by exposing the cells to gemcitabine prior to irradiation, that radiosensitisation of the cells would occur due the known

radiosensitising activity of gemcitabine seen in literature [185], which in turn should enhance the effect of EXBR. In schedule 2, this combination of gemcitabine + EXBR was overall less effective in respect to reduction in clonogenicity in both Panc-1 and Mia PaCa-2, when tested in the 2D cell model via the clonogenic assay (**figure 3.13C & D**) as the combination did not achieve more reduction in clonogenicity when compared with the single agents alone. However, despite this result, the combination was still taken forward for further analysis as this scheduled approach showed promise with both DMF and MMF. The trend observed in the 2D cell model translated into the 3D spheroid model, as the combination did not induce a reduction in spheroid growth when compared with gemcitabine monotherapy in spheroids of both Panc-1 and Mia PaCa-2 (**figures 3.14 & 3.15**), implying that the agents were of no additional benefit in spheroids, which was unexpected as both Panc-1 and Mia PaCa-2 spheroids showed high sensitivity to both gemcitabine and EXBR when given as single agents. Upon reviewing the literature, this schedule of the combination of gemcitabine + EXBR in which gemcitabine is administered as a neoadjuvant chemotherapy before radiotherapy has not been used clinically, however many studies have been carried out investigating the role of neoadjuvant therapy in the treatment of pancreatic cancer. Typically, the role of neoadjuvant therapy in the treatment of pancreatic cancer is to facilitate resection in patients with initially unresectable pancreatic cancer by shrinking the tumour [186]. Different combinations of chemotherapies, such as gemcitabine + capecitabine; gemcitabine + nab-paclitaxel and FOLFIRINOX have been interrogated in clinical trials as a neoadjuvant for the treatment of pancreatic cancer, as well as different combinations of chemoradiotherapy, such as radiotherapy + gemcitabine and radiotherapy + capecitabine have been utilised to varying levels of success [187]. Some studies have investigated the use of gemcitabine monotherapy as a neoadjuvant chemotherapy. For example, one study compared FOLFIRINOX with gemcitabine monotherapy as a

neoadjuvant chemotherapy and the median overall survival of patients treated with gemcitabine was 6.8 months versus 11.1 months in patients treated with FOLFIRINOX [132]. Similarly, another study found that the median overall survival in patients treated with gemcitabine monotherapy was 6.7 months, versus 8.5 months in patients treated with nab-paclitaxel + gemcitabine [135]. These findings suggest that gemcitabine is a poor candidate for neoadjuvant chemotherapy and could perhaps explain the lesser reduction in clonogenicity in the 2D cell model and lowered reduction in spheroid volume results obtained when interrogating the schedule 2 combination therapy of gemcitabine + EXBR.

Overall, gemcitabine in combination with EXBR regardless of schedule was ineffective, especially in pancreatic cancer cell spheroids, where gemcitabine monotherapy was equally as effective. The exact mechanism in which gemcitabine induces radiosensitisation is currently unknown, but it is thought that the inhibition of DNA synthesis itself is a key factor in the reported radiosensitisation effect of gemcitabine [188]. Cytidine deaminase, a ubiquitous enzyme involved in the recycling of free pyrimidines, has been implemented as a key factor in limiting the anticancer effectiveness of gemcitabine [133, 189, 190]. Cytidine deaminase inactivates and degrades gemcitabine and is known to be more highly expressed in PDAC tumour tissue when compared with healthy tissue [189]. Therefore, it may be possible that gemcitabine did not work in combination with radiotherapy overall due to the action of cytidine deaminase, which prevented gemcitabine from inducing its radiosensitising effect, and subsequently enhancing the effect of EXBR. This hypothesis is further supported by the fact that a study identified that cytidine deaminase expression is increased in both Panc-1 and Mia PaCa-2, with cytidine deaminase expression being higher in Panc-1 when compared with Mia PaCa-2 [191]. Additionally, as gemcitabine is known to preferentially induce synthesis phase (S phase) cell cycle arrest, which is

reported to be the most radioresistant phase of the cell cycle, this could account for the effects obtained experimentally when given in combination with EXBR, which is known to be most effective in the G2/M phase of the cell cycle [192-194].

### **3.5.2: DMF + EXBR**

It was hypothesised that the schedule 1 combination of DMF + EXBR would be effective in Panc-1 and Mia PaCa-2 cells, as previous studies carried out in our lab utilising glioblastoma and medulloblastoma cancer cell lines indicated that this simultaneous combination of DMF + EXBR induced greater reduction in clonogenicity when compared with the individual agents alone [195, 196]. In schedule 1, the combination of DMF + EXBR were given simultaneously, and this combination was only effective in Mia PaCa-2 cells (**figure 3.2B**), as in Panc-1 cells (**figure 3.2A**) the combination did not induce additional reduction in clonogenicity over the single agents of DMF and EXBR alone, when tested in a 2D cell model via the clonogenic assay. Based on this result, it was decided to not take this combination forward for further analysis. However, the combination was tested in a 3D spheroid model in both Panc-1 and Mia PaCa-2 (**figure 3.11**), and again the combination was only of additional benefit in Mia PaCa-2 spheroids, where the combination induced a greater reduction in spheroid growth than both DMF and EXBR alone, while in Panc-1 there was no additional reduction in spheroid growth when comparing the combination with the individual agents. These results were somewhat unexpected as previously mentioned studies in our lab indicated that this combination would be effective, however given these studies were in other type of cancer, and thus these cancers have different molecular pathologies this could contribute to the obtained result. Interestingly, the combination did show some promise in Mia PaCa-2 cells, but not in Panc-1 cells, which suggests that there may be some fundamental difference between the two cell lines attributing to this effect. A study found that DMF is preferentially cytotoxic to

cancer cells with KRAS mutation, particularly those harbouring a G12V KRAS mutation [112]. In pancreatic cancers, KRAS mutation occurs most frequently in the G12 position, however Mia PaCa-2 has the less frequently occurring G12C KRAS mutation, which occurs in approximately 1% of pancreatic cancers, whereas Panc-1 has a KRAS G12D mutation which occurs in 41% of pancreatic cancers [197, 198]. This difference in KRAS mutation between Panc-1 and Mia PaCa-2 could perhaps be attributed to the observed difference in combination cytotoxicity, however further studies would be required to confirm this hypothesis utilising other KRAS mutant pancreatic cancer cell lines.

For schedule 2 of the DMF + EXBR combination, where DMF was given 24 hours before irradiation with 0.5 Gy EXBR, it was hypothesised that this combination would be effective due to the reported inhibition of the oxidative response, via reduction of glutathione, reported in literature by DMF, which when given as a neoadjuvant chemotherapy, DMF could enhance the effect of radiotherapy as the ROS produced as a result of EXBR would not be diminished by the oxidative response. When given in schedule 2, the combination of DMF + EXBR was of additional benefit when compared with the monotherapies in both Panc-1 and Mia PaCa-2 cells (**figure 3.16**) when tested in the 2D cell model via the clonogenic assay as the combination induced greater reduction in clonogenicity than the individual agents of DMF and EXBR alone. This translated into 3D spheroids, with the combination being of additional benefit over the single agents alone in both Panc-1 and Mia Paca-2 spheroids as the combination induced a greater reduction in spheroid growth when compared with both single agents alone. This result would indicate that DMF did indeed reduce glutathione levels and enhance the effect of EXBR, and later studies will be carried out in **chapter 4** to test this hypothesis. When looking in the literature no studies utilising DMF and radiotherapy in this scheduled manner could be found.

Overall, the combination of DMF + EXBR was most effective when given in schedule 2. However, it was noted that in both schedules the combination of DMF + EXBR exhibited a greater effect in the spheroid model in both Panc-1 and Mia PaCa-2 cells. Interestingly, a study identified that DMF induces a radiosensitising effect on hypoxic cells [199], which could perhaps explain the enhanced effect of the combination in spheroids, as spheroids contain a large population of hypoxic cells. Further supporting this hypothesis is that NRF2 is upregulated in response to hypoxia, and DMF is reported to be an inhibitor of NRF2 activity, meaning DMF would enhance hypoxic conditions within spheroids [111, 200].

### **3.5.3: MMF + EXBR**

In schedule 1, MMF and EXBR were given simultaneously, and it was hypothesised that this scheduled combination would be highly effective as both Panc-1 and Mia PaCa-2 cells/spheroids exhibited a high degree of sensitivity to both single agents as shown in **chapter 2**. Given that MMF is the active metabolite of DMF, the same considerations made for the schedule 1 combination of DMF + EXBR can be applied here. The schedule 1 combination of MMF + EXBR was highly effective in both Panc-1 and Mia PaCa-2 cells (**figure 3.2**) when assessed in 2D cells via the clonogenic assay, as indicated by the increased reduction in clonogenicity by the combination when compared with its single components of MMF and EXBR. When testing this combination in Panc-1 and Mia PaCa-2 spheroids, the combination induced a greater reduction in spheroid growth when compared with the individual agents in Panc-1 spheroids, however in Mia PaCa-2 spheroids (**figure 3.5**) the combination was of no additional benefit over the single agents as the combination was unable to induce a greater reduction in spheroid growth when compared with MMF monotherapy. This result was unexpected as the clonogenic data (**figure 3.4**) indicated that the combination would be of additional benefit in Mia PaCa-2, but this result can perhaps

be explained by how effective MMF monotherapy was on Mia PaCa-2 spheroids as seen in **chapter 2**.

In schedule 2, MMF was given first and incubated for 24 hours prior to irradiation with 0.5 Gy EXBR. For this schedule it was hypothesised that similarly to DMF, neoadjuvant treatment with MMF would decrease the antioxidant response, allowing the full effect of the radiotherapy to be achieved, therefore the agents would work effectively in combination using this schedule. When given in schedule 2, the combination of MMF + EXBR was of additional benefit in both Panc-1 and Mia PaCa-2 cells, as indicated by the increased reduction in clonogenicity by the combination when compared with the individual agents alone. This did not translate into spheroids in the Panc-1 cell line, as the combination did not induce a greater reduction in Panc-1 spheroid growth when compared with both single agents alone (**figure 3.19**), however in Mia PaCa-2 the combination was of additional benefit over both single agents as the combination induced a greater reduction in spheroid growth when compared with MMF and EXBR alone.

Overall, the combination of MMF + EXBR was highly effective regardless of schedule in 2D monolayers in both Panc-1 and Mia PaCa-2, however this did not universally translate into the 3D spheroid model, highlighting the challenges in treating spheroids, which more accurately reflect the *in vivo* conditions of a tumour. Upon reviewing the literature this combination has not yet been tested; therefore, no comparisons could be drawn.

#### **3.5.4: DMF + gemcitabine**

In schedule 1 DMF and gemcitabine were given simultaneously to Panc-1 and Mia PaCa-2 cells/spheroids. It was hypothesised that this combination would be effective as gemcitabine is known to increase the expression of Glutathione S-transferases, which are a key enzyme in the antioxidant response, therefore administering

gemcitabine with DMF could be beneficial if DMF reduces the level of glutathione in the cell, preventing the cell from evading damage induced by gemcitabine therapy [201]. In Mia PaCa-2 cells the combination induced a greater amount of reduction in clonogenicity over the individual components. Interestingly, when the combination was tested in 3D spheroids, the combination was effective in Panc-1 (**figure 3.9**) spheroids, as the combination induced a greater decrease in spheroid growth when compared with the individual components. In Mia PaCa-2 spheroids, the combination was of no additional benefit over gemcitabine monotherapy, which is not entirely unexpected given that as previously described in **chapter 2** Mia PaCa-2 is less suited to 3D spheroid studies when compared with Panc-1 due to Mia PaCa-2 cells forming looser spheroids [161]. Upon reviewing the literature, no studies utilising this combination of DMF + gemcitabine have been published; therefore, no comparisons can be made at this time.

When the combination of DMF + gemcitabine was given in schedule 3, cells/spheroids were incubated with DMF first for 24 hours, followed by the addition of gemcitabine for an additional 24 hours. As with the schedule 1 variant of this combination, it was hypothesised that this combination would be of additional benefit over the monotherapies. The combination was ineffective in Panc-1 as the combination did not induce a greater amount of reduction in clonogenicity when compared with the individual agents alone following the clonogenic assay. However, in Mia PaCa-2 (**figure 3.21**) the combination was effective as when assessing the level of reduction in clonogenicity via the clonogenic assay the combination induced a greater reduction in clonogenicity when compared with the single agents alone. The results from the clonogenic assay translated into spheroids, as in Panc-1 spheroids the combination did not induce a greater reduction in spheroid growth when compared with gemcitabine monotherapy, whereas in Mia PaCa-2 spheroids (**figure 3.22**), the

combination was of additional benefit over gemcitabine monotherapy. Overall, this combination was effective in Mia PaCa-2 only, which could be attributed to the higher sensitivity of Mia PaCa-2 to DMF as seen in **chapter 2**. As with the schedule 1 variant of this combination, when searching the literature, no studies utilising this scheduled combination of DMF + gemcitabine could be found, therefore no comparisons can be made.

Overall, this combination of DMF and gemcitabine worked best when given in schedule 3. Interestingly, neither scheduled approach of this combination worked universally in both Panc-1 and Mia PaCa-2, perhaps highlighting that this combination would be a poor candidate for further studies due to the variability in its effectiveness seen *in vitro*.

### **3.5.5: MMF + gemcitabine**

In schedule 1, MMF + gemcitabine was administered simultaneously to Panc-1 and Mia PaCa-2 cells/spheroids. It was hypothesised that this combination would be highly effective as both cell lines displayed a high degree of sensitivity to both single agents that make up the combination, as indicated in the results presented in **chapter 2**. The schedule 1 combination of MMF + gemcitabine was of additional benefit in Panc-1 cells (**figure 3.6**) as indicated by the greater reduction in clonogenicity induced by the combination than its individual agents as assessed via the clonogenic assay. This translated into Panc-1 spheroids, as the combination induced a greater reduction in spheroid growth when compared with the individual agents alone. In Mia PaCa-2 cells (**figure 3.6**), the combination was not of additional benefit, as indicated by the combination inducing a lesser reduction in clonogenicity than the individual agents. This trend translated into Mia PaCa-2 spheroids, as the combination did not induce a greater reduction in spheroid growth when compared with gemcitabine monotherapy.

Upon reviewing the literature, no other studies utilising this combination could be found, therefore no comparisons could be made.

In schedule 3, Panc-1 and Mia PaCa-2 cells/spheroids were incubated with MMF for 24 hours before the addition of gemcitabine, and a further 24-hour incubation. It was hypothesised that this combination would be effective as both Panc-1 and Mia PaCa-2 displayed a high degree of sensitivity to both MMF and gemcitabine monotherapy, additionally it was thought that by pre-treating cells with MMF, gemcitabine effectiveness would be enhanced to the reduction of glutathione. When given in schedule 3, this combination was overall of additional benefit in Panc-1 and Mia PaCa-2 cells (**figure 3.21**), as indicated by the combination inducing a greater reduction in clonogenicity than the individual agents when assessed via the clonogenic assay. The results obtained from schedule 1 of this combination indicate that for this combination of drugs to work effectively they must be given simultaneously, as staggering them was less effective at inducing a reduction in clonogenicity. There are multiple theories for this result, with one possibility being that the glutathione reducing properties of MMF have already passed by the time gemcitabine is administered, meaning gemcitabine therapy would be less effective due to the presences of the antioxidant response. Another possibility is that MMF is upregulating NRF2 activity, because as previously discussed the action of DMF, and therefore MMF, is concentration dependent and there can be a fine line between the drug activating or inactivating NRF2. Interestingly, the effectiveness seen in both Panc-1 and Mia PaCa-2 cells did not translate into the 3D spheroid model, as the combination was unable to induce a greater reduction in spheroid growth when compared with gemcitabine monotherapy in both Panc-1 and Mia PaCa-2 spheroids. However, this result was not entirely unexpected as previously shown in **chapter 2**, both Panc-1 and Mia PaCa-2 spheroids are incredibly sensitive to gemcitabine

monotherapy when compared with 2D culture, meaning seeing the effect of the combination is challenging due to the reduction in spheroid volume achieved by gemcitabine alone. Upon reviewing the literature, no other studies utilising this combination could be found, therefore no comparisons could be made.

Overall, this combination worked best when given in schedule 1, as the combination induced a greater amount of reduction in clonogenicity when compared with the individual agents in both Panc-1 and Mia PaCa-2 cells and was able to reduce the growth of Panc-1 spheroids when compared with gemcitabine monotherapy.

### **3.5.6: Summary of combination therapies**

Overall, the combinations involving MMF were more effective in Panc-1 cells, whereas DMF combination were more effective in Mia PaCa-2 cells. Out of all the combination developed and tested, no combination in this schedule was effective in both cell lines in both 2D and 3D cell models. The difference in DMF cell cytotoxicity seen between Panc-1 and Mia PaCa-2 could be due to differences in *KRAS* mutation as previously mentioned. Mia PaCa-2 has a G12C *KRAS* mutation, whereas Panc-1 has a G12D *KRAS* mutation [137] and DMF is known to have greater toxicity towards *KRAS* mutated cells [111], however it is currently unclear from the literature if DMF preferentially targets particular *KRAS* mutants over others, but this could perhaps explain the differences in responses observed when using DMF in Mia PaCa-2 and Panc-1.

A prevailing observation throughout this chapter of work is that gemcitabine monotherapy is very effective in pancreatic spheroids, which makes seeing the effects of a combination challenging and we believe that the majority of the observed effect in the combinations in spheroids is due to the gemcitabine.

Based on all the obtained results, the schedule 1 combination of MMF + EXBR and MMF + gemcitabine; the schedule 2 combinations of MMF + EXBR and DMF + EXBR; and finally, the schedule 3 combination of MMF + gemcitabine was selected for further mechanistic studies in **chapter 4** to try and elucidate the mechanisms of action underpinning the combinations. We believe this selection of combination to be the most promising out of those tested according to the obtained results, and due to time and budgetary constraints we couldn't take everything forward for mechanistic studies.

The schedule 3 combination of DMF + gemcitabine was not taken forward for mechanistic studies as we believed the schedule 3 combination of MMF + gemcitabine to be the more efficacious combination overall, as MMF requires lower doses to induce a cytotoxic effect when compared with DMF and was more consistent in both cell lines. Additionally, due to time and budget constraints we were unable to take every combination forward for further studies meaning we had to remove some combinations. We do however note that the schedule 3 combination of DMF + gemcitabine shows some promise, and it may be explored in further studies at a later date.

## **CHAPTER 4: Mechanistic studies of developed combinations**

## **4.1: INTRODUCTION**

In the previous chapter (**chapter 3**), novel combinations for the treatment of pancreatic cancer were assessed. We selected what we believed to be the most promising combinations, based on the results obtained, to go forward for further investigation to elucidate the mechanism of action underpinning the promising treatments with respect to potential combination therapies. In an effort to determine the mechanism of action, the effects of the chosen combination treatments on the distribution of cells in the cell cycle; whether or not the combination induced apoptosis; the effect of the combination on glutathione levels within the cell; and to investigate if the combination induced DNA damage.

### **4.1.1: Cell Cycle**

The normal cell cycle functions to ensure that duplicated DNA is equally distributed amongst two daughter cells following DNA replication/chromosomal segregation and perhaps more importantly that genomic integrity is maintained [202]. Understanding the cell cycle's dynamics is crucial for developing cancer therapies for several reasons. Cancer cells typically have higher proliferation rates compared to normal cells, which can be exploited by chemotherapeutic agents and radiotherapy. We assess the distribution of cells in the cell cycle to determine if both the single agents and the selected combinations are inducing cell cycle arrest, and if so, in which phase. Determining the phase of cell cycle arrest allows us to better understand and design combination therapies, as certain agents preferentially target cells in specific phases of the cell cycle, for example radiotherapy is most effective in cells in G2 and M phase of the cell cycle [193]. Studies reported in the literature indicate that DMF induces G1 phase arrest [203, 204]. Gemcitabine is known to induce G1/S phase arrest [84].

As previously mentioned, in somatic cells the cell cycle is composed of four phases: G1; S phase G2; and M phase. Sub G1 (sG1) refers to a population of cells that are

fragmented with unrepaired DNA damage and an indicator of apoptosis [202, 205, 206].

In normal cells, the cell cycle is a highly regulated process, with various cell cycle checkpoints throughout to ensure each step occurs in the right sequence and to ensure DNA, and therefore genomic integrity is maintained via DNA repair checkpoints [207, 208]. There are three cell cycle checkpoints which function to assess DNA integrity and carry out any necessary repairs: the G1/S checkpoint; the intra-S checkpoint; and finally, the G2/M phase checkpoint [209-212]. However, in cancer cells mutation of the proteins involved in these cell cycle checkpoints occur frequently, with mutation occurring most frequently in the G1/S checkpoint, allowing cancer cells to replicate unregulated, leading to a high degree of genomic instability [207].

To distinguish what phase of the cell cycle dividing cells are in, the fluorescent DNA stain propidium iodide (PI) is used. Cells are permeabilised to allow PI to enter the cell, and the greater the amount of DNA, the greater the amount of PI that will bind, therefore cells in S phase will uptake a greater amount of PI stain, than those in G1 as they will have the double the DNA content. The differences in PI quantity can then be determined by analysing fluorescence via flow cytometry. The main goal of carrying out cell cycle analysis was to try and elucidate what the combination were doing mechanistically to the cell cycle.

#### **4.1.2: Apoptosis**

Apoptosis is a form of programmed cell death, which occurs naturally as a homeostatic mechanism to maintain cell populations in tissues and as a defence mechanism to eliminate cells damaged by disease or noxious substances [213]. We chose to assess apoptosis to determine if the selected combinations are inducing cell death as previous work carried out in our lab and in the literature suggests that DMF

induces apoptosis rather than other modes of cell death such as senescence or autophagy [111, 203, 214].

In healthy cells, the lipid phosphatidylserine (PS) is restricted to the inner leaflet of the plasma membrane, however during apoptosis the plasma membrane loses its structural integrity and PS becomes exposed on the outer leaflet of the plasma membrane [215]. Annexin V is a calcium dependent cellular protein which binds to PS, and therefore can be targeted as a means of detecting apoptotic cells. Fluorescently labelled annexin V (annexin V conjugated to fluorescein isothiocyanate (FITC)) in conjunction with PI is an effective means of detecting apoptotic and necrotic cells via flow cytometry [22, 215]. A healthy non-apoptotic cell will not express PS as the plasma membrane is intact, meaning neither annexin V nor PI will be able to bind [215]. Early apoptotic cells will stain positive for annexin V only as the membrane is still intact and PI will be unable to bind to the DNA within the cell. Late apoptotic cells will have a compromised membrane, meaning both annexin V and PI can bind. Necrotic cells will only be positive for PI, and therefore can be distinguished from late apoptotic cells [22, 206, 213, 215].

#### **4.1.3: DNA damage**

As previously mentioned, treating cells with radiotherapy and chemotherapeutic agents induces DNA damage. The ultimate aim of many cancer therapies is inducing enough DNA damage that the cell is unable to repair it, ultimately leading to cell death, therefore it is important to assess not only DNA damage, but also the DNA repair [91, 216]. To achieve this goal, we used the comet assay to assay the DNA damage and repair induced by the selected combination therapies over a time course as previous studies carried out in the lab indicated that DMF induces DNA damage.

The comet assay is a sensitive assay which can be used to detect and visualise both double stranded and single stranded DNA breaks. Under an electric field, fragmented

DNA migrates out of the nucleoid body, or comet head, and forms a DNA stain in the agarose gel known as the comet tail. To quantify the amount of DNA damage, an index of the distance of DNA migration (comet tail) and the quantity of DNA present in the comet tail, known as the tail moment, is utilised [91, 178, 216].

#### **4.1.4: Glutathione**

As previously mentioned, glutathione is involved in the antioxidant response triggered by the presence of free radicals, and a key player in the cells ability to overcome damage caused by oxidative stress [97]. As glutathione reduction is one of the key mechanisms of action proposed for DMF/MMF in the literature, it was therefore decided to assess the glutathione level within the cells following treatment with both single agents and combination therapies to determine if DMF/MMF is in fact targeting the NRF2 pathway as suggested in the literature [111].

#### **4.2: AIMS**

The aims of this chapter were therefore to investigate the effects of the selected developed combinations on the distribution of cells in the cell cycle; apoptosis; glutathione levels within the cell; and DNA damage and repair, to determine the mechanism of action of the combinations. It was hypothesised that the combination treatments containing DMF/MMF would result in a decrease in glutathione levels, which would coincide with an increase in DNA damage and apoptosis. Additionally, it was hypothesised that combination treatments containing DMF would induce G1 phase arrest.

#### **4.3: MATERIALS AND METHODS**

##### **4.3.1: Cell Lines and Culture Conditions**

Cells were cultured as described previously in **section 2.3.1**.

#### **4.3.2: Treatments**

Treatments were prepared and carried out as previously described in **section 3.3.2**. For post treatment timings, zero hours post treatment refers to immediately after the treatment regime has been completed, i.e. after 48 hours with the relevant agent(s). At this time point media containing the treatment(s) was removed and replaced with fresh complete DMEM media. Each subsequent time point takes place after the zero hours post treatment time point.

#### **4.3.3: Cell Cycle Analysis**

Cells were seeded in 6-well plates (Thermo Fisher Scientific, Perth, UK) at a cell density of 10,000 cells per well in a final volume of 5 mL of complete DMEM media. Following a 24-hour incubation, DMEM media was removed and replaced with 2 mL of complete DMEM media containing the desired treatment(s) depending on the treatment schedule. For schedules including EXBR, cells were irradiated with 0.5 Gy EXBR using the X-Rad225 irradiator (Precision X-Ray, Connecticut, USA) at a dose rate of 2.3 Gy/min. Following treatment, the DMEM media containing the treatments was removed and replaced with 5 mL fresh complete DMEM media. Cells were then harvested at set time intervals post treatment: 0 hours; 1 hour; 4 hours; 24 hours; and 36 hours. To harvest cells, DMEM media was removed, and the cell washed with 1X PBS and detached with 1X 0.05% trypsin-EDTA solution, before finally being neutralised with complete DMEM media to create a cell suspension. The resulting cell suspension was centrifuged at 216 x g for 5 minutes to create a cell pellet, and the supernatant removed before the addition of ice cold 70% ethanol to fix the cells. The cell pellets were stored in 70% ethanol at -20°C prior to use for a maximum duration of 3 months.

On the day of the assay, the fixed pellets were centrifuged at 216 x g for 5 minutes and the supernatant discarded, then washed twice with 1X PBS. A staining solution

was prepared composed of Ribonuclease A (RNase A) at a final concentration of 50 µg/mL (Sigma Aldrich, Irvine, UK); PI at a final concentration of 10 µg /mL (Sigma Aldrich, Irvine, UK); and distilled water. To each cell pellet 250 µL of staining solution was added, and the samples incubated on ice for one hour in the dark. Following incubation, the samples were analysed using an Attune™ NxT Flow Cytometer (Thermo Fisher Scientific, Perth, UK) to determine the distribution of cells throughout the cell cycle following treatment. An exemplar FSC/SSC and gating strategy for flow cytometry data can be found in **appendix 1**. Each cell cycle experiment was carried out in three biological repeats, with one technical repeat per biological repeat.

#### **4.3.4: Apoptosis Assay**

Cells were seeded in 6-well plates (Thermo Fisher Scientific, Perth, UK) at a cell density of 10,000 cells per well in a final volume of 5 mL of complete DMEM media. Following a 24-hour incubation, DMEM media was removed and replaced with 2 mL of complete DMEM media containing the desired treatment(s) depending on the treatment schedule. For schedules including EXBR, cells were irradiated with 0.5 Gy EXBR using the X-Rad225 irradiator (Precision X-Ray, Connecticut, USA) at a dose rate of 2.3 Gy/min. Following treatment, the DMEM media containing the treatments was removed and replaced with 5 mL fresh complete DMEM media. Cells were then harvested at set time intervals post treatment: 0 hours; 1 hour; 4 hours; 24 hours; and 36 hours. To harvest cells, DMEM media was removed, and the cell washed with 1X PBS and detached with 1X 0.05% trypsin-EDTA solution, before finally being neutralised with complete DMEM media to create a cell suspension. The resulting cell suspension was centrifuged at 216 x g for 5 minutes to create a cell pellet, and the supernatant discarded, then washed twice with 1X PBS, before the addition of staining solution.

To stain cells, the BD Pharmingen™ FITC Annexin V Apoptosis Detection Kit I (BD Biosciences, UK; catalogue number: 556547). In brief, 5 µL of FITC Annexin V; 5 µL PI; and 100 µL of 1X binding buffer was added to each sample and vortexed briefly, before incubation for 15 minutes at room temperature in the dark. Following incubation, 400 µL of 1X binding buffer was added to each sample before analysis using an Attune™ NxT Flow Cytometer (Thermo Fisher Scientific, Perth, UK) to determine the percentage of non-apoptotic; early apoptotic; late apoptotic; and necrotic cells following treatment. An exemplar FSC/SSC and gating strategy for flow cytometry data can be found in **appendix 1**. Each apoptosis experiment was carried out in three biological repeats, with one technical repeat per biological repeat.

#### **4.3.5: Comet Assay (single cell gel electrophoresis)**

To prepare cells for the comet assay, cells were seeded in T-25 flasks (Thermo Fisher Scientific, Perth, UK) at a cell density of 100,000 cells per well in a final volume of 5 mL of complete DMEM media. Following a 24-hour incubation, DMEM media was removed and replaced with 1.5 mL of complete DMEM media containing the desired treatment(s) depending on the treatment schedule. For schedules including EXBR, cells were irradiated with 0.5 Gy EXBR using the X-Rad225 irradiator (Precision X-Ray, Connecticut, USA) at a dose rate of 2.3 Gy/min. Following treatment, the DMEM media containing the treatments was removed and replaced with 5 mL fresh complete DMEM media. Cells were then harvested at set time intervals post treatment: 0 hours; 1 hour; 4 hours; 24 hours; and 36 hours. To harvest cells, DMEM media was removed, and the cell washed with 1X PBS and detached with 1X 0.05% trypsin-EDTA solution, before finally being neutralised with complete DMEM media to create a cell suspension. The resulting cell suspension was passed through a 23-gauge needle to create a single cell suspension and counted using a haemocytometer to create a  $1 \times 10^5$  cells/mL solution.

To carry out the comet assay, the Enzo Comet SCGE assay kit was utilised according to the manufacturer's instructions (Enzo Life Sciences, USA; catalogue number: ADI-900-166). Briefly, to 500  $\mu$ L of molten 1% low melting point (LM) agarose (Enzo Life Sciences, USA) at 37°C, 50  $\mu$ L of cell suspension was added and gently mixed before pipetting 75  $\mu$ L of the resulting mixture onto comet slides (Enzo Life Sciences, USA), ensuring even coverage of the sample area. Comet slides were then left in the dark at 4°C to allow the gel to set. The slides were then immersed in prechilled lysis solution (Enzo Life Sciences, USA) for 60 minutes. Whilst incubating, fresh alkaline solution was prepared by dissolving 12 grams of sodium hydroxide pellets (Thermo Fisher Scientific, Perth, UK) in one litre of deionised water and 2 mL of 500 mM EDTA (Enzo Life Sciences, USA) added. Following incubation in the lysis solution, the slides were immersed in the freshly prepared alkaline solution (pH >13) and incubated for 60 minutes. Slides were then removed from the alkaline solution and immersed in Tris Borate EDTA (TBE) buffer (Sigma Aldrich, Irvine, UK) for 10 minutes. Following incubation, the slides were placed into a gel electrophoresis tank filled with 1X TBE buffer and electrophoresis undertaken at 45 V for 10 minutes.

Following electrophoresis, the slides were immersed in 70% ethanol for 5 minutes and then allowed to fully dry. Once dry, 100  $\mu$ L of 1X SYBR green stain (Enzo Life Sciences, USA) was added to each sample and then slides incubated in the dark for 30 minutes to allow for visualization of DNA comets. Following staining slides were washed in deionised water and allowed to fully dry before fluorescent imaging (482/25 nm Excitation; 524/24 nm Emission) using an EVOS FL auto microscope (Life Technologies, Paisley, UK).

To analyse the obtained images of comets, the Image J plugin OpenComet (Gyori *et al.*, 2014), was used to determine the tail moment of each comet. A minimum of 100 comets were analysed per sample. The tail moment of each sample was standardised

as a fraction of the tail moment of the untreated control, and the average tail moment for each treatment group presented.

#### **4.3.6: Glutathione Assay**

To prepare cells for the glutathione assay, cells were seeded in T-25 flasks (Thermo Fisher Scientific, Perth, UK) at a cell density of 100,000 cells per flask in a final volume of 5 mL of complete DMEM media. Following a 24-hour incubation, DMEM media was removed and replaced with 1.5 mL of complete DMEM media containing the desired treatment(s) depending on the treatment schedule. For schedules including EXBR, cells were irradiated with 0.5 Gy EXBR using the X-Rad225 irradiator (Precision X-Ray, Connecticut, USA) at a dose rate of 2.3 Gy/min. Following treatment, the DMEM media containing the treatments was removed and replaced with 5 mL fresh complete DMEM media. Cells were then harvested at set time intervals post treatment: 0 hours; 1 hour; 4 hours; 24 hours; and 36 hours. To harvest cells, DMEM media was removed, and the cells washed with 1X PBS and detached with 1X 0.05% trypsin-EDTA solution, before finally being neutralised with complete DMEM media to create a cell suspension. Cells were then centrifuged at 216 x g for 5 minutes to create a cell pellet, and the supernatant discarded. To each cell pellet three volumes of 5% salicylic acid solution (Sigma Aldrich, Irvine, UK) was added and the pellet vortexed. The resulting suspension was then freeze-thawed twice using liquid nitrogen and a 37°C heating block. The resulting solution was then centrifuged at 12,879 x g, and the resulting supernatant collected for further analysis.

To carry out the glutathione assay, a Glutathione Colorimetric Detection Kit (Thermo Fisher Scientific, Perth, UK; catalogue number: EIAGSHC) was used. The reaction mixture was prepared using 1 mL NADPH; 1 mL glutathione reductase concentrate; and 8 mL assay buffer, and the colorimetric detection reagent was prepared using 1 mL of colorimetric detection concentrate and 9 mL assay buffer. To each well of a

clear flat bottom 96-well half area plate, 50  $\mu\text{L}$  of sample; 25  $\mu\text{L}$  of colorimetric detection reagent; and 25  $\mu\text{L}$  of reaction mixture were added and gently mixed before being incubated for 20 minutes at room temperature. Following the incubation, total GSH content in the samples was determined by reading the absorbance of the plate(s) at 405 nm using a Flexstation 3 Multi-Mode Microplate Reader (Molecular Devices, California, USA) to measure the colorimetric change as a result of the colorimetric detection reagent reacting with the free thiol group present in GSH to produce a yellow-coloured product. To determine the concentration of glutathione in each sample, the absorbance values were compared with the concentration curve generated using absorbance readings obtained from the oxidised glutathione standards provided with the kit. Each glutathione experiment was carried out in three biological repeats, with three technical repeats per biological repeat.

#### **4.3.7: Statistical Analysis**

All statistical analysis was carried out using Graphpad Prism 10.1.2. Significance was assigned at an alpha ( $\alpha$ ) value  $\leq 0.05$ . Prior to carrying out any analysis on data, a Shapiro-Wilk normality test was used to determine if the data conformed to normal distribution (parametric or nonparametric), to allow for the selection of an appropriate statistical test. For all the data presented in this chapter a two-way ANOVA with Tukey post hoc test was used. The following labelling was used to convey significance: ns = not significant; \* =  $P \leq 0.05$ ; \*\* =  $P \leq 0.01$ , \*\*\* =  $P \leq 0.001$ ; and \*\*\*\* =  $P \leq 0.0001$ .

## **4.4: RESULTS**

### **4.4.1: Cell cycle studies on developed combinations**

To investigate the effects of the developed combinations on the distribution of cells in the cell cycle in Panc-1 cells, the cell cycle assay was carried out as described in **section 4.3.3**, and the results presented in **figure 4.1**. In **appendix 2 – 6**, tables containing the average values for the distribution of cells throughout the cell cycle following treatment can be found.

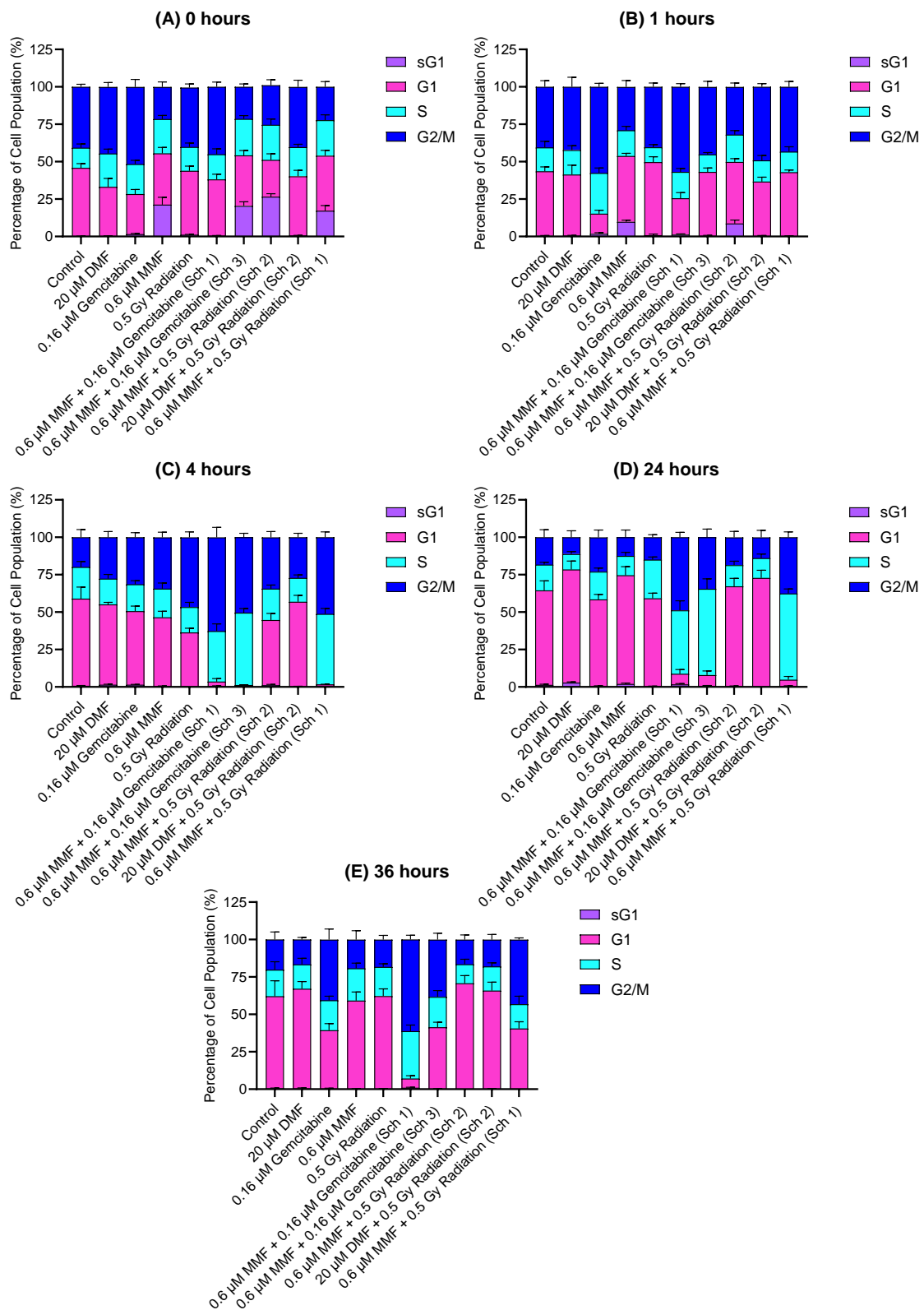


**Figure 4.1: Cell cycle analysis of combination therapies in Panc-1.** Cells were incubated and harvested at specific time points post treatment before undergoing flow cytometry to determine cell cycle distribution. (A) Distribution of cells 0 hours post treatment. (B) Distribution of cells 1 hour post treatment. (C) Distribution of cells 4 hours post treatment. (D) Distribution of cells 24 hours post treatment. (E) Distribution of cells 36 hours post treatment. All data is represented as an average of three independent experiments  $\pm$  the standard deviation.

As can be seen in **figure 4.1A**, in Panc-1 cells 0.6  $\mu$ M MMF, 0.6  $\mu$ M MMF + 0.5 Gy EXBR (Schedule 1), 0.6  $\mu$ M MMF + 0.5 Gy EXBR (Schedule 2), and 0.6  $\mu$ M MMF + 0.16  $\mu$ M gemcitabine (Schedule 3) induced a statistically significant increase in the number of cells in sG1 phase when compared with the untreated control zero hours post treatment ( $P < 0.0001$ ). When looking at G1 phase, 0.6  $\mu$ M MMF, 20  $\mu$ M DMF, 0.16  $\mu$ M gemcitabine, 0.6  $\mu$ M MMF + 0.5 Gy EXBR (Schedule 1), 0.6  $\mu$ M MMF + 0.5 Gy EXBR (Schedule 2), and 0.6  $\mu$ M MMF + 0.16  $\mu$ M gemcitabine (Schedule 3) induced a statistically significant decrease in the number of cells in G1 phase when compared with the untreated control zero hours post treatment ( $P \leq 0.169$ ). When looking at S phase, 0.6  $\mu$ M MMF, 20  $\mu$ M DMF, 0.6  $\mu$ M MMF + 0.5 Gy EXBR (Schedule 2), and 0.6  $\mu$ M MMF + 0.16  $\mu$ M gemcitabine (Schedule 3) induced a statistically significant increase in the number of cells in S phase when compared with the untreated control zero hours post treatment ( $P \leq 0.0032$ ). When looking at G2/M phase, 0.6  $\mu$ M MMF, 0.6  $\mu$ M MMF + 0.5 Gy EXBR (Schedule 1), 0.6  $\mu$ M MMF + 0.5 Gy EXBR (Schedule 2), and 0.6  $\mu$ M MMF + 0.16  $\mu$ M gemcitabine (Schedule 3) induced a statistically significant decrease in the number of cells in G2/M phase when compared with the untreated control zero hours post treatment ( $P < 0.0001$ ). Conversely, 0.16  $\mu$ M gemcitabine induced a statistically significant increase in the number of cells in G2/M phase when compared with the untreated control zero hours post treatment ( $P = 0.0007$ ).

As can be seen in **figure 4.1B**, in Panc-1 cells only 0.6  $\mu$ M MMF and 0.6  $\mu$ M MMF + 0.5 Gy EXBR (Schedule 2) caused a statistically significant increase in the number of cells in sG1 phase when compared with the untreated control one hour post treatment ( $P \leq 0.0049$ ). When looking at G1 phase, both 0.16  $\mu$ M gemcitabine and 0.6  $\mu$ M MMF + 0.16  $\mu$ M gemcitabine (Schedule 1) induced a statistically significant decrease in the number of cells in G1 phase when compared with the untreated control one hour post

treatment ( $P < 0.0001$ ). Only 0.16  $\mu\text{M}$  gemcitabine induced a statistically significant increase in the number of cells in S phase when compared with the untreated control one hour post treatment ( $P < 0.0001$ ). When looking at G2/M phase, both 0.6  $\mu\text{M}$  MMF and 0.6  $\mu\text{M}$  MMF + 0.5 Gy EXBR (Schedule 2) induced a statistically significant decrease in the number of cells in G2/M phase when compared with the untreated control one hour post treatment ( $P \leq 0.0033$ ). Conversely, 0.16  $\mu\text{M}$  gemcitabine, 0.6  $\mu\text{M}$  MMF + 0.16  $\mu\text{M}$  gemcitabine (Schedule 1), and 20  $\mu\text{M}$  DMF + 0.5 Gy EXBR (Schedule 2) induced a statistically significant increase in the number of cells in G2/M phase when compared with the untreated control one hour post treatment ( $P \leq 0.0180$ ).

As can be seen in **figure 4.1C**, in Panc-1 cells no treatments caused a statistically significant change in the number of cells in sG1 phase when compared with the untreated control four hours post treatment ( $P > 0.9999$ ). When looking at G1 phase, 0.6  $\mu\text{M}$  MMF, 0.16  $\mu\text{M}$  gemcitabine, 0.5 Gy EXBR, 0.6  $\mu\text{M}$  MMF + 0.5 Gy EXBR (Schedule 1), 0.6  $\mu\text{M}$  MMF + 0.5 Gy EXBR (Schedule 2), 0.6  $\mu\text{M}$  MMF + 0.16  $\mu\text{M}$  gemcitabine (Schedule 1), and 0.6  $\mu\text{M}$  MMF + 0.16  $\mu\text{M}$  gemcitabine (Schedule 3) induced a statistically significant decrease in the number of cells in G1 phase when compared with the untreated control four hours post treatment ( $P \leq 0.0384$ ). When looking at S phase, 0.6  $\mu\text{M}$  MMF + 0.5 Gy EXBR (Schedule 1), 0.6  $\mu\text{M}$  MMF + 0.16  $\mu\text{M}$  gemcitabine (Schedule 1), and 0.6  $\mu\text{M}$  MMF + 0.16  $\mu\text{M}$  gemcitabine (Schedule 3) induced a statistically significant increase in the number of cells in S phase when compared with the untreated control four hours post treatment ( $P \leq 0.0019$ ). When looking at G2/M phase, 0.6  $\mu\text{M}$  MMF, 0.16  $\mu\text{M}$  gemcitabine, 20  $\mu\text{M}$  DMF, 0.5 Gy EXBR, 0.6  $\mu\text{M}$  MMF + 0.5 Gy EXBR (Schedule 1), 0.6  $\mu\text{M}$  MMF + 0.5 Gy EXBR (Schedule 2), 0.6  $\mu\text{M}$  MMF + 0.16  $\mu\text{M}$  gemcitabine (Schedule 1), and 0.6  $\mu\text{M}$  MMF + 0.16  $\mu\text{M}$  gemcitabine (Schedule 3) induced a statistically significant increase in the

number of cells in G2/M phase when compared with the untreated control 4 hours post treatment ( $P \leq 0.0452$ ).

As can be seen in **figure 4.1D**, in Panc-1 cells no treatments caused a statistically significant change in the number of cells in sG1 phase when compared with the untreated control 24 hours post treatment ( $P > 0.9999$ ). When looking at G1 phase, 0.6  $\mu$ M MMF, 20  $\mu$ M DMF, and 20  $\mu$ M DMF + 0.5 Gy EXBR induced a statistically significant increase in the number of cells in G1 phase 24 hours post treatment when compared with the untreated control 24 hours post treatment ( $P \leq 0.0135$ ). Conversely, 0.6  $\mu$ M MMF + 0.5 Gy EXBR (Schedule 1), 0.6  $\mu$ M MMF + 0.16  $\mu$ M gemcitabine (Schedule 1), and 0.6  $\mu$ M MMF + 0.16  $\mu$ M gemcitabine (Schedule 3) induced a statistically significant decrease in the number of cells in G1 phase when compared with the untreated control 24 hours post treatment ( $P < 0.0001$ ). When looking at S phase, 0.5 Gy EXBR, 0.6  $\mu$ M MMF + 0.5 Gy EXBR (Schedule 1), 0.6  $\mu$ M MMF + 0.16  $\mu$ M gemcitabine (Schedule 1), and 0.6  $\mu$ M MMF + 0.16  $\mu$ M gemcitabine (Schedule 3) induced a statistically significant increase in the number of cells in S phase when compared with the untreated control 24 hours post treatment ( $P \leq 0.0183$ ). When looking at G2/M phase, 0.6  $\mu$ M MMF + 0.5 Gy EXBR (Schedule 1), 0.6  $\mu$ M MMF + 0.16  $\mu$ M gemcitabine (Schedule 1), and 0.6  $\mu$ M MMF + 0.16  $\mu$ M gemcitabine (Schedule 3) induced a statistically significant increase in the number of cells in G2/M phase when compared with the untreated control 24 hours post treatment ( $P \leq 0.0001$ ).

As can be seen in **figure 4.1E**, in Panc-1 cells no treatments caused a statistically significant change in the number of cells in sG1 phase when compared with the untreated control 36 hours post treatment ( $P > 0.9999$ ). When looking at G1 phase, 0.16  $\mu$ M gemcitabine, 0.6  $\mu$ M MMF + 0.5 Gy EXBR (Schedule 1), 0.6  $\mu$ M MMF + 0.16  $\mu$ M gemcitabine (Schedule 1), and 0.6  $\mu$ M MMF + 0.16  $\mu$ M gemcitabine (Schedule 3)

induced a statistically significant increase in the number of cells in G1 phase when compared with the untreated control 36 hours post treatment ( $P < 0.0001$ ). When looking at S phase, only 0.6  $\mu\text{M}$  MMF + 0.16  $\mu\text{M}$  gemcitabine (Schedule 1) induced a statistically significant increase in the number of cells in S phase when compared with the untreated control 36 hours post treatment ( $P = 0.0047$ ). When looking at G2/M phase, 0.16  $\mu\text{M}$  gemcitabine, 0.6  $\mu\text{M}$  MMF + 0.5 Gy EXBR (Schedule 1), 0.6  $\mu\text{M}$  MMF + 0.16  $\mu\text{M}$  gemcitabine (Schedule 1), and 0.6  $\mu\text{M}$  MMF + 0.16  $\mu\text{M}$  gemcitabine (Schedule 3) induced a statistically significant increase in the number of cells in G2/M phase when compared with the untreated control 36 hours post treatment ( $P \leq 0.0003$ ).

Some changes were observed in the untreated control over the time course, with a statistically significant increase in the number of cells in G1 phase at the 4-hour timepoint ( $P = 0.0090$ ), however this did not change for the remainder of the time course ( $P \geq 0.6541$ ). The other change observed was that there was a statistically significant increase in the number of cells in G2/M phase at the 4-hour timepoint ( $P \leq 0.0001$ ), however this did not change for the remainder of the time course ( $P \geq 0.9932$ ).

A summary of all statistical comparisons carried out between the untreated control and therapies, and between combination therapies and individual components over the time course in Panc-1 cells following two-way ANOVA with Bonferroni post hoc test can be found in **tables 4.1 – 4.10**.

**Table 4.1: Statistical comparisons of the distribution of treated Panc-1 cells throughout the cell cycle versus the untreated control zero hours post treatment.** Sch = schedule, M = MMF, D = MMF, G = gemcitabine, R = EXBR, ns = not significant.

Comparison	Phase of cell cycle	Summary	P-value
Control vs DMF	sG1	ns	>0.9999
	G1	****	<0.0001
	S	**	0.0032
	G2/M	ns	0.6360
Control vs MMF	sG1	****	<0.0001
	G1	***	0.0003
	S	**	0.0028
	G2/M	****	<0.0001
Control vs gemcitabine	sG1	ns	>0.9999
	G1	****	<0.0001
	S	ns	0.0769
	G2/M	***	0.0007
Control vs EXBR	sG1	ns	>0.9999
	G1	ns	>0.9999
	S	ns	>0.9999
	G2/M	ns	>0.9999
Control vs M+R Sch 1	sG1	****	<0.0001
	G1	**	0.0054
	S	**	0.0011
	G2/M	****	<0.0001
Control vs M+R Sch 2	sG1	****	<0.0001
	G1	****	<0.0001
	S	**	0.0016
	G2/M	****	<0.0001
Control vs D+R Sch 2	sG1	ns	>0.9999
	G1	ns	0.0765
	S	ns	0.0755
	G2/M	ns	>0.9999
Control vs M+G Sch 1	sG1	ns	>0.9999
	G1	*	0.0169
	S	ns	>0.9999
	G2/M	ns	0.5244
Control vs M+G Sch 3	sG1	****	<0.0001
	G1	***	0.0001
	S	***	0.0004
	G2/M	****	<0.0001

**Table 4.2: Statistical comparisons of the distribution of treated Panc-1 cells throughout the cell cycle versus monotherapies zero hours post treatment.** Sch = schedule, M = MMF, D = MMF, G = gemcitabine, R = EXBR, ns = not significant.

Comparison	Phase of cell cycle	Summary	P-value
M+R Sch 1 vs MMF	sG1	ns	0.6391
	G1	ns	>0.9999
	S	ns	>0.9999
	G2/M	ns	>0.9999
M+R Sch 1 vs EXBR	sG1	****	<0.0001
	G1	ns	0.1259
	S	*	0.0193
	G2/M	****	<0.0001
M+R Sch 2 vs MMF	sG1	ns	0.2328
	G1	**	0.0024
	S	ns	>0.9999
	G2/M	ns	0.3073
M+R Sch 2 vs EXBR	sG1	****	<0.0001
	G1	****	<0.0001
	S	*	0.0275
	G2/M	****	<0.0001
D+R Sch 2 vs DMF	sG1	ns	>0.9999
	G1	*	0.0370
	S	ns	>0.9999
	G2/M	ns	0.4253
D+R Sch 2 vs EXBR	sG1	ns	>0.9999
	G1	ns	>0.9999
	S	ns	0.8018
	G2/M	ns	>0.9999
M+G Sch 1 vs MMF	sG1	****	<0.0001
	G1	ns	>0.9999
	S	ns	0.1059
	G2/M	****	<0.0001
M+G Sch 1 vs gemcitabine	sG1	ns	>0.9999
	G1	***	0.0007
	S	ns	>0.9999
	G2/M	ns	0.0782
M+G Sch 3 vs MMF	sG1	ns	>0.9999
	G1	ns	>0.9999
	S	ns	>0.9999
	G2/M	ns	>0.9999
M+G Sch 3 vs gemcitabine	sG1	****	<0.0001
	G1	*	0.0388
	S	ns	0.4565
	G2/M	****	<0.0001

**Table 4.3: Statistical comparisons of the distribution of treated Panc-1 cells throughout the cell cycle versus the untreated control one hour post treatment.**  
 Sch = schedule, M = MMF, D = MMF, G = gemcitabine, R = EXBR, ns = not significant.

Comparison	Phase of cell cycle	Summary	P-value
Control vs DMF	sG1	ns	>0.9999
	G1	ns	>0.9999
	S	ns	>0.9999
	G2/M	ns	>0.9999
Control vs MMF	sG1	**	0.0013
	G1	ns	>0.9999
	S	ns	>0.9999
	G2/M	****	<0.0001
Control vs gemcitabine	sG1	ns	>0.9999
	G1	****	<0.0001
	S	****	<0.0001
	G2/M	****	<0.0001
Control vs EXBR	sG1	ns	>0.9999
	G1	ns	0.0990
	S	ns	0.0710
	G2/M	ns	>0.9999
Control vs M+R Sch 1	sG1	ns	>0.9999
	G1	ns	>0.9999
	S	ns	>0.9999
	G2/M	ns	>0.9999
Control vs M+R Sch 2	sG1	**	0.0049
	G1	ns	>0.9999
	S	ns	>0.9999
	G2/M	**	0.0033
Control vs D+R Sch 2	sG1	ns	>0.9999
	G1	ns	0.1053
	S	ns	>0.9999
	G2/M	*	0.0180
Control vs M+G Sch 1	sG1	ns	>0.9999
	G1	****	<0.0001
	S	ns	>0.9999
	G2/M	****	<0.0001
Control vs M+G Sch 3	sG1	ns	>0.9999
	G1	ns	>0.9999
	S	ns	0.3995
	G2/M	ns	0.2485

**Table 4.4: Statistical comparisons of the distribution of treated Panc-1 cells throughout the cell cycle versus monotherapies one hour post treatment.** Sch = schedule, M = MMF, D = MMF, G = gemcitabine, R = EXBR, ns = not significant.

Comparison	Phase of cell cycle	Summary	P-value
M+R Sch 1 vs MMF	sG1	***	0.0009
	G1	ns	>0.9999
	S	ns	0.8075
	G2/M	****	<0.0001
M+R Sch 1 vs EXBR	sG1	ns	>0.9999
	G1	ns	0.0629
	S	ns	0.5978
	G2/M	ns	>0.9999
M+R Sch 2 vs MMF	sG1	ns	>0.9999
	G1	ns	>0.9999
	S	ns	>0.9999
	G2/M	ns	>0.9999
M+R Sch 2 vs EXBR	sG1	**	0.0083
	G1	ns	0.0948
	S	**	0.0043
	G2/M	**	0.0038
D+R Sch 2 vs DMF	sG1	ns	>0.9999
	G1	ns	0.6136
	S	ns	>0.9999
	G2/M	ns	0.0984
D+R Sch 2 vs EXBR	sG1	ns	>0.9999
	G1	***	0.0004
	S	ns	0.8210
	G2/M	*	0.0162
M+G Sch 1 vs MMF	sG1	**	0.0034
	G1	****	<0.0001
	S	ns	>0.9999
	G2/M	****	<0.0001
M+G Sch 1 vs gemcitabine	sG1	ns	>0.9999
	G1	***	0.0002
	S	***	0.0009
	G2/M	ns	>0.9999
M+G Sch 3 vs MMF	sG1	**	0.0010
	G1	ns	>0.9999
	S	ns	0.1147
	G2/M	****	<0.0001
M+G Sch 3 vs gemcitabine	sG1	ns	>0.9999
	G1	****	<0.0001
	S	****	<0.0001
	G2/M	****	<0.0001

**Table 4.5: Statistical comparisons of the distribution of treated Panc-1 cells throughout the cell cycle versus the untreated control four hours post treatment.** Sch = schedule, M = MMF, D = MMF, G = gemcitabine, R = EXBR, ns = not significant.

Comparison	Phase of cell cycle	Summary	P-value
Control vs DMF	sG1	ns	>0.9999
	G1	ns	0.5735
	S	ns	0.9634
	G2/M	*	0.0452
Control vs MMF	sG1	ns	>0.9999
	G1	***	0.0010
	S	ns	>0.9999
	G2/M	***	0.0001
Control vs gemcitabine	sG1	ns	>0.9999
	G1	*	0.0384
	S	ns	>0.9999
	G2/M	**	0.0051
Control vs EXBR	sG1	ns	>0.9999
	G1	****	<0.0001
	S	ns	0.9360
	G2/M	****	<0.0001
Control vs M+R Sch 1	sG1	ns	>0.9999
	G1	****	<0.0001
	S	****	<0.0001
	G2/M	****	<0.0001
Control vs M+R Sch 2	sG1	ns	>0.9999
	G1	***	0.0001
	S	ns	>0.9999
	G2/M	***	0.0002
Control vs D+R Sch 2	sG1	ns	>0.9999
	G1	ns	>0.9999
	S	ns	0.3780
	G2/M	ns	0.0699
Control vs M+G Sch 1	sG1	ns	>0.9999
	G1	****	<0.0001
	S	**	0.0019
	G2/M	****	<0.0001
Control vs M+G Sch 3	sG1	ns	>0.9999
	G1	****	<0.0001
	S	****	<0.0001
	G2/M	****	<0.0001

**Table 4.6: Statistical comparisons of the distribution of treated Panc-1 cells throughout the cell cycle versus monotherapies four hours post treatment.** Sch = schedule, M = MMF, D = MMF, G = gemcitabine, R = EXBR, ns = not significant.

Comparison	Phase of cell cycle	Summary	P-value
M+R Sch 1 vs MMF	sG1	ns	>0.9999
	G1	****	<0.0001
	S	****	<0.0001
	G2/M	****	<0.0001
M+R Sch 1 vs EXBR	sG1	ns	>0.9999
	G1	****	<0.0001
	S	****	<0.0001
	G2/M	ns	0.7200
M+R Sch 2 vs MMF	sG1	>0.9999	>0.9999
	G1	>0.9999	>0.9999
	S	ns	>0.9999
	G2/M	ns	>0.9999
M+R Sch 2 vs EXBR	sG1	>0.9999	>0.9999
	G1	ns	0.0971
	S	ns	>0.9999
	G2/M	**	0.0014
D+R Sch 2 vs DMF	sG1	ns	>0.9999
	G1	ns	>0.9999
	S	ns	>0.9999
	G2/M	ns	>0.9999
D+R Sch 2 vs EXBR	sG1	ns	>0.9999
	G1	****	<0.0001
	S	ns	>0.9999
	G2/M	****	<0.0001
M+G Sch 1 vs MMF	sG1	ns	>0.9999
	G1	****	<0.0001
	S	***	0.0003
	G2/M	****	<0.0001
M+G Sch 1 vs gemcitabine	sG1	ns	>0.9999
	G1	****	<0.0001
	S	***	0.0001
	G2/M	****	<0.0001
M+G Sch 3 vs MMF	sG1	ns	>0.9999
	G1	****	<0.0001
	S	****	<0.0001
	G2/M	****	<0.0001
M+G Sch 3 vs gemcitabine	sG1	ns	>0.9999
	G1	****	<0.0001
	S	****	<0.0001
	G2/M	****	<0.0001

**Table 4.7: Statistical comparisons of the distribution of treated Panc-1 cells throughout the cell cycle versus the untreated control 24 hours post treatment.**  
 Sch = schedule, M = MMF, D = MMF, G = gemcitabine, R = EXBR, ns = not significant.

Comparison	Phase of cell cycle	Summary	P-value
Control vs DMF	sG1	ns	>0.9999
	G1	***	0.0007
	S	ns	0.1334
	G2/M	ns	0.1100
Control vs MMF	sG1	ns	>0.9999
	G1	**	0.0095
	S	ns	0.7820
	G2/M	ns	0.2387
Control vs gemcitabine	sG1	ns	>0.9999
	G1	ns	0.6231
	S	ns	>0.9999
	G2/M	ns	0.8663
Control vs EXBR	sG1	ns	>0.9999
	G1	ns	0.7145
	S	*	0.0183
	G2/M	ns	>0.9999
Control vs M+R Sch 1	sG1	ns	>0.9999
	G1	****	<0.0001
	S	****	<0.0001
	G2/M	****	<0.0001
Control vs M+R Sch 2	sG1	ns	>0.9999
	G1	ns	>0.9999
	S	ns	>0.9999
	G2/M	ns	>0.9999
Control vs D+R Sch 2	sG1	ns	>0.9999
	G1	*	0.0135
	S	ns	>0.9999
	G2/M	ns	0.7805
Control vs M+G Sch 1	sG1	ns	>0.9999
	G1	****	<0.0001
	S	****	<0.0001
	G2/M	****	<0.0001
Control vs M+G Sch 3	sG1	ns	>0.9999
	G1	****	<0.0001
	S	****	<0.0001
	G2/M	***	0.0001

**Table 4.8: Statistical comparisons of the distribution of treated Panc-1 cells throughout the cell cycle versus monotherapies 24 hours post treatment.** Sch = schedule, M = MMF, D = MMF, G = gemcitabine, R = EXBR, ns = not significant.

Comparison	Phase of cell cycle	Summary	P-value
M+R Sch 1 vs MMF	sG1	ns	>0.9999
	G1	****	<0.0001
	S	****	<0.0001
	G2/M	****	<0.0001
M+R Sch 1 vs EXBR	sG1	ns	>0.9999
	G1	****	<0.0001
	S	****	<0.0001
	G2/M	****	<0.0001
M+R Sch 2 vs MMF	sG1	ns	>0.9999
	G1	ns	0.3294
	S	ns	>0.9999
	G2/M	ns	0.2583
M+R Sch 2 vs EXBR	sG1	ns	>0.9999
	G1	ns	0.0564
	S	**	0.0019
	G2/M	ns	>0.9999
D+R Sch 2 vs DMF	sG1	ns	>0.9999
	G1	ns	>0.9999
	S	ns	>0.9999
	G2/M	ns	>0.9999
D+R Sch 2 vs EXBR	sG1	ns	>0.9999
	G1	***	0.0002
	S	***	0.0006
	G2/M	ns	>0.9999
M+G Sch 1 vs MMF	sG1	ns	>0.9999
	G1	****	<0.0001
	S	****	<0.0001
	G2/M	****	<0.0001
M+G Sch 1 vs gemcitabine	sG1	ns	>0.9999
	G1	****	<0.0001
	S	****	<0.0001
	G2/M	****	<0.0001
M+G Sch 3 vs MMF	sG1	ns	>0.9999
	G1	****	<0.0001
	S	****	<0.0001
	G2/M	****	<0.0001
M+G Sch 3 vs gemcitabine	sG1	ns	>0.9999
	G1	****	<0.0001
	S	****	<0.0001
	G2/M	**	0.0081

**Table 4.9: Statistical comparisons of the distribution of treated Panc-1 cells throughout the cell cycle versus the untreated control 36 hours post treatment.**  
 Sch = schedule, M = MMF, D = MMF, G = gemcitabine, R = EXBR, ns = not significant.

Comparison	Phase of cell cycle	Summary	P-value
Control vs DMF	sG1	ns	>0.9999
	G1	ns	0.8993
	S	ns	>0.9999
	G2/M	ns	>0.9999
Control vs MMF	sG1	ns	>0.9999
	G1	ns	>0.9999
	S	ns	>0.9999
	G2/M	ns	>0.9999
Control vs gemcitabine	sG1	ns	>0.9999
	G1	****	<0.0001
	S	ns	>0.9999
	G2/M	****	<0.0001
Control vs EXBR	sG1	ns	>0.9999
	G1	ns	>0.9999
	S	ns	>0.9999
	G2/M	ns	>0.9999
Control vs M+R Sch 1	sG1	ns	>0.9999
	G1	****	<0.0001
	S	ns	>0.9999
	G2/M	****	<0.0001
Control vs M+R Sch 2	sG1	ns	>0.9999
	G1	ns	0.1212
	S	ns	>0.9999
	G2/M	ns	>0.9999
Control vs D+R Sch 2	sG1	ns	>0.9999
	G1	ns	>0.9999
	S	ns	>0.9999
	G2/M	ns	>0.9999
Control vs M+G Sch 1	sG1	ns	>0.9999
	G1	****	<0.0001
	S	**	0.0047
	G2/M	****	<0.0001
Control vs M+G Sch 3	sG1	ns	>0.9999
	G1	****	<0.0001
	S	ns	>0.9999
	G2/M	***	0.0003

**Table 4.10: Statistical comparisons of the distribution of treated Panc-1 cells throughout the cell cycle versus monotherapies 36 hours post treatment.** Sch = schedule, M = MMF, D = MMF, G = gemcitabine, R = EXBR, ns = not significant.

Comparison	Phase of cell cycle	Summary	P-value
M+R Sch 1 vs MMF	sG1	ns	>0.9999
	G1	****	<0.0001
	S	ns	0.9263
	G2/M	****	<0.0001
M+R Sch 1 vs EXBR	sG1	ns	>0.9999
	G1	****	<0.0001
	S	ns	>0.9999
	G2/M	****	<0.0001
M+R Sch 2 vs MMF	sG1	ns	>0.9999
	G1	*	0.0219
	S	ns	0.1282
	G2/M	ns	>0.9999
M+R Sch 2 vs EXBR	sG1	ns	>0.9999
	G1	ns	0.1526
	S	ns	0.4396
	G2/M	ns	>0.9999
D+R Sch 2 vs DMF	sG1	ns	>0.9999
	G1	ns	>0.9999
	S	ns	>0.9999
	G2/M	ns	>0.9999
D+R Sch 2 vs EXBR	sG1	ns	>0.9999
	G1	ns	>0.9999
	S	ns	>0.9999
	G2/M	ns	>0.9999
M+G Sch 1 vs MMF	sG1	ns	>0.9999
	G1	****	<0.0001
	S	ns	0.0697
	G2/M	****	<0.0001
M+G Sch 1 vs gemcitabine	sG1	ns	>0.9999
	G1	****	<0.0001
	S	*	0.0258
	G2/M	****	<0.0001
M+G Sch 3 vs MMF	sG1	ns	>0.9999
	G1	***	0.0004
	S	ns	>0.9999
	G2/M	***	0.0002
M+G Sch 3 vs gemcitabine	sG1	ns	>0.9999
	G1	ns	>0.9999
	S	ns	>0.9999
	G2/M	ns	>0.9999

### **Summary of cell cycle analysis in Panc-1**

Overall, in Panc-1 cells, it took until four hours post treatment for the effects of the MMF + EXBR schedule 1 combination to induce any changes in the distribution of cells in the cell cycle when compared with the untreated control. The combination caused the cells to begin accumulating in both S phase and G2/M of the cell cycle in Panc-1 cells. However, as time progressed cells began to accumulate in G2/M phase 36 hours post treatment in Panc-1 cells. MMF monotherapy initially induced an increase in sG1 phase, indicating damaged cells, however this resolved by 36 hours post treatment. EXBR alone caused cells to accumulate in the G2/M phase four hours post treatment, indicating activation of the G2/M checkpoint due to DNA damage, however this resolved by 36 hours post treatment.

Initially the schedule 1 combination of 0.6  $\mu$ M MMF + 0.16  $\mu$ M gemcitabine did not appear to have any effect on the distribution of cells in the cell cycle, however as the time course continued the combination caused the cells to accumulate in G2/M phase of the cell cycle in the Panc-1 cell line, indicating DNA damage has occurred, activating the G2/M checkpoint. Overall gemcitabine monotherapy induced G2/M arrest, indicating DNA damage and the subsequent activation of the G2/M checkpoint. MMF monotherapy initially induced an increase in sG1 phase, indicating damaged cells, however this resolved by 36 hours post treatment.

Overall, the schedule 2 combination of 0.6  $\mu$ M MMF + 0.5 Gy EXBR induced an increase in the number of cells in sG1 phase immediately post treatment when compared with the untreated control, indicating the cells were damaged, which continued until four hours post treatment where the cell began to accumulate in G2/M phase, suggesting the G2/M checkpoint had been activated due to the presence of DNA damage. However, from 24 to 36 hours post treatment the distribution of cells in the cell cycle did not differ from the untreated control, indicating any DNA damage

inflicted by the combination was able to be resolved. MMF monotherapy initially induced an increase in sG1 phase, indicating damaged cells, however this resolved by 36 hours post treatment. EXBR alone caused cells to accumulate in the G2/M phase four hours post treatment, indicating activation of the G2/M checkpoint due to DNA damage, however this was resolved by 36 hours post treatment. Therefore, these results indicate that the combination is not promising for the treatment of pancreatic cancer.

Overall, the schedule 2 combination of 20  $\mu$ M DMF + 0.5 Gy EXBR had no significant effect on the cell cycle in the Panc-1 cell line as the G1 arrest seen 24 hours post treatment had resolved 36 hours post treatment. DMF monotherapy overall had no effect on the distribution of the cells throughout the cell cycle when compared with the untreated control. EXBR alone caused cells to accumulate in the G2/M phase four hours post treatment, indicating activation of the G2/M checkpoint due to DNA damage, however this resolved by 36 hours post treatment when compared with the untreated control.

Overall, the schedule 3 combination of MMF + gemcitabine caused the cells to accumulate in S phase of the cell cycle in the Panc-1 cell line up to 24 hours post treatment, indicating the cells had suffered DNA damage, activating the intra-S phase cell cycle checkpoint, however 36 hours post treatment the cells began to accumulate in G2/M phase, indicating the cells had begun transitioning from S phase to G2/M phase when compared to the untreated control. Overall gemcitabine monotherapy induced G2/M arrest, indicating DNA damage and the subsequent activation of the G2/M checkpoint when compared with the untreated control. MMF monotherapy initially induced an increase in sG1 phase, indicating damaged cells, however this resolved by 36 hours post treatment. This result indicates that the combination shows promise.

To investigate the effects of the developed combinations on the distribution of cells in the cell cycle in Mia PaCa-2 cells, the cell cycle assay was carried out as described in **section 4.3.3**, and the results presented in **figure 4.2**. In **appendix 7 – 11**, tables containing the average values for the distribution of cells throughout the cell cycle following treatment can be found.

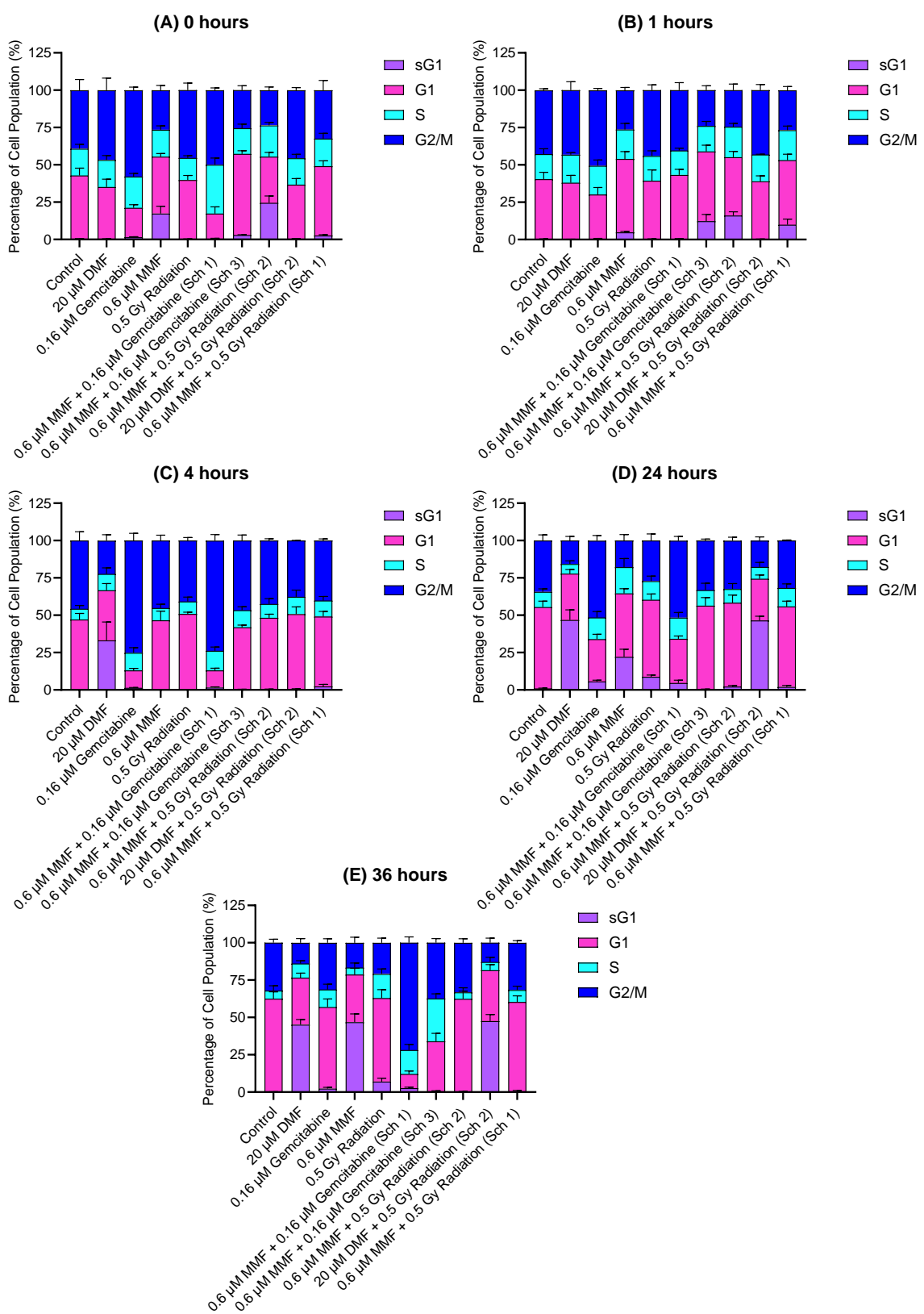


**Figure 4.2: Cell cycle analysis of combination therapies in Mia PaCa-2.** Cells were incubated and harvested at specific time points post treatment before undergoing flow cytometry to determine cell cycle distribution. (A) Distribution of cells 0 hours post treatment. (B) Distribution of cells 1 hour post treatment. (C) Distribution of cells 4 hours post treatment. (D) Distribution of cells 24 hours post treatment. (E) Distribution of cells 36 hours post treatment. All data is represented as an average of three independent experiments  $\pm$  the standard deviation.

As can be seen in **figure 4.2A**, in Mia PaCa-2 cells only 0.6  $\mu$ M MMF and 0.6  $\mu$ M MMF + 0.5 Gy EXBR (Schedule 2) induced a statistically significant increase in the number of cells in sG1 phase when compared with the untreated control zero hours post treatment ( $P < 0.0001$ ). When looking at G1 phase, 0.16  $\mu$ M gemcitabine and 0.6  $\mu$ M MMF + 0.16  $\mu$ M gemcitabine (Schedule 1) induced a statistically significant decrease in the number of cells in G1 phase when compared with the untreated control zero hours post treatment ( $P < 0.0001$ ). Conversely, 0.6  $\mu$ M MMF + 0.5 Gy EXBR (Schedule 2) and 0.16  $\mu$ M gemcitabine and 0.6  $\mu$ M MMF + 0.16  $\mu$ M gemcitabine (Schedule 3) induced a statistically significant increase in the number of cells in G1 phase when compared with the untreated control zero hours post treatment ( $P \leq 0.0021$ ). When looking at S phase, only 0.6  $\mu$ M MMF + 0.16  $\mu$ M gemcitabine (Schedule 1) induced a statistically significant increase in the number of cells in S phase when compared with the untreated control zero hours post treatment ( $P < 0.0001$ ). When looking at G2/M phase, 0.6  $\mu$ M MMF and 0.16  $\mu$ M gemcitabine and 0.6  $\mu$ M MMF + 0.16  $\mu$ M gemcitabine (Schedule 3) induced a statistically significant decrease in the number of cells in G2/M phase when compared with the untreated control zero hours post treatment ( $P \leq 0.0017$ ).

As can be seen in **figure 4.2B**, in Mia PaCa-2 cells 0.6  $\mu$ M MMF and 0.6  $\mu$ M MMF + 0.5 Gy EXBR (Schedule 1), 0.6  $\mu$ M MMF and 0.6  $\mu$ M MMF + 0.5 Gy EXBR (Schedule 2), and 0.6  $\mu$ M MMF + 0.16  $\mu$ M gemcitabine (Schedule 3) induced a statistically significant increase in the number of cells in sG1 phase when compared with the untreated control one hour post treatment ( $P \leq 0.0132$ ). When looking at G1 phase, only 0.6  $\mu$ M MMF induced a statistically significant increase in the number of cells in G1 phase when compared with the untreated control one hour post treatment ( $P = 0.0216$ ). Conversely, 0.16  $\mu$ M gemcitabine induced a statistically significant decrease in the number of cells in G1 phase when compared with the untreated control one

hour post treatment ( $P = 0.0018$ ). When looking at S phase, no treatments induced a statistically significant change in the number of cells in S phase when compared with the untreated control one hour post treatment ( $P > 0.9999$ ). When looking at G2/M phase, 0.6  $\mu\text{M}$  MMF, 0.6  $\mu\text{M}$  MMF + 0.5 Gy EXBR (Schedule 1), 0.6  $\mu\text{M}$  MMF + 0.5 Gy EXBR (Schedule 2), and 0.6  $\mu\text{M}$  MMF + 0.16  $\mu\text{M}$  gemcitabine (Schedule 3) induced a statistically significant decrease in the number of cells in G2/M phase when compared with the untreated control one hour post treatment ( $P < 0.0001$ ). Conversely, 0.16  $\mu\text{M}$  gemcitabine was the only treatment to induce a statistically significant increase in the number of cells in G2/M phase one hour post treatment when compared with the untreated control one hour post treatment ( $P = 0.0292$ ).

As can be seen in **figure 4.2C**, in Mia PaCa-2 cells only 20  $\mu\text{M}$  DMF induced a statistically significant increase in the number of cells in sG1 phase when compared with the untreated control four hours post treatment ( $P < 0.0001$ ). When looking at G1 phase, 0.16  $\mu\text{M}$  gemcitabine, 20  $\mu\text{M}$  DMF, and 0.6  $\mu\text{M}$  MMF + 0.16  $\mu\text{M}$  gemcitabine (Schedule 1) induced a statistically significant increase in the number of cells in G1 phase when compared with the untreated control four hours post treatment ( $P \leq 0.0051$ ). When looking at S phase, no treatments induced a statistically significant change in the number of cells in S phase when compared with the untreated control four hours post treatment ( $P \geq 0.2150$ ). When looking at G2/M phase, 0.16  $\mu\text{M}$  gemcitabine and 0.6  $\mu\text{M}$  MMF + 0.16  $\mu\text{M}$  gemcitabine (Schedule 1) induced a statistically significant increase in the number of cells in G2/M phase when compared with the untreated control four hours post treatment ( $P < 0.0001$ ). Whereas 20  $\mu\text{M}$  DMF was the only treatment to induce a statistically significant decrease in the number of cells in G2/M phase when compared with the untreated control four hours post treatment ( $P < 0.0001$ ).

As can be seen in **figure 4.2D**, in Mia PaCa-2 cells 0.6  $\mu\text{M}$  MMF, 0.5 Gy EXBR, 20  $\mu\text{M}$  DMF, 0.6  $\mu\text{M}$  MMF + 0.5 Gy EXBR (Schedule 1), and 20  $\mu\text{M}$  DMF + 0.5 Gy EXBR (Schedule 2) induced a statistically significant increase in the number of cells in sG1 phase when compared with the untreated control 24 hours post treatment ( $P \leq 0.0493$ ). When looking at G1 phase, 0.6  $\mu\text{M}$  MMF, 0.16  $\mu\text{M}$  gemcitabine, 20  $\mu\text{M}$  DMF, 0.6  $\mu\text{M}$  MMF + 0.5 Gy EXBR (Schedule 1), and 20  $\mu\text{M}$  DMF + 0.5 Gy EXBR (Schedule 2) induced a statistically significant decrease in the number of cells in G1 phase when compared with the untreated control 24 hours post treatment ( $P \leq 0.0009$ ). When looking at S phase, no treatments induced a statistically significant change in the number of cells in S phase when compared with the untreated control 24 hours post treatment ( $P \geq 0.0722$ ). When looking at G2/M phase, only 0.6  $\mu\text{M}$  MMF induced a statistically significant decrease in the number of cells in G2/M phase when compared with the untreated control 24 hours post treatment ( $P < 0.0001$ ). Whereas 0.16  $\mu\text{M}$  gemcitabine and 0.6  $\mu\text{M}$  MMF + 0.16  $\mu\text{M}$  gemcitabine (Schedule 1) induced a statistically significant increase in the number of cells in G2/M phase when compared with the untreated control 24 hours post treatment ( $P < 0.0001$ ).

As can be seen in **figure 4.2E**, in Mia PaCa-2 cells 0.6  $\mu\text{M}$  MMF, 20  $\mu\text{M}$  DMF, and 20  $\mu\text{M}$  DMF + 0.5 Gy EXBR (Schedule 2) induced a statistically significant increase in the number of cells in sG1 phase when compared with the untreated control 36 hours post treatment ( $P < 0.0001$ ). When looking at G1 phase, 0.6  $\mu\text{M}$  MMF, 20  $\mu\text{M}$  DMF, 0.6  $\mu\text{M}$  MMF + 0.16  $\mu\text{M}$  gemcitabine (Schedule 1), 0.6  $\mu\text{M}$  MMF + 0.16  $\mu\text{M}$  gemcitabine (Schedule 3), and 20  $\mu\text{M}$  DMF + 0.5 Gy EXBR (Schedule 2) induced a statistically significant decrease in the number of cells in G1 phase when compared with the untreated control 36 hours post treatment ( $P < 0.0001$ ). When looking at S phase, 0.5 Gy EXBR, 0.6  $\mu\text{M}$  MMF + 0.16  $\mu\text{M}$  gemcitabine (Schedule 1), and 0.6  $\mu\text{M}$  MMF + 0.16  $\mu\text{M}$  gemcitabine (Schedule 3) induced a statistically significant increase

in the number of cells in S phase when compared with the untreated control 36 hours post treatment ( $P \leq 0.0040$ ). When looking at G2/M phase, 0.6  $\mu\text{M}$  MMF, 20  $\mu\text{M}$  DMF, 0.5 Gy EXBR, and 20  $\mu\text{M}$  DMF + 0.5 Gy EXBR (Schedule 2) induced a statistically significant decrease in the number of cells in G2/M phase when compared with the untreated control 36 hours post treatment ( $P \leq 0.0023$ ). Conversely, 0.6  $\mu\text{M}$  MMF + 0.16  $\mu\text{M}$  gemcitabine (Schedule 1) was the only treatment to induce a statistically significant increase in the number of cells in G2/M phase when compared with the untreated control 36 hours post treatment ( $P < 0.0001$ ).

Some changes were observed in the untreated control over the time course, with a statistically significant increase in the number of cells in G1 phase at the 24-hour timepoint ( $P = 0.0013$ ), however this did not change for the remainder of the time course ( $P = 0.0659$ ). The other change observed was that there was a statistically significant decrease in the number of cells in S phase at the 4- and 36-hour timepoint ( $P \leq 0.0050$ ).

A summary of all statistical comparisons carried out between the untreated control and therapies, and between combination therapies and individual components over the time course in Panc-1 cells following two-way ANOVA with Bonferroni post hoc test can be found in **tables 4.1 – 4.20**.

**Table 4.11: Statistical comparisons of the distribution of treated Mia PaCa-2 cells throughout the cell cycle versus the untreated control zero hours post treatment.** Sch = schedule, M = MMF, D = MMF, G = gemcitabine, R = EXBR, ns = not significant.

Comparison	Phase of cell cycle	Summary	P-value
Control vs DMF	sG1	ns	>0.9999
	G1	ns	0.1415
	S	ns	>0.9999
	G2/M	ns	0.1511
Control vs MMF	sG1	****	<0.0001
	G1	ns	>0.9999
	S	ns	>0.9999
	G2/M	**	0.0017
Control vs gemcitabine	sG1	ns	>0.9999
	G1	****	<0.0001
	S	ns	>0.9999
	G2/M	****	<0.0001
Control vs EXBR	sG1	ns	>0.9999
	G1	ns	>0.9999
	S	ns	>0.9999
	G2/M	ns	0.3392
Control vs M+R Sch 1	sG1	ns	>0.9999
	G1	ns	>0.9999
	S	ns	>0.9999
	G2/M	ns	0.2211
Control vs M+R Sch 2	sG1	****	<0.0001
	G1	**	0.0021
	S	ns	>0.9999
	G2/M	****	<0.0001
Control vs D+R Sch 2	sG1	ns	>0.9999
	G1	ns	0.3680
	S	ns	0.3393
	G2/M	ns	>0.9999
Control vs M+G Sch 1	sG1	ns	>0.9999
	G1	****	<0.0001
	S	****	<0.0001
	G2/M	**	0.0033
Control vs M+G Sch 3	sG1	ns	>0.9999
	G1	ns	0.6801
	S	ns	>0.9999
	G2/M	****	<0.0001

**Table 4.12: Statistical comparisons of the distribution of treated Mia PaCa-2 cells throughout the cell cycle versus monotherapies zero hours post treatment.** Sch = schedule, M = MMF, D = MMF, G = gemcitabine, R = EXBR, ns = not significant.

Comparison	Phase of cell cycle	Summary	P-value
M+R Sch 1 vs MMF	sG1	***	0.0003
	G1	ns	0.0681
	S	ns	>0.9999
	G2/M	ns	0.4016
M+R Sch 1 vs EXBR	sG1	ns	>0.9999
	G1	ns	0.1909
	S	ns	>0.9999
	G2/M	**	0.0013
M+R Sch 2 vs MMF	sG1	ns	0.1078
	G1	ns	0.0999
	S	ns	0.0999
	G2/M	ns	0.0999
M+R Sch 2 vs EXBR	sG1	****	<0.0001
	G1	*	0.0311
	S	ns	0.2530
	G2/M	****	<0.0001
D+R Sch 2 vs DMF	sG1	ns	>0.9999
	G1	ns	>0.9999
	S	ns	>0.9999
	G2/M	ns	>0.9999
D+R Sch 2 vs EXBR	sG1	ns	>0.9999
	G1	ns	>0.9999
	S	ns	>0.9999
	G2/M	ns	>0.9999
M+G Sch 1 vs MMF	sG1	****	<0.0001
	G1	****	<0.0001
	S	****	<0.0001
	G2/M	****	<0.0001
M+G Sch 1 vs gemcitabine	sG1	ns	>0.9999
	G1	ns	>0.9999
	S	**	0.0011
	G2/M	*	0.0452
M+G Sch 3 vs MMF	sG1	****	<0.0001
	G1	****	<0.0001
	S	ns	>0.9999
	G2/M	****	<0.0001
M+G Sch 3 vs gemcitabine	sG1	ns	>0.9999
	G1	****	<0.0001
	S	ns	>0.9999
	G2/M	****	<0.0001

**Table 4.13: Statistical comparisons of the distribution of treated Mia PaCa-2 cells throughout the cell cycle versus the untreated control one hour post treatment.** Sch = schedule, M = MMF, D = MMF, G = gemcitabine, R = EXBR, ns = not significant.

Comparison	Phase of cell cycle	Summary	P-value
Control vs DMF	sG1	ns	>0.9999
	G1	ns	>0.9999
	S	ns	>0.9999
	G2/M	ns	>0.9999
Control vs MMF	sG1	ns	0.7438
	G1	*	0.0216
	S	ns	>0.9999
	G2/M	****	<0.0001
Control vs gemcitabine	sG1	ns	>0.9999
	G1	**	0.0018
	S	ns	>0.9999
	G2/M	*	0.0292
Control vs EXBR	sG1	ns	>0.9999
	G1	ns	>0.9999
	S	ns	>0.9999
	G2/M	ns	>0.9999
Control vs M+R Sch 1	sG1	*	0.0132
	G1	ns	>0.9999
	S	ns	>0.9999
	G2/M	****	<0.0001
Control vs M+R Sch 2	sG1	****	<0.0001
	G1	ns	>0.9999
	S	ns	>0.9999
	G2/M	****	<0.0001
Control vs D+R Sch 2	sG1	ns	>0.9999
	G1	ns	>0.9999
	S	ns	>0.9999
	G2/M	ns	>0.9999
Control vs M+G Sch 1	sG1	ns	>0.9999
	G1	ns	>0.9999
	S	ns	>0.9999
	G2/M	ns	>0.9999
Control vs M+G Sch 3	sG1	***	0.0006
	G1	ns	0.1177
	S	ns	>0.9999
	G2/M	****	<0.0001

**Table 4.14: Statistical comparisons of the distribution of treated Mia PaCa-2 cells throughout the cell cycle versus monotherapies one hour post treatment.**  
 Sch = schedule, M = MMF, D = MMF, G = gemcitabine, R = EXBR, ns = not significant.

Comparison	Phase of cell cycle	Summary	P-value
M+R Sch 1 vs MMF	sG1	ns	0.5388
	G1	ns	0.2954
	S	ns	>0.9999
	G2/M	ns	>0.9999
M+R Sch 1 vs EXBR	sG1	*	0.0135
	G1	ns	0.9164
	S	ns	>0.9999
	G2/M	****	<0.0001
M+R Sch 2 vs MMF	sG1	**	0.0028
	G1	**	0.0087
	S	ns	>0.9999
	G2/M	ns	>0.9999
M+R Sch 2 vs EXBR	sG1	****	<0.0001
	G1	ns	>0.9999
	S	ns	>0.9999
	G2/M	****	<0.0001
D+R Sch 2 vs DMF	sG1	ns	>0.9999
	G1	ns	>0.9999
	S	ns	>0.9999
	G2/M	ns	>0.9999
D+R Sch 2 vs EXBR	sG1	ns	>0.9999
	G1	ns	>0.9999
	S	ns	>0.9999
	G2/M	ns	>0.9999
M+G Sch 1 vs MMF	sG1	ns	0.5467
	G1	ns	0.1269
	S	ns	>0.9999
	G2/M	****	<0.0001
M+G Sch 1 vs gemcitabine	sG1	ns	>0.9999
	G1	****	<0.0001
	S	ns	>0.9999
	G2/M	**	0.0023
M+G Sch 3 vs MMF	sG1	ns	0.0542
	G1	ns	>0.9999
	S	ns	>0.9999
	G2/M	ns	>0.9999
M+G Sch 3 vs gemcitabine	sG1	***	0.0006
	G1	****	<0.0001
	S	ns	>0.9999
	G2/M	****	<0.0001

**Table 4.15: Statistical comparisons of the distribution of treated Mia PaCa-2 cells throughout the cell cycle versus the untreated control four hours post treatment.** Sch = schedule, M = MMF, D = MMF, G = gemcitabine, R = EXBR, ns = not significant.

Comparison	Phase of cell cycle	Summary	P-value
Control vs DMF	sG1	****	<0.0001
	G1	**	0.0051
	S	ns	>0.9999
	G2/M	****	<0.0001
Control vs MMF	sG1	ns	>0.9999
	G1	ns	>0.9999
	S	ns	>0.9999
	G2/M	ns	>0.9999
Control vs gemcitabine	sG1	ns	>0.9999
	G1	****	<0.0001
	S	ns	0.6164
	G2/M	****	<0.0001
Control vs EXBR	sG1	ns	>0.9999
	G1	ns	0.8576
	S	ns	>0.9999
	G2/M	ns	0.3643
Control vs M+R Sch 1	sG1	ns	>0.9999
	G1	ns	>0.9999
	S	ns	>0.9999
	G2/M	ns	0.2055
Control vs M+R Sch 2	sG1	ns	>0.9999
	G1	ns	>0.9999
	S	ns	>0.9999
	G2/M	ns	>0.9999
Control vs D+R Sch 2	sG1	ns	>0.9999
	G1	ns	>0.9999
	S	ns	>0.9999
	G2/M	ns	0.2047
Control vs M+G Sch 1	sG1	ns	>0.9999
	G1	****	<0.0001
	S	ns	0.2150
	G2/M	****	<0.0001
Control vs M+G Sch 3	sG1	ns	>0.9999
	G1	ns	0.3471
	S	ns	0.7044
	G2/M	ns	>0.9999

**Table 4.16: Statistical comparisons of the distribution of treated Mia PaCa-2 cells throughout the cell cycle versus monotherapies four hours post treatment.** Sch = schedule, M = MMF, D = MMF, G = gemcitabine, R = EXBR, ns = not significant.

Comparison	Phase of cell cycle	Summary	P-value
M+R Sch 1 vs MMF	sG1	ns	>0.9999
	G1	ns	>0.9999
	S	ns	>0.9999
	G2/M	ns	0.3093
M+R Sch 1 vs EXBR	sG1	ns	>0.9999
	G1	ns	0.7854
	S	ns	>0.9999
	G2/M	ns	>0.9999
M+R Sch 2 vs MMF	sG1	ns	>0.9999
	G1	ns	>0.9999
	S	ns	>0.9999
	G2/M	ns	>0.9999
M+R Sch 2 vs EXBR	sG1	ns	>0.9999
	G1	ns	>0.9999
	S	ns	>0.9999
	G2/M	ns	>0.9999
D+R Sch 2 vs DMF	sG1	****	<0.0001
	G1	***	0.0003
	S	ns	>0.9999
	G2/M	**	0.0011
D+R Sch 2 vs EXBR	sG1	ns	>0.9999
	G1	ns	>0.9999
	S	ns	>0.9999
	G2/M	ns	>0.9999
M+G Sch 1 vs MMF	sG1	ns	>0.9999
	G1	****	<0.0001
	S	ns	0.4453
	G2/M	****	<0.0001
M+G Sch 1 vs gemcitabine	sG1	ns	>0.9999
	G1	ns	>0.9999
	S	ns	>0.9999
	G2/M	ns	>0.9999
M+G Sch 3 vs MMF	sG1	ns	>0.9999
	G1	ns	0.4698
	S	ns	>0.9999
	G2/M	ns	>0.9999
M+G Sch 3 vs gemcitabine	sG1	ns	>0.9999
	G1	****	<0.0001
	S	ns	>0.9999
	G2/M	****	<0.0001

**Table 4.17: Statistical comparisons of the distribution of treated Mia PaCa-2 cells throughout the cell cycle versus the untreated control 24 hours post treatment.** Sch = schedule, M = MMF, D = MMF, G = gemcitabine, R = EXBR, ns = not significant.

Comparison	Phase of cell cycle	Summary	P-value
Control vs DMF	sG1	****	<0.0001
	G1	****	<0.0001
	S	ns	>0.9999
	G2/M	****	<0.0001
Control vs MMF	sG1	****	<0.0001
	G1	***	0.0009
	S	ns	0.0722
	G2/M	****	<0.0001
Control vs gemcitabine	sG1	ns	0.6223
	G1	****	<0.0001
	S	ns	0.7999
	G2/M	****	<0.0001
Control vs EXBR	sG1	*	0.0493
	G1	ns	>0.9999
	S	ns	>0.9999
	G2/M	ns	0.0873
Control vs M+R Sch 1	sG1	ns	>0.9999
	G1	ns	>0.9999
	S	ns	>0.9999
	G2/M	ns	>0.9999
Control vs M+R Sch 2	sG1	ns	>0.9999
	G1	ns	>0.9999
	S	ns	>0.9999
	G2/M	ns	>0.9999
Control vs D+R Sch 2	sG1	****	<0.0001
	G1	****	<0.0001
	S	ns	>0.9999
	G2/M	****	<0.0001
Control vs M+G Sch 1	sG1	ns	>0.9999
	G1	****	<0.0001
	S	ns	0.9673
	G2/M	****	<0.0001
Control vs M+G Sch 3	sG1	ns	>0.9999
	G1	ns	>0.9999
	S	ns	>0.9999
	G2/M	ns	>0.9999

**Table 4.18: Statistical comparisons of the distribution of treated Mia PaCa-2 cells throughout the cell cycle versus monotherapies 24 hours post treatment.**  
 Sch = schedule, M = MMF, D = MMF, G = gemcitabine, R = EXBR, ns = not significant.

Comparison	Phase of cell cycle	Summary	P-value
M+R Sch 1 vs MMF	sG1	****	<0.0001
	G1	**	0.0018
	S	ns	0.4306
	G2/M	***	0.0001
M+R Sch 1 vs EXBR	sG1	ns	0.1231
	G1	ns	>0.9999
	S	ns	>0.9999
	G2/M	ns	0.6625
M+R Sch 2 vs MMF	sG1	****	<0.0001
	G1	***	0.0004
	S	*	0.0442
	G2/M	***	0.0001
M+R Sch 2 vs EXBR	sG1	ns	0.1957
	G1	ns	0.7523
	S	ns	>0.9999
	G2/M	ns	0.4853
D+R Sch 2 vs DMF	sG1	ns	>0.9999
	G1	ns	>0.9999
	S	ns	>0.9999
	G2/M	ns	>0.9999
D+R Sch 2 vs EXBR	sG1	****	<0.0001
	G1	****	<0.0001
	S	ns	0.5988
	G2/M	**	0.0079
M+G Sch 1 vs MMF	sG1	****	<0.0001
	G1	***	0.0003
	S	ns	>0.9999
	G2/M	****	<0.0001
M+G Sch 1 vs gemcitabine	sG1	ns	>0.9999
	G1	ns	>0.9999
	S	ns	>0.9999
	G2/M	ns	>0.9999
M+G Sch 3 vs MMF	sG1	****	<0.0001
	G1	***	0.0004
	S	ns	0.1235
	G2/M	****	<0.0001
M+G Sch 3 vs gemcitabine	sG1	ns	0.5239
	G1	****	<0.0001
	S	ns	>0.9999
	G2/M	****	<0.0001

**Table 4.19: Statistical comparisons of the distribution of treated Mia PaCa-2 cells throughout the cell cycle versus the untreated control 36 hours post treatment.** Sch = schedule, M = MMF, D = MMF, G = gemcitabine, R = EXBR, ns = not significant.

Comparison	Phase of cell cycle	Summary	P-value
Control vs DMF	sG1	****	<0.0001
	G1	****	<0.0001
	S	ns	0.8910
	G2/M	****	<0.0001
Control vs MMF	sG1	****	<0.0001
	G1	****	<0.0001
	S	ns	>0.9999
	G2/M	****	<0.0001
Control vs gemcitabine	sG1	ns	>0.9999
	G1	ns	0.0595
	S	ns	0.1891
	G2/M	ns	>0.9999
Control vs EXBR	sG1	ns	0.1293
	G1	ns	0.1896
	S	**	0.0037
	G2/M	**	0.0023
Control vs M+R Sch 1	sG1	ns	>0.9999
	G1	ns	>0.9999
	S	ns	>0.9999
	G2/M	ns	>0.9999
Control vs M+R Sch 2	sG1	ns	>0.9999
	G1	ns	>0.9999
	S	ns	>0.9999
	G2/M	ns	>0.9999
Control vs D+R Sch 2	sG1	****	<0.0001
	G1	****	<0.0001
	S	ns	>0.9999
	G2/M	****	<0.0001
Control vs M+G Sch 1	sG1	ns	>0.9999
	G1	****	<0.0001
	S	**	0.0040
	G2/M	****	<0.0001
Control vs M+G Sch 3	sG1	ns	>0.9999
	G1	****	<0.0001
	S	****	<0.0001
	G2/M	ns	0.4748

**Table 4.20: Statistical comparisons of the distribution of treated Mia PaCa-2 cells throughout the cell cycle versus monotherapies 36 hours post treatment.**  
 Sch = schedule, M = MMF, D = MMF, G = gemcitabine, R = EXBR, ns = not significant.

Comparison	Phase of cell cycle	Summary	P-value
M+R Sch 1 vs MMF	sG1	****	<0.0001
	G1	****	<0.0001
	S	ns	>0.9999
	G2/M	****	<0.0001
M+R Sch 1 vs EXBR	sG1	ns	0.1767
	G1	ns	>0.9999
	S	*	0.0463
	G2/M	**	0.0037
M+R Sch 2 vs MMF	sG1	****	<0.0001
	G1	****	<0.0001
	S	ns	>0.9999
	G2/M	****	<0.0001
M+R Sch 2 vs EXBR	sG1	ns	0.1710
	G1	ns	0.2568
	S	**	0.0022
	G2/M	**	0.0013
D+R Sch 2 vs DMF	sG1	ns	>0.9999
	G1	ns	>0.9999
	S	ns	>0.9999
	G2/M	ns	>0.9999
D+R Sch 2 vs EXBR	sG1	****	<0.0001
	G1	****	<0.0001
	S	**	0.0034
	G2/M	*	0.0350
M+G Sch 1 vs MMF	sG1	****	<0.0001
	G1	****	<0.0001
	S	**	0.0021
	G2/M	****	<0.0001
M+G Sch 1 vs gemcitabine	sG1	ns	>0.9999
	G1	****	<0.0001
	S	ns	0.8257
	G2/M	****	<0.0001
M+G Sch 3 vs MMF	sG1	****	<0.0001
	G1	ns	>0.9999
	S	****	<0.0001
	G2/M	****	<0.0001
M+G Sch 3 vs gemcitabine	sG1	ns	>0.9999
	G1	****	<0.0001
	S	****	<0.0001
	G2/M	ns	0.2799

## **Summary of cell cycle analysis in Mia PaCa-2**

Overall, the schedule 1 combination of 0.6  $\mu$ M MMF + 0.5 Gy EXBR initially appeared to cause Mia PaCa-2 cells to accumulate in G1 phase, however as time progressed the cells continued to progress through the cell cycle unhindered. Surprisingly, MMF monotherapy caused cells to continue to accumulate in sG1 phase as time progressed, which would suggest the cells were damaged and possibly undergoing apoptosis. EXBR alone overall had no effect on the distribution of cells throughout the cell cycle, however 36 hours post treatment it began to cause cells to accumulate in S phase, indicating DNA damage and subsequent activation of the intra-S checkpoint.

The schedule 1 combination of MMF + gemcitabine caused the cells to accumulate in G2/M phase of the cell cycle in the Mia PaCa-2 cell line, with the number of cells in the G2/M phase continuing to increase as the time course progressed, indicating the activation of the G2/M checkpoint in response to DNA damage. As the cells continued to accumulate in G2/M this would suggest the cells are unable to repair the DNA damage that was induced by the combination induced. MMF monotherapy caused cells to continue to accumulate in sG1 phase as time progressed, which would suggest the cells were damaged and possibly undergoing apoptosis. Overall gemcitabine monotherapy induced G2/M arrest, indicating DNA damage and the subsequent activation of the G2/M checkpoint.

Overall, the schedule 2 combination of 0.6  $\mu$ M MMF + 0.5 Gy EXBR had no effect on the distribution of cells in the cell cycle when compared with the untreated control in the Mia PaCa-2 cell line, despite the initial increase in the number of cells in sG1 phase which indicated the cells were damaged. EXBR alone overall had no effect on the distribution of cells throughout the cell cycle, however 36 hours post treatment it began to cause cells to accumulate in S phase, indicating DNA damage and subsequent activation of the intra-S checkpoint. MMF monotherapy initially induced

an increase in sG1 phase, indicating damaged cells, however this resolved by 36 hours post treatment.

Initially the schedule 2 combination of 20  $\mu$ M DMF + 0.5 Gy had no effect on the distribution of cells throughout the cell cycle, until 24 hours post treatment and beyond, where it caused cells to accumulate in sG1 phase in the Mia PaCa-2 cell line. This indicates that the cells are damaged and possibly undergoing apoptosis. EXBR alone overall had no effect on the distribution of cells throughout the cell cycle, however 36 hours post treatment it began to cause cells to accumulate in S phase, indicating DNA damage and subsequent activation of the intra-S checkpoint. DMF monotherapy initially had no effect on the distribution of cells throughout the cell cycle, however 4 hours post treatment it began to induce an increase in the number of cells in sG1 phase, which continued to increase until 36 hours post treatment, indicating the cells were damaged and possibly undergoing apoptosis.

Initially, the schedule 1 combination of MMF + gemcitabine had no effect on the distribution of cells in the cell cycle until 36 hours post treatment, where it caused cells to accumulate in caused the cells to accumulate in S phase of the cell cycle in Mia PaCa-2 cells, indicating DNA damage and subsequent activation of the intra-S phase cell cycle checkpoint. MMF monotherapy caused cells to continue to accumulate in sG1 phase as time progressed, which would suggest the cells were damaged and possibly undergoing apoptosis. Overall gemcitabine monotherapy induced G2/M arrest, indicating DNA damage and the subsequent activation of the G2/M checkpoint.

#### **4.4.2: Apoptosis studies on developed combinations**

To investigate if the selected combinations were inducing cell death via apoptosis in the Panc-1 cell line, the apoptosis assay was carried out as described in **section 4.3.4**, and the results presented in ***figure 4.3***.

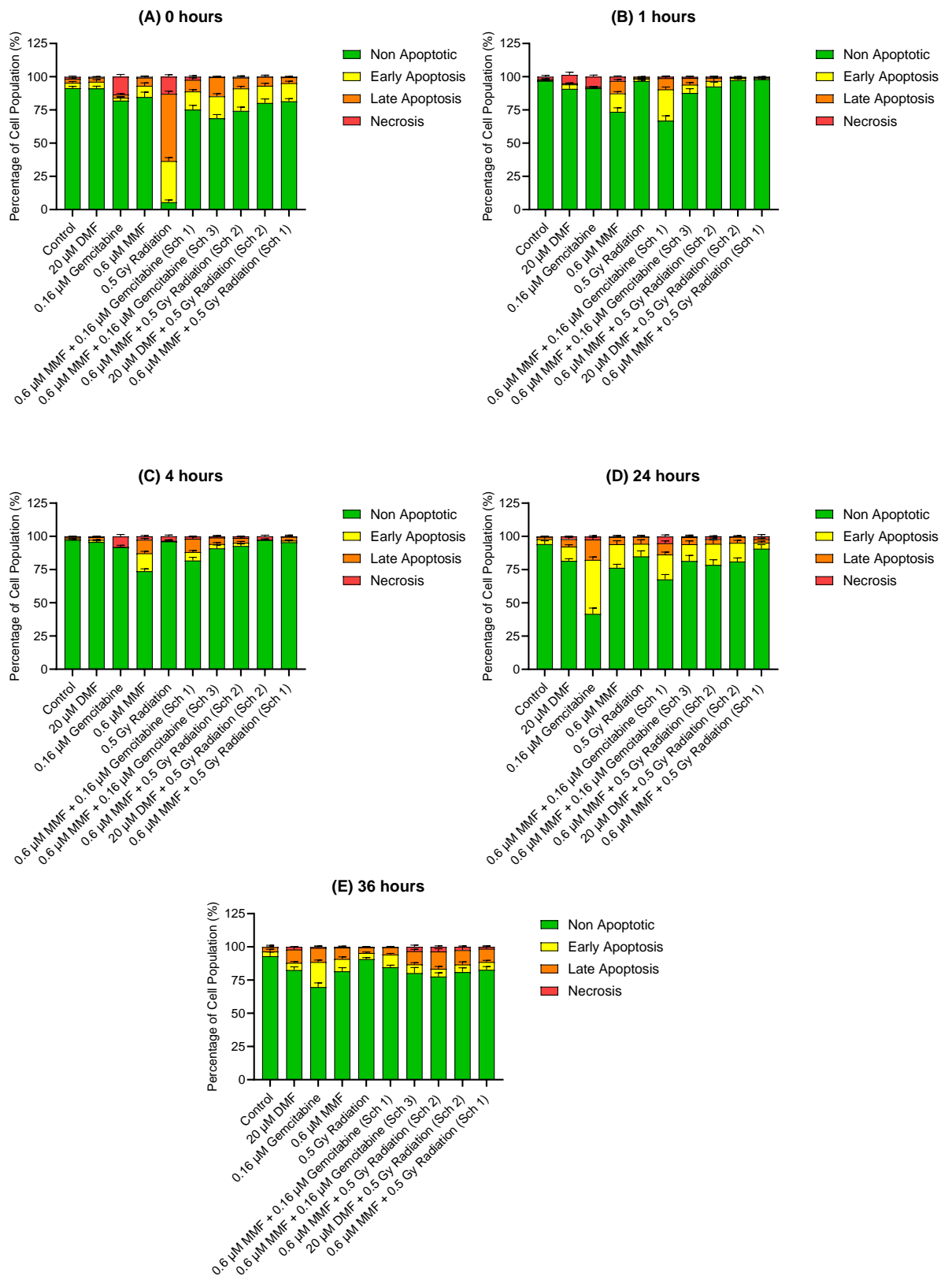


**Figure 4.3: Apoptosis analysis of combination therapies in Panc-1.** Cells were incubated and harvested at specific time points post treatment before undergoing flow cytometry to determine the stage of apoptosis. (A) Distribution of cells 0 hours post treatment. (B) Distribution of cells 1 hour post treatment. (C) Distribution of cells 4 hours post treatment. (D) Distribution of cells 24 hours post treatment. (E) Distribution of cells 36 hours post treatment. All data is represented as an average of three independent experiments  $\pm$  the standard deviation.

As can be seen in **figure 4.3A**, in Panc-1 cells 0.6  $\mu\text{M}$  MMF, 0.5 Gy EXBR, 0.6  $\mu\text{M}$  MMF + 0.5 Gy EXBR (Schedule 1), 0.6  $\mu\text{M}$  MMF + 0.5 Gy EXBR (Schedule 2), 0.6  $\mu\text{M}$  MMF + 0.16  $\mu\text{M}$  gemcitabine (Schedule 1), 0.6  $\mu\text{M}$  MMF + 0.16  $\mu\text{M}$  gemcitabine (Schedule 3), and 20  $\mu\text{M}$  DMF + 0.5 Gy EXBR (Schedule 2) induced a statistically significant increase in the number of early apoptotic cells when compared with the untreated control zero hours post treatment ( $P \leq 0.0223$ ). When looking at late apoptosis, 0.5 Gy EXBR, 0.6  $\mu\text{M}$  MMF + 0.16  $\mu\text{M}$  gemcitabine (Schedule 1), 0.6  $\mu\text{M}$  MMF + 0.16  $\mu\text{M}$  gemcitabine (Schedule 3), 0.6  $\mu\text{M}$  MMF + 0.5 Gy EXBR (Schedule 2), and 20  $\mu\text{M}$  DMF + 0.5 Gy EXBR (Schedule 2) induced a statistically significant increase in the number of late apoptotic cells when compared with the untreated control zero hours post treatment ( $P \leq 0.0230$ ). When looking at necrosis, only 0.5 Gy EXBR and 0.16  $\mu\text{M}$  gemcitabine induced a statistically significant increase in the number of necrotic cells when compared with the untreated control zero hours post treatment ( $P < 0.0001$ ).

As can be seen in **figure 4.3B**, in Panc-1 cells 0.6  $\mu\text{M}$  MMF, 20  $\mu\text{M}$  DMF, 0.6  $\mu\text{M}$  MMF + 0.16  $\mu\text{M}$  gemcitabine (Schedule 1), 0.6  $\mu\text{M}$  MMF + 0.16  $\mu\text{M}$  gemcitabine (Schedule 3), and 0.6  $\mu\text{M}$  MMF + 0.5 Gy EXBR (Schedule 2) induced a statistically significant increase in the number of early apoptotic cells when compared with the untreated control one hour post treatment ( $P \leq 0.0112$ ). When looking at late apoptosis, 0.6  $\mu\text{M}$  MMF, 0.6  $\mu\text{M}$  MMF + 0.16  $\mu\text{M}$  gemcitabine (Schedule 1), and 0.6  $\mu\text{M}$  MMF + 0.16  $\mu\text{M}$  gemcitabine (Schedule 3) induced a statistically significant increase in the number of late apoptotic cells when compared with the untreated control one hour post treatment ( $P \leq 0.0095$ ). When looking at necrosis, only 0.16  $\mu\text{M}$  gemcitabine and 20  $\mu\text{M}$  DMF induced a statistically significant increase in the number of necrotic cells when compared with the untreated control one hour post treatment ( $P \leq 0.0005$ ).

As can be seen in **figure 4.3C**, in Panc-1 cells only 0.6  $\mu\text{M}$  MMF and 0.6  $\mu\text{M}$  MMF + 0.16  $\mu\text{M}$  gemcitabine (Schedule 1) induced a statistically significant increase in the number of early apoptotic cells when compared with the untreated control four hours post treatment ( $P < 0.0001$ ). When looking at late apoptosis, 0.6  $\mu\text{M}$  MMF, 0.6  $\mu\text{M}$  MMF + 0.16  $\mu\text{M}$  gemcitabine (Schedule 1), 0.6  $\mu\text{M}$  MMF + 0.16  $\mu\text{M}$  gemcitabine (Schedule 3), and 0.6  $\mu\text{M}$  MMF + 0.5 Gy EXBR (Schedule 2) induced a statistically significant increase in the number of late apoptotic cells when compared with the untreated control ( $P \leq 0.0208$ ). When looking at necrosis, 0.6  $\mu\text{M}$  MMF, 0.5 Gy EXBR, 0.16  $\mu\text{M}$  gemcitabine, and 20  $\mu\text{M}$  DMF + 0.5 Gy EXBR (Schedule 2) induced a statistically significant increase in the number of necrotic cells when compared with the untreated control four hours post treatment ( $P \leq 0.0317$ ).

As can be seen in **figure 4.3D**, in Panc-1 cells 0.6  $\mu\text{M}$  MMF, 0.5 Gy EXBR, 0.16  $\mu\text{M}$  gemcitabine, 20  $\mu\text{M}$  DMF, 0.6  $\mu\text{M}$  MMF + 0.16  $\mu\text{M}$  gemcitabine (Schedule 1), 0.6  $\mu\text{M}$  MMF + 0.5 Gy EXBR (Schedule 2), and 20  $\mu\text{M}$  DMF + 0.5 Gy EXBR (Schedule 2) induced a statistically significant increase in the number of early apoptotic cells when compared with the untreated control 24 hours post treatment ( $P \leq 0.0127$ ). When looking at late apoptosis, only 0.16  $\mu\text{M}$  gemcitabine and 0.6  $\mu\text{M}$  MMF + 0.16  $\mu\text{M}$  gemcitabine (Schedule 1) induced a statistically significant increase in the number of late apoptotic cells when compared with the untreated control 24 hours post treatment ( $P \leq 0.0031$ ). When looking at necrosis, only 0.6  $\mu\text{M}$  MMF + 0.16  $\mu\text{M}$  gemcitabine (Schedule 1) induced a statistically significant increase in the number of necrotic cells when compared with the untreated control 24 hours post treatment ( $P = 0.0430$ ).

As can be seen in **figure 4.3E**, in Panc-1 cells 0.6  $\mu\text{M}$  MMF, 0.16  $\mu\text{M}$  gemcitabine, and 0.6  $\mu\text{M}$  MMF + 0.16  $\mu\text{M}$  gemcitabine (Schedule 1) induced a statistically significant increase in the number of early apoptotic cells when compared with the

untreated control 36 hours post treatment ( $P \leq 0.0006$ ). When looking at late apoptosis, 0.6  $\mu\text{M}$  MMF, 20  $\mu\text{M}$  DMF, 0.16  $\mu\text{M}$  gemcitabine, 0.6  $\mu\text{M}$  MMF + 0.5 Gy EXBR (Schedule 1), 0.6  $\mu\text{M}$  MMF + 0.5 Gy EXBR (Schedule 2), 20  $\mu\text{M}$  DMF + 0.5 Gy EXBR (Schedule 2), and 0.6  $\mu\text{M}$  MMF + 0.16  $\mu\text{M}$  gemcitabine (Schedule 3) induced a statistically significant increase in the number of late apoptotic cells when compared with the untreated control 36 hours post treatment ( $P \leq 0.0015$ ). No treatments induced a statistically significant change in the number of necrotic cells when compared with the untreated control 36 hours post treatment ( $P \geq 0.1001$ ).

A summary of all statistical comparisons carried out between the untreated control and therapies, and between combination therapies and individual components over the time course in Panc-1 cells following two-way ANOVA with Bonferroni post hoc test can be found in **tables 4.21 – 4.30**.

**Table 4.21: Statistical comparisons of the distribution of apoptotic Panc-1 cells versus the untreated control zero hours post treatment.** Sch = schedule, M = MMF, D = MMF, G = gemcitabine, R = EXBR, ns = not significant.

Comparison	Mode of Cell Death	Summary	P-value
Control vs DMF	Early Apoptosis	ns	0.8774
	Late Apoptosis	ns	0.9962
	Necrosis	ns	0.8733
Control vs MMF	Early Apoptosis	*	0.0223
	Late Apoptosis	ns	0.1261
	Necrosis	ns	>0.9999
Control vs gemcitabine	Early Apoptosis	ns	0.5353
	Late Apoptosis	ns	0.9888
	Necrosis	****	<0.0001
Control vs EXBR	Early Apoptosis	****	<0.0001
	Late Apoptosis	****	<0.0001
	Necrosis	****	<0.0001
Control vs M+R Sch 1	Early Apoptosis	****	<0.0001
	Late Apoptosis	ns	>0.9999
	Necrosis	ns	>0.9999
Control vs M+R Sch 2	Early Apoptosis	****	<0.0001
	Late Apoptosis	**	0.0050
	Necrosis	ns	0.9137
Control vs D+R Sch 2	Early Apoptosis	****	<0.0001
	Late Apoptosis	*	0.0230
	Necrosis	ns	0.6121
Control vs M+G Sch 1	Early Apoptosis	****	<0.0001
	Late Apoptosis	**	0.0021
	Necrosis	ns	0.9512
Control vs M+G Sch 3	Early Apoptosis	****	<0.0001
	Late Apoptosis	****	<0.0001
	Necrosis	ns	0.8097

**Table 4.22: Statistical comparisons of the distribution of apoptotic Panc-1 cells versus monotherapies zero hours post treatment.** Sch = schedule, M = MMF, D = MMF, G = gemcitabine, R = EXBR, ns = not significant.

Comparison	Mode of Cell Death	Summary	P-value
M+R Sch 1 vs MMF	Early Apoptosis	**	0.0039
	Late Apoptosis	ns	>0.9999
	Necrosis	ns	>0.9999
M+R Sch 1 vs EXBR	Early Apoptosis	****	<0.0001
	Late Apoptosis	****	<0.0001
	Necrosis	****	<0.0001
M+R Sch 2 vs MMF	Early Apoptosis	****	<0.0001
	Late Apoptosis	ns	0.5448
	Necrosis	ns	>0.9999
M+R Sch 2 vs EXBR	Early Apoptosis	****	<0.0001
	Late Apoptosis	****	<0.0001
	Necrosis	****	<0.0001
D+R Sch 2 vs DMF	Early Apoptosis	****	<0.0001
	Late Apoptosis	*	0.0387
	Necrosis	****	<0.0001
D+R Sch 2 vs EXBR	Early Apoptosis	****	<0.0001
	Late Apoptosis	****	<0.0001
	Necrosis	ns	0.9641
M+G Sch 1 vs MMF	Early Apoptosis	**	0.0049
	Late Apoptosis	ns	0.3478
	Necrosis	ns	0.6373
M+G Sch 1 vs gemcitabine	Early Apoptosis	****	<0.0001
	Late Apoptosis	***	0.0009
	Necrosis	****	<0.0001
M+G Sch 3 vs MMF	Early Apoptosis	****	<0.0001
	Late Apoptosis	****	<0.0001
	Necrosis	ns	0.9965
M+G Sch 3 vs gemcitabine	Early Apoptosis	****	<0.0001
	Late Apoptosis	****	<0.0001
	Necrosis	****	<0.0001

**Table 4.23: Statistical comparisons of the distribution of apoptotic Panc-1 cells versus the untreated control one hour post treatment.** Sch = schedule, M = MMF, D = MMF, G = gemcitabine, R = EXBR, ns = not significant.

Comparison	Mode of Cell Death	Summary	P-value
Control vs DMF	Early Apoptosis	**	0.0068
	Late Apoptosis	ns	>0.9999
	Necrosis	****	<0.0001
Control vs MMF	Early Apoptosis	****	<0.0001
	Late Apoptosis	****	<0.0001
	Necrosis	ns	0.3386
Control vs gemcitabine	Early Apoptosis	ns	>0.9999
	Late Apoptosis	ns	>0.9999
	Necrosis	***	0.0005
Control vs EXBR	Early Apoptosis	ns	0.4064
	Late Apoptosis	ns	0.9987
	Necrosis	ns	0.4294
Control vs M+R Sch 1	Early Apoptosis	ns	0.9290
	Late Apoptosis	ns	0.9931
	Necrosis	ns	0.3282
Control vs M+R Sch 2	Early Apoptosis	*	0.0112
	Late Apoptosis	ns	0.5838
	Necrosis	ns	0.8082
Control vs D+R Sch 2	Early Apoptosis	ns	0.5320
	Late Apoptosis	ns	0.9943
	Necrosis	ns	0.3133
Control vs M+G Sch 1	Early Apoptosis	****	<0.0001
	Late Apoptosis	****	<0.0001
	Necrosis	ns	0.9433
Control vs M+G Sch 3	Early Apoptosis	***	0.0001
	Late Apoptosis	**	0.0095
	Necrosis	ns	0.9144

**Table 4.24: Statistical comparisons of the distribution of apoptotic Panc-1 cells versus monotherapies one hour post treatment.** Sch = schedule, M = MMF, D = MMF, G = gemcitabine, R = EXBR, ns = not significant.

Comparison	Mode of Cell Death	Summary	P-value
M+R Sch 1 vs MMF	Early Apoptosis	****	<0.0001
	Late Apoptosis	****	<0.0001
	Necrosis	**	0.0087
M+R Sch 1 vs EXBR	Early Apoptosis	ns	0.7682
	Late Apoptosis	ns	0.9746
	Necrosis	ns	0.9975
M+R Sch 2 vs MMF	Early Apoptosis	****	<0.0001
	Late Apoptosis	****	<0.0001
	Necrosis	ns	0.1772
M+R Sch 2 vs EXBR	Early Apoptosis	ns	0.1392
	Late Apoptosis	ns	0.6495
	Necrosis	ns	0.9976
D+R Sch 2 vs DMF	Early Apoptosis	ns	0.1557
	Late Apoptosis	ns	0.9952
	Necrosis	****	<0.0001
D+R Sch 2 vs EXBR	Early Apoptosis	ns	0.9978
	Late Apoptosis	ns	0.9779
	Necrosis	ns	0.9942
M+G Sch 1 vs MMF	Early Apoptosis	****	<0.0001
	Late Apoptosis	ns	0.8919
	Necrosis	ns	0.3592
M+G Sch 1 vs gemcitabine	Early Apoptosis	****	<0.0001
	Late Apoptosis	****	<0.0001
	Necrosis	***	0.0001
M+G Sch 3 vs MMF	Early Apoptosis	****	<0.0001
	Late Apoptosis	**	0.0037
	Necrosis	ns	0.2819
M+G Sch 3 vs gemcitabine	Early Apoptosis	***	0.0001
	Late Apoptosis	*	0.0113
	Necrosis	****	<0.0001

**Table 4.25: Statistical comparisons of the distribution of apoptotic Panc-1 cells versus the untreated control four hours post treatment.** Sch = schedule, M = MMF, D = MMF, G = gemcitabine, R = EXBR, ns = not significant.

Comparison	Mode of Cell Death	Summary	P-value
Control vs DMF	Early Apoptosis	ns	0.7476
	Late Apoptosis	ns	0.2839
	Necrosis	ns	0.9636
Control vs MMF	Early Apoptosis	****	<0.0001
	Late Apoptosis	****	<0.0001
	Necrosis	*	0.0317
Control vs gemcitabine	Early Apoptosis	ns	0.6733
	Late Apoptosis	ns	0.5404
	Necrosis	****	<0.0001
Control vs EXBR	Early Apoptosis	ns	0.6323
	Late Apoptosis	ns	0.5277
	Necrosis	**	0.0016
Control vs M+R Sch 1	Early Apoptosis	ns	0.9982
	Late Apoptosis	ns	0.1759
	Necrosis	ns	>0.9999
Control vs M+R Sch 2	Early Apoptosis	ns	0.2912
	Late Apoptosis	*	0.0208
	Necrosis	ns	0.6551
Control vs D+R Sch 2	Early Apoptosis	ns	0.1480
	Late Apoptosis	ns	0.0725
	Necrosis	***	0.0001
Control vs M+G Sch 1	Early Apoptosis	****	<0.0001
	Late Apoptosis	****	<0.0001
	Necrosis	ns	0.3803
Control vs M+G Sch 3	Early Apoptosis	ns	0.1306
	Late Apoptosis	**	0.0024
	Necrosis	ns	0.9423

**Table 4.26: Statistical comparisons of the distribution of apoptotic Panc-1 cells versus monotherapies four hours post treatment.** Sch = schedule, M = MMF, D = MMF, G = gemcitabine, R = EXBR, ns = not significant.

Comparison	Mode of Cell Death	Summary	P-value
M+R Sch 1 vs MMF	Early Apoptosis	****	<0.0001
	Late Apoptosis	****	<0.0001
	Necrosis	*	0.0343
M+R Sch 1 vs EXBR	Early Apoptosis	ns	0.5265
	Late Apoptosis	**	0.0079
	Necrosis	**	0.0018
M+R Sch 2 vs MMF	Early Apoptosis	****	<0.0001
	Late Apoptosis	****	<0.0001
	Necrosis	ns	0.3024
M+R Sch 2 vs EXBR	Early Apoptosis	*	0.0246
	Late Apoptosis	***	0.0005
	Necrosis	*	0.0294
D+R Sch 2 vs DMF	Early Apoptosis	*	0.0158
	Late Apoptosis	***	0.0007
	Necrosis	***	0.0005
D+R Sch 2 vs EXBR	Early Apoptosis	ns	0.9934
	Late Apoptosis	ns	0.9859
	Necrosis	ns	0.4332
M+G Sch 1 vs MMF	Early Apoptosis	****	<0.0001
	Late Apoptosis	ns	0.9966
	Necrosis	ns	0.8442
M+G Sch 1 vs gemcitabine	Early Apoptosis	****	<0.0001
	Late Apoptosis	****	<0.0001
	Necrosis	****	<0.0001
M+G Sch 3 vs MMF	Early Apoptosis	****	<0.0001
	Late Apoptosis	****	<0.0001
	Necrosis	ns	0.2813
M+G Sch 3 vs gemcitabine	Early Apoptosis	*	0.0104
	Late Apoptosis	****	<0.0001
	Necrosis	****	<0.0001

**Table 4.27: Statistical comparisons of the distribution of apoptotic Panc-1 cells versus the untreated control 24 hours post treatment.** Sch = schedule, M = MMF, D = MMF, G = gemcitabine, R = EXBR, ns = not significant.

Comparison	Mode of Cell Death	Summary	P-value
Control vs DMF	Early Apoptosis	***	0.0003
	Late Apoptosis	ns	0.0774
	Necrosis	ns	0.6749
Control vs MMF	Early Apoptosis	****	<0.0001
	Late Apoptosis	ns	0.1578
	Necrosis	ns	0.9996
Control vs gemcitabine	Early Apoptosis	****	<0.0001
	Late Apoptosis	****	<0.0001
	Necrosis	ns	0.6601
Control vs EXBR	Early Apoptosis	**	0.0063
	Late Apoptosis	ns	0.1730
	Necrosis	ns	>0.9999
Control vs M+R Sch 1	Early Apoptosis	ns	0.9523
	Late Apoptosis	ns	0.9572
	Necrosis	ns	0.7153
Control vs M+R Sch 2	Early Apoptosis	****	<0.0001
	Late Apoptosis	ns	0.7440
	Necrosis	ns	0.8024
Control vs D+R Sch 2	Early Apoptosis	****	<0.0001
	Late Apoptosis	ns	0.2928
	Necrosis	ns	>0.9999
Control vs M+G Sch 1	Early Apoptosis	****	<0.0001
	Late Apoptosis	**	0.0031
	Necrosis	*	0.0430
Control vs M+G Sch 3	Early Apoptosis	ns	0.0724
	Late Apoptosis	ns	0.0699
	Necrosis	ns	>0.9999

**Table 4.28: Statistical comparisons of the distribution of apoptotic Panc-1 cells versus monotherapies 24 hours post treatment.** Sch = schedule, M = MMF, D = MMF, G = gemcitabine, R = EXBR, ns = not significant.

Comparison	Mode of Cell Death	Summary	P-value
M+R Sch 1 vs MMF	Early Apoptosis	****	<0.0001
	Late Apoptosis	ns	0.3663
	Necrosis	ns	0.7753
M+R Sch 1 vs EXBR	Early Apoptosis	*	0.0238
	Late Apoptosis	ns	0.3928
	Necrosis	ns	0.7126
M+R Sch 2 vs MMF	Early Apoptosis	ns	0.7241
	Late Apoptosis	ns	0.7620
	Necrosis	ns	0.8505
M+R Sch 2 vs EXBR	Early Apoptosis	**	0.0068
	Late Apoptosis	ns	0.7870
	Necrosis	ns	0.8001
D+R Sch 2 vs DMF	Early Apoptosis	ns	0.1663
	Late Apoptosis	ns	0.8916
	Necrosis	ns	0.6896
D+R Sch 2 vs EXBR	Early Apoptosis	*	0.0296
	Late Apoptosis	ns	0.9628
	Necrosis	ns	>0.9999
M+G Sch 1 vs MMF	Early Apoptosis	ns	0.9293
	Late Apoptosis	ns	0.3076
	Necrosis	ns	0.0540
M+G Sch 1 vs gemcitabine	Early Apoptosis	****	<0.0001
	Late Apoptosis	**	0.0020
	Necrosis	ns	0.3807
M+G Sch 3 vs MMF	Early Apoptosis	ns	0.3569
	Late Apoptosis	ns	0.4381
	Necrosis	ns	>0.9999
M+G Sch 3 vs gemcitabine	Early Apoptosis	****	<0.0001
	Late Apoptosis	****	<0.0001
	Necrosis	***	0.0001

**Table 4.29: Statistical comparisons of the distribution of apoptotic Panc-1 cells versus the untreated control 36 hours post treatment.** Sch = schedule, M = MMF, D = MMF, G = gemcitabine, R = EXBR, ns = not significant.

Comparison	Mode of Cell Death	Summary	P-value
Control vs DMF	Early Apoptosis	ns	0.5410
	Late Apoptosis	***	0.0002
	Necrosis	ns	0.5575
Control vs MMF	Early Apoptosis	***	0.0006
	Late Apoptosis	**	0.0013
	Necrosis	ns	0.9942
Control vs gemcitabine	Early Apoptosis	****	<0.0001
	Late Apoptosis	****	<0.0001
	Necrosis	ns	0.9747
Control vs EXBR	Early Apoptosis	ns	0.8615
	Late Apoptosis	ns	0.8640
	Necrosis	ns	0.9995
Control vs M+R Sch 1	Early Apoptosis	ns	0.3130
	Late Apoptosis	****	<0.0001
	Necrosis	ns	0.7693
Control vs M+R Sch 2	Early Apoptosis	ns	0.3667
	Late Apoptosis	****	<0.0001
	Necrosis	ns	0.1001
Control vs D+R Sch 2	Early Apoptosis	ns	0.4007
	Late Apoptosis	****	<0.0001
	Necrosis	ns	0.3883
Control vs M+G Sch 1	Early Apoptosis	***	0.0005
	Late Apoptosis	ns	0.4281
	Necrosis	ns	0.9990
Control vs M+G Sch 3	Early Apoptosis	ns	0.2873
	Late Apoptosis	**	0.0015
	Necrosis	ns	0.2362

**Table 4.30: Statistical comparisons of the distribution of apoptotic Panc-1 cells versus monotherapies 36 hours post treatment.** Sch = schedule, M = MMF, D = MMF, G = gemcitabine, R = EXBR, ns = not significant.

Comparison	Mode of Cell Death	Summary	P-value
M+R Sch 1 vs MMF	Early Apoptosis	ns	0.0565
	Late Apoptosis	ns	0.7492
	Necrosis	ns	0.8913
M+R Sch 1 vs EXBR	Early Apoptosis	ns	0.7660
	Late Apoptosis	***	0.0007
	Necrosis	ns	0.8280
M+R Sch 2 vs MMF	Early Apoptosis	ns	0.0710
	Late Apoptosis	*	0.0119
	Necrosis	ns	0.1608
M+R Sch 2 vs EXBR	Early Apoptosis	ns	0.8032
	Late Apoptosis	****	<0.0001
	Necrosis	ns	0.1241
D+R Sch 2 vs DMF	Early Apoptosis	ns	0.9951
	Late Apoptosis	ns	0.9265
	Necrosis	ns	0.4462
D+R Sch 2 vs EXBR	Early Apoptosis	ns	0.8226
	Late Apoptosis	***	0.0003
	Necrosis	ns	0.9914
M+G Sch 1 vs MMF	Early Apoptosis	ns	0.9907
	Late Apoptosis	ns	0.0946
	Necrosis	ns	0.9996
M+G Sch 1 vs gemcitabine	Early Apoptosis	****	<0.0001
	Late Apoptosis	**	0.0023
	Necrosis	ns	0.9923
M+G Sch 3 vs MMF	Early Apoptosis	ns	0.3383
	Late Apoptosis	ns	0.8659
	Necrosis	ns	0.3267
M+G Sch 3 vs gemcitabine	Early Apoptosis	****	<0.0001
	Late Apoptosis	ns	0.9599
	Necrosis	ns	0.4049

### Summary of apoptosis analysis in Panc-1

The schedule 1 combination of 0.6  $\mu$ M MMF + 0.5 Gy EXBR induced a low level of apoptosis in Panc-1 cells initially post treatment, however as time progressed the combination did not appear to induce apoptosis until the final time point at 36 hours post treatment, suggesting an alternative mechanism of cell death is at play. MMF monotherapy induced apoptosis, which continued to increase as the time course progressed, however by 36 hours post treatment the number of apoptotic cells began

to decrease. Initially EXBR alone induced a significant level of apoptosis, however this decreased as the time course progressed. Overall, in these experiments, the single agents induced more apoptosis than the combination.

Overall, the schedule 1 combination of MMF + gemcitabine induced apoptosis in Panc-1 cell line from zero hours post treatment to 24 hours post treatment, however the population of apoptotic cells began to decline at the 36-hour post treatment timepoint, indicating the late apoptotic cells previously seen have been eliminated from the population of cells. MMF monotherapy induced apoptosis, which continued to increase as the time course progressed, however by 36 hours post treatment the number of apoptotic cells began to decrease. Initially EXBR alone induced significant apoptosis, however this decreased as the time course progressed. Overall, the combination induced more apoptosis than the single agents until 24 hours post treatment, where gemcitabine induced more apoptosis than the combination.

Overall, the schedule 2 combination of 0.6  $\mu$ M MMF + 0.5 Gy EXBR induced apoptosis immediately post treatment, which decreased between one to four hours post treatment, indicating the apoptotic population of cells had been eliminated. However, from 24 to 36 hours post treatment the combination began to induce apoptosis once again, indicating the combination is inducing cell death. Initially EXBR alone induced higher levels of apoptosis, however this decreased as the time course progressed. MMF monotherapy induced apoptosis, which continued to increase as the time course progressed, however by 36 hours post treatment the number of apoptotic cells began to decrease. The combination overall did not induce more apoptosis than the single agents and would therefore not be considered as a promising treatment strategy based on this result.

Overall, the schedule 2 combination of 20  $\mu$ M DMF + 0.5 Gy EXBR induced a low level of apoptosis in the Panc-1 cell line when compared with the untreated control.

However, DMF monotherapy was just as effective at inducing apoptosis as the combination and EXBR alone initially induced a great deal of apoptosis, however this decreased as the time course progressed.

The schedule 3 combination of MMF + gemcitabine induced apoptosis in the Panc-1 cell line when compared to the untreated control, which increased as the time course progressed. Gemcitabine monotherapy initially induced necrosis, however 24 hours post treatment it began to induce apoptosis when compared with the untreated control. MMF monotherapy induced apoptosis when compared with the untreated control, which continued to increase as the time course progressed, however by 36 hours post treatment the number of apoptotic cells began to decrease. Overall, gemcitabine monotherapy induced more apoptosis than the combination, suggesting the combination was of no additional benefit.

To investigate if the selected combinations were inducing cell death via apoptosis in the Mia PaCa-2 cell line, the apoptosis assay was carried out as described in **section 4.3.4**, and the results presented in **figure 4.4**.

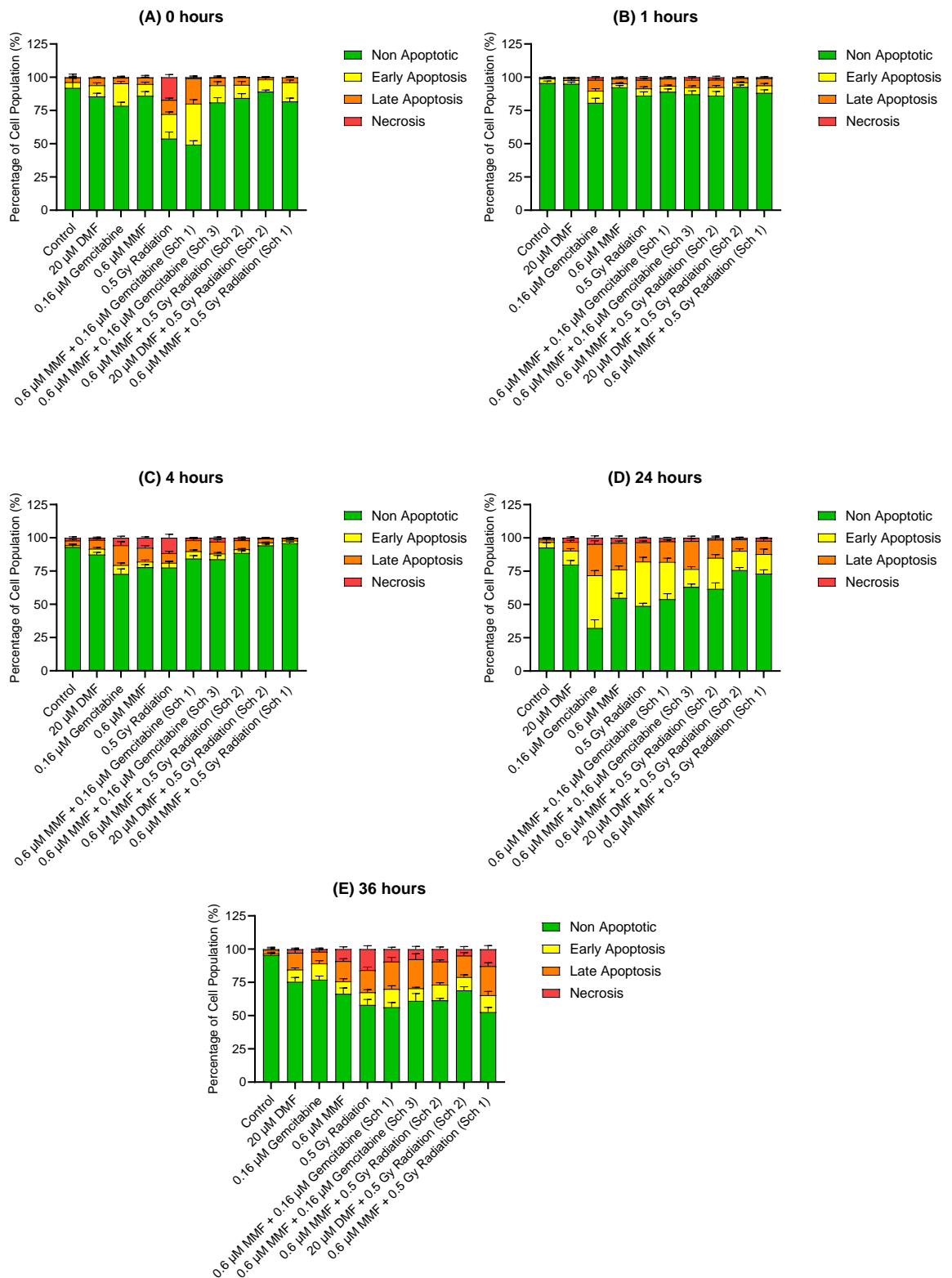


**Figure 4.4: Apoptosis analysis of combination therapies in Mia PaCa-2.** Cells were incubated and harvested at specific time points post treatment before undergoing flow cytometry to determine the stage of apoptosis. (A) Distribution of cells 0 hours post treatment. (B) Distribution of cells 1 hour post treatment. (C) Distribution of cells 4 hours post treatment. (D) Distribution of cells 24 hours post treatment. (E) Distribution of cells 36 hours post treatment. All data is represented as an average of three independent experiments  $\pm$  the standard deviation.

As can be seen in **figure 4.4A**, in Mia PaCa-2 cells 0.16  $\mu\text{M}$  gemcitabine, 0.5 Gy EXBR, 0.6  $\mu\text{M}$  MMF + 0.5 Gy EXBR (Schedule 1), 0.6  $\mu\text{M}$  MMF + 0.16  $\mu\text{M}$  gemcitabine (Schedule 1), and 0.6  $\mu\text{M}$  MMF + 0.16  $\mu\text{M}$  gemcitabine (Schedule 3) induced a statistically significant increase in the number of early apoptotic cells when compared with the untreated control zero hours post treatment ( $P \leq 0.0032$ ). When looking at late apoptosis, only 0.5 Gy EXBR and 0.6  $\mu\text{M}$  MMF + 0.16  $\mu\text{M}$  gemcitabine (Schedule 1) induced a statistically significant increase in the number of late apoptotic cells when compared with the untreated control zero hours post treatment ( $P \leq 0.0270$ ). Only 0.5 Gy EXBR induced a statistically significant increase in the number of necrotic cells when compared with the untreated control zero hours post treatment ( $P < 0.0001$ ).

As can be seen in **figure 4.4B**, in Mia PaCa-2 cells only 0.16  $\mu\text{M}$  gemcitabine induced a statistically significant increase in the number of early apoptotic cells when compared with the untreated control one hour post treatment ( $P < 0.0001$ ). When looking at late apoptosis, 0.6  $\mu\text{M}$  MMF, 0.5 Gy EXBR, 0.16  $\mu\text{M}$  gemcitabine, 0.6  $\mu\text{M}$  MMF + 0.5 Gy EXBR (Schedule 1), 0.6  $\mu\text{M}$  MMF + 0.5 Gy EXBR (Schedule 2), 0.6  $\mu\text{M}$  MMF + 0.16  $\mu\text{M}$  gemcitabine (Schedule 1), and 0.6  $\mu\text{M}$  MMF + 0.16  $\mu\text{M}$  gemcitabine (Schedule 3) induced a statistically significant increase in the number of late apoptotic cells when compared with the untreated control one hour post treatment ( $P \leq 0.0161$ ). No treatments induced a statistically significant change in the number of necrotic cells when compared with the untreated control one hour post treatment ( $P \geq 0.4087$ ).

As can be seen in **figure 4.4C**, in Mia PaCa-2 cells 0.16  $\mu\text{M}$  gemcitabine and 0.6  $\mu\text{M}$  MMF + 0.16  $\mu\text{M}$  gemcitabine (Schedule 1) induced a statistically significant increase in the number of early apoptotic cells when compared with the untreated control four hours post treatment ( $P \leq 0.0322$ ). When looking at late apoptosis, 0.6  $\mu\text{M}$  MMF, 0.16

$\mu\text{M}$  gemcitabine,  $0.6 \mu\text{M}$  MMF +  $0.16 \mu\text{M}$  gemcitabine (Schedule 1), and  $0.6 \mu\text{M}$  MMF +  $0.16 \mu\text{M}$  gemcitabine (Schedule 3) induced a statistically significant increase in the number of late apoptotic cells when compared with the untreated control four hours post treatment ( $P \leq 0.0110$ ). When looking at necrosis,  $0.6 \mu\text{M}$  MMF and  $0.5 \text{ Gy}$  EXBR induced a statistically significant increase in the number of necrotic cells when compared with the untreated control four hours post treatment ( $P \leq 0.0038$ ).

As can be seen in **figure 4.4D**, in Mia PaCa-2 cells  $0.6 \mu\text{M}$  MMF,  $0.5 \text{ Gy}$  EXBR,  $0.16 \mu\text{M}$  gemcitabine,  $0.6 \mu\text{M}$  MMF +  $0.5 \text{ Gy}$  EXBR (Schedule 1),  $0.6 \mu\text{M}$  MMF +  $0.5 \text{ Gy}$  EXBR (Schedule 2),  $0.6 \mu\text{M}$  MMF +  $0.16 \mu\text{M}$  gemcitabine (Schedule 1), and  $0.6 \mu\text{M}$  MMF +  $0.16 \mu\text{M}$  gemcitabine (Schedule 3) induced an increase in the number of early apoptotic cells when compared with the untreated control 24 hours post treatment ( $P \leq 0.0006$ ). When looking at late apoptosis,  $0.6 \mu\text{M}$  MMF,  $0.5 \text{ Gy}$  EXBR,  $0.16 \mu\text{M}$  gemcitabine,  $0.6 \mu\text{M}$  MMF +  $0.5 \text{ Gy}$  EXBR (Schedule 1),  $0.6 \mu\text{M}$  MMF +  $0.5 \text{ Gy}$  EXBR (Schedule 2),  $0.6 \mu\text{M}$  MMF +  $0.16 \mu\text{M}$  gemcitabine (Schedule 1), and  $0.6 \mu\text{M}$  MMF +  $0.16 \mu\text{M}$  gemcitabine (Schedule 3) induced an increase in the number of late apoptotic cells when compared with the untreated control 24 hours post treatment ( $P \leq 0.0006$ ). No treatments induced a statistically significant change in the number of necrotic cells when compared with the untreated control 24 hours post treatment ( $P \geq 0.4694$ ).

As can be seen in **figure 4.4E**, in Mia PaCa-2 cells  $0.6 \mu\text{M}$  MMF,  $0.5 \text{ Gy}$  EXBR,  $0.16 \mu\text{M}$  gemcitabine,  $0.6 \mu\text{M}$  MMF +  $0.5 \text{ Gy}$  EXBR (Schedule 1),  $0.6 \mu\text{M}$  MMF +  $0.5 \text{ Gy}$  EXBR (Schedule 2),  $0.6 \mu\text{M}$  MMF +  $0.16 \mu\text{M}$  gemcitabine (Schedule 1),  $0.6 \mu\text{M}$  MMF +  $0.16 \mu\text{M}$  gemcitabine (Schedule 3), and  $20 \mu\text{M}$  DMF +  $0.5 \text{ Gy}$  EXBR (Schedule 2) induced an increase in the number of early apoptotic cells when compared with the untreated control 36 hours post treatment ( $P \leq 0.0018$ ). When looking at late apoptosis,  $0.6 \mu\text{M}$  MMF,  $0.5 \text{ Gy}$  EXBR,  $0.16 \mu\text{M}$  gemcitabine,  $0.6 \mu\text{M}$  MMF +  $0.5 \text{ Gy}$  EXBR (Schedule 1),  $0.6 \mu\text{M}$  MMF +  $0.5 \text{ Gy}$  EXBR (Schedule 2),  $0.6$

$\mu\text{M}$  MMF + 0.16  $\mu\text{M}$  gemcitabine (Schedule 1), 0.6  $\mu\text{M}$  MMF + 0.16  $\mu\text{M}$  gemcitabine (Schedule 3), and 20  $\mu\text{M}$  DMF + 0.5 Gy EXBR (Schedule 2) induced an increase in the number of late apoptotic cells when compared with the untreated control 36 hours post treatment ( $P \leq 0.0173$ ). When looking at necrosis, 0.6  $\mu\text{M}$  MMF, 0.5 Gy EXBR, 0.16  $\mu\text{M}$  gemcitabine, 0.6  $\mu\text{M}$  MMF + 0.5 Gy EXBR (Schedule 1), 0.6  $\mu\text{M}$  MMF + 0.5 Gy EXBR (Schedule 2), and 0.6  $\mu\text{M}$  MMF + 0.16  $\mu\text{M}$  gemcitabine (Schedule 3) induced a statistically significant increase in the number of necrotic cells when compared with the untreated control 36 hours post treatment ( $P \leq 0.0090$ ).

A summary of all statistical comparisons carried out between the untreated control and therapies, and between combination therapies and individual components over the time course in Mia PaCa-2 cells following two-way ANOVA with Bonferroni post hoc test can be found in **tables 4.31 – 4.40**.

**Table 4.31: Statistical comparisons of the distribution of apoptotic Mia PaCa-2 cells versus the untreated control zero hours post treatment.** Sch = schedule, M = MMF, D = MMF, G = gemcitabine, R = EXBR, ns = not significant.

Comparison	Mode of Cell Death	Summary	P-value
Control vs DMF	Early Apoptosis	ns	0.2835
	Late Apoptosis	ns	0.2835
	Necrosis	ns	0.9997
Control vs MMF	Early Apoptosis	ns	0.3776
	Late Apoptosis	ns	>0.9999
	Necrosis	ns	>0.9999
Control vs gemcitabine	Early Apoptosis	****	<0.0001
	Late Apoptosis	ns	0.9937
	Necrosis	ns	0.9998
Control vs EXBR	Early Apoptosis	****	<0.0001
	Late Apoptosis	*	0.0270
	Necrosis	****	<0.0001
Control vs M+R Sch 1	Early Apoptosis	***	0.0008
	Late Apoptosis	ns	>0.9999
	Necrosis	ns	>0.9999
Control vs M+R Sch 2	Early Apoptosis	ns	0.1154
	Late Apoptosis	ns	0.8117
	Necrosis	ns	>0.9999
Control vs D+R Sch 2	Early Apoptosis	ns	0.1548
	Late Apoptosis	ns	0.8345
	Necrosis	ns	0.9998
Control vs M+G Sch 1	Early Apoptosis	****	<0.0001
	Late Apoptosis	****	<0.0001
	Necrosis	ns	0.9954
Control vs M+G Sch 3	Early Apoptosis	**	0.0032
	Late Apoptosis	ns	0.7642
	Necrosis	ns	>0.9999

**Table 4.32: Statistical comparisons of the distribution of apoptotic Mia PaCa-2 cells versus monotherapies zero hours post treatment.** Sch = schedule, M = MMF, D = MMF, G = gemcitabine, R = EXBR, ns = not significant.

Comparison	Mode of Cell Death	Summary	P-value
M+R Sch 1 vs MMF	Early Apoptosis	ns	0.1364
	Late Apoptosis	ns	>0.9999
	Necrosis	ns	>0.9999
M+R Sch 1 vs EXBR	Early Apoptosis	ns	0.6237
	Late Apoptosis	*	0.0331
	Necrosis	****	<0.0001
M+R Sch 2 vs MMF	Early Apoptosis	ns	0.9711
	Late Apoptosis	ns	0.9842
	Necrosis	ns	0.9996
M+R Sch 2 vs EXBR	Early Apoptosis	**	0.0068
	Late Apoptosis	ns	0.1779
	Necrosis	****	<0.0001
D+R Sch 2 vs DMF	Early Apoptosis	ns	0.9854
	Late Apoptosis	ns	0.2978
	Necrosis	ns	0.9983
D+R Sch 2 vs EXBR	Early Apoptosis	**	0.0014
	Late Apoptosis	**	0.0017
	Necrosis	****	<0.0001
M+G Sch 1 vs MMF	Early Apoptosis	****	<0.0001
	Late Apoptosis	****	<0.0001
	Necrosis	ns	0.9973
M+G Sch 1 vs gemcitabine	Early Apoptosis	****	<0.0001
	Late Apoptosis	****	<0.0001
	Necrosis	ns	0.9988
M+G Sch 3 vs MMF	Early Apoptosis	ns	0.2871
	Late Apoptosis	ns	0.9762
	Necrosis	ns	>0.9999
M+G Sch 3 vs gemcitabine	Early Apoptosis	ns	0.3171
	Late Apoptosis	ns	0.8894
	Necrosis	ns	>0.9999

**Table 4.33: Statistical comparisons of the distribution of apoptotic Mia PaCa-2 cells versus the untreated control one hour post treatment.** Sch = schedule, M = MMF, D = MMF, G = gemcitabine, R = EXBR, ns = not significant.

Comparison	Mode of Cell Death	Summary	P-value
Control vs DMF	Early Apoptosis	ns	0.8886
	Late Apoptosis	ns	0.6607
	Necrosis	ns	0.9992
Control vs MMF	Early Apoptosis	ns	0.9818
	Late Apoptosis	*	0.0289
	Necrosis	ns	0.9266
Control vs gemcitabine	Early Apoptosis	****	<0.0001
	Late Apoptosis	****	<0.0001
	Necrosis	ns	0.5014
Control vs EXBR	Early Apoptosis	ns	0.1946
	Late Apoptosis	****	<0.0001
	Necrosis	ns	0.4087
Control vs M+R Sch 1	Early Apoptosis	ns	0.1214
	Late Apoptosis	***	0.0003
	Necrosis	ns	0.9876
Control vs M+R Sch 2	Early Apoptosis	ns	0.0525
	Late Apoptosis	***	0.0006
	Necrosis	ns	0.5352
Control vs D+R Sch 2	Early Apoptosis	ns	0.9996
	Late Apoptosis	*	0.0211
	Necrosis	ns	0.9971
Control vs M+G Sch 1	Early Apoptosis	ns	0.7540
	Late Apoptosis	***	0.0006
	Necrosis	ns	0.9505
Control vs M+G Sch 3	Early Apoptosis	ns	0.3880
	Late Apoptosis	***	0.0006
	Necrosis	ns	0.6121

**Table 4.34: Statistical comparisons of the distribution of apoptotic Mia PaCa-2 cells versus monotherapies one hour post treatment.** Sch = schedule, M = MMF, D = MMF, G = gemcitabine, R = EXBR, ns = not significant.

Comparison	Mode of Cell Death	Summary	P-value
M+R Sch 1 vs MMF	Early Apoptosis	ns	0.0552
	Late Apoptosis	ns	0.3530
	Necrosis	ns	0.9916
M+R Sch 1 vs EXBR	Early Apoptosis	ns	0.9944
	Late Apoptosis	ns	0.7534
	Necrosis	ns	0.6046
M+R Sch 2 vs MMF	Early Apoptosis	*	0.0236
	Late Apoptosis	ns	0.3236
	Necrosis	ns	0.8576
M+R Sch 2 vs EXBR	Early Apoptosis	ns	0.8469
	Late Apoptosis	ns	0.8898
	Necrosis	ns	0.9998
D+R Sch 2 vs DMF	Early Apoptosis	ns	0.9253
	Late Apoptosis	ns	0.2385
	Necrosis	ns	0.9999
D+R Sch 2 vs EXBR	Early Apoptosis	ns	0.0990
	Late Apoptosis	*	0.0144
	Necrosis	ns	0.4130
M+G Sch 1 vs MMF	Early Apoptosis	ns	0.5434
	Late Apoptosis	ns	0.3581
	Necrosis	ns	>0.9999
M+G Sch 1 vs gemcitabine	Early Apoptosis	**	0.0012
	Late Apoptosis	ns	0.0818
	Necrosis	ns	0.8156
M+G Sch 3 vs MMF	Early Apoptosis	ns	0.2317
	Late Apoptosis	ns	0.2827
	Necrosis	ns	0.9017
M+G Sch 3 vs gemcitabine	Early Apoptosis	*	0.0118
	Late Apoptosis	ns	0.1671
	Necrosis	ns	0.9995

**Table 4.35: Statistical comparisons of the distribution of apoptotic Mia PaCa-2 cells versus the untreated control four hours post treatment.** Sch = schedule, M = MMF, D = MMF, G = gemcitabine, R = EXBR, ns = not significant.

Comparison	Mode of Cell Death	Summary	P-value
Control vs DMF	Early Apoptosis	ns	0.1430
	Late Apoptosis	ns	0.1228
	Necrosis	ns	0.9786
Control vs MMF	Early Apoptosis	ns	0.1902
	Late Apoptosis	***	0.0002
	Necrosis	**	0.0038
Control vs gemcitabine	Early Apoptosis	**	0.0039
	Late Apoptosis	****	<0.0001
	Necrosis	ns	0.0784
Control vs EXBR	Early Apoptosis	ns	0.4480
	Late Apoptosis	ns	0.0603
	Necrosis	****	<0.0001
Control vs M+R Sch 1	Early Apoptosis	ns	0.9603
	Late Apoptosis	ns	0.5870
	Necrosis	ns	0.6407
Control vs M+R Sch 2	Early Apoptosis	ns	0.7446
	Late Apoptosis	ns	0.1457
	Necrosis	ns	0.9992
Control vs D+R Sch 2	Early Apoptosis	ns	0.9300
	Late Apoptosis	ns	0.9802
	Necrosis	ns	0.6957
Control vs M+G Sch 1	Early Apoptosis	*	0.0322
	Late Apoptosis	*	0.0110
	Necrosis	ns	0.9994
Control vs M+G Sch 3	Early Apoptosis	ns	0.2114
	Late Apoptosis	**	0.0048
	Necrosis	ns	0.9367

**Table 4.36: Statistical comparisons of the distribution of apoptotic Mia PaCa-2 cells versus monotherapies four hours post treatment.** Sch = schedule, M = MMF, D = MMF, G = gemcitabine, R = EXBR, ns = not significant.

Comparison	Mode of Cell Death	Summary	P-value
M+R Sch 1 vs MMF	Early Apoptosis	****	<0.0001
	Late Apoptosis	ns	0.4143
	Necrosis	****	<0.0001
M+R Sch 1 vs EXBR	Early Apoptosis	****	<0.0001
	Late Apoptosis	ns	0.7448
	Necrosis	**	0.0025
M+R Sch 2 vs MMF	Early Apoptosis	ns	0.7558
	Late Apoptosis	ns	0.0788
	Necrosis	**	0.0034
M+R Sch 2 vs EXBR	Early Apoptosis	ns	0.9685
	Late Apoptosis	ns	0.9836
	Necrosis	****	<0.0001
D+R Sch 2 vs DMF	Early Apoptosis	ns	0.3913
	Late Apoptosis	ns	0.0545
	Necrosis	ns	0.8971
D+R Sch 2 vs EXBR	Early Apoptosis	ns	0.7767
	Late Apoptosis	*	0.0196
	Necrosis	****	<0.0001
M+G Sch 1 vs MMF	Early Apoptosis	ns	0.8453
	Late Apoptosis	ns	0.4190
	Necrosis	**	0.0024
M+G Sch 1 vs gemcitabine	Early Apoptosis	ns	0.8371
	Late Apoptosis	***	0.0003
	Necrosis	ns	0.0608
M+G Sch 3 vs MMF	Early Apoptosis	ns	>0.9999
	Late Apoptosis	ns	0.7297
	Necrosis	*	0.0219
M+G Sch 3 vs gemcitabine	Early Apoptosis	ns	0.3990
	Late Apoptosis	**	0.0017
	Necrosis	ns	0.2833

**Table 4.37: Statistical comparisons of the distribution of apoptotic Mia PaCa-2 cells versus the untreated control 24 hours post treatment.** Sch = schedule, M = MMF, D = MMF, G = gemcitabine, R = EXBR, ns = not significant.

Comparison	Mode of Cell Death	Summary	P-value
Control vs DMF	Early Apoptosis	ns	0.1430
	Late Apoptosis	ns	0.1228
	Necrosis	ns	0.9786
Control vs MMF	Early Apoptosis	****	<0.0001
	Late Apoptosis	****	<0.0001
	Necrosis	ns	0.5073
Control vs gemcitabine	Early Apoptosis	****	<0.0001
	Late Apoptosis	****	<0.0001
	Necrosis	ns	0.4694
Control vs EXBR	Early Apoptosis	****	<0.0001
	Late Apoptosis	****	<0.0001
	Necrosis	ns	0.6481
Control vs M+R Sch 1	Early Apoptosis	****	<0.0001
	Late Apoptosis	***	0.0006
	Necrosis	ns	0.9485
Control vs M+R Sch 2	Early Apoptosis	****	<0.0001
	Late Apoptosis	****	<0.0001
	Necrosis	ns	0.9998
Control vs D+R Sch 2	Early Apoptosis	ns	0.9300
	Late Apoptosis	ns	0.9802
	Necrosis	ns	0.6957
Control vs M+G Sch 1	Early Apoptosis	****	<0.0001
	Late Apoptosis	****	<0.0001
	Necrosis	ns	0.9321
Control vs M+G Sch 3	Early Apoptosis	***	0.0007
	Late Apoptosis	****	<0.0001
	Necrosis	ns	0.9418

**Table 4.38: Statistical comparisons of the distribution of apoptotic Mia PaCa-2 cells versus monotherapies 24 hours post treatment.** Sch = schedule, M = MMF, D = MMF, G = gemcitabine, R = EXBR, ns = not significant.

Comparison	Mode of Cell Death	Summary	P-value
M+R Sch 1 vs MMF	Early Apoptosis	**	0.0046
	Late Apoptosis	****	<0.0001
	Necrosis	ns	0.8242
M+R Sch 1 vs EXBR	Early Apoptosis	****	<0.0001
	Late Apoptosis	ns	0.0887
	Necrosis	ns	0.9208
M+R Sch 2 vs MMF	Early Apoptosis	ns	0.7689
	Late Apoptosis	*	0.0142
	Necrosis	ns	0.5992
M+R Sch 2 vs EXBR	Early Apoptosis	****	<0.0001
	Late Apoptosis	ns	0.9802
	Necrosis	ns	0.7304
D+R Sch 2 vs DMF	Early Apoptosis	ns	0.3913
	Late Apoptosis	ns	0.0545
	Necrosis	ns	0.8971
D+R Sch 2 vs EXBR	Early Apoptosis	ns	0.7767
	Late Apoptosis	*	0.0196
	Necrosis	****	<0.0001
M+G Sch 1 vs MMF	Early Apoptosis	*	0.0317
	Late Apoptosis	ns	0.2256
	Necrosis	ns	0.9512
M+G Sch 1 vs gemcitabine	Early Apoptosis	****	<0.0001
	Late Apoptosis	**	0.0059
	Necrosis	ns	0.8211
M+G Sch 3 vs MMF	Early Apoptosis	***	0.0007
	Late Apoptosis	****	<0.0001
	Necrosis	ns	0.9418
M+G Sch 3 vs gemcitabine	Early Apoptosis	****	<0.0001
	Late Apoptosis	ns	0.6027
	Necrosis	ns	0.7438

**Table 4.39: Statistical comparisons of the distribution of apoptotic Mia PaCa-2 cells versus the untreated control 36 hours post treatment.** Sch = schedule, M = MMF, D = MMF, G = gemcitabine, R = EXBR, ns = not significant.

Comparison	Mode of Cell Death	Summary	P-value
Control vs DMF	Early Apoptosis	***	0.0004
	Late Apoptosis	****	<0.0001
	Necrosis	ns	0.5865
Control vs MMF	Early Apoptosis	**	0.0018
	Late Apoptosis	****	<0.0001
	Necrosis	**	0.0015
Control vs gemcitabine	Early Apoptosis	****	<0.0001
	Late Apoptosis	*	0.0173
	Necrosis	ns	0.8584
Control vs EXBR	Early Apoptosis	**	0.0018
	Late Apoptosis	****	<0.0001
	Necrosis	****	<0.0001
Control vs M+R Sch 1	Early Apoptosis	****	<0.0001
	Late Apoptosis	****	<0.0001
	Necrosis	****	<0.0001
Control vs M+R Sch 2	Early Apoptosis	****	<0.0001
	Late Apoptosis	****	<0.0001
	Necrosis	***	0.0002
Control vs D+R Sch 2	Early Apoptosis	***	0.0001
	Late Apoptosis	****	<0.0001
	Necrosis	ns	0.0930
Control vs M+G Sch 1	Early Apoptosis	****	<0.0001
	Late Apoptosis	****	<0.0001
	Necrosis	***	0.0002
Control vs M+G Sch 3	Early Apoptosis	**	0.0016
	Late Apoptosis	****	<0.0001
	Necrosis	**	0.0090

**Table 4.40: Statistical comparisons of the distribution of apoptotic Mia PaCa-2 cells versus monotherapies 36 hours post treatment.** Sch = schedule, M = MMF, D = MMF, G = gemcitabine, R = EXBR, ns = not significant.

Comparison	Mode of Cell Death	Summary	P-value
M+R Sch 1 vs MMF	Early Apoptosis	ns	0.3940
	Late Apoptosis	*	0.0163
	Necrosis	ns	0.2814
M+R Sch 1 vs EXBR	Early Apoptosis	ns	0.3958
	Late Apoptosis	ns	0.0819
	Necrosis	ns	0.4798
M+R Sch 2 vs MMF	Early Apoptosis	ns	0.5819
	Late Apoptosis	ns	0.6316
	Necrosis	ns	0.9977
M+R Sch 2 vs EXBR	Early Apoptosis	ns	0.5842
	Late Apoptosis	ns	0.9787
	Necrosis	**	0.0058
D+R Sch 2 vs DMF	Early Apoptosis	ns	0.9669
	Late Apoptosis	ns	0.2232
	Necrosis	ns	0.6620
D+R Sch 2 vs EXBR	Early Apoptosis	ns	0.9868
	Late Apoptosis	ns	0.9882
	Necrosis	****	<0.0001
M+G Sch 1 vs MMF	Early Apoptosis	ns	0.1108
	Late Apoptosis	*	0.0291
	Necrosis	ns	0.9980
M+G Sch 1 vs gemcitabine	Early Apoptosis	ns	0.8318
	Late Apoptosis	****	<0.0001
	Necrosis	**	0.0019
M+G Sch 3 vs MMF	Early Apoptosis	ns	>0.9999
	Late Apoptosis	*	0.0165
	Necrosis	ns	0.9096
M+G Sch 3 vs gemcitabine	Early Apoptosis	ns	0.5804
	Late Apoptosis	****	<0.0001
	Necrosis	*	0.0494

### Summary of apoptosis analysis in Mia PaCa-2

Overall, the schedule 1 combination of 0.6  $\mu$ M MMF + 0.5 Gy EXBR induced apoptosis in Mia PaCa-2 cells, which transitioned from early apoptosis in the earlier timepoints to late apoptosis and necrosis by the final 36 hours post treatment timepoint, suggesting cells continued to undergo apoptosis post treatment. MMF monotherapy induced apoptosis, which continued to increase as the time course progressed, and 4 hours post treatment MMF began to induce necrosis. EXBR

alone initially induced apoptosis and necrosis, which increased as the time course progressed. However, the combination did not induce more apoptosis or necrosis than either single agent alone overall.

Overall, the schedule 1 combination of 0.6  $\mu\text{M}$  MMF + 0.16  $\mu\text{M}$  gemcitabine induced apoptosis in the Mia PaCa-2 cell line, which continued to increase over the time course and necrosis began to occur by 36 hours post treatment. MMF induced apoptosis, which continued to increase as the time course progressed, and 4 hours post treatment it began to induce necrosis. Gemcitabine continued to induce apoptosis until 36 hours post treatment, where the number of apoptotic cells began to decrease. Overall, the combination induced more apoptosis than both single agents overall by the time 36 hours post treatment was reached suggesting the combination is of additional benefit as hypothesised.

Overall, the schedule 2 combination of 0.6  $\mu\text{M}$  MMF + 0.5 Gy EXBR induced more apoptosis than the untreated control in the Mia PaCa-2 cell line, which increased as the time course progressed and led to necrosis 36 hours post treatment. MMF induced apoptosis, which continued to increase as the time course progressed, and 4 hours post treatment it began to induce necrosis. EXBR alone initially induced apoptosis and necrosis, which increased as the time course progressed. The combination overall did not induce more apoptosis/necrosis than EXBR alone, suggesting the combination was of no additional benefit.

The schedule 2 combination of 20  $\mu\text{M}$  DMF + 0.5 Gy EXBR initially induced apoptosis in the Mia PaCa-2 cell line immediately post treatment, however the number of apoptotic cells decreased until 36 hours post treatment when the number of apoptotic cells again began to increase when compared with the untreated control. EXBR alone initially induced apoptosis and necrosis, which increased as the time course progressed compared with the untreated control. DMF monotherapy

induced apoptosis, which increased as the time course progressed when compared with the untreated control. Overall, the combination did not induce more apoptosis than EXBR alone, indicating the combination was of no additional benefit when compared with the EXBR alone.

Overall, the schedule 1 combination of 0.6  $\mu$ M MMF + 0.16  $\mu$ M gemcitabine induced apoptosis in the Mia PaCa-2 cell line, which increased as the time course progressed, with the greatest amount of apoptosis induced 36 hours post treatment. MMF induced apoptosis, which continued to increase as the time course progressed, and 4 hours post treatment it began to induce necrosis. Gemcitabine continued to induce apoptosis until 36 hours post treatment, where the number of apoptotic cells began to decrease. The combination induced more apoptosis overall than both single agents.

#### **4.4.3: DNA damage studies on developed combinations**

To investigate if the selected combinations were inducing DNA damage in the Panc-1 cell line, the comet assay was carried out as described in **section 4.3.5**, and the results presented in **figure 4.5**.

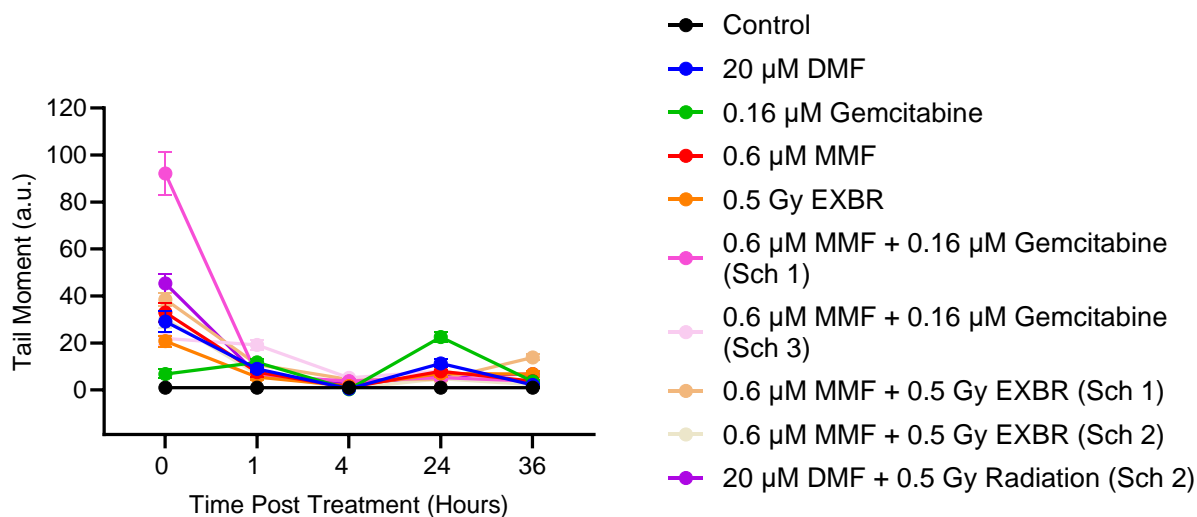


**Figure 4.5: DNA damage analysis of combination therapies in Panc-1.** Cells were incubated and harvested at specific time points post treatment before undergoing comet assay to determine if DNA damage had been induced. All data is represented as an average of three independent experiments  $\pm$  the standard error of the mean.

As can be seen in **figure 4.5**, in Panc-1 cells, 20  $\mu\text{M}$  DMF, 0.6  $\mu\text{M}$  MMF, 0.5 Gy EXBR, 0.6  $\mu\text{M}$  MMF + 0.16  $\mu\text{M}$  gemcitabine (Schedule 1), 0.6  $\mu\text{M}$  MMF + 0.16  $\mu\text{M}$  gemcitabine (Schedule 3), 0.6  $\mu\text{M}$  MMF + 0.5 Gy EXBR (Schedule 1), 0.6  $\mu\text{M}$  MMF + 0.5 Gy EXBR (Schedule 2), and 20  $\mu\text{M}$  DMF + 0.5 Gy EXBR (Schedule 2) induced a statistically significantly greater amount of DNA damage when compared with the untreated control zero hours post treatment ( $P < 0.0001$ ).

One hour post treatment in Panc-1 cells, 20  $\mu\text{M}$  DMF, 0.16  $\mu\text{M}$  gemcitabine, 0.6  $\mu\text{M}$  MMF + 0.16  $\mu\text{M}$  gemcitabine (Schedule 3), and 0.6  $\mu\text{M}$  MMF + 0.5 Gy EXBR (Schedule 1) induced a statistically significantly greater amount of DNA damage when compared with the untreated control one hour post treatment ( $P \leq 0.0191$ ).

Four hours post treatment in Panc-1 cells, no treatments induced a statistically significant amount of DNA damage when compared with the untreated control four hours post treatment ( $P \geq 0.9604$ ).

24 hours post treatment in Panc-1 cells, only 20  $\mu\text{M}$  DMF and 0.16  $\mu\text{M}$  gemcitabine induced a statistically significantly greater amount of DNA damage when compared with the untreated control 24 hours post treatment ( $P \leq 0.0065$ ).

36 hours post treatment in Panc-1 cells, only 0.6  $\mu\text{M}$  MMF + 0.5 Gy EXBR (Schedule 1) induced a statistically significantly greater amount of DNA damage when compared with the untreated control 36 hours post treatment ( $P < 0.0001$ ).

A summary of all statistical comparisons carried out between the untreated control and therapies, and between combination therapies and individual components over the time course in Panc-1 cells following two-way ANOVA with Bonferroni post hoc test can be found in **tables 4.41 and 4.42**.

**Table 4.41: Statistical comparisons of DNA damage of treated Panc-1 cells throughout the time course versus the untreated control.** Sch = schedule, M = MMF, D = MMF, G = gemcitabine, R = EXBR, ns = not significant.

Comparison	Time Point (hrs)	Summary	P-value
Control vs DMF	0	****	<0.0001
	1	*	0.0191
	4	ns	>0.9999
	24	**	0.0065
	36	ns	0.9996
Control vs MMF	0	****	<0.0001
	1	ns	0.2645
	4	ns	>0.9999
	24	ns	0.1394
	36	ns	0.8273
Control vs gemcitabine	0	ns	0.3260
	1	***	0.0001
	4	ns	>0.9999
	24	****	<0.0001
	36	ns	0.9047
Control vs EXBR	0	****	<0.0001
	1	ns	0.7931
	4	ns	>0.9999
	24	ns	0.5037
	36	ns	0.3097
Control vs M+R Sch 1	0	****	<0.0001
	1	**	0.0091
	4	ns	0.9604
	24	ns	0.9583
	36	****	<0.0001
Control vs M+R Sch 2	0	****	<0.0001
	1	ns	0.4228
	4	ns	>0.9999
	24	ns	0.9453
	36	ns	>0.9999
Control vs M+G Sch 1	0	****	<0.0001
	1	ns	0.6078
	4	ns	0.9916
	24	ns	0.8909
	36	ns	0.8612
Control vs M+G Sch 3	0	****	<0.0001
	1	****	<0.0001
	4	ns	0.8928
	24	ns	0.2590
	36	ns	0.9863
Control vs D+R Sch 2	0	****	<0.0001
	1	ns	0.5065
	4	ns	>0.9999
	24	ns	0.7525
	36	ns	0.2152

**Table 4.42: Statistical comparisons of DNA damage of treated Panc-1 cells throughout the time course versus the untreated control.** Sch = schedule, M = MMF, D = MMF, G = gemcitabine, R = EXBR, ns = not significant.

Comparison	Time Point (hrs)	Summary	P-value
D+R Sch 2 vs DMF	0	****	<0.0001
	1	ns	0.9948
	4	ns	0.9996
	24	ns	0.6087
	36	ns	0.4530
D+R Sch 2 vs EXBR	0	****	<0.0001
	1	ns	>0.9999
	4	ns	>0.9999
	24	ns	>0.9999
	36	ns	>0.9999
M+G Sch 1 vs MMF	0	****	<0.0001
	1	ns	>0.9999
	4	ns	0.9952
	24	ns	0.9845
	36	ns	>0.9999
M+G Sch 1 vs gemcitabine	0	****	<0.0001
	1	ns	0.4853
	4	ns	0.9359
	24	****	<0.0001
	36	ns	>0.9999
M+G Sch 3 vs MMF	0	**	0.0039
	1	**	0.0011
	4	ns	0.9215
	24	ns	>0.9999
	36	ns	>0.9999
M+G Sch 3 vs gemcitabine	0	****	<0.0001
	1	ns	0.0694
	4	ns	0.6830
	24	****	<0.0001
	36	ns	>0.9999
M+R Sch 1 vs MMF	0	ns	0.6086
	1	ns	0.9837
	4	ns	0.9738
	24	ns	0.9165
	36	***	0.0002
M+R Sch 1 vs EXBR	0	****	<0.0001
	1	ns	0.6876
	4	ns	0.9925
	24	ns	0.9961
	36	ns	0.2512
M+R Sch 2 vs MMF	0	ns	0.9934
	1	ns	>0.9999
	4	ns	>0.9999
	24	ns	0.9571
	36	ns	0.9994
M+R Sch 2 vs EXBR	0	*	0.0176
	1	ns	>0.9999
	4	ns	>0.9999
	24	ns	0.9986
	36	ns	0.7991

### Summary of DNA damage following treatment in Panc-1 cells

Overall, the DNA damage induced by the schedule 1 combination of 0.6  $\mu\text{M}$  MMF + 0.5 Gy EXBR was unable to be fully repaired in Panc-1 cells, as the DNA damage was statistically significantly greater 36 hours post treatment when compared with the untreated control, whereas the single agent damage was able to be repaired. This result implies the combination may have therapeutic efficacy as the combination is inducing DNA damage the cell is unable to repair, which could lead to cancer cell death.

Overall, the DNA damage induced by the schedule 1 combination of 0.6  $\mu\text{M}$  MMF + 0.16  $\mu\text{M}$  gemcitabine was fully repaired in the Panc-1 cells, despite the initial peak of DNA damage seen immediately post treatment.

Overall, the DNA damage induced by the schedule 2 combination of 0.6  $\mu\text{M}$  MMF + 0.5 Gy EXBR was able to be fully repaired in the Panc-1 cells over the analysed time course, indicating the combination was no different from that of the untreated control.

Overall, the DNA damage induced by the schedule 2 combination of 20  $\mu\text{M}$  DMF + 0.5 Gy EXBR was able to be fully repaired in the Panc-1 cells over the analysed time course as it did not differ from the untreated control.

Overall, the DNA damage induced by the schedule 1 combination of 0.6  $\mu\text{M}$  MMF + 0.16  $\mu\text{M}$  gemcitabine was able to be fully repaired in the Panc-1 cells as the DNA damage decreased over time and returned to that of the untreated control 36 hours post treatment, suggesting the combination was of no additional benefit.

To investigate if the selected combinations were inducing DNA damage in the Mia PaCa-2 cell line, the comet assay was carried out as described in **section 4.3.5**, and the results presented in **figure 4.6**.

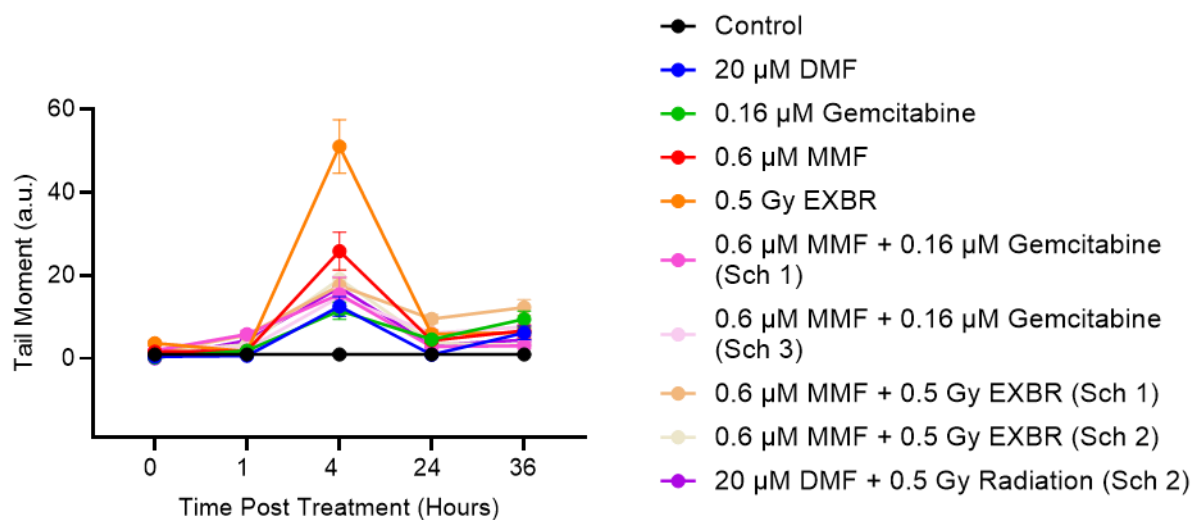


**Figure 4.6: DNA damage analysis of combination therapies in Mia PaCa-2.** Cells were incubated and harvested at specific time points post treatment before undergoing comet assay to determine if DNA damage had been induced. All data is represented as an average of three independent experiments  $\pm$  the standard error of the mean.

As can be seen in **figure 4.6**, in Mia PaCa-2 cells, 0.16  $\mu$ M gemcitabine, 0.5 Gy EXBR, 0.6  $\mu$ M MMF + 0.16  $\mu$ M gemcitabine (Schedule 1), 0.6  $\mu$ M MMF + 0.16  $\mu$ M gemcitabine (Schedule 3), 0.6  $\mu$ M MMF + 0.5 Gy EXBR (Schedule 2), and 20  $\mu$ M DMF + 0.5 Gy EXBR (Schedule 2) induced a statistically significantly greater amount of DNA damage when compared with the untreated control zero hours post treatment ( $P \leq 0.0367$ ).

One hour post treatment in Mia PaCa-2 cells, 0.6  $\mu$ M MMF, 0.16  $\mu$ M gemcitabine, 0.5 Gy EXBR, 0.6  $\mu$ M MMF + 0.16  $\mu$ M gemcitabine (Schedule 1), 0.6  $\mu$ M MMF + 0.16  $\mu$ M gemcitabine (Schedule 3), 0.6  $\mu$ M MMF + 0.5 Gy EXBR (Schedule 2), 0.6  $\mu$ M MMF + 0.5 Gy EXBR (Schedule 1) and 20  $\mu$ M DMF + 0.5 Gy EXBR (Schedule 2) induced a statistically significantly greater amount of DNA damage when compared with the untreated control one hour post treatment ( $P \leq 0.0004$ ).

Four hours post treatment in Mia PaCa-2 cells, all tested monotherapies and combination therapies induced a statistically significantly greater amount of DNA damage when compared with the untreated control four hours post treatment ( $P < 0.0001$ ).

24 hours post treatment in Mia PaCa-2 cells, all tested monotherapies and combination therapies, with the exception of 20  $\mu$ M DMF, induced a statistically significantly greater amount of DNA damage when compared with the untreated control 24 hours post treatment ( $P < 0.0001$ ).

36 hours post treatment in Mia PaCa-2 cells, all tested monotherapies and combination therapies induced a statistically significantly greater amount of DNA damage when compared with the untreated control 36 hours post treatment ( $P < 0.0001$ ).

A summary of all statistical comparisons carried out between the untreated control and therapies, and between combination therapies and individual components over the time course in Mia PaCa-2 cells following two-way ANOVA with Bonferroni post hoc test can be found in **tables 4.43 and 4.44**.

**Table 4.43: Statistical comparisons of DNA damage of treated Mia PaCa-2 cells throughout the time course versus the untreated control.** Sch = schedule, M = MMF, D = MMF, G = gemcitabine, R = EXBR, ns = not significant.

Comparison	Time Point (hrs)	Summary	P-value
Control vs DMF	0	ns	0.3814
	1	ns	0.6807
	4	****	<0.0001
	24	ns	>0.9999
	36	****	<0.0001
Control vs MMF	0	ns	0.0927
	1	****	<0.0001
	4	****	<0.0001
	24	****	<0.0001
	36	****	<0.0001
Control vs gemcitabine	0	*	0.0367
	1	***	0.0004
	4	****	<0.0001
	24	****	<0.0001
	36	****	<0.0001
Control vs EXBR	0	****	<0.0001
	1	ns	0.0559
	4	****	<0.0001
	24	****	<0.0001
	36	****	<0.0001
Control vs M+R Sch 1	0	ns	0.5040
	1	****	<0.0001
	4	****	<0.0001
	24	****	<0.0001
	36	****	<0.0001
Control vs M+R Sch 2	0	*	0.0332
	1	****	<0.0001
	4	****	<0.0001
	24	****	<0.0001
	36	****	<0.0001
Control vs M+G Sch 1	0	**	0.0017
	1	****	<0.0001
	4	****	<0.0001
	24	****	<0.0001
	36	****	<0.0001
Control vs M+G Sch 3	0	****	<0.0001
	1	****	<0.0001
	4	****	<0.0001
	24	****	<0.0001
	36	****	<0.0001
Control vs D+R Sch 2	0	**	0.0012
	1	****	<0.0001
	4	****	<0.0001
	24	****	<0.0001
	36	****	<0.0001

**Table 4.44: Statistical comparisons of DNA damage of treated Mia PaCa-2 cells throughout the time course versus the untreated control.** Sch = schedule, M = MMF, D = MMF, G = gemcitabine, R = EXBR, ns = not significant.

Comparison	Time Point (hrs)	Summary	P-value
D+R Sch 2 vs DMF	0	ns	0.7028
	1	****	<0.0001
	4	****	<0.0001
	24	****	<0.0001
	36	****	<0.0001
D+R Sch 2 vs EXBR	0	****	<0.0001
	1	****	<0.0001
	4	****	<0.0001
	24	****	<0.0001
	36	****	<0.0001
M+G Sch 1 vs MMF	0	ns	0.9704
	1	****	<0.0001
	4	****	<0.0001
	24	****	<0.0001
	36	****	<0.0001
M+G Sch 1 vs gemcitabine	0	****	<0.0001
	1	****	<0.0001
	4	****	<0.0001
	24	****	<0.0001
	36	****	<0.0001
M+G Sch 3 vs MMF	0	****	<0.0001
	1	ns	0.2483
	4	****	<0.0001
	24	****	<0.0001
	36	****	<0.0001
M+G Sch 3 vs gemcitabine	0	****	<0.0001
	1	ns	0.7070
	4	****	<0.0001
	24	****	<0.0001
	36	****	<0.0001
M+R Sch 1 vs MMF	0	ns	0.9973
	1	****	<0.0001
	4	****	<0.0001
	24	****	<0.0001
	36	****	<0.0001
M+R Sch 1 vs EXBR	0	****	<0.0001
	1	****	<0.0001
	4	****	<0.0001
	24	****	<0.0001
	36	****	<0.0001
M+R Sch 2 vs MMF	0	ns	>0.9999
	1	****	<0.0001
	4	****	<0.0001
	24	ns	0.0993
	36	****	<0.0001
M+R Sch 2 vs EXBR	0	****	<0.0001
	1	****	<0.0001
	4	****	<0.0001
	24	****	<0.0001
	36	****	<0.0001

### **Summary of DNA damage following treatment in Mia PaCa-2 cells**

Overall, the DNA damage induced by the schedule 1 combination of 0.6  $\mu\text{M}$  MMF + 0.5 Gy EXBR was unable to be fully repaired in the Mia PaCa-2 cells, as the induced DNA damage continued to increase until 36 hours post treatment, whereas the damage induced by both single agents began to decrease, indicating DNA repair.

Overall, the DNA damage induced by the schedule 1 combination of 0.6  $\mu\text{M}$  MMF + 0.16  $\mu\text{M}$  gemcitabine was fully repaired in the Mia PaCa-2 cells, with the single agents inducing more damage overall when compared with the untreated control, surprisingly suggesting that the cytotoxicity induced combination is related to DNA damage.

Overall, the DNA damage induced by the schedule 1 combination of 0.6  $\mu\text{M}$  MMF + 0.5 Gy EXBR was able to be fully repaired in the Mia PaCa-2 cells, as the DNA damage induced by the combination 36 hours post treatment did not statistically significantly differ from the DNA damage initially induced by the combination zero hours post treatment.

Overall, the DNA damage induced by the schedule 1 combination of 20  $\mu\text{M}$  DMF + 0.5 Gy EXBR was not fully repaired in the Mia PaCa-2 cells, as the DNA damage 36 hours post treatment was greater than that of the untreated control, however the monotherapies induced more DNA damage overall, indicating this combination was of no additional benefit.

Overall, the DNA damage induced by the schedule 1 combination of 0.6  $\mu\text{M}$  MMF + 0.16  $\mu\text{M}$  gemcitabine was repaired in the Mia PaCa-2 cells, however the DNA damage induced by the single agents was also repaired. This suggest that the combination was of no additional benefit.

#### **4.4.4: Glutathione studies on developed combinations**

To investigate the effects of the developed combinations on glutathione levels within Panc-1 cells, the glutathione assay was carried out as described in **section 4.3.6**, and the results presented in **figure 4.7**.

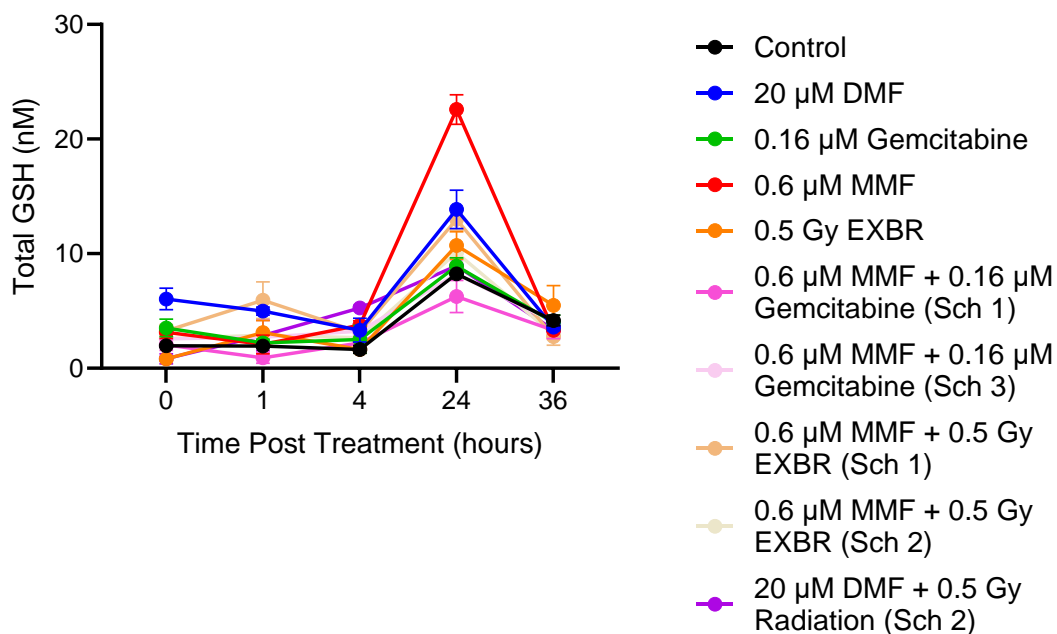


**Figure 4.7: Glutathione analysis of combination therapies in Panc-1.** Cells were incubated and harvested at specific time points post treatment before undergoing glutathione assay to determine if the glutathione levels within the cell had been altered following treatment. All data is represented as an average of three independent experiments  $\pm$  the standard deviation.

As can be seen in **figure 4.7**, in Panc-1 cells only 20  $\mu$ M DMF induced a statistically significant increase in the glutathione level when compared with the untreated control zero hours post treatment ( $P < 0.0001$ ).

One hour post treatment in Panc-1 cells, 20  $\mu$ M DMF and 0.6  $\mu$ M MMF + 0.5 Gy EXBR (Schedule 1) induced a statistically significant increase in the glutathione level when compared with the untreated control one hour post treatment ( $P \leq 0.0002$ ).

Four hours post treatment in Panc-1 cells, only 0.6  $\mu$ M MMF and 0.6  $\mu$ M + 0.5 Gy EXBR (Schedule 1) induced a statistically significant increase in the glutathione level when compared with the untreated control four hours post treatment ( $P \leq 0.0351$ ).

24 hours post treatment in Panc-1 cells, only 0.6  $\mu$ M MMF, 0.5 Gy EXBR, 20  $\mu$ M DMF, and 0.6  $\mu$ M + 0.5 Gy EXBR (Schedule 1) induced a statistically significant increase in the glutathione level when compared with the untreated control 24 hours post treatment ( $P \leq 0.0062$ ).

36 hours post treatment in Panc-1 cells single agents or combination therapies induced a statistically significant change in the glutathione level when compared with the untreated control 36 hours post treatment ( $P \geq 0.4449$ ).

A summary of all statistical comparisons carried out between the untreated control and therapies, and between combination therapies and individual components over the time course in Panc-1 cells following two-way ANOVA with Bonferroni post hoc test can be found in **tables 4.45 and 4.46**.

**Table 4.45: Statistical comparisons of glutathione levels in treated Panc-1 cells throughout the time course versus the untreated control.** Sch = schedule, M = MMF, D = MMF, G = gemcitabine, R = EXBR, ns = not significant.

Comparison	Time Point (hrs)	Summary	P-value
Control vs DMF	0	****	<0.0001
	1	***	0.0002
	4	ns	0.2020
	24	****	<0.0001
	36	ns	0.9956
Control vs MMF	0	ns	0.6891
	1	ns	>0.9999
	4	*	0.0351
	24	****	<0.0001
	36	ns	0.9320
Control vs gemcitabine	0	ns	0.3011
	1	ns	>0.9999
	4	ns	0.9298
	24	ns	0.9881
	36	ns	>0.9999
Control vs EXBR	0	ns	0.7002
	1	ns	0.6833
	4	ns	>0.9999
	24	**	0.0062
	36	ns	0.5414
Control vs M+R Sch 1	0	ns	0.5509
	1	****	<0.0001
	4	****	<0.0001
	24	****	<0.0001
	36	ns	0.4449
Control vs M+R Sch 2	0	ns	0.9935
	1	ns	0.8892
	4	ns	0.8332
	24	ns	0.1065
	36	ns	0.6594
Control vs M+G Sch 1	0	ns	>0.9999
	1	ns	0.8332
	4	ns	0.9962
	24	ns	0.0609
	36	ns	0.9390
Control vs M+G Sch 3	0	ns	0.9946
	1	ns	0.9672
	4	ns	0.2572
	24	ns	>0.9999
	36	ns	>0.9999
Control vs D+R Sch 2	0	ns	0.7258
	1	ns	0.8892
	4	ns	0.9053
	24	ns	0.9818
	36	ns	0.9553

**Table 4.46: Statistical comparisons of glutathione levels in treated Panc-1 cells throughout the time course versus the untreated control.** Sch = schedule, M = MMF, D = MMF, G = gemcitabine, R = EXBR, ns = not significant.

Comparison	Time Point (hrs)	Summary	P-value
D+R Sch 2 vs DMF	0	****	<0.0001
	1	*	0.0332
	4	ns	0.0757
	24	****	<0.0001
	36	ns	>0.9999
D+R Sch 2 vs EXBR	0	ns	>0.9999
	1	ns	>0.9999
	4	****	<0.0001
	24	ns	0.1526
	36	*	0.0343
M+G Sch 1 vs MMF	0	ns	0.7545
	1	ns	0.7113
	4	ns	0.3017
	24	****	<0.0001
	36	ns	>0.9999
M+G Sch 1 vs gemcitabine	0	ns	0.3612
	1	ns	0.5654
	4	ns	>0.9999
	24	**	0.0021
	36	ns	0.9843
M+G Sch 3 vs MMF	0	ns	0.9952
	1	ns	0.9910
	4	ns	0.9982
	24	****	<0.0001
	36	ns	0.9724
M+G Sch 3 vs gemcitabine	0	ns	0.8805
	1	ns	0.9985
	4	ns	0.9760
	24	ns	0.9819
	36	ns	>0.9999
M+R Sch 1 vs MMF	0	ns	>0.9999
	1	****	<0.0001
	4	ns	0.9914
	24	****	<0.0001
	36	ns	0.9974
M+R Sch 1 vs EXBR	0	**	0.0059
	1	***	0.0008
	4	ns	0.3456
	24	*	0.0152
	36	**	0.0015
M+R Sch 2 vs MMF	0	ns	0.9960
	1	ns	0.9540
	4	ns	0.7715
	24	****	<0.0001
	36	ns	>0.9999
M+R Sch 2 vs EXBR	0	ns	0.1444
	1	ns	>0.9999
	4	ns	0.8189
	24	ns	0.9936
	36	**	0.0046

### **Summary of glutathione levels following treatment in Panc-1 cells**

Overall, none of the developed combinations influenced the glutathione levels within the cell, as the glutathione levels did not statistically significantly vary from that of the untreated control overall. Unexpectedly, MMF monotherapy caused an increase in glutathione levels in Panc-1 cells 24 hours post treatment, however this returned to that of the untreated control 36 hours post treatment. This result contradicts our hypothesis that MMF would decrease glutathione. As the glutathione levels rose in the untreated control over the time course, this suggests an experimental error and the results may not be a true representative of what was happening with glutathione levels within the cell.

To investigate the effects of the developed combinations on glutathione levels within Mia PaCa-2 cells, the glutathione assay was carried out as described in **section 4.3.6**, and the results presented in **figure 4.8**.

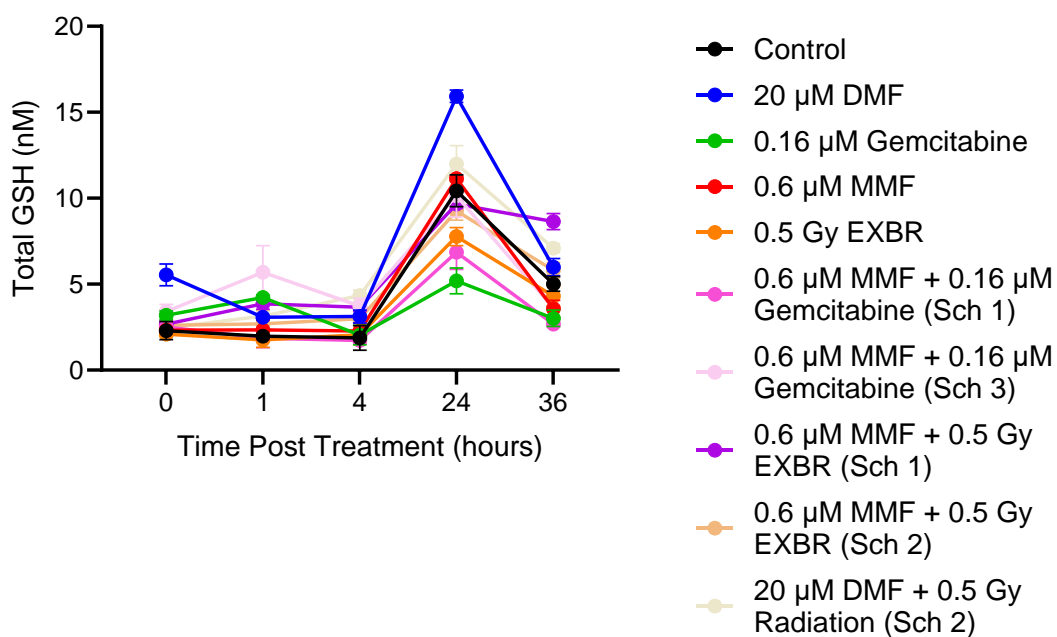


**Figure 4.8: Glutathione analysis of combination therapies in Mia PaCa-2.** Cells were incubated and harvested at specific time points post treatment before undergoing glutathione assay to determine if the glutathione levels within the cell had been altered following treatment. All data is represented as an average of three independent experiments  $\pm$  the standard deviation.

As can be seen in **figure 4.8** in Mia PaCa-2 cells, only 20  $\mu\text{M}$  DMF induced a statistically significant increase in glutathione levels when compared with the untreated control zero hours post treatment ( $P = 0.0223$ ).

One hour post treatment in Mia PaCa-2 cells, 20  $\mu\text{M}$  DMF + 0.5 Gy EXBR and 0.6  $\mu\text{M}$  MMF + 0.16  $\mu\text{M}$  gemcitabine (Schedule 3) induced a statistically significant increase in glutathione levels when compared with the untreated control one hour post treatment ( $P \leq 0.0044$ ).

Four hours post treatment in Mia PaCa-2 cells, no monotherapies or combination therapies induced a statistically significant change in glutathione levels when compared with the untreated control four hours post treatment ( $P = 0.2035$ ).

24 hours post treatment in Mia PaCa-2 cells, 0.16  $\mu\text{M}$  gemcitabine and 0.6  $\mu\text{M}$  MMF + 0.16  $\mu\text{M}$  gemcitabine (Schedule 1) induced a statistically significant reduction in glutathione levels when compared with the untreated control 24 hours post treatment ( $P \leq 0.0071$ ). Conversely, 20  $\mu\text{M}$  DMF induced a statistically significant increase in glutathione levels when compared with the untreated control 24 hours post treatment ( $P < 0.0001$ ).

36 hours post treatment in Mia PaCa-2 cells, only 0.6  $\mu\text{M}$  MMF + 0.5 Gy EXBR (Schedule 1) induced a statistically significant increase in glutathione levels when compared with the untreated control 36 hours post treatment ( $P = 0.0059$ ).

A summary of all statistical comparisons carried out between the untreated control and therapies, and between combination therapies and individual components over the time course in Mia PaCa-2 cells following two-way ANOVA with Bonferroni post hoc test can be found in **tables 4.47 and 4.48**.

**Table 4.47: Statistical comparisons of glutathione levels in treated Mia PaCa-2 cells throughout the time course versus the untreated control.** Sch = schedule, M = MMF, D = MMF, G = gemcitabine, R = EXBR, ns = not significant.

Comparison	Time Point (hrs)	Summary	P-value
Control vs DMF	0	*	0.0223
	1	ns	0.9710
	4	ns	0.9393
	24	****	<0.0001
	36	ns	0.9879
Control vs MMF	0	ns	>0.9999
	1	ns	>0.9999
	4	ns	>0.9999
	24	ns	0.9987
	36	ns	0.8608
Control vs gemcitabine	0	ns	0.9936
	1	ns	0.3152
	4	ns	>0.9999
	24	****	<0.0001
	36	ns	0.4860
Control vs EXBR	0	ns	>0.9999
	1	ns	>0.9999
	4	ns	>0.9999
	24	ns	0.1265
	36	ns	0.9989
Control vs M+R Sch 1	0	ns	>0.9999
	1	ns	0.5666
	4	ns	0.6451
	24	ns	0.9980
	36	**	0.0059
Control vs M+R Sch 2	0	ns	0.9898
	1	*	0.0355
	4	ns	0.9688
	24	ns	0.9588
	36	ns	0.9973
Control vs M+G Sch 1	0	ns	>0.9999
	1	ns	>0.9999
	4	ns	>0.9999
	24	**	0.0071
	36	ns	0.2662
Control vs M+G Sch 3	0	ns	0.9696
	1	****	<0.0001
	4	ns	0.6046
	24	ns	>0.9999
	36	ns	0.8826
Control vs D+R Sch 2	0	ns	0.5529
	1	**	0.0044
	4	ns	0.2035
	24	ns	0.7987
	36	ns	0.4306

**Table 4.48: Statistical comparisons of glutathione levels in treated Mia PaCa-2 cells throughout the time course versus the untreated control.** Sch = schedule, M = MMF, D = MMF, G = gemcitabine, R = EXBR, ns = not significant.

Comparison	Time Point (hrs)	Summary	P-value
D+R Sch 2 vs DMF	0	ns	0.9098
	1	ns	0.1456
	4	ns	0.9482
	24	**	0.0018
	36	ns	0.9713
D+R Sch 2 vs EXBR	0	ns	0.4056
	1	**	0.0019
	4	ns	0.3020
	24	***	0.0006
	36	ns	0.0897
M+G Sch 1 vs MMF	0	ns	>0.9999
	1	ns	>0.9999
	4	ns	0.9998
	24	***	0.0004
	36	ns	0.9937
M+G Sch 1 vs gemcitabine	0	ns	0.9992
	1	ns	0.2525
	4	ns	>0.9999
	24	ns	0.7339
	36	ns	>0.9999
M+G Sch 3 vs MMF	0	ns	0.9734
	1	***	0.0001
	4	ns	0.8659
	24	ns	0.9851
	36	ns	>0.9999
M+G Sch 3 vs gemcitabine	0	ns	>0.9999
	1	ns	0.1192
	4	ns	0.7288
	24	****	<0.0001
	36	ns	0.9997
M+R Sch 1 vs MMF	0	ns	>0.9999
	1	ns	0.8204
	4	ns	0.8908
	24	ns	0.8420
	36	****	<0.0001
M+R Sch 1 vs EXBR	0	ns	0.9998
	1	ns	0.4102
	4	ns	0.7730
	24	ns	0.5683
	36	***	0.0004
M+R Sch 2 vs MMF	0	ns	0.9914
	1	ns	0.1042
	4	ns	0.9988
	24	ns	0.5703
	36	ns	0.3211
M+R Sch 2 vs EXBR	0	ns	0.9624
	1	*	0.0177
	4	ns	0.9910
	24	ns	0.8406
	36	ns	0.8316

### **Summary of glutathione levels following treatment in Mia PaCa-2 cells**

Overall, none of the developed combinations influenced the glutathione levels within the cell, as the glutathione levels did not statistically significantly vary from that of the untreated control overall. Unexpectedly, DMF monotherapy caused an increase in glutathione levels in Panc-1 cells 24 hours post treatment, however this returned to that of the untreated control 36 hours post treatment. This result contradicts our hypothesis that DMF would decrease glutathione. As the glutathione levels rose in the untreated control over the time course, this suggests an experimental error and the results may not be a true representative of what was happening with glutathione levels within the cell.

An overall summary of all mechanistic studies carried out can be found in **table 49 and 50**.

**Table 4.49: Summary of mechanistic results for combination therapies in Panc-1 cells vs the untreated control**

<b>Schedule 1 MMF + EXBR</b>					
	<b>0 hours</b>	<b>1 hour</b>	<b>4 hours</b>	<b>24 hours</b>	<b>36 hours</b>
<b>Cell Cycle</b>	↑ sG1	No change	↑ S & G2/M	↑ S & G2/M	↑ G2/M
<b>Apoptosis</b>	↑ apoptosis	No change	No change	No change	↑ apoptosis
<b>DNA Damage</b>	↑ DNA damage	No change	No change	No change	↑ DNA damage
<b>Glutathione Level</b>	No change	↑ glutathione	No change	↑ glutathione	No change
<b>Schedule 1 MMF + gemcitabine</b>					
	<b>0 hours</b>	<b>1 hour</b>	<b>4 hours</b>	<b>24 hours</b>	<b>36 hours</b>
<b>Cell Cycle</b>	No change	↑ G2/M	↑ S & G2/M	↑ S & G2/M	↑ S & G2/M
<b>Apoptosis</b>	↑ apoptosis	↑ apoptosis	↑ apoptosis	↑ apoptosis	↑ apoptosis
<b>DNA Damage</b>	↑ DNA damage	No change	No change	No change	No change
<b>Glutathione Level</b>	No change	No change	No change	No change	No change
<b>Schedule 2 MMF + EXBR</b>					
	<b>0 hours</b>	<b>1 hour</b>	<b>4 hours</b>	<b>24 hours</b>	<b>36 hours</b>
<b>Cell Cycle</b>	↑ sG1	↑ sG1	↑ G2/M	No change	No change
<b>Apoptosis</b>	↑ apoptosis	↑ apoptosis	↑ apoptosis	↑ apoptosis	↑ apoptosis
<b>DNA Damage</b>	↑ DNA damage	No change	No change	No change	No change
<b>Glutathione Level</b>	No change	No change	No change	No change	No change
<b>Schedule 2 DMF + EXBR</b>					
	<b>0 hours</b>	<b>1 hour</b>	<b>4 hours</b>	<b>24 hours</b>	<b>36 hours</b>
<b>Cell Cycle</b>	No change	↑ G2/M	No change	↑ G1	No change
<b>Apoptosis</b>	↑ apoptosis	No change	No change	↑ apoptosis	↑ apoptosis
<b>DNA Damage</b>	↑ DNA damage	No change	No change	No change	No change
<b>Glutathione Level</b>	No change	No change	↑ glutathione	No change	No change
<b>Schedule 3 MMF + gemcitabine</b>					
	<b>0 hours</b>	<b>1 hour</b>	<b>4 hours</b>	<b>24 hours</b>	<b>36 hours</b>
<b>Cell Cycle</b>	↑ sG1 & S	No change	↑ S & G2/M	↑ S & G2/M	↑ G2/M
<b>Apoptosis</b>	↑ apoptosis	↑ apoptosis	↑ apoptosis	↑ apoptosis	↑ apoptosis
<b>DNA Damage</b>	↑ DNA damage	↑ DNA damage	No change	No change	No change
<b>Glutathione Level</b>	No change	No change	No change	No change	No change

**Table 4.50: Summary of mechanistic results for combination therapies in Mia PaCa-2 cells vs the untreated control**

<b>Schedule 1 MMF + EXBR</b>					
	<b>0 hours</b>	<b>1 hour</b>	<b>4 hours</b>	<b>24 hours</b>	<b>36 hours</b>
<b>Cell Cycle</b>	No change	↑ sG1	No change	No change	No change
<b>Apoptosis</b>	↑ apoptosis	↑ apoptosis	No change	↑ apoptosis	↑ apoptosis
<b>DNA Damage</b>	No change	↑ DNA damage	↑ DNA damage	↑ DNA damage	↑ DNA damage
<b>Glutathione Level</b>	No change	No change	No change	No change	↑ glutathione
<b>Schedule 1 MMF + gemcitabine</b>					
	<b>0 hours</b>	<b>1 hour</b>	<b>4 hours</b>	<b>24 hours</b>	<b>36 hours</b>
<b>Cell Cycle</b>	↑ S & G2/M	No change	↑ G2/M	↑ G2/M	↑ G2/M
<b>Apoptosis</b>	↑ apoptosis	↑ apoptosis	↑ apoptosis	↑ apoptosis	↑ apoptosis
<b>DNA Damage</b>	↑ DNA damage	↑ DNA damage	↑ DNA damage	↑ DNA damage	↑ DNA damage
<b>Glutathione Level</b>	No change	No change	No change	↓ glutathione	No change
<b>Schedule 2 MMF + EXBR</b>					
	<b>0 hours</b>	<b>1 hour</b>	<b>4 hours</b>	<b>24 hours</b>	<b>36 hours</b>
<b>Cell Cycle</b>	↑ sG1	↑ sG1	No change	No change	No change
<b>Apoptosis</b>	↑ apoptosis	↑ apoptosis	↑ apoptosis	↑ apoptosis	↑ apoptosis
<b>DNA Damage</b>	↑ DNA damage	↑ DNA damage	↑ DNA damage	↑ DNA damage	↑ DNA damage
<b>Glutathione Level</b>	No change	↑ glutathione	No change	No change	No change
<b>Schedule 2 DMF + EXBR</b>					
	<b>0 hours</b>	<b>1 hour</b>	<b>4 hours</b>	<b>24 hours</b>	<b>36 hours</b>
<b>Cell Cycle</b>	No change	No change	No change	↑ sG1	↑ sG1
<b>Apoptosis</b>	No change	↑ apoptosis	No change	No change	↑ apoptosis
<b>DNA Damage</b>	No change	↑ DNA damage	↑ DNA damage	↑ DNA damage	↑ DNA damage
<b>Glutathione Level</b>	No change	↑ glutathione	No change	No change	No change
<b>Schedule 3 MMF + gemcitabine</b>					
	<b>0 hours</b>	<b>1 hour</b>	<b>4 hours</b>	<b>24 hours</b>	<b>36 hours</b>
<b>Cell Cycle</b>	↑ G1	↑ sG1	No change	No change	↑ S
<b>Apoptosis</b>	↑ apoptosis	↑ apoptosis	↑ apoptosis	↑ apoptosis	↑ apoptosis
<b>DNA Damage</b>	↑ DNA damage	↑ DNA damage	↑ DNA damage	↑ DNA damage	↑ DNA damage
<b>Glutathione Level</b>	No change	↑ glutathione	No change	No change	No change

## **4.5: DISCUSSION**

### **4.5.1: Monotherapies**

As a monotherapy MMF induced an increase in the number of cells in sG1 phase in both Panc-1 and Mia PaCa-2 cell lines, which corresponded with an increase in the number of apoptotic cells and an increase in DNA damage. In Panc-1 cells MMF caused glutathione levels to fall below that of the untreated control 36 hours post treatment, however in Mia PaCa-2 cells MMF had no effect on glutathione levels. In the literature no studies looking at the effects of MMF and glutathione could be found, however as the active metabolite of DMF, it was assumed that MMF would lower glutathione levels as is reported in the literature for DMF [117]. A possible explanation for the obtained results is both Panc-1 and Mia PaCa-2 cell lines have p53 missense mutations, and in the literature it has been reported that p53 missense mutant cancers upregulate NRF2 activity [217], therefore the mutant p53 activity may be counteracting the NRF2 inhibition reported to be induced by DMF in the literature [117]. Additionally, no studies looking at the mechanism of cell death induced by MMF could be found in the literature, however for DMF it has been reported that DMF induced apoptosis, as a investigating the effects of DMF on human colon carcinoma cell lines found DMF induced apoptosis [203]. Therefore, it was assumed that MMF would also induce apoptosis as it is the active metabolite of DMF, and this was reflected in the obtained results as MMF did induce apoptosis in the pancreatic cancer cell lines. Unfortunately, no studies could be found in the literature investigating the effects of MMF on the cell cycle, however it has been reported that DMF induces G1 phase arrest, however this effect was not seen in the obtained results as MMF induced an increase in the number of cells in sG1 in both cell lines [111, 203, 204].

DMF monotherapy caused cells to accumulate in G1 phase until 24 hours post treatment, where the cells then appeared to continue cycling similar to the untreated

control in Panc-1, which is supported by studies in the literature [203, 204]. However, in Mia PaCa-2, DMF monotherapy caused an increase in the number of cells in sG1 phase, similarly to the effect seen with MMF in the cell line. As previously mentioned, DMF has been shown to be preferentially cytotoxic to cancer cells with KRAS mutation in the literature [112], and Mia PaCa-2 has a different KRAS mutation to Panc-1 (G12C vs G12D) which is rarer and may make it more sensitive to DMF therapy, however further studies would be required to conform this hypothesis. As seen with MMF, the glutathione reducing effect of DMF was not seen experimentally, indicating that the effect was missed with the selected time points, or that DMF is acting differently than as was expected as reported in the literature [112, 203].

Gemcitabine monotherapy induced G2/M arrest in both Panc-1 and Mia PaCa-2 cell lines, which was unexpected as in the literature it was reported that gemcitabine induces G1/S phase arrest [84]. However, studies in the literature utilising the Mia PaCa-2 cell line found that treatment with gemcitabine induced an increase in G2/M phase [218], as we observed experimentally, and that incubation with gemcitabine induced G2/M checkpoint activation, causing cells to accumulate in G2/M phase [194]. Gemcitabine induced apoptosis, which coincided with findings reported in the literature [87, 219, 220].

In the literature radiation is reported to induce cell cycle arrest in all phases of the cell cycle, which is dependent on the dose of radiation and whether the cell is p53 competent [193, 221, 222]. In this study we found that EXBR induced G2/M arrest in Panc-1 cells and S phase arrest in Mia PaCa-2 cells. In the literature, a study found that irradiating Panc-1 and Mia PaCa-2 cells with 4 Gy of ionizing radiation induced G2/M arrest [223], supporting our findings in Panc-1, but not in Mia PaCa-2. Our findings in Mia PaCa-2 may be due to the low dose of radiation utilised (0.5 Gy). We found that 0.5 Gy EXBR induced DNA damage and apoptosis in both Panc-1 and Mia

PaCa-2 cells over the time course, which is supported by the literature as studies have shown that radiation induces apoptosis [222].

#### **4.5.2: MMF + EXBR**

As seen in **chapter 3**, the schedule 1 combination of MMF + EXBR, where both agents were administered simultaneously, was of additional benefit over the monotherapies in both Panc-1 and Mia PaCa-2 cells, which resulted in decreased clonogenicity. In an attempt to uncover the mechanism underpinning this combination, the effect of the combination on the cell cycle, apoptosis, DNA damage and glutathione was investigated.

In Panc-1 the schedule 1 combination of MMF + EXBR initially caused an increase in the number of cells in sG1 phase, which corresponded with an increase in apoptosis and DNA damage, however the glutathione level remained unchanged from the untreated control. Later (1 – 24 hours post treatment) the cells began to arrest in S phase, indicating the high level of DNA damage induced initially caused the cells to arrest in S phase due to the activation of the intra-S checkpoint. During this time, the glutathione level increased, and the DNA damage and number of apoptotic cells decreased, indicating that the cells began to repair the damage induced initially. By 36 hours post treatment the cells were arresting in G2/M phase, indicating the cells were unable to continue repairing the damage previously induced which corresponded with an increase in apoptosis and DNA damage, with a decrease in glutathione levels within the cell.

In Mia PaCa-2 the schedule 1 combination of MMF + EXBR initially caused an increase in the number of cells in sG1 phase, which corresponded with an increase in apoptosis. Later (1 – 36 hours post treatment) the DNA damage induced began to increase, as did the number of apoptotic cells and glutathione levels within the cells, however the distribution of cells in the cell cycle remained unchanged when compared

with the untreated control, which suggests that the damaged and apoptotic cells had been disintegrated and removed from the cell population at this time point.

In both cell lines the combination induced apoptosis, however the overall percentage of apoptotic cells was low 36 hours post treatment (15.8% in Panc-1 and 34.6% in Mia PaCa-2), suggesting that an alternative mechanism of cell death may be occurring. Previous studies have shown that there is a link between DMF, and therefore MMF, and the induction of autophagy via NRF2 activity [203, 224]. Autophagy is a highly conserved recycling process in which damaged organelles and proteins are degraded via the lysosome and turned into metabolites to fuel further metabolic processes and pathways [225, 226]. Additionally, autophagy is known to be upregulated in pancreatic cancers (but not in healthy pancreatic tissue) and thought to be one of the main driving factors in disease progression and therapy resistance [226, 227]. It could therefore be the case that the MMF in the combination is further promoting autophagy in the cells to deal with the damage inflicted, hence the low level of apoptosis seen, however further studies would be required to confirm this hypothesis.

As seen in **chapter 3**, the schedule 2 combination of MMF + EXBR, where MMF was incubated with the cells for 24 hours before irradiation, was of additional benefit over the monotherapies in both Panc-1 and Mia PaCa-2, which resulted in decreased clonogenicity. In an attempt to uncover the mechanism underpinning this combination, the effect of the combination on the cell cycle, apoptosis, DNA damage and glutathione was investigated.

In Panc-1 and Mia PaCa-2 cells, immediately post treatment the schedule 2 combination of MMF + EXBR caused an increase in the number of sG1 cells, which corresponded with an increase in apoptosis and DNA damage. One to four hours post treatment the cell cycle remained largely unaffected, and the amount of DNA damage

and apoptosis decreased. Between 24 – 36 hours post treatment the cell cycle remained unaffected, however the level of apoptosis increased despite the DNA damage decreasing. The lack of DNA damage seen could be attributed to the fact that the comet assay was performed under neutral conditions, which is less sensitive at detecting smaller amounts of DNA damage when compared with the alkaline comet assay [91]. To confirm this hypothesis the combination would have to be tested using the alkaline comet assay, or an alternative DNA damage assessing assay such as the  $\gamma$ -H2AX assay [206]. In both cell lines the schedule 2 combination of MMF + EXBR had no effect on the level of glutathione in the cell when compared with the untreated control.

Overall, the combination of MMF + EXBR was highly effective in both Panc-1 and Mia PaCa-2 cells regardless of schedule, however when looking at the mechanistic results when given in schedule 1 (simultaneously) the combination induced sustained cell cycle arrest, as well as DNA damage that was unable to be repaired, suggesting that this schedule of the combination was more effective when compared with the schedule 2 variant. Thus, the schedule 2 combination of MMF + EXBR looks like a promising candidate scheme for investigation *in vivo* and possible clinical translation, however *in vivo* side effects would first have to be assessed.

#### **4.5.3: MMF + gemcitabine**

As seen in **chapter 3**, the schedule 1 combination of MMF + gemcitabine, where both agents were administered simultaneously, was of additional benefit over the monotherapies in Panc-1, however in Mia PaCa-2, the combination was of no additional benefit and did not reduce clonogenicity when compared with the monotherapies. To uncover the mechanism underpinning this combination, the effect of the combination on the cell cycle, apoptosis, DNA damage and glutathione was investigated.

In both Panc-1 and Mia PaCa-2, immediately post treatment with the schedule 1 combination of MMF + gemcitabine, there was an increase in apoptotic cells, which corresponded with an increase in DNA damage, but the cell cycle was initially unaffected in Panc-1, whereas in Mia PaCa-2 the cells began accumulating in S and G2/M phase, indicating the DNA damage induced activated the cell cycle checkpoints to undergo DNA repair. Following this initial increase in DNA damage and apoptotic cells, 1 – 36 hours post treatment the amount of DNA damage present decreased, as did the number of apoptotic cells, however the cells were consistently arresting in G2/M phase for the remainder of the time course, indicating the cells were struggling to deal with the DNA damage initially induced and activation of the G2/M checkpoint. Again, the overall level of apoptosis was low, supporting the hypothesis of an alternative mode of cell death, however the combination did induce more apoptosis than both single agents in both Mia PaCa-2 and Panc-1. However, it may be that an alternative mechanism of apoptosis was at play, and that the cells were apoptosing via caspase cleavage or PAPR cleavage for example, however further studies would be required to confirm this as time did not permit for an alternative assay to be carried out [228, 229].

The glutathione levels within the Panc-1 and Mia PaCa-2 cells remained unchanged throughout the time course when compared with the untreated control, suggesting the MMF indeed reduced glutathione levels within the cell as hypothesised and preventing them from rising in response to ROS resulting from treatment. The reasoning behind the result seen in Mia PaCa-2 is currently unclear, as mechanistically the combination worked almost identically in both cell lines. As Mia PaCa-2 was highly sensitive to gemcitabine monotherapy (**chapter 2**), the added benefit of the combination may have been difficult to determine, therefore the experiment should be repeated using lower doses of gemcitabine that are not highly

cytotoxic alone, to allow any benefit between MMF and gemcitabine in this schedule to be seen. Unfortunately, this combination has not been reported in the literature, therefore no comparisons could be made.

As seen in **chapter 3**, the schedule 3 combination of MMF + gemcitabine, where MMF was incubated with the cells for 24 hours prior to the addition of gemcitabine, was highly effective in both Panc-1 and Mia PaCa-2 when given at lower concentrations. To uncover the mechanism underpinning this combination, the effect of the combination on the cell cycle, apoptosis, DNA damage and glutathione was investigated.

In Panc-1, the schedule 3 combination of MMF + gemcitabine induced an increase in the number of sG1 cells immediately post treatment, which corresponded with an increase in both apoptosis and DNA damage. Between 1 – 4 hours post treatment the number of apoptotic cells decreased, which coincided with a decrease in DNA damage, however the cells began to accumulate in both S phase and G2/M phase. Following this the number of apoptotic cells began to increase between 24 – 36 hours post treatment, with the cells ultimately arresting in G2/M phase, implying that the cells were unable to fully repair the damage induced initially post treatment. Overall, this combination had no effect on the glutathione level of the cell as it remained the same as the untreated control throughout the time course.

In Mia PaCa-2, 0 – 1 hours post treatment, the schedule 3 combination of MMF + gemcitabine induced an increase in the number of sG1 cells, which coincided with an increase in apoptosis and DNA damage. Between 4 – 36 hours the cells began to ultimately arrest in S phase, which corresponded with increasing DNA damage and apoptosis. Following treatment with this combination, the glutathione levels in Mia PaCa-2 increased from 0 – 4 hours, suggesting that there was a large increase in ROS at this time interval, which gemcitabine is known to induce [230]. The glutathione

level then returned to the same level as that of the untreated control 24 – 36 hours post treatment.

As this combination and MMF itself are novel in the treatment of pancreatic cancer there were no other studies available in the literature with which to draw comparisons. It was however noted that in both Panc-1 and Mia PaCa-2 cells in both schedules of MMF + gemcitabine, gemcitabine monotherapy induced more apoptosis than the combination, suggesting that the interaction between MMF and gemcitabine is inducing an alternative mode of cell death, such as autophagy, as previously mentioned DMF is known to induce autophagy, which would imply MMF does as well [203, 224].

#### **4.5.4: DMF + EXBR**

As seen in **chapter 3**, the schedule 2 combination of DMF + EXBR, where cells were incubated with DMF for 24 hours prior to irradiation, was highly effective in both cell lines tested, however the combination was only of additional benefit over the individual components in Mia PaCa-2 cells. In an attempt to uncover the mechanism underpinning this combination, the effect of the combination on the cell cycle, apoptosis, DNA damage and glutathione was investigated.

In Panc-1, the schedule 2 combination of DMF + EXBR overall had no effect on the cell cycle, which was unexpected as the single agents of DMF and EXBR induced G1, and G2/M arrest zero hours post treatment respectively, then the cells began to cycle like the untreated control. This result suggests that the agents are cancelling out each other's effect on the cell cycle. Immediately post treatment the combination induced an increase in both apoptosis and DNA damage, with no change to cellular glutathione levels. Between 1 – 4 hours post treatment the amount of DNA damage and the number of apoptotic cells decreased, which corresponded with an increase in glutathione levels. Between 24 – 36 hours post treatment the amount of apoptotic

cells and DNA damage increased, with the glutathione levels remaining the same as the untreated control. The reduced effectiveness of the schedule 2 combination seen in Panc-1, could be in part due to the inability of the combination to induce any kind of cell cycle arrest. Compared with the single therapies, the schedule 2 combination of DMF + EXBR did not induce more apoptosis or DNA damage in Panc-1, suggesting there is another mechanism underpinning the combination.

In Mia PaCa-2, initially post treatment with the schedule 2 combination of DMF + EXBR induced an increase in apoptosis, however no changes were observed in the cell cycle, DNA damage and glutathione levels. Between 1 – 4 hours post treatment the number of apoptotic cells decreased overall, but the level of DNA damage increased, which could in part be due to the observed increase in glutathione levels. This subsequently led to an increase in the number of sG1 cells 24 – 36 hours post treatment, which coincided with an increase in DNA damage and apoptosis. This result was not unexpected as previous studies have demonstrated DMF inducing apoptosis in pancreatic cancer, as well as other cancers [214, 231]. EXBR alone induced more apoptosis than the combination in Mia PaCa-2, again suggesting as previously mentioned that an alternative mode of cell death is being induced by the combination. The combination did not have a significant effect on the cell cycle, when compared with DMF monotherapy, suggesting that much of the activity from the combination observed in Mia PaCa-2 comes from DMF and not EXBR.

Again, the overall level of apoptosis observed was low after treatment in both cell lines, reinforcing the hypothesis that an alternative mechanism of cell death is at play, and the combination did not induce more DNA damage than the single therapies or alter the cell cycle, suggesting that overall, the combination of DMF + EXBR is inducing its cytotoxic effect in an alternative manner to those tested in this study. To confirm this hypothesis further studies would be required.

#### **4.5.5: Summary**

Overall DMF and MMF did not function as expected over the analysed time course, as both as a single agent and in combination the glutathione levels did not differ from the untreated control, suggesting that the concentration of the drugs was insufficiently high to inhibit NRF2 activity, or that the reduction of glutathione occurs earlier more immediately after administration of the drugs.

In the literature, a limited number of studies have shown that DMF induces G1 phase arrest, and although no studies utilising MMF could be found, as it is the active metabolite of DMF we assume it will exhibit the same effect. From our studies, we cannot conclude what effect DMF and MMF have on the cell cycle, as the results varied between each of the two cell lines used in this study and there was no clear phase of cell cycle arrest when given as a single agent. In combination with gemcitabine or EXBR, MMF appears to induce S and or G2/M arrest. DMF in combination with EXBR had no effect on the cell cycle overall.

In Panc-1 cells, only MMF + EXBR (schedule 1) induced sustained DNA damage by the end of the time course. The DNA damage induced by the remaining combinations was resolved by the end of the time course in Panc-1 cells. In Mia PaCa-2 cells, all combinations tested induced sustained DNA damage by the end of the time course. This suggests that DDR mechanisms are more upregulated in the Panc-1 cell line.

Unexpectedly, the glutathione levels increased in the control of both cell lines starting at 24 hours post treatment. One possible explanation of this is that studies have shown that total glutathione levels increase within the cell during G1 phase of the cell cycle as the cell begins to transition to S phase [232]. Therefore, it may be possible that the increase in glutathione observed 24 hours post treatment could be due to cells preparing to enter the S phase, as both cell lines have a doubling time of approximately 24 hours, so at this time point they may have been preparing to enter

another round of cell division. However, this hypothesis could not be confirmed by the cell cycle data obtained as there was no increase in G1 phase at this time point, although this was for different cell populations under different experimental conditions than those used in the glutathione assay.

As previously discussed, the overall level of apoptosis induced by the various therapies was low given the results seen in previous chapters that suggest the drugs to be highly cytotoxic, suggesting that an alternative mechanism of cell death, such as autophagy or ferroptosis, is at play or that the assay chosen to measure apoptosis was inefficient in this cell line.

Overall, the combination of MMF + EXBR, regardless of schedule, showed the most promise for the treatment of pancreatic cancers. Additionally, we believe MMF + gemcitabine (schedule 1) showed promise; however, it was more effective in Panc-1 than Mia PaCa-2, suggesting its effectiveness might not be universal.

## **CHAPTER 5: Discussion, conclusions, & future work**

## 5.2: Discussion & Future work

Pancreatic cancer is one of the most lethal cancers, with the average five-year survival rate being 9% globally [44]. This appalling survival rate is mainly due to two factors: late diagnosis and chemoresistance, with the current gold standard therapy gemcitabine being only effective for 20% of patients [88], which leaves patients with limited options, highlighting the need for alternative therapies. We identified DMF and MMF as a potential candidate for the treatment of pancreatic cancers due to its reported ability to reduce glutathione levels within the cell, which we hypothesised would lead to the chemo- and radio-sensitisation of pancreatic cancer cells [111]. Therefore, we aimed to develop novel combination therapies utilising both DMF and MMF.

Firstly, we characterised the cytotoxic effects of both DMF and MMF alone. From our data overall, MMF was more effective as a cytotoxic agent than DMF, as MMF induced a greater proportion of cytotoxicity in both Panc-1 and Mia PaCa-2 cell lines both in 2D and 3D cell models. However, it was noted that Mia PaCa-2 cells exhibited a higher sensitivity to DMF when compared with Panc-1, although this effect was still lesser than that of MMF, which we propose is due to the rarer KRAS mutation present in this cell line, as DMF is known to have preferential activity in specific KRAS mutants [112]. However further studies would be required to confirm this hypothesis. Given the difference in cytotoxicity observed between DMF and MMF monotherapy, this leads us to believe that the prodrug DMF was not being hydrolysed into MMF at a high rate as in the body DMF is reported to have a half-life of 12 minutes, implying that 24 and 48-hour incubation times should have been more than sufficient for conversion into MMF. The hydrolysis of DMF into MMF is carried out by digestive esterases present within the GI tract, and it is unclear if such enzymes are present in *in vitro* cell cultures, which could account for the differences in cytotoxicity observed

as only a small fraction of DMF may have been converted into MMF [122-125]. A study in the literature found that carboxylesterase 1 (CES1) is the digestive esterase responsible for the hydrolysis of DMF into MMF and methanol, with the authors hypothesising that alcohol (methanol) limits the effectiveness of DMF/MMF [233]. The Panc-1 cell line has a higher expression of CES1 when compared with Mia PaCa-2 (32.5 vs 0.3 nTPM), which we believe could account for the difference in activity, as DMF will be hydrolysed more readily in Panc-1 cells, methanol will build up in the cells at a greater rate when compared with Mia PaCa-2 cells, therefore limiting the overall effectiveness of the drug. A diagrammatic representation of this hypothesised mechanism is displayed in **appendix 12**. Therefore, giving DMF in the active metabolite form (MMF) circumvents the build-up of methanol and allows the cytotoxic effect to be seen [233, 234]. However, despite Panc-1 expressing a far greater amount of CES1 than Mia PaCa-2, overall, the pancreatic cancer cell lines express a reduced level of CES1 when compared to gallbladder or liver cancer [234].

While we speculate that KRAS mutation and drug metabolism could account for the differences observed in cytotoxicity between DMF and MMF, we also believe that the drugs may be working entirely differently despite being regarded as prodrug and active metabolite. To confirm this hypothesis further studies would be required that are out with the scope of this project.

When we assessed both DMF and MMF as part of combination therapies, the trend observed between DMF and MMF monotherapy continued into the developed combinations, with MMF based combinations being more effective overall as they reduced spheroid growth more than the individual agents.

The literature has proposed that the anticancer mechanism of action for DMF/MMF was inhibition of the transcription factor NRF2, and reduction of glutathione levels within the cell, which would leave the cancer cell more vulnerable to oxidative damage

via ROS and ultimately cell death [117]. However, this mechanism was unable to be confirmed in the studies carried out as the glutathione level was never observed to be decreased by the administration of the drugs over the selected time course. However, it may be that the selected time points were too late after the initial administration of the drug to see the effect, as other studies within our lab indicate that DMF reduces glutathione levels within hours of administering the drug, therefore this suggests that the selected time points for analysis of glutathione levels in this study were incorrect [195]. Additionally, as the half-life of DMF and MMF (12 & 30 minutes respectively) is short, it may be that by the time the samples were collected for glutathione analysis, the drugs had been fully metabolised, and therefore no longer reducing the glutathione levels within the cell. To answer this hypothesis the glutathione levels should be checked immediately following treatment administration, not post treatment and an alternative mode of measurement of glutathione levels should be investigated as we believe the kit that was utilised was not optimal. Another possible explanation for the lack of effect on glutathione levels observed may be due to both Panc-1 and Mia PaCa-2 being p53 mutants, which has been reported in the literature to upregulate NRF2 activity, therefore the anti NRF2 activity reported by DMF may have been counteracted by mutant p53 activity, causing the cells to have neither an increase nor decrease in glutathione levels [217]. As an alternative means of assessing if DMF/MMF inhibits NRF2 activity, we could have assessed NRF2 expression via Western blotting to determine if the drugs were having the hypothesised effect of inhibiting NRF2 expression.

The mechanism of cell death caused by DMF/MMF was unclear from the data obtained, as both agents consistently induced a low level of apoptosis, which did not correspond with the high levels of cytotoxicity observed. Literature suggests that DMF induces apoptosis, however an alternative mechanism of apoptosis may also have

occurred in Panc-1 and Mia PaCa-2 cells, which would not have been detected by the apoptosis assay utilised, as we only looked for the presence of annexin V, therefore other apoptotic markers such as PARP cleavage or caspase cleavage should have been explored, however due to time constraints this was not feasible [203, 228, 229]. Alternatively, an alternative mechanism of cell death is at play, with autophagy appearing to be a likely suspect due to the links between DMF and autophagy upregulation observed in the literature [203, 224] and the well documented upregulation of autophagy in pancreatic cancers [226-229]. To determine if this hypothesis is correct an assay to quantify autophagy would have to be carried out. This was attempted, but due to time constraints and issues in obtaining a signal in the positive control, it was unable to be determined if autophagy was taking place. However, we are developing alternative protocols within the lab group to quantify autophagy utilising Western blotting. Alternatively, in the literature it has been shown that DMF induces ferroptosis, which is known to be involved in cell death in KRAS mutant pancreatic cells [214, 235, 236]. Additionally, the dysregulation of NRF2 activity is speculated to be involved in the ferroptosis pathway [236]. Therefore, DMF and MMF may be inducing ferroptosis in Panc-1 and Mia PaCa-2 cells which is being mediated by dysregulation of the NRF2 pathway, however further studies would be required to investigate this hypothesis.

When looking at the effects of DMF and MMF on the cell cycle and DNA damage/repair, we found that MMF induced an increase in the number of cells in sG1 phase in both Panc-1 and Mia PaCa-2. DMF however had different effects on the cell cycle depending on the cell line, as in Panc-1 it induced cells to accumulate in G1 phase, whereas in Mia PaCa-2 it caused cells to accumulate in sG1 phase. This data again suggests DMF has differential activity in the two cell lines, which we believe to be due to the difference in KRAS mutation between Panc-1 and Mia PaCa-2 [112].

Interestingly, the DNA damage induced by DMF/MMF monotherapy in Panc-1 was fully repaired by the end of the time course (0 – 36 hours post treatment) analysed in this study, however in Mia PaCa-2 the induced DNA damage was not fully repaired, again suggesting that the Mia PaCa-2 cell line is more sensitive to fumarates overall. In combination the effects of DMF/MMF on the cell cycle differed, with the majority of the developed novel combinations inducing an increase in the number of cells in G2/M phase, suggesting that the fumarates are working in an alternative manner in combination EXBR and gemcitabine.

We found the combinations of MMF + EXBR; DMF + EXBR; and MMF + gemcitabine exhibited significantly greater effectiveness in 2D cell models in both Panc-1 and Mia PaCa-2 cells when analysed via the clonogenic assay. However, this rarely translated into the 3D spheroid model, with combinations being of no additional benefit over the individual agents when tested in the 3D spheroid model. We hypothesise that the reduced effectiveness of the combinations in Panc-1 and Mia PaCa-2 spheroids was due to the monotherapies being highly effective at reducing spheroid growth alone. To further test the combinations in a 3D cell model, the combinations should be tested in an *in vivo* model, such as the chick embryo model, which we have been establishing in our lab to enable us to assess promising combination schedules *in vivo* without the need to utilise murine cancer models [237, 238]. This would adhere to the principles of the 3Rs as the model is cheaper, higher throughput and partially replaces the use of rodents [237, 238]. Unfortunately, the model has yet to be reproducibly established in our lab, however preliminary studies show promise that the model would be a suitable and cost-effective means of assessing the developed combinations *in vivo*. However, alternative considerations may have to be made when assessing DMF and MMF *in vivo* as it has been reported in the literature that DMF induces changes in the distribution of immune cells, which could have an impact on the anti-cancer effects,

therefore an alternative animal model may have to be utilised, such as a syngeneic mouse model or a humanised mouse model [239].

Future work would include finding an alternative way of assessing glutathione levels within the cell and testing for changes in glutathione at much earlier time points to see if DMF/MMF is indeed reducing glutathione as proposed in the literature. Additionally, Western blotting experiments would be carried out to determine if autophagy is the mode of cell death as hypothesised. Finally, the combinations should be tested in an *in vivo* model to further assess the validity of the combinations.

## **5.2: Limitations**

The limitations of this study are that both DMF/MMF and the developed combinations were only tested in immortalised pancreatic cancer cell lines, which are noted to have several disadvantages over primary pancreatic tumour cells such as: altered phenotype and epigenetic changes that less adequately reflect a patient [240]. As this study was not carried out in primary cells or in an *in vivo* model, we cannot definitively conclude that the effects seen *in vitro* would translate clinically. Additionally, it was hoped to trial the developed combinations in an in house developed cell line that was resistant to gemcitabine monotherapy to allow the efficacy of the combinations to be assessed as a means of overcoming gemcitabine resistance, however all attempts to create this cell line resulted in cells that were more sensitive to gemcitabine than the original parental cells.

As the combination therapy experiments carried out in this study only consisted of three concentrations of each combination, no conclusions could be made surrounding synergy or antagonism of the developed combinations. To enable synergism to be analysed the combinations would have to be assessed with a minimum of four concentrations. Additionally, the SynergyFinder+ software should be used to interpret

synergism, rather than other software that rely on combination index analysis that utilise the Chou-Talalay method.

As the cell cycle studies carried out did not utilise an antibody, such as phosphor-histone H3 which is expressed exclusively in M phase, to distinguish between G2 and M phase, some information about the effects of treatments on the cell cycle may have been lost. Therefore, to improve these experiments the inclusion of such an antibody would allow us to distinguish between G2 and M phase.

We don't believe the glutathione assay kit we used was an adequate means of determining the glutathione levels within the cell as we encountered multiple issues when using this kit and believe an alternative means of assessing glutathione would have yielded more representative results and allowed us to see the reported effect of DMF in which it depletes glutathione. If these experiments were to be repeated, monochlorobimane could be used. Monochlorobimane is a cell permeable fluorescent probe that binds to intracellular glutathione to create a fluorescent product which can then be detected by a fluorimeter. This would be more advantageous as the cell's glutathione levels could be analysed live, opposed to the kit we utilised where cells had to be harvested, lysed, etc before the glutathione levels could be assessed, which may have allowed time for glutathione levels to be altered due to stress induced by the harvesting process.

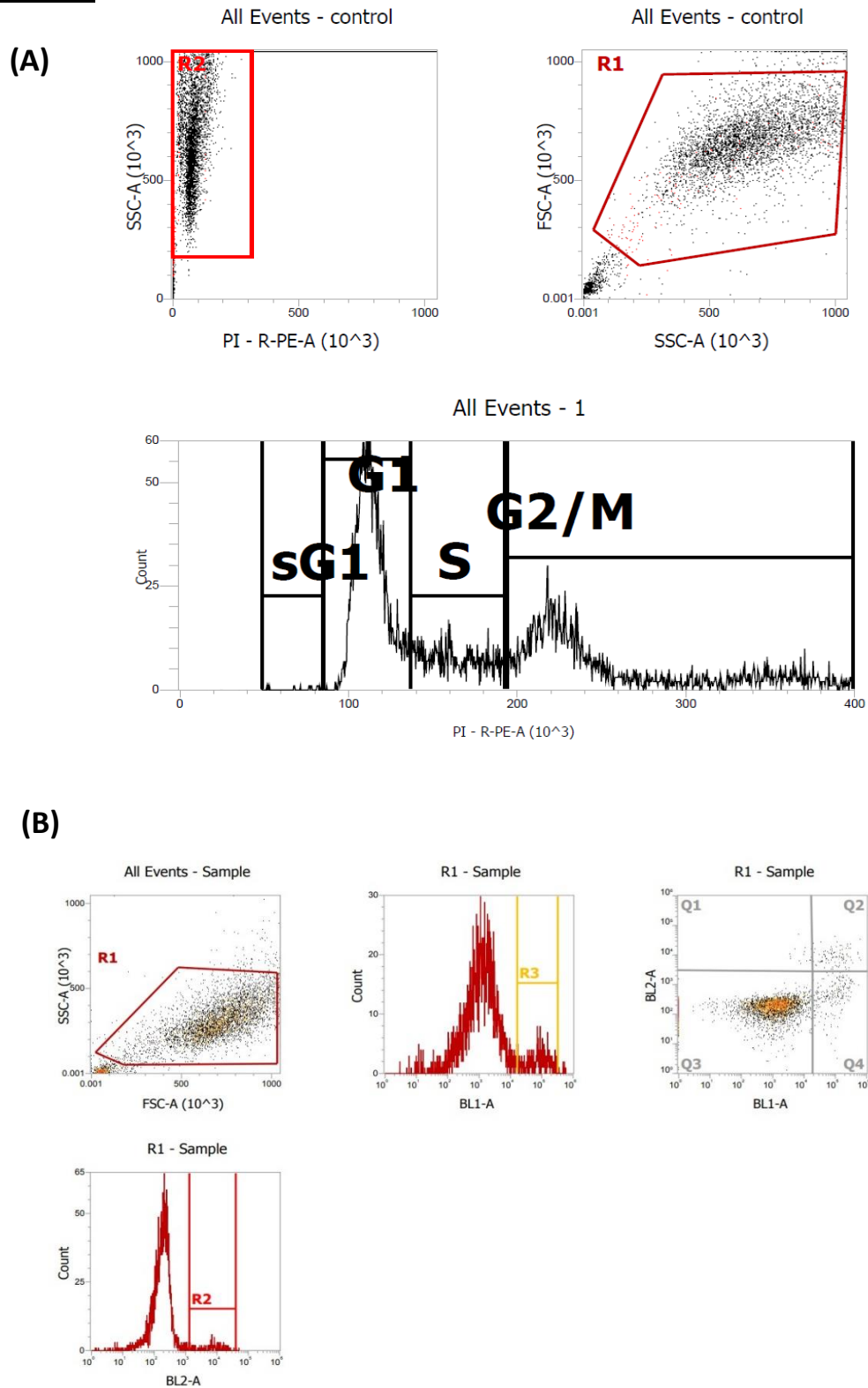
### **5.3: Final Conclusions**

We conclude that MMF shows promise as a chemotherapeutic agent for the treatment of pancreatic cancers, and that out of all the combinations assessed the schedule 1 (simultaneous administration) combination of MMF + EXBR shows the most promise as a combination therapy for the treatment of pancreatic cancers. However, further studies to elucidate the specific mechanism of action of MMF and *in vivo* studies would be required to fully assess the drug as both a monotherapy and in combination.

Overall, DMF was less potent than MMF, and less efficacious in combination when compared with MMF. The schedule 2 combination of DMF + EXBR only showed promise in the Mia PaCa-2 cell line, however it effectively reduced the growth of spheroids in both cell lines, suggesting this combination may have some efficacy, but further studies would be required to confirm this hypothesis.

Additionally, the schedule 1 combination of MMF + gemcitabine showed some promise, although the major drawback of this combination is that it contains gemcitabine, which as has been discussed throughout has limited efficacy in the clinical due to a multitude of reasons, therefore the benefit of this combination clinically could be limited. Therefore, further *in vivo* studies would be required before considering this combination to be truly efficacious.

## APPENDIX



**Appendix 1: Representative flow cytometry plots.** (A) Cell cycle FSC/SSC and gating strategies. (B) Annexin V FSC/SSC and gating strategies. BL1 = FITC, BL2 = PI, Q1 = necrosis, Q2 = late apoptosis, Q3 = non apoptotic cells and Q4 = early apoptosis.

**Appendix 2: Distribution of Panc-1 cells in the cell cycle zero hours post treatment**

<b>Treatment</b>	<b>% of cells in sG1 phase</b>	<b>% of cells in G1 phase</b>	<b>% of cells in S phase</b>	<b>% of cells in G2/M</b>
Control	0.19	45.64	13.47	40.68
Gemcitabine	1.64	26.77	20.0	51.57
DMF	0.32	32.83	22.33	44.50
MMF	21.32	34.26	22.94	21.46
EXBR	1.20	42.65	16.01	39.70
MMF + EXBR (Schedule 1)	17.28	36.74	23.76	22.20
MMF + gemcitabine (Schedule 1)	0.58	37.62	16.73	45.05
MMF + EXBR (Schedule 2)	26.57	24.64	23.44	26.40
DMF + EXBR (Schedule 2)	0.65	39.57	19.55	40.20
MMF + gemcitabine (Schedule 3)	20.48	33.75	24.39	21.36

**Appendix 3: Distribution of Panc-1 cells in the cell cycle one hour post treatment**

<b>Treatment</b>	<b>% of cells in sG1 phase</b>	<b>% of cells in G1 phase</b>	<b>% of cells in S phase</b>	<b>% of cells in G2/M</b>
Control	0.51	43.12	15.91	40.44
Gemcitabine	1.77	13.43	27.22	57.56
DMF	0.55	40.89	16.26	42.28
MMF	9.79	43.97	17.17	29.05
EXBR	0.93	48.77	9.95	40.33
MMF + EXBR (Schedule 1)	0.22	42.70	13.74	43.32
MMF + gemcitabine (Schedule 1)	1.27	24.27	17.67	56.77
MMF + EXBR (Schedule 2)	8.70	41.11	18.24	31.93
DMF + EXBR (Schedule 2)	0.40	36.32	14.10	49.16
MMF + gemcitabine (Schedule 3)	0.42	42.71	11.73	45.12

**Appendix 4: Distribution of Panc-1 cells in the cell cycle four hours post treatment**

<b>Treatment</b>	<b>% of cells in sG1 phase</b>	<b>% of cells in G1 phase</b>	<b>% of cells in S phase</b>	<b>% of cells in G2/M</b>
Control	0.73	58.30	21.14	19.82
Gemcitabine	1.47	49.15	17.99	31.37
DMF	1.55	53.58	17.19	27.66
MMF	0.42	46.08	19.18	34.31
EXBR	0.37	36.01	16.97	46.63
MMF + EXBR (Schedule 1)	0.25	1.42	47.10	51.21
MMF + gemcitabine (Schedule 1)	0.59	2.97	33.78	62.63
MMF + EXBR (Schedule 2)	1.23	43.51	20.90	34.34
DMF + EXBR (Schedule 2)	0.29	56.68	15.84	27.17
MMF + gemcitabine (Schedule 3)	0.62	0.67	48.32	50.37

**Appendix 5: Distribution of Panc-1 cells in the cell cycle 24 hours post treatment**

<b>Treatment</b>	<b>% of cells in sG1 phase</b>	<b>% of cells in G1 phase</b>	<b>% of cells in S phase</b>	<b>% of cells in G2/M</b>
Control	1.36	63.19	17.12	18.31
Gemcitabine	0.45	57.98	18.58	22.97
DMF	2.84	75.62	10.28	11.24
MMF	2.02	72.56	12.91	12.49
EXBR	0.37	58.85	25.82	14.94
MMF + EXBR (Schedule 1)	0.39	4.46	57.53	37.59
MMF + gemcitabine (Schedule 1)	1.73	7.05	42.40	48.80
MMF + EXBR (Schedule 2)	0.40	66.82	14.19	18.57
DMF + EXBR (Schedule 2)	0.25	72.64	13.19	13.89
MMF + gemcitabine (Schedule 3)	0.52	7.44	57.58	34.45

**Appendix 6: Distribution of Panc-1 cells in the cell cycle 36 hours post treatment**

<b>Treatment</b>	<b>% of cells in sG1 phase</b>	<b>% of cells in G1 phase</b>	<b>% of cells in S phase</b>	<b>% of cells in G2/M</b>
Control	0.57	61.57	17.64	20.20
Gemcitabine	0.32	39.06	20.06	40.54
DMF	0.49	66.67	16.25	16.58
MMF	0.18	59.05	21.56	19.19
EXBR	0.31	61.94	19.48	18.25
MMF + EXBR (Schedule 1)	0.34	40.23	16.19	43.22
MMF + gemcitabine (Schedule 1)	1.01	6.07	31.70	61.21
MMF + EXBR (Schedule 2)	0.26	70.51	12.71	16.49
DMF + EXBR (Schedule 2)	0.31	65.55	16.20	17.93
MMF + gemcitabine (Schedule 3)	0.23	41.11	20.33	38.31

**Appendix 7: Distribution of Mia PaCa-2 cells in the cell cycle zero hours post treatment**

<b>Treatment</b>	<b>% of cells in sG1 phase</b>	<b>% of cells in G1 phase</b>	<b>% of cells in S phase</b>	<b>% of cells in G2/M</b>
Control	0.19	45.64	13.47	40.68
Gemcitabine	1.64	26.77	20.0	51.57
DMF	0.32	32.83	22.33	44.50
MMF	21.32	34.26	22.94	21.46
EXBR	1.20	42.65	16.01	39.70
MMF + EXBR (Schedule 1)	17.28	36.74	23.76	22.20
MMF + gemcitabine (Schedule 1)	0.58	37.62	16.73	45.05
MMF + EXBR (Schedule 2)	26.57	24.64	23.44	26.40
DMF + EXBR (Schedule 2)	0.65	39.57	19.55	40.20
MMF + gemcitabine (Schedule 3)	20.48	33.75	24.39	21.36

**Appendix 8: Distribution of Mia PaCa-2 cells in the cell cycle one hour post treatment**

<b>Treatment</b>	<b>% of cells in sG1 phase</b>	<b>% of cells in G1 phase</b>	<b>% of cells in S phase</b>	<b>% of cells in G2/M</b>
Control	0.51	43.12	15.91	40.44
Gemcitabine	1.77	13.43	27.22	57.56
DMF	0.55	40.89	16.26	42.28
MMF	9.79	43.97	17.17	29.05
EXBR	0.93	48.77	9.95	40.33
MMF + EXBR (Schedule 1)	0.22	42.70	13.74	43.32
MMF + gemcitabine (Schedule 1)	1.27	24.27	17.67	56.77
MMF + EXBR (Schedule 2)	8.70	41.11	18.24	31.93
DMF + EXBR (Schedule 2)	0.40	36.32	14.10	49.16
MMF + gemcitabine (Schedule 3)	0.42	42.71	11.73	45.12

**Appendix 9: Distribution of Mia PaCa-2 cells in the cell cycle four hours post treatment**

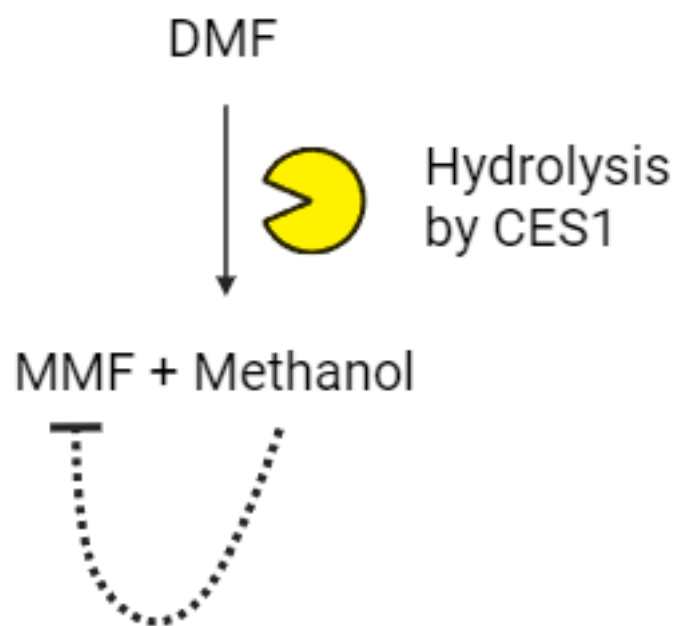
<b>Treatment</b>	<b>% of cells in sG1 phase</b>	<b>% of cells in G1 phase</b>	<b>% of cells in S phase</b>	<b>% of cells in G2/M</b>
Control	0.73	58.30	21.14	19.82
Gemcitabine	1.47	49.15	17.99335	31.37
DMF	1.55	53.58	17.19	27.66
MMF	0.42	46.08	19.18	34.31
EXBR	0.37	36.01	16.97	46.63
MMF + EXBR (Schedule 1)	0.25	1.42	47.10	51.21
MMF + gemcitabine (Schedule 1)	0.59	2.97	33.78	62.63
MMF + EXBR (Schedule 2)	1.23	43.51	20.90	34.34
DMF + EXBR (Schedule 2)	0.29	56.68	15.84	27.17
MMF + gemcitabine (Schedule 3)	0.62	0.67	48.32	50.37

**Appendix 10: Distribution of Mia PaCa-2 cells in the cell cycle 24 hours post treatment**

<b>Treatment</b>	<b>% of cells in sG1 phase</b>	<b>% of cells in G1 phase</b>	<b>% of cells in S phase</b>	<b>% of cells in G2/M</b>
Control	1.36	63.19	17.12	18.31
Gemcitabine	0.45	57.98	18.58	22.97
DMF	2.84	75.62	10.28	11.24
MMF	2.02	72.56	12.91	12.49
EXBR	0.37	58.8	25.82	14.94
MMF + EXBR (Schedule 1)	0.39	4.4	57.53	37.59
MMF + gemcitabine (Schedule 1)	1.73	7.05	42.40	48.80
MMF + EXBR (Schedule 2)	0.40	66.82	14.19	18.57
DMF + EXBR (Schedule 2)	0.25	72.64	13.19	13.89
MMF + gemcitabine (Schedule 3)	0.52	7.44	57.58	34.45

**Appendix 11: Distribution of Mia PaCa-2 cells in the cell cycle 36 hours post treatment**

<b>Treatment</b>	<b>% of cells in sG1 phase</b>	<b>% of cells in G1 phase</b>	<b>% of cells in S phase</b>	<b>% of cells in G2/M</b>
Control	0.57	61.57	17.64	20.20
Gemcitabine	0.32	39.06	20.06	40.54
DMF	0.49	66.67	16.25	16.58
MMF	0.18	59.05	21.56	19.19
EXBR	0.31	61.94	19.48	18.25
MMF + EXBR (Schedule 1)	0.34	40.23	16.19	43.22
MMF + gemcitabine (Schedule 1)	1.01	6.07	31.70	61.21
MMF + EXBR (Schedule 2)	0.26	70.51	12.71	16.49
DMF + EXBR (Schedule 2)	0.31	65.55	16.20	17.93
MMF + gemcitabine (Schedule 3)	0.23	41.11	20.33	38.31



Created in BioRender.com bio

**Appendix 12: Inhibition of MMF via production of methanol.** DMF is hydrolysed by the digestive esterase CES1 into MMF and methanol. Alcohol is known to inhibit MMF activity, therefore cell lines that highly express CES1 may reduce MMF effectiveness.

## REFERENCES

1. World Health Organization. *Cancer*. 2023 [8 January 2024]; Available from: <https://www.who.int/news-room/fact-sheets/detail/cancer>
2. World Cancer Research Fund International. *Pancreatic cancer statistics*. 2023 [8 January 2024]; Available from: <https://www.wcrf.org/cancer-trends/pancreatic-cancer-statistics/>
3. International Agency for Research on Cancer. *Estimated number of new cases in 2020, World, both sexes, all ages (excl. NMSC)*. 2023 [8 January 2024]; Available from: <https://gco.iarc.fr/today/online-analysis-table>
4. Shelton, J., et al., *25 year trends in cancer incidence and mortality among adults aged 35-69 years in the UK, 1993-2018: retrospective secondary analysis*. *BMJ*, 2024. **384**: p. e076962.
5. Kim, H.I., H. Lim, and A. Moon, *Sex Differences in Cancer: Epidemiology, Genetics and Therapy*. *Biomol Ther (Seoul)*, 2018. **26**(4): p. 335-342.
6. Sung, H., et al., *Global Cancer Statistics 2020: GLOBOCAN Estimates of Incidence and Mortality Worldwide for 36 Cancers in 185 Countries*. *CA: A Cancer Journal for Clinicians*, 2021. **71**(3): p. 209-249.
7. Nenciarelli, P. and K.J. Harrington, *The biology of cancer*. *Medicine*, 2020. **48**(2): p. 67-72.
8. Olafsson, S. and C.A. Anderson, *Somatic mutations provide important and unique insights into the biology of complex diseases*. *Trends in Genetics*, 2021. **37**(10): p. 872-881.
9. Hanahan, D., *Hallmarks of Cancer: New Dimensions*. *Cancer Discovery*, 2022. **12**(1): p. 31-46.
10. Dagogo-Jack, I. and A.T. Shaw, *Tumour heterogeneity and resistance to cancer therapies*. *Nature Reviews Clinical Oncology*, 2018. **15**(2): p. 81-94.
11. Ye, Z., et al., *Function and Molecular Mechanism of the DNA Damage Response in Immunity and Cancer Immunotherapy*. *Frontiers in Immunology*, 2021. **12**.
12. Choi, W. and E.S. Lee, *Therapeutic Targeting of DNA Damage Response in Cancer*. *International Journal of Molecular Sciences*, 2022. **23**(3): p. 1701.
13. Alberts, B., Johnson, A., Lewis, J., Raff, M., Roberts, K., & Walter, P., *Molecular Biology of the Cell*. 4th ed. 2002, New York: Garland Science.
14. Cooper, G.M., & Hausman, R. E., *The Cell: A Molecular Approach*. 5th ed. 2007, Washington D.C: ASM Press.
15. Lodish, H., Berk, A., Kaiser, C. A., Krieger, M., Bretscher, A., Ploegh, H., Amon, A., & Scott, M. P., *Molecular Cell Biology*. 8th ed. 2016, New York: W.H. Freeman.
16. Morgan, D.O., *Cell Cycle: Principles of Control*. 2006, London: New Science Press.
17. Weinberg, R.A., *The Biology of Cancer*. 2nd ed. 2013: Garland Science.
18. Zhou, B.B. and S.J. Elledge, *The DNA damage response: putting checkpoints in perspective*. *Nature*, 2000. **408**(6811): p. 433-9.
19. Bartek, J. and J. Lukas, *Chk1 and Chk2 kinases in checkpoint control and cancer*. *Cancer Cell*, 2003. **3**(5): p. 421-9.
20. Cimprich, K.A. and D. Cortez, *ATR: an essential regulator of genome integrity*. *Nat Rev Mol Cell Biol*, 2008. **9**(8): p. 616-27.
21. Byun, T.S., et al., *Functional uncoupling of MCM helicase and DNA polymerase activities activates the ATR-dependent checkpoint*. *Genes Dev*, 2005. **19**(9): p. 1040-52.

22. Elmore, S., *Apoptosis: A Review of Programmed Cell Death*. Toxicologic Pathology, 2007. **35**(4): p. 495-516.
23. Taylor, R.C., S.P. Cullen, and S.J. Martin, *Apoptosis: controlled demolition at the cellular level*. Nature Reviews Molecular Cell Biology, 2008. **9**(3): p. 231-241.
24. Fuchs, Y. and H. Steller, *Programmed cell death in animal development and disease*. Cell, 2011. **147**(4): p. 742-58.
25. Green, D.R. and F. Llambi, *Cell Death Signaling*. Cold Spring Harb Perspect Biol, 2015. **7**(12).
26. Green, D.R., L. Galluzzi, and G. Kroemer, *Mitochondria and the autophagy-inflammation-cell death axis in organismal aging*. Science, 2011. **333**(6046): p. 1109-12.
27. Kumar, V., Abbas, A. K., & Aster, J. C., *Robbins and Cotran Pathologic Basis of Disease*. 10th ed. 2021: Elsevier.
28. Fink, S.L. and B.T. Cookson, *Apoptosis, pyroptosis, and necrosis: mechanistic description of dead and dying eukaryotic cells*. Infect Immun, 2005. **73**(4): p. 1907-16.
29. Karsch-Bluman, A., et al., *Tissue necrosis and its role in cancer progression*. Oncogene, 2019. **38**(11): p. 1920-1935.
30. Levy, J.M.M., C.G. Towers, and A. Thorburn, *Targeting autophagy in cancer*. Nat Rev Cancer, 2017. **17**(9): p. 528-542.
31. Shintani, T. and D.J. Klionsky, *Autophagy in health and disease: a double-edged sword*. Science, 2004. **306**(5698): p. 990-5.
32. Dixon, S.J., et al., *Ferroptosis: an iron-dependent form of nonapoptotic cell death*. Cell, 2012. **149**(5): p. 1060-72.
33. Yang, W.S. and B.R. Stockwell, *Ferroptosis: Death by Lipid Peroxidation*. Trends Cell Biol, 2016. **26**(3): p. 165-176.
34. Feng, H. and B.R. Stockwell, *Unsolved mysteries: How does lipid peroxidation cause ferroptosis?* PLoS Biol, 2018. **16**(5): p. e2006203.
35. Li, J., et al., *Ferroptosis: past, present and future*. Cell Death & Disease, 2020. **11**(2): p. 88.
36. Talathi, S.S., Zimmerman, R. and Young, M, *Anatomy, Abdomen and Pelvis, Pancreas*. 2023, Treasure Island (FL): StatPearls Publishing.
37. Mahadevan, V., *Anatomy of the pancreas and spleen*. Surgery - Oxford International Edition, 2019. **37**(6): p. 297-301.
38. S.J., P., *The Exocrine Pancreas*. 2013, San Rafael (CA): Morgan & Claypool Life Sciences.
39. Sarantis, P., et al., *Pancreatic ductal adenocarcinoma: Treatment hurdles, tumor microenvironment and immunotherapy*. World J Gastrointest Oncol, 2020. **12**(2): p. 173-181.
40. Ro, C., et al., *Pancreatic neuroendocrine tumors: biology, diagnosis, and treatment*. Chin J Cancer, 2013. **32**(6): p. 312-24.
41. Mizrahi, J.D., et al., *Pancreatic cancer*. The Lancet, 2020. **395**(10242): p. 2008-2020.
42. Li, D., et al., *Pancreatic cancer*. The Lancet, 2004. **363**(9414): p. 1049-1057.
43. Bliss, D., *Pancreas, Duodenum, and Small Intestine* 2001, National Cancer Institute.
44. Rawla, P., T. Sunkara, and V. Gaduputi, *Epidemiology of Pancreatic Cancer: Global Trends, Etiology and Risk Factors*. World J Oncol, 2019. **10**(1): p. 10-27.
45. Park, W., A. Chawla, and E.M. O'Reilly, *Pancreatic Cancer: A Review*. Jama, 2021. **326**(9): p. 851-862.

46. American Cancer Society. *Pancreatic Cancer Risk Factors*. 2023 [8 January 2024]; Available from: <https://www.cancer.org/cancer/types/pancreatic-cancer/causes-risks-prevention/risk-factors.html>
47. Pancreatic Cancer Action Network. *Staging*. 2023 [8 January 2024]; Available from: <https://pancan.org/facing-pancreatic-cancer/diagnosis/staging/>
48. Vincent, A., et al., *Pancreatic cancer*. *Lancet*, 2011. **378**(9791): p. 607-20.
49. Hidalgo, M., *Pancreatic Cancer*. *New England Journal of Medicine*, 2010. **362**(17): p. 1605-1617.
50. American Cancer Society. *Pancreatic Cancer Stages*. 2023 [8 January 2024]; Available from: <https://www.cancer.org/cancer/types/pancreatic-cancer/detection-diagnosis-staging/staging.html>
51. Ilic, I. and M. Ilic, *International patterns in incidence and mortality trends of pancreatic cancer in the last three decades: A joinpoint regression analysis*. *World J Gastroenterol*, 2022. **28**(32): p. 4698-4715.
52. Cancer Research UK. *Cancer Statistics for the UK*. 2023 [8 January 2024]; Available from: <https://www.cancerresearchuk.org/health-professional/cancer-statistics-for-the-uk>
53. National Cancer Institute. *Cancer Stat Facts: Pancreatic Cancer*. 2023 [8 January 2024]; Available from: <https://seer.cancer.gov/statfacts/html/pancreas.html>
54. International, W.C.R.F. *Global cancer data by country*. 2023 [8 January 2024]; Available from: <https://www.wcrf.org/cancer-trends/global-cancer-data-by-country/>
55. Kamisawa, T., et al., *Pancreatic cancer*. *The Lancet*, 2016. **388**(10039): p. 73-85.
56. Wang, F., et al., *SMAD4 Gene Mutation Renders Pancreatic Cancer Resistance to Radiotherapy through Promotion of Autophagy*. *Clinical Cancer Research*, 2018. **24**(13): p. 3176-3185.
57. American Cancer Society. *Survival Rates for Pancreatic Cancer*. 2023 [8 January 2024]; Available from: <https://www.cancer.org/cancer/types/pancreatic-cancer/detection-diagnosis-staging/survival-rates.html>.
58. Zhang, L., S. Sanagapalli, and A. Stoita, *Challenges in diagnosis of pancreatic cancer*. *World J Gastroenterol*, 2018. **24**(19): p. 2047-2060.
59. Kleeff, J., et al., *Distal Pancreatectomy: Risk Factors for Surgical Failure in 302 Consecutive Cases*. *Annals of Surgery*, 2007. **245**(4): p. 573-582.
60. Karim, S.A.M., et al., *The outcomes and complications of pancreaticoduodenectomy (Whipple procedure): Cross sectional study*. *International Journal of Surgery*, 2018. **52**: p. 383-387.
61. De La Cruz, M.S., A.P. Young, and M.T. Ruffin, *Diagnosis and management of pancreatic cancer*. *Am Fam Physician*, 2014. **89**(8): p. 626-32.
62. Maeda, S., M. Unno, and J. Yu, *Adjuvant and neoadjuvant therapy for pancreatic cancer*. *Journal of Pancreatology*, 2019. **2**(3): p. 100-106.
63. Pappalardo, A., et al., *Adjuvant Treatment in Pancreatic Cancer: Shaping the Future of the Curative Setting*. *Frontiers in Oncology*, 2021. **11**.
64. Janssen, Q.P., et al., *Neoadjuvant Treatment in Patients With Resectable and Borderline Resectable Pancreatic Cancer*. *Frontiers in Oncology*, 2020. **10**.
65. van Roessel, S., et al., *Evaluation of Adjuvant Chemotherapy in Patients With Resected Pancreatic Cancer After Neoadjuvant FOLFIRINOX Treatment*. *JAMA Oncology*, 2020. **6**(11): p. 1733-1740.

66. Jones, O.P., J.D. Melling, and P. Ghaneh, *Adjuvant therapy in pancreatic cancer*. World J Gastroenterol, 2014. **20**(40): p. 14733-46.
67. Garnier, J., et al., *Outcomes of patients with initially locally advanced pancreatic adenocarcinoma who did not benefit from resection: a prospective cohort study*. BMC Cancer, 2020. **20**(1): p. 203.
68. White, R.R., S. Reddy, and D.S. Tyler, *The role of chemoradiation therapy in locally advanced pancreatic cancer*. HPB (Oxford), 2005. **7**(2): p. 109-13.
69. Wu, L., et al., *Consolidative Chemoradiotherapy After Induced Chemotherapy Is an Optimal Regimen for Locally Advanced Pancreatic Cancer*. Frontiers in Oncology, 2020. **9**.
70. Simoni, N., et al., *Ablative Radiotherapy (ART) for Locally Advanced Pancreatic Cancer (LAPC): Toward a New Paradigm?* Life, 2022. **12**(4): p. 465.
71. Reyngold, M., P. Parikh, and C.H. Crane, *Ablative radiation therapy for locally advanced pancreatic cancer: techniques and results*. Radiation Oncology, 2019. **14**(1): p. 95.
72. Sawicka, E., et al., *Chemoradiotherapy for locally advanced pancreatic cancer patients: is it still an open question?* Contemp Oncol (Pozn), 2016. **20**(2): p. 102-8.
73. Brown, J.M., D.J. Carlson, and D.J. Brenner, *The Tumor Radiobiology of SRS and SBRT: Are More Than the 5 Rs Involved?* International Journal of Radiation Oncology, Biology, Physics, 2014. **88**(2): p. 254-262.
74. Goldsmith, C., et al., *Stereotactic ablative radiotherapy (SABR) as primary, adjuvant, consolidation and re-treatment option in pancreatic cancer: scope for dose escalation and lessons for toxicity*. Radiation Oncology, 2018. **13**(1): p. 204.
75. Ghaly, M., et al., *New Potential Options for SBRT in Pancreatic Cancer*. Cancer Med J, 2021. **4**(Suppl 3): p. 41-50.
76. Abi Jaoude, J., et al., *Stereotactic Versus Conventional Radiation Therapy for Patients With Pancreatic Cancer in the Modern Era*. Advances in Radiation Oncology, 2021. **6**(6).
77. Ghosn, M., et al., *Optimum chemotherapy in the management of metastatic pancreatic cancer*. World J Gastroenterol, 2014. **20**(9): p. 2352-7.
78. Hall, E.J.a.G., A.J. , *Radiobiology for the Radiologist*. 8th ed. 2018, Lippincott (PA): Williams & Wilkins.
79. Riley, P.A., *Free Radicals in Biology: Oxidative Stress and the Effects of Ionizing Radiation*. International Journal of Radiation Biology, 1994. **65**(1): p. 27-33.
80. Halliwell, B., et al., *Hydroxyl radical is a significant player in oxidative DNA damage in vivo*. Chemical Society Reviews, 2021. **50**(15): p. 8355-8360.
81. Falco, M., B. Masojć, and T. Sulikowski, *Radiotherapy in Pancreatic Cancer: To Whom, When, and How?* Cancers, 2023. **15**(13): p. 3382.
82. Wang, S., et al., *The molecular biology of pancreatic adenocarcinoma: translational challenges and clinical perspectives*. Signal Transduction and Targeted Therapy, 2021. **6**(1): p. 249.
83. Zeng, S., et al., *Chemoresistance in Pancreatic Cancer*. International Journal of Molecular Sciences, 2019. **20**(18): p. 4504.
84. de Sousa Cavalcante, L. and G. Monteiro, *Gemcitabine: Metabolism and molecular mechanisms of action, sensitivity and chemoresistance in pancreatic cancer*. European Journal of Pharmacology, 2014. **741**: p. 8-16.
85. Huang, P., et al., *Action of 2',2'-difluorodeoxycytidine on DNA synthesis*. Cancer Res, 1991. **51**(22): p. 6110-7.

86. Mini, E., et al., *Cellular pharmacology of gemcitabine*. Ann Oncol, 2006. **17 Suppl 5**: p. v7-12.
87. Huang, P. and W. Plunkett, *Induction of apoptosis by gemcitabine*. Semin Oncol, 1995. **22**(4 Suppl 11): p. 19-25.
88. Yin, T., et al., *Bmi1 inhibition enhances the sensitivity of pancreatic cancer cells to gemcitabine*. Oncotarget, 2016. **7**(24): p. 37192-37204.
89. Amrutkar, M. and I.P. Gladhaug, *Pancreatic Cancer Chemoresistance to Gemcitabine*. Cancers, 2017. **9**(11): p. 157.
90. Tamburrino, A., et al., *Mechanisms of resistance to chemotherapeutic and anti-angiogenic drugs as novel targets for pancreatic cancer therapy*. Frontiers in Pharmacology, 2013. **4**.
91. Liu, Y., Y. Lu, and C. Yang, *Evaluating In Vitro DNA Damage Using Comet Assay*. JoVE, 2017(128): p. e56450.
92. Shi, X., et al., *Acquired Resistance of Pancreatic Cancer Cells towards 5-Fluorouracil and Gemcitabine Is Associated with Altered Expression of Apoptosis-Regulating Genes*. Oncology, 2002. **62**(4): p. 354-362.
93. Low, Z.Y., I.A. Farouk, and S.K. Lal, *Drug Repositioning: New Approaches and Future Prospects for Life-Debilitating Diseases and the COVID-19 Pandemic Outbreak*. Viruses, 2020. **12**(9): p. 1058.
94. Kim, J.H. and A.R. Scialli, *Thalidomide: The Tragedy of Birth Defects and the Effective Treatment of Disease*. Toxicological Sciences, 2011. **122**(1): p. 1-6.
95. Michael Cox, David L. Nelson, and A.L. Lehninger, *Lehninger Principles of Biochemistry*. 4th ed. 2008: Palgrave Macmillan.
96. Lubert Stryer, Jeremy M. Berg, and J. Tymoczko, *Biochemistry*. 5th ed. 2002: W.H.Freeman & Co Ltd.
97. Pizzorno, J., *Glutathione!* Integr Med (Encinitas), 2014. **13**(1): p. 8-12.
98. Balak, D.M., *Fumaric acid esters in the management of psoriasis*. Psoriasis (Auckl), 2015. **5**: p. 9-23.
99. Carlström, K.E., et al., *Therapeutic efficacy of dimethyl fumarate in relapsing-remitting multiple sclerosis associates with ROS pathway in monocytes*. Nature Communications, 2019. **10**(1): p. 3081.
100. National Institute for Health and Care Excellence. *Dimethyl fumarate for treating relapsing remitting multiple sclerosis*. 2023 [8 January 2024]; Available from: <https://www.nice.org.uk/guidance/ta320/chapter/1-Guidance>.
101. U.S. Food & Drug Administration. *Drug Approval Package*. 2023 [8 January 2024]; Available from: [https://www.accessdata.fda.gov/drugsatfda\\_docs/nda/2013/204063orig1s000toc.cfm](https://www.accessdata.fda.gov/drugsatfda_docs/nda/2013/204063orig1s000toc.cfm).
102. European Medicines Agency. *Skilarence*. 2023 [8 January 2024]; Available from: <https://www.ema.europa.eu/en/medicines/human/EPAR/skilarence>
103. National Institute for Health and Care Excellence. *Dimethyl fumarate for treating moderate to severe plaque psoriasis*. 2023 [8 January 2024]; Available from: <https://www.nice.org.uk/guidance/ta475>.
104. Manai, F., et al., *Dimethyl Fumarate and Intestine: From Main Suspect to Potential Ally against Gut Disorders*. International Journal of Molecular Sciences, 2023. **24**(12): p. 9912.
105. Berger, A.A., et al., *Monomethyl Fumarate (MMF, Bafiertam) for the Treatment of Relapsing Forms of Multiple Sclerosis (MS)*. Neurology International, 2021. **13**(2): p. 207-223.
106. U.S. Food & Drug Administration. *The U.S. Food and Drug Administration Highlights of Prescribing Information*. 2023 [8 January 2024]; Available from: [https://www.accessdata.fda.gov/drugsatfda\\_docs/label/2020/210296s000lbl.pdf](https://www.accessdata.fda.gov/drugsatfda_docs/label/2020/210296s000lbl.pdf).

107. Mills, E.A., et al., *Emerging Understanding of the Mechanism of Action for Dimethyl Fumarate in the Treatment of Multiple Sclerosis*. *Frontiers in Neurology*, 2018. **9**.
108. Sánchez-Sanz, A., et al., *Dimethyl fumarate-related immune and transcriptional signature is associated with clinical response in multiple sclerosis-treated patients*. *Frontiers in Immunology*, 2023. **14**.
109. Loewe, R., et al., *Dimethylfumarate Impairs Melanoma Growth and Metastasis*. *Cancer Research*, 2006. **66**(24): p. 11888-11896.
110. Yamazoe, Y., et al., *Dimethylfumarate inhibits tumor cell invasion and metastasis by suppressing the expression and activities of matrix metalloproteinases in melanoma cells*. *Cell Biology International*, 2009. **33**(10): p. 1087-1094.
111. Saidu, N.E.B., et al., *Dimethyl Fumarate Controls the NRF2/DJ-1 Axis in Cancer Cells: Therapeutic Applications*. *Molecular Cancer Therapeutics*, 2017. **16**(3): p. 529-539.
112. Edward Bennett Saidu, N., et al., *Dimethyl fumarate is highly cytotoxic in KRAS mutated cancer cells but spares non-tumorigenic cells*. *Oncotarget*, 2018. **9**(10).
113. Rupp, T., et al., *Therapeutic Potential of Fingolimod and Dimethyl Fumarate in Non-Small Cell Lung Cancer Preclinical Models*. *International Journal of Molecular Sciences*, 2022. **23**(15): p. 8192.
114. Xie, X., et al., *Dimethyl fumarate induces necroptosis in colon cancer cells through GSH depletion/ROS increase/MAPKs activation pathway*. *British Journal of Pharmacology*, 2015. **172**(15): p. 3929-3943.
115. Tsurushima, K., et al., *Dimethyl Fumarate Induces Apoptosis via Inhibition of NF- $\kappa$ B and Enhances the Effect of Paclitaxel and Adriamycin in Human TNBC Cells*. *International Journal of Molecular Sciences*, 2022. **23**(15): p. 8681.
116. Shafer, D., et al., *Phase I trial of dimethyl fumarate, temozolomide, and radiation therapy in glioblastoma*. *Neuro-Oncology Advances*, 2020. **2**(1).
117. Saidu, N.E.B., et al., *Dimethyl fumarate, a two-edged drug: Current status and future directions*. *Medicinal Research Reviews*, 2019. **39**(5): p. 1923-1952.
118. Chio, I.I.C., et al., *NRF2 Promotes Tumor Maintenance by Modulating mRNA Translation in Pancreatic Cancer*. *Cell*, 2016. **166**(4): p. 963-976.
119. Jaganjac, M., et al., *The NRF2, Thioredoxin, and Glutathione System in Tumorigenesis and Anticancer Therapies*. *Antioxidants*, 2020. **9**(11): p. 1151.
120. Franklin, C.C., et al., *Structure, function, and post-translational regulation of the catalytic and modifier subunits of glutamate cysteine ligase*. *Molecular Aspects of Medicine*, 2009. **30**(1): p. 86-98.
121. Lu, S.C., *Glutathione synthesis*. *Biochimica et Biophysica Acta (BBA) - General Subjects*, 2013. **1830**(5): p. 3143-3153.
122. Gafson, A.R., et al., *Breaking the cycle*. *Neurology Neuroimmunology & Neuroinflammation*, 2019. **6**(3): p. e562.
123. Hoogendoorn, A., et al., *Emerging Therapeutic Applications for Fumarates*. *Trends in Pharmacological Sciences*, 2021. **42**(4): p. 239-254.
124. Al-Jaderi, Z. and A.A. Maghazachi, *Utilization of Dimethyl Fumarate and Related Molecules for Treatment of Multiple Sclerosis, Cancer, and Other Diseases*. *Frontiers in Immunology*, 2016. **7**.
125. Landeck, L., et al., *Dimethyl fumarate (DMF) vs. monoethyl fumarate (MEF) salts for the treatment of plaque psoriasis: a review of clinical data*. *Archives of Dermatological Research*, 2018. **310**(6): p. 475-483.

126. Wynn, D., et al., *Monomethyl fumarate has better gastrointestinal tolerability profile compared with dimethyl fumarate*. Multiple Sclerosis and Related Disorders, 2020. **45**.
127. Vaziri-Gohar, A., et al., *Increased glucose availability sensitizes pancreatic cancer to chemotherapy*. bioRxiv, 2022: p. 2022.04.29.490090.
128. Kogawa, T., et al., *Chemoprevention of pancreatic cancer by inhibition of glutathione-S transferase P1*. Investigational New Drugs, 2021. **39**(6): p. 1484-1492.
129. Jagust, P., et al., *Glutathione metabolism is essential for self-renewal and chemoresistance of pancreatic cancer stem cells*. World J Stem Cells, 2020. **12**(11): p. 1410-1428.
130. Burris, H.A., 3rd, et al., *Improvements in survival and clinical benefit with gemcitabine as first-line therapy for patients with advanced pancreas cancer: a randomized trial*. J Clin Oncol, 1997. **15**(6): p. 2403-13.
131. Moore, M.J., et al., *Erlotinib plus gemcitabine compared with gemcitabine alone in patients with advanced pancreatic cancer: a phase III trial of the National Cancer Institute of Canada Clinical Trials Group*. J Clin Oncol, 2007. **25**(15): p. 1960-6.
132. Conroy, T., et al., *FOLFIRINOX versus gemcitabine for metastatic pancreatic cancer*. N Engl J Med, 2011. **364**(19): p. 1817-25.
133. Ciccolini, J., et al., *Pharmacokinetics and pharmacogenetics of Gemcitabine as a mainstay in adult and pediatric oncology: an EORTC-PAMM perspective*. Cancer Chemotherapy and Pharmacology, 2016. **78**(1): p. 1-12.
134. Olive, K.P., et al., *Inhibition of Hedgehog signaling enhances delivery of chemotherapy in a mouse model of pancreatic cancer*. Science, 2009. **324**(5933): p. 1457-61.
135. Hoff, D.D.V., et al., *Increased Survival in Pancreatic Cancer with nab-Paclitaxel plus Gemcitabine*. New England Journal of Medicine, 2013. **369**(18): p. 1691-1703.
136. Michl, P. and T.M. Gress, *Current concepts and novel targets in advanced pancreatic cancer*. Gut, 2013. **62**(2): p. 317-26.
137. Deer, E.L., et al., *Phenotype and Genotype of Pancreatic Cancer Cell Lines*. Pancreas, 2010. **39**(4): p. 425-435.
138. Franken, N.A.P., et al., *Clonogenic assay of cells in vitro*. Nature Protocols, 2006. **1**(5): p. 2315-2319.
139. McMillan, K.S., et al., *Emulsion technologies for multicellular tumour spheroid radiation assays*. Analyst, 2016. **141**(1): p. 100-110.
140. Zaroni, M., et al., *3D tumor spheroid models for in vitro therapeutic screening: a systematic approach to enhance the biological relevance of data obtained*. Scientific Reports, 2016. **6**(1): p. 19103.
141. Chen, W., et al., *High-throughput image analysis of tumor spheroids: a user-friendly software application to measure the size of spheroids automatically and accurately*. J Vis Exp, 2014(89).
142. Cellosaurus. *Cellosaurus PANC-1 (CVCL\_0480)*. 2023 [29th January 2024]; Available from: [https://www.cellosaurus.org/CVCL\\_0480](https://www.cellosaurus.org/CVCL_0480).
143. Miura, K., et al., *Establishment and characterization of new cell lines of anaplastic pancreatic cancer, which is a rare malignancy: OCUP-A1 and OCUP-A2*. BMC Cancer, 2016. **16**(1): p. 268.
144. Watanabe, M., et al., *Metabolic Profiling Comparison of Human Pancreatic Ductal Epithelial Cells and Three Pancreatic Cancer Cell Lines using NMR Based Metabonomics*. J Mol Biomark Diagn, 2012. **3**(2).

145. Brix, N., et al., *The clonogenic assay: robustness of plating efficiency-based analysis is strongly compromised by cellular cooperation*. Radiation Oncology, 2020. **15**(1): p. 248.
146. Puck, T.T. and P.I. Marcus, *Action of x-rays on mammalian cells*. J Exp Med, 1956. **103**(5): p. 653-66.
147. Chang, Z., et al., *GATA1 Promotes Gemcitabine Resistance in Pancreatic Cancer through Antiapoptotic Pathway*. Journal of Oncology, 2019. **2019**(1): p. 9474273.
148. Huanwen, W., et al., *Intrinsic chemoresistance to gemcitabine is associated with constitutive and laminin-induced phosphorylation of FAK in pancreatic cancer cell lines*. Molecular Cancer, 2009. **8**(1): p. 125.
149. Amrutkar, M., et al., *Differential Gemcitabine Sensitivity in Primary Human Pancreatic Cancer Cells and Paired Stellate Cells Is Driven by Heterogenous Drug Uptake and Processing*. Cancers, 2020. **12**(12): p. 3628.
150. Kurata, N., et al., *Predicting the chemosensitivity of pancreatic cancer cells by quantifying the expression levels of genes associated with the metabolism of gemcitabine and 5-fluorouracil*. Int J Oncol, 2011. **39**(2): p. 473-482.
151. Awasthi, N., et al., *Comparative benefits of Nab-paclitaxel over gemcitabine or polysorbate-based docetaxel in experimental pancreatic cancer*. Carcinogenesis, 2013. **34**(10): p. 2361-2369.
152. Fryer, R.A., et al., *Mechanisms underlying gemcitabine resistance in pancreatic cancer and sensitisation by the iMiD™ lenalidomide*. Anticancer Res, 2011. **31**(11): p. 3747-56.
153. Hagmann, W., R. Jesnowski, and J.M. Löhr, *Interdependence of Gemcitabine Treatment, Transporter Expression, and Resistance in Human Pancreatic Carcinoma Cells*. Neoplasia, 2010. **12**(9): p. 740-747.
154. Dufau, I., et al., *Multicellular tumor spheroid model to evaluate spatio-temporal dynamics effect of chemotherapeutics: application to the gemcitabine/CHK1 inhibitor combination in pancreatic cancer*. BMC Cancer, 2012. **12**(1): p. 15.
155. Longati, P., et al., *3D pancreatic carcinoma spheroids induce a matrix-rich, chemoresistant phenotype offering a better model for drug testing*. BMC Cancer, 2013. **13**(1): p. 95.
156. Valeria, P.d.L. and B.-R. Raúl, *Changes in P-glycoprotein activity are mediated by the growth of a tumour cell line as multicellular spheroids*. Cancer Cell International, 2005. **5**(1): p. 20.
157. Harpstrite, S.E., et al., *Interrogation of multidrug resistance (MDR1) P-glycoprotein (ABCB1) expression in human pancreatic carcinoma cells: correlation of: 99m: Tc-Sestamibi uptake with western blot analysis*. Nuclear Medicine Communications, 2014. **35**(10): p. 1067-1070.
158. Bergman, A.M., et al., *Increased sensitivity to gemcitabine of P-glycoprotein and multidrug resistance-associated protein-overexpressing human cancer cell lines*. British Journal of Cancer, 2003. **88**(12): p. 1963-1970.
159. Giovannetti, E., et al., *Synergistic Cytotoxicity and Pharmacogenetics of Gemcitabine and Pemetrexed Combination in Pancreatic Cancer Cell Lines*. Clinical Cancer Research, 2004. **10**(9): p. 2936-2943.
160. Kapałczyńska, M., et al., *2D and 3D cell cultures – a comparison of different types of cancer cell cultures*. Archives of Medical Science, 2018. **14**(4): p. 910-919.
161. Vinci, M., et al., *Advances in establishment and analysis of three-dimensional tumor spheroid-based functional assays for target validation and drug evaluation*. BMC Biology, 2012. **10**(1): p. 29.

162. Matsuda, Y., et al., *Morphological and cytoskeletal changes of pancreatic cancer cells in three-dimensional spheroidal culture*. Medical Molecular Morphology, 2010. **43**(4): p. 211-217.
163. Powan, P., et al., *Detachment-induced E-cadherin expression promotes 3D tumor spheroid formation but inhibits tumor formation and metastasis of lung cancer cells*. American Journal of Physiology-Cell Physiology, 2017. **313**(5): p. C556-C566.
164. Nguyen, L., et al., *Impact of DNA repair and reactive oxygen species levels on radioresistance in pancreatic cancer*. Radiotherapy and Oncology, 2021. **159**: p. 265-276.
165. Schwarz, K., et al., *Modification of radiosensitivity by Curcumin in human pancreatic cancer cell lines*. Scientific Reports, 2020. **10**(1): p. 3815.
166. Unkel, S., C. Belka, and K. Lauber, *On the analysis of clonogenic survival data: Statistical alternatives to the linear-quadratic model*. Radiation Oncology, 2016. **11**(1): p. 11.
167. Onozato, Y., et al., *Radiosensitivity of quiescent and proliferating cells grown as multicellular tumor spheroids*. Cancer Science, 2017. **108**(4): p. 704-712.
168. Mokhtari, R.B., et al., *Combination therapy in combating cancer*. Oncotarget, 2017. **8**(23).
169. Chou, T.-C., *Drug Combination Studies and Their Synergy Quantification Using the Chou-Talalay Method*. Cancer Research, 2010. **70**(2): p. 440-446.
170. Chou, T.-C., *Theoretical Basis, Experimental Design, and Computerized Simulation of Synergism and Antagonism in Drug Combination Studies*. Pharmacological Reviews, 2006. **58**(3): p. 621-681.
171. Iwata, K., et al., *The Relationship between Treatment Time of Gemcitabine and Development of Hematologic Toxicity in Cancer Patients*. Biological and Pharmaceutical Bulletin, 2011. **34**(11): p. 1765-1768.
172. Patwardhan, G.A., et al., *Treatment scheduling effects on the evolution of drug resistance in heterogeneous cancer cell populations*. npj Breast Cancer, 2021. **7**(1): p. 60.
173. Modest, D.P., et al., *Sequential Versus Combination Therapy of Metastatic Colorectal Cancer Using Fluoropyrimidines, Irinotecan, and Bevacizumab: A Randomized, Controlled Study—XELAVIRI (AIO KRK0110)*. Journal of Clinical Oncology, 2019. **37**(1): p. 22-32.
174. Poole, C.J., et al., *Optimized sequence of drug administration and schedule leads to improved dose delivery for gemcitabine and paclitaxel in combination: a phase I trial in patients with recurrent ovarian cancer*. Int J Gynecol Cancer, 2006. **16**(2): p. 507-14.
175. De Souza, R., et al., *Chemotherapy Dosing Schedule Influences Drug Resistance Development in Ovarian Cancer*. Molecular Cancer Therapeutics, 2011. **10**(7): p. 1289-1299.
176. Liu, W.M., A.J. Lawrence, and S.P. Joel, *The importance of drug scheduling and recovery phases in determining drug activity: improving etoposide efficacy in BCR-ABL-positive CML cells*. European Journal of Cancer, 2002. **38**(6): p. 842-850.
177. Blackwood, E., et al., *Combination Drug Scheduling Defines a “Window of Opportunity” for Chemopotiation of Gemcitabine by an Orally Bioavailable, Selective ChK1 Inhibitor, GNE-900*. Molecular Cancer Therapeutics, 2013. **12**(10): p. 1968-1980.
178. McCluskey, A.G., et al., *Inhibition of Poly(ADP-Ribose) Polymerase Enhances the Toxicity of <sup>131</sup>I-Metaiodobenzylguanidine/Topotecan Combination Therapy to Cells and*

- Xenografts That Express the Noradrenaline Transporter*. Journal of Nuclear Medicine, 2012. **53**(7): p. 1146-1154.
179. Inamura, A., S. Muraoka-Hirayama, and K. Sakurai, *Loss of Mitochondrial DNA by Gemcitabine Triggers Mitophagy and Cell Death*. Biological and Pharmaceutical Bulletin, 2019. **42**(12): p. 1977-1987.
  180. Okusaka, T., et al., *Phase II study of radiotherapy combined with gemcitabine for locally advanced pancreatic cancer*. British Journal of Cancer, 2004. **91**(4): p. 673-677.
  181. Cengiz, M., et al., *Concurrent gemcitabine and radiotherapy for locally advanced pancreatic cancer*. Medical Oncology, 2007. **24**(2): p. 239-243.
  182. Jr, W.S., et al., *Full-Dose Gemcitabine With Concurrent Radiation Therapy in Patients With Nonmetastatic Pancreatic Cancer: A Multicenter Phase II Trial*. Journal of Clinical Oncology, 2008. **26**(6): p. 942-947.
  183. Sr, P.J.L., et al., *Gemcitabine Alone Versus Gemcitabine Plus Radiotherapy in Patients With Locally Advanced Pancreatic Cancer: An Eastern Cooperative Oncology Group Trial*. Journal of Clinical Oncology, 2011. **29**(31): p. 4105-4112.
  184. Cardenes, H.R., et al., *A Phase II Study of Gemcitabine in Combination With Radiation Therapy in Patients With Localized, Unresectable, Pancreatic Cancer: A Hoosier Oncology Group Study*. American Journal of Clinical Oncology, 2011. **34**(5): p. 460-465.
  185. Kobashigawa, S., et al., *Gemcitabine Induces Radiosensitization Through Inhibition of RAD51-dependent Repair for DNA Double-strand Breaks*. Anticancer Res, 2015. **35**(5): p. 2731-7.
  186. Andrén-Sandberg, A., *Pancreatic cancer: chemotherapy and radiotherapy*. N Am J Med Sci, 2011. **3**(1): p. 1-12.
  187. Springfield, C., et al., *Neoadjuvant therapy for pancreatic cancer*. Nature Reviews Clinical Oncology, 2023. **20**(5): p. 318-337.
  188. Wouters, A., et al., *The radiosensitising effect of gemcitabine and its main metabolite dFdU under low oxygen conditions is in vitro not dependent on functional HIF-1 protein*. BMC Cancer, 2014. **14**(1): p. 594.
  189. Patki, M., et al., *In vitro assessment of a synergistic combination of gemcitabine and zebularine in pancreatic cancer cells*. Exp Cell Res, 2021. **405**(2): p. 112660.
  190. Frances, A. and P. Cordelier, *The Emerging Role of Cytidine Deaminase in Human Diseases: A New Opportunity for Therapy?* Molecular Therapy, 2020. **28**(2): p. 357-366.
  191. Bjånes, T.K., et al., *Intracellular Cytidine Deaminase Regulates Gemcitabine Metabolism in Pancreatic Cancer Cell Lines*. Drug Metabolism and Disposition, 2020. **48**(3): p. 153-158.
  192. Pawlik, T.M. and K. Keyomarsi, *Role of cell cycle in mediating sensitivity to radiotherapy*. International Journal of Radiation Oncology, Biology, Physics, 2004. **59**(4): p. 928-942.
  193. Lonati, L., et al., *Radiation-induced cell cycle perturbations: a computational tool validated with flow-cytometry data*. Scientific Reports, 2021. **11**(1): p. 925.
  194. Hamed, S.S., R.M. Straubinger, and W.J. Jusko, *Pharmacodynamic modeling of cell cycle and apoptotic effects of gemcitabine on pancreatic adenocarcinoma cells*. Cancer Chemotherapy and Pharmacology, 2013. **72**(3): p. 553-563.
  195. Scott, D., *Personal Communication*. 2019.
  196. ALQahtani, R.K.N., *Personal Communication*. 2022.

197. Brown, W.S., et al., *Overcoming Adaptive Resistance to KRAS and MEK Inhibitors by Co-targeting mTORC1/2 Complexes in Pancreatic Cancer*. *Cell Reports Medicine*, 2020. **1**(8).
198. Zhang, J., et al., *Targeting KRAS for the potential treatment of pancreatic ductal adenocarcinoma: Recent advancements provide hope (Review)*. *Oncol Rep*, 2023. **50**(5): p. 206.
199. Held, K.D., et al., *Effect of Dimethyl Fumarate on the Radiation Sensitivity of Mammalian Cells in Vitro*. *Radiation Research*, 1988. **115**(3): p. 495-502.
200. Kolamunne, R.T., et al., *Nrf2 activation supports cell survival during hypoxia and hypoxia/reoxygenation in cardiomyoblasts; the roles of reactive oxygen and nitrogen species*. *Redox Biology*, 2013. **1**(1): p. 418-426.
201. Peng, L., et al., *Downregulation of GSTM2 enhances gemcitabine chemosensitivity of pancreatic cancer in vitro and in vivo*. *Pancreatology*, 2021. **21**(1): p. 115-123.
202. Sherr, C.J. and J. Bartek, *Cell Cycle–Targeted Cancer Therapies*. *Annual Review of Cancer Biology*, 2017. **1**(Volume 1, 2017): p. 41-57.
203. Kaluzki, I., et al., *Dimethylfumarate Inhibits Colorectal Carcinoma Cell Proliferation: Evidence for Cell Cycle Arrest, Apoptosis and Autophagy*. *Cells*, 2019. **8**(11): p. 1329.
204. Oh, C.J., et al., *Dimethylfumarate attenuates restenosis after acute vascular injury by cell-specific and Nrf2-dependent mechanisms*. *Redox Biology*, 2014. **2**: p. 855-864.
205. Cooper, *The Cell: A Molecular Approach*. 2nd ed. 2000, Sunderland (MA): Sinauer Associates.
206. Plesca, D., S. Mazumder, and A. Almasan, *Chapter 6 DNA Damage Response and Apoptosis*, in *Methods in Enzymology*. 2008, Academic Press. p. 107-122.
207. Molinari, M., *Cell cycle checkpoints and their inactivation in human cancer*. *Cell Proliferation*, 2000. **33**(5): p. 261-274.
208. Kastan, M.B. and J. Bartek, *Cell-cycle checkpoints and cancer*. *Nature*, 2004. **432**(7015): p. 316-323.
209. Hustedt, N. and D. Durocher, *The control of DNA repair by the cell cycle*. *Nature Cell Biology*, 2017. **19**(1): p. 1-9.
210. Iyer, D.R. and N. Rhind, *The Intra-S Checkpoint Responses to DNA Damage*. *Genes*, 2017. **8**(2): p. 74.
211. de Gooijer, M.C., et al., *The G2 checkpoint—a node-based molecular switch*. *FEBS Open Bio*, 2017. **7**(4): p. 439-455.
212. Ventura, E. and A. Giordano, *Cell Cycle*, in *Reference Module in Life Sciences*. 2019, Elsevier.
213. Wong, R.S.Y., *Apoptosis in cancer: from pathogenesis to treatment*. *Journal of Experimental & Clinical Cancer Research*, 2011. **30**(1): p. 87.
214. Chen, K., et al., *Dimethyl Fumarate Induces Metabolic Crisis to Suppress Pancreatic Carcinoma*. *Frontiers in Pharmacology*, 2021. **12**.
215. Crowley, L.C., et al., *Quantitation of Apoptosis and Necrosis by Annexin V Binding, Propidium Iodide Uptake, and Flow Cytometry*. *Cold Spring Harb Protoc*, 2016. **2016**(11).
216. Hellman, B., H. Vaghef, and B. Boström, *The concepts of tail moment and tail inertia in the single cell gel electrophoresis assay*. *Mutation Research/DNA Repair*, 1995. **336**(2): p. 123-131.
217. Mantovani, F., L. Collavin, and G. Del Sal, *Mutant p53 as a guardian of the cancer cell*. *Cell Death & Differentiation*, 2019. **26**(2): p. 199-212.

218. N'Guessan, K.F., et al., *Enhanced Efficacy of Combination of Gemcitabine and Phosphatidylserine-Targeted Nanovesicles against Pancreatic Cancer*. *Molecular Therapy*, 2020. **28**(8): p. 1876-1886.
219. Hill, R., et al., *Gemcitabine-mediated tumour regression and p53-dependent gene expression: implications for colon and pancreatic cancer therapy*. *Cell Death & Disease*, 2013. **4**(9): p. e791-e791.
220. Chandler, N.M., J.J. Canete, and M.P. Callery, *Caspase-3 drives apoptosis in pancreatic cancer cells after treatment with gemcitabine*. *Journal of Gastrointestinal Surgery*, 2004. **8**(8): p. 1072-1078.
221. Teyssier, F., et al., *[Cell cycle regulation after exposure to ionizing radiation]*. *Bull Cancer*, 1999. **86**(4): p. 345-57.
222. Sia, J., et al., *Molecular Mechanisms of Radiation-Induced Cancer Cell Death: A Primer*. *Frontiers in Cell and Developmental Biology*, 2020. **8**.
223. Chen, X.-Y., et al., *Pim-3 contributes to radioresistance through regulation of the cell cycle and DNA damage repair in pancreatic cancer cells*. *Biochemical and Biophysical Research Communications*, 2016. **473**(1): p. 296-302.
224. Lee, Y.-S., et al., *Anti-Inflammatory Effects of Dimethyl Fumarate in Microglia via an Autophagy Dependent Pathway*. *Frontiers in Pharmacology*, 2021. **12**.
225. Parzych, K.R. and D.J. Klionsky, *An Overview of Autophagy: Morphology, Mechanism, and Regulation*. *Antioxidants & Redox Signaling*, 2014. **20**(3): p. 460-473.
226. Piffoux, M., E. Eriau, and P.A. Cassier, *Autophagy as a therapeutic target in pancreatic cancer*. *British Journal of Cancer*, 2021. **124**(2): p. 333-344.
227. Yang, S., et al., *Pancreatic cancers require autophagy for tumor growth*. *Genes Dev*, 2011. **25**(7): p. 717-29.
228. Jakubowska, K., et al., *Reduced expression of caspase-8 and cleaved caspase-3 in pancreatic ductal adenocarcinoma cells*. *Oncol Lett*, 2016. **11**(3): p. 1879-1884.
229. Zhu, H., et al., *PARP inhibitors in pancreatic cancer: molecular mechanisms and clinical applications*. *Molecular Cancer*, 2020. **19**(1): p. 49.
230. Zhao, H., et al., *ROS/KRAS/AMPK Signaling Contributes to Gemcitabine-Induced Stem-like Cell Properties in Pancreatic Cancer*. *Molecular Therapy - Oncolytics*, 2019. **14**: p. 299-312.
231. Zhang, J., et al., *Dual Effects of N,N-dimethylformamide on Cell Proliferation and Apoptosis in Breast Cancer*. *Dose-Response*, 2017. **15**(4): p. 1559325817744450.
232. Diaz Vivancos, P., et al., *A nuclear glutathione cycle within the cell cycle*. *Biochemical Journal*, 2010. **431**(2): p. 169-178.
233. Yang, B., et al., *Alcohol inhibits the metabolism of dimethyl fumarate to the active metabolite responsible for decreasing relapse frequency in the treatment of multiple sclerosis*. *PLoS One*, 2022. **17**(11): p. e0278111.
234. The Human Protein Atlas. *CES1*. 2024 [18 March 2024]; Available from: <https://www.proteinatlas.org/ENSG00000198848-CES1/cell+line>
235. Schmitt, A., et al., *Dimethyl fumarate induces ferroptosis and impairs NF- $\kappa$ B/STAT3 signaling in DLBCL*. *Blood*, 2021. **138**(10): p. 871-884.
236. Liu, J., R. Kang, and D. Tang, *The Art of War: Ferroptosis and Pancreatic Cancer*. *Frontiers in Pharmacology*, 2021. **12**.
237. Kain, K.H., et al., *The chick embryo as an expanding experimental model for cancer and cardiovascular research*. *Developmental Dynamics*, 2014. **243**(2): p. 216-228.
238. Miebach, L., J. Berner, and S. Bekeschus, *In ovo model in cancer research and tumor immunology*. *Frontiers in Immunology*, 2022. **13**.

239. Montes Diaz, G., et al., *Dimethyl fumarate induces a persistent change in the composition of the innate and adaptive immune system in multiple sclerosis patients*. Scientific Reports, 2018. **8**(1): p. 8194.
240. Irfan Maqsood, M., et al., *Immortality of cell lines: challenges and advantages of establishment*. Cell Biology International, 2013. **37**(10): p. 1038-1045.